

Tuning tolerance

**Modulating adaptive immune responses for
therapeutic purposes**

Manon Aleida Adriana Jansen

Tuning tolerance

Modulating adaptive immune responses for therapeutic purposes

Afstemmen van tolerantie

Moduleren van adaptieve immuun responsen voor therapeutische doeleinden
(met een samenvatting in het Nederlands)

Proefschrift

ter verkrijging van de graad van doctor aan de Universiteit Utrecht op gezag van de rector magnificus, prof.dr. H.R.B.M. Kummeling, ingevolge het besluit van het college voor promoties in het openbaar te verdedigen op donderdag 14 februari 2019 des middags te 12.45 uur

door

Manon Aleida Adriana Jansen

geboren op 17 november 1990
te Sint Michielsgestel

colofon

© 2018 Manon AA jansen

ISBN: 978-90-393-7073-5

All rights reserved. No part of this thesis may be reproduced, stored or transmitted in any form or by any means without prior permission of the author.

The research described in this thesis was carried out at the Division of Immunology, Department of Infectious diseases & Immunology, Utrecht University, Utrecht, the Netherlands.

The research described in chapter 3 and 4 was part of the AFACTT project (Action to Focus and Accelerate Cell-based Tolerance-inducing Therapies; BM1305) from European Cooperation in Science and Technology (COST). COST is part of the EU Framework Programme Horizon 2020.

Lay-out and printing: proefschrift-aio.nl

Printing of this thesis was financially supported by the Infection & Immunity center Utrecht.

Contents

Promotoren: Prof.dr. W. van Eden
Prof.dr. F. Broere

Chapter 1.	General introduction	7
Chapter 2.	Generation of the first TCR transgenic mouse with CD4 ⁺ T cells recognizing an anti-inflammatory regulatory T cell-inducing HSP70 peptide.	31
Chapter 3.	Matured tolerogenic dendritic cells modulate pre-activated and naïve CD4 ⁺ T cells and ameliorate proteoglycan induced arthritis in mice.	55
Chapter 4.	Targeting of tolerogenic dendritic cells to heat-shock proteins in inflammatory arthritis.	83
Chapter 5.	Lipidoid-polymer hybrid nanoparticles loaded with TNF siRNA suppress inflammation after intra-articular administration in a murine experimental arthritis model.	105
Chapter 6.	Routing dependent immune responses after experimental R848-adjuvated vaccination.	135
Chapter 7.	Summarizing discussion	163
Chapter 8.	Addendum	179
	Samenvatting	180
	Dankwoord/Acknowledgements	186
	Curriculum Vitae	190
	List of publications	191

Chapter 1

General introduction



Immune tolerance

To protect the body from infections, the immune system must recognize and establish responses against several pathogens such as bacteria, viruses and parasites. Antigens of these pathogens trigger the activation of both innate and adaptive immune cells to clear the pathogen. However, it is also possible that self-antigens are recognized by immune cells. This can generate inappropriate activation of the immune system and can lead to tissue damage and autoimmunity. In western countries, about 8% of the population is affected by autoimmune diseases^{1,2}.

T cells play an important role in the recognition of microbes but also in the maintenance of self-tolerance. In healthy individuals, self-tolerance is maintained at different levels: central and peripheral tolerance. Central tolerance for T cells takes place in the thymus when T lymphocytes are in development. Thymic medullary cells, under the control of autoimmune regulator (AIRE), present self-antigens in their MHC. Immature T cells that have a high affinity for self-antigens are deleted or inactivated before they develop into fully immunocompetent cells. Tolerance induced against self-antigens when the lymphocytes have left the primary lymphoid organs is known as peripheral tolerance. Since not all self-antigens are expressed in the primary lymphoid tissues, self-recognizing T cells that do not recognize self in the central lymphoid organs need to be killed or inactivated in the periphery. Peripheral tolerance roughly entails four processes: (1) Deletion, self-recognizing T cells are deleted after T cell receptor (TCR) engagement. (2) Ignorance, by never encountering their self-antigen through sequestration of self-antigens. (3) Anergy, induced functional unresponsiveness and (4) suppression of self-recognizing T cells by regulatory T cells (Tregs). Tregs are described in the mouse as CD4⁺CD25⁺FoxP3⁺ (CD4⁺CD127^{low}CD25⁺ in humans) and originate in the thymus (natural occurring Tregs; nTregs) or are induced in the periphery (induced Tregs; iTregs)^{3,4}. Tregs can suppress other cells via several mechanisms including cell-cell interaction (e.g. CTLA-4)⁵, cytokine production (e.g. IL-10 and TGFβ)^{6,7} and cytotoxicity via the release of granzymes or perforin⁸. By being able to suppress self-recognizing T cells, Tregs play a major role in preventing autoimmunity. For this reason, several studies were performed in which Treg presence and function was investigated in patients with autoimmune diseases, among which Rheumatoid arthritis (RA). There is a lot of controversy in this area, while some studies report that Tregs are decreasing in RA^{9,10}, others have reported an unchanged presence^{11,12} or even an increase in Tregs¹³. In addition to cell number, the functionality of the Tregs is important, which is also unclear in RA patients¹³⁻¹⁵.

Rheumatoid arthritis

RA is a chronic systemic autoimmune disease characterized by inflammation in the joints with pain, stiffness and often cartilage and bone destruction as a result. However, the etiology of RA is unclear. New research shows that not all patients can be categorized to the same group since the presence of autoantibodies differs. In RA, there are various autoantibodies described but the best known, and used in the clinic, are rheumatoid factor (RF) and anti-citrullinated protein antibodies (ACPA). The presence of RF, autoantibodies directed against self-IgG-Fc, has already been described in 1940. RF is not specific for RA but occurs also in other inflammatory diseases. ACPA are more specific for RA than RF, ACPA are present in only 2% of healthy individuals. Autoantibodies such as RF and ACPA are found in blood before patients experience any rheumatic symptoms. At this moment, there is no definite causal autoantigen known but, it is believed that the continuous increase in autoantibodies is due to epitope spreading, which means that there is an increase in recognition of citrullinated antigens secondary to the release of self-antigens¹⁶. Next to an accumulation of autoantigens with multiple specificities, there was also a correlation found between the increase in autoantibodies (e.g. ACPA) and pro-inflammatory cytokines such as TNF and IFN-γ in the serum of patients¹⁷. Immunogenetic studies have shown that 90% of the RA patients who are ACPA positive (70-80%) also share an HLA class-II epitope in the DRB1 chain (HLA-DRB1 *0101, *0401, *0404). This so-called shared epitope increases the risk of developing RA and is also associated with ACPAs; shared epitope-positive patients are predisposed to having ACPAs^{18,19}. Feitsma *et al* identified two HLA-DRB1 restricted CD4⁺ T cell clones that recognized citrullinated vimentin and were also present in the inflamed joint of RA patients. This indicates that CD4⁺ T cells can respond to naturally processed epitopes from an autoantigen¹⁸. The finding that ACPAs were present in inflamed joints of patients but not in the joints of healthy individuals, together with the discovery that citrullinated autoantigen specific CD4⁺ T cells were only found in PBMCs from RA patients, suggests that both the ACPAs and these CD4⁺ T cells play a significant role in the pathogenesis of RA^{19,20}. Scally *et al* (and others) provide molecular evidence on how CD4⁺ T cells are able to recognize citrullinated antigens²¹⁻²³. They also showed that in the autoantigen recognizing CD4⁺ T cell population of HLA-DRB1*04:01⁺ RA patients, the percentage Tregs (both activated and resting) was reduced, whereas the populations of naïve and effector memory CD4⁺ T cells were increased compared to healthy subjects²¹. These results indicate that citrullinated peptides are (one of the) autoantigens in RA but it does not provide proof that they are causal autoantigens. Next to citrullinated peptides, there are other peptides which are found to be present in RA for example peptides from heat shock proteins (HSPs). HSPs are highly expressed on sites of

inflammation and are evolutionary conserved, which has caused considerable sequence similarities between microbial and mammalian homologs²². Also they have been found to be present in synovial fluid from RA patients²⁴⁻²⁶. Since HSPs are generally produced under conditions of inflammation, they are general antigens and thus potential targets for therapy. This will be discussed in further detail in the section *HSPs as surrogate autoantigens for autoimmunity*.

Pathogenesis of Rheumatoid arthritis

The precise mechanisms that trigger immunity against self-peptides are unknown. Some studies however have shown that together with the shared epitope, smoking is a risk factor for the development of ACPA positive RA^{27,28}. The particles in the smoke possibly trigger toll like receptor (TLR) activation and increase the expression of peptidyl-arginine deiminases (PADs)²⁷. PADs are associated with the presence of citrullinated peptides and were found in the lungs of both RA patients and healthy smokers²⁹. The amount of citrullinated peptides in healthy non-smokers was significantly lower. Furthermore, particles present in smoke can activate local APCs and trigger T cell activation to self-antigen. These CD4⁺ T cells in turn are able to activate B cells which differentiate into plasma cells and start producing autoantibodies such as ACPA. Thus, it is possible that the initiation of RA starts in the lungs. But how do these inflammatory responses target the joints specifically? Research shows that ACPA against citrullinated vimentin are able to induce osteoclast differentiation and bone resorption³⁰. The citrullinated vimentin ACPA induce tumor necrosis factor (TNF) production by osteoclast precursors. TNF in turn stimulates the differentiation into osteoclasts and therefore the induction of bone resorption³⁰. Next to ACPA, initiation of innate immune responses triggers also the production of pro-inflammatory cytokines such as TNF. Moreover, immunocomplexes from ACPA with citrullinated peptides can be recognized by APCs (e.g. macrophages) which triggers the production of TNF and IL-6, cytokines that are regularly found in RA patients³¹. These pro-inflammatory cytokines recruit more immune cells to migrate to the synovium. Next to recruitment of immune cells, pro-inflammatory cytokines such as TNF and IL-1 can activate fibroblast-like synoviocytes. The synovium in a joint is built up from two layers: the outer layer (subintima) and the inner layer (intima). About 33% of the intima consists of fibroblast-like synoviocytes and specialized macrophages. In normal tissue, fibroblast-like synoviocytes have a barrier function and produce lubricating molecules for efficient movement of the joint³². In a (pre) rheumatic joint, these cells express matrixmetalloproteases (MMPs) after activation by pro-inflammatory cytokines. The MMPs consecutively degrade extracellular matrix components which causes cartilage destruction³³. This together with the inflammatory reactions in the joint can cause severe pain and joint demolition.

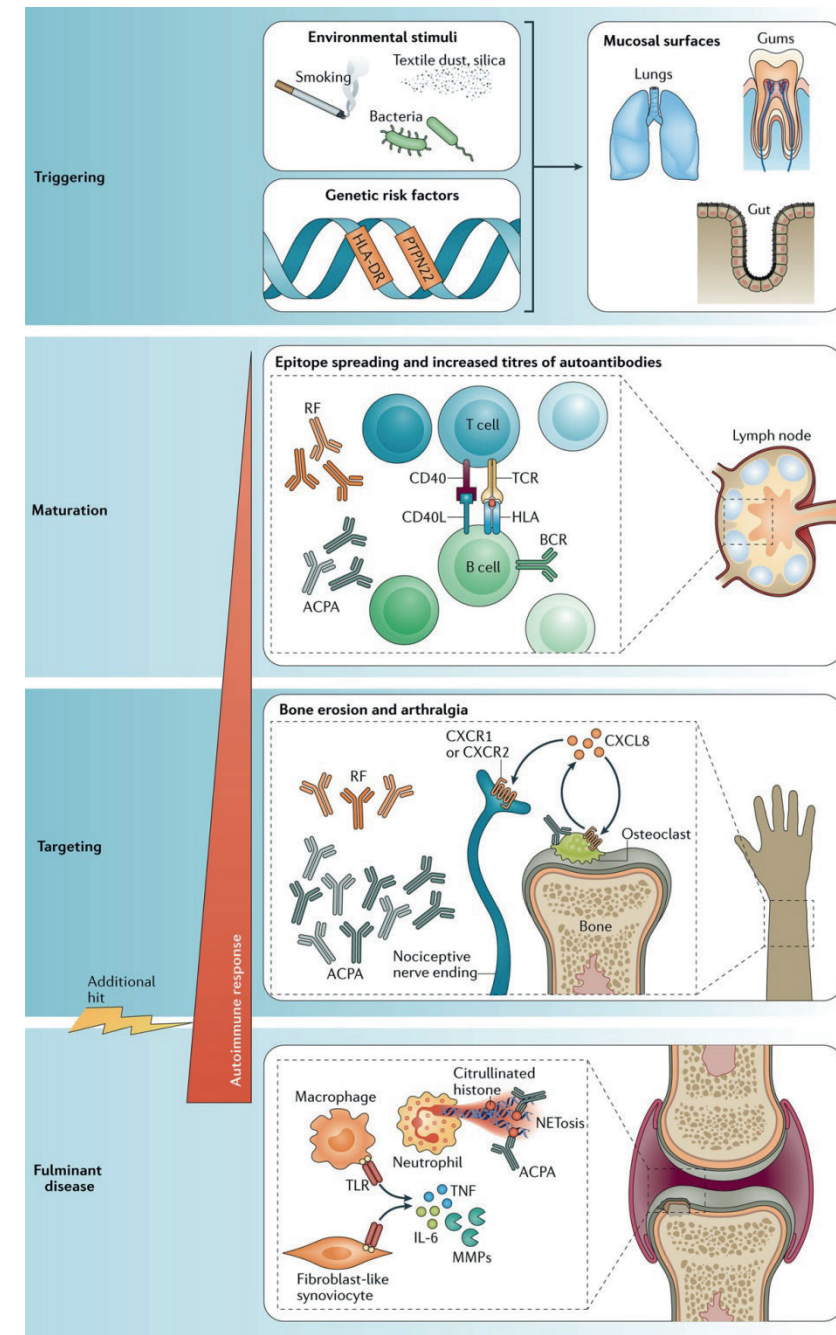


Figure 1. Pathogenesis of seropositive Rheumatoid arthritis
 Adapted from Malmström, Catrina & Klareskog. *The immunopathogenesis of seropositive rheumatoid arthritis: from triggering to targeting*. Nat Rev Immunol. 2017 Jan;17(1):60-75. doi: 10.1038/nri.2016.124.

Treatment of Rheumatoid arthritis

Although a lot is known about the pathogenesis of RA, the knowledge about relevant autoantigen(s) is insufficient. Citrullinated peptides seem a candidate but only 70-80% of the RA patients has autoantibodies against these peptides. Since the pathogenesis is not completely elucidated, current medication is directed towards a relief of symptoms rather than a cure. Nonsteroidal anti-inflammatory drugs (NSAIDs) are the most commonly used drugs for pain relief. These drugs inhibit the biosynthesis of prostaglandins by blocking the activation enzyme cyclooxygenase (COX). This happens at sites of inflammation but also in other tissues causing adverse effects³⁴. Disease-modifying anti-rheumatic drugs (DMARDs) non-specifically target the immune inflammatory response, and thus reduce swelling of the joints and pain. Methotrexate is the most commonly used DMARD in RA patients³⁵. Next to NSAIDs and DMARDs, biological therapeutics have been developed to target the inflammatory responses. Most biological agents are directed against pro-inflammatory cytokines TNF and IL-6, since they are known to play a role in RA (as discussed above in *Pathogenesis of Rheumatoid arthritis*). These biological agents consist mainly of antibodies (e.g. Etanercept, Infliximab, Tocilizumab) which prevent binding of the cytokine (e.g. TNF or IL-6) to the receptor³⁶.

Although these antibodies have proven to be effective, the antibodies hamper the inflammation at protein level. Inhibiting the production of these cytokines at RNA level would be more efficient and long-lasting, with the result that patients need fewer injections than with antibody treatment. However, delivering small interfering RNA (siRNA) across the cell membrane has proven to be difficult. Therefore, drug delivery systems such as nanoparticles are needed. The siRNA can be packaged within these nanoparticles and transferred across the cell membrane to be delivered inside the cell. Several types of nanoparticles can be used as drug delivery systems. Poly-lactic-co-glycolic acid (PLGA) nanoparticles are known to have a high loading capacity and are biodegradable³⁷. Furthermore, they were shown to sustain a gradual release of siRNA for two months *in vitro*. It has already been shown that the administration of nanoparticles can modulate the immune response. PLGA nanoparticles enhanced the expression of RALDH enzymes in DCs *in vitro*, which resulted in induction of FoxP3⁺ Tregs³⁸. After intranasal delivery in a mouse, the FoxP3 expression in local lymphoid tissue was increased³⁹. Recently, lipid-polymer hybrid nanoparticles were developed since it has been shown that the immunogenicity of these particles is lower compared to the more established PLGA nanoparticles^{40,41}. These nanoparticles are a promising drug delivery system for the induction of immune tolerance since the particles as such do not induce cytotoxicity or activation of the immune system *in vitro*. However, more research is needed to establish a therapy with nanoparticles.

Tolerogenic dendritic cells as a therapeutic tool

Instead of dampening inflammation with drugs, restoration of immune tolerance is a promising therapeutic way of relieving patients of their inflammatory symptoms. One method to achieve this is by using tolerogenic dendritic cells (toDCs). Dendritic cells (DCs) are a heterogeneous family of professional antigen-presenting cells that can be classified on the basis of their ontogeny, surface marker expression profile and anatomical location (reviewed in ⁴²). DCs are as important for the induction of effective immunity against invading pathogens as they are for the maintenance of immune tolerance. Patients with primary immunodeficiency with mutations in GATA2 have defective DC function, resulting in enhanced susceptibility not only to infection and cancer, but also to autoimmune conditions, most likely due to a reduction in Tregs⁴³. The role of DCs in instigating immunity versus tolerance is largely determined by their maturation status. Under steady-state conditions, tissue DCs are immature, expressing low levels of MHC class II and co-stimulatory molecules; their 'default' setting is to induce tolerance. These immature DCs can become immunogenic when they sense pathogen-associated molecular patterns and danger-associated molecular patterns via pattern recognition receptors. These include Toll-like receptors, retinoic-acid-inducible gene I-like receptors, and nucleotide-binding oligomerization domain-like receptors. Pattern recognition receptor mediated signaling plays a central role in the maturation process that DCs need to undergo to acquire potent T-cell stimulatory properties⁴⁴. Fully matured DCs express high levels of MHC class II, co-stimulatory markers (e.g. CD86) and pro-inflammatory cytokines (e.g. IL-12p70, IL-23, tumor necrosis factor), all required for the efficient induction of T effector cell responses. Furthermore, during DC maturation the expression of chemokine receptors is modulated (e.g. CCR5 is down-regulated and CCR7 is up-regulated) enabling DC migration towards lymphoid tissues to present antigen to naive T cells. However, the outcome of maturation of DCs is not always the generation of DCs with immunogenic properties. Certain danger-associated molecular patterns and immune suppressive compounds have been shown to drive the maturation of DCs with tolerogenic properties (i.e. toIDCs)⁴⁵⁻⁴⁸. These toIDCs may be phenotypically mature (i.e. high levels of MHC class II and co-stimulatory molecules), but may express co-inhibitory molecules [e.g. programmed death ligand 1 (PD-L1), PD-L2, immunoglobulin-like transcript 3], lack expression of pro-inflammatory cytokines and instead produce immunosuppressive cytokines and compounds (e.g. IL-10, TGF- β , IDO). The maturation status of these DC has been referred to as 'semi-mature'. Thus, there is plasticity with regard to the functional maturation of DC, and the environmental cues that DC receive during the maturation process determines whether they become immunogenic or tolerogenic.

DCs are able to mediate tolerance via several mechanisms. They can induce iTregs through, for example, membrane-bound PD-L1, which blocks the Akt/mTOR pathway to preferentially stimulate naive T cells to become iTregs⁴⁹. Furthermore, PD-L1 and PD-L2 provide inhibitory signals to both CD8⁺ and CD4⁺ T cells which drives the T cell into a state of tolerance⁴⁹. Secreted compounds such as IL-10, IL-27, TGF- β , retinoic acid and IDO, can convert naive T cells into iTregs. DC can also promote T cell tolerance through T cell killing, and the induction of T-cell hyporesponsiveness (anergy)^{50,51}.

The importance of DC in maintaining immune tolerance has led to exploring the therapeutic use of DC. Various ways have been described to create DC with stable tolerogenic properties, called tolDCs. The tolerogenic properties of these in vitro generated tolDCs depend on the specific method used (reviewed in ⁵²). For example, tolDCs generated with the immunosuppressive agents dexamethasone and/or the active form of Vitamin D3 (1 α ,25-Dihydroxyvitamin D3) are characterized by a semi-mature phenotype, with high levels of MHC II, intermediate levels of co-stimulatory molecules, low levels of pro-inflammatory cytokines and high levels of immunosuppressive cytokines IL-10 and TGF- β ⁵³⁻⁵⁷. TolDCs can also be genetically engineered, for example through the transduction of immunosuppressive or pro-apoptotic molecules (e.g. IL-10, CTLA-4, FasL) or silencing of immunostimulatory molecules (e.g. CD80/CD86, IL-12) (Reviewed in ⁵⁸). These different types of tolDCs have been shown to reduce or prevent autoimmune diseases or transplant rejection in animal models, providing important proof of principle evidence that these cells can be applied therapeutically⁵⁷⁻⁶². Their therapeutic benefit is associated with a reduction of pro-inflammatory effector T cells and NK cells, and the induction of regulatory T-cells or IL-10-producing T cells^{57,58,63-65}.

Efforts have been made to translate these findings from animal studies to the clinical setting. Good Manufacturing Protocols to generate tolDCs from human donor cells have been developed^{56,66}, and methods to preserve the tolDCs and reduce the production costs are being explored⁵⁸. Since there are diverse methods of generating tolDCs and other types of tolerogenic APC (tolAPC), a minimal information model for tolAPC (MITAP) was generated. MITAP enables researchers to report their data in a standardized and more transparent manner, facilitating data comparison and interpretation, ultimately paving the way for the development of standardized protocols for the production of tolDCs and other tolAPC for therapeutic application⁶⁷. A number of tolDCs have been tested in phase I clinical trials, including for type I diabetes⁵⁹, Crohn's disease⁶⁸ and rheumatoid arthritis^{69,70}. Encouragingly, tolDCs therapy in all these studies was found to be feasible and safe, providing rationale to conduct further studies into their efficacy.

The problem of targeting autoantigen(s) – which ones?

One of the main advantages of tolDC therapy is the specific targeting of pathogenic immune responses. Many of the drugs that are currently used to treat autoimmune diseases are non-antigen specific, leading to general immunosuppression. With tolDCs autoreactive T cells can, theoretically, be exclusively targeted. But how to achieve this is still a debate. A number of studies have provided clear evidence that tolDCs need to be loaded with a disease-relevant antigen to exert their beneficial immune modulatory action. Loading of tolDCs with type II collagen was required, for example, for antigen-specific disease remission in the collagen-induced arthritis model^{57,71,72}. More recent research shows that this is also applicable in other autoimmune diseases⁷³. Furthermore, when comparing the therapeutic action of unloaded tolDCs and tolDCs loaded with a disease relevant peptide (MOG40-55) in the experimental autoimmune encephalomyelitis (EAE) model, Mansilla *et al* showed that although the unloaded tolDCs inhibited disease symptoms, the MOG40-55 loaded tolDCs diminished disease even more⁷⁴. In contrast, other studies have shown that disease remission can be established when administering unloaded tolDCs^{75,76}. This may suggest that tolDCs are able to take up the relevant antigen *in vivo*. It has been hypothesized that unloaded tolDCs induce T cell anergy rather than promoting Tregs. These anergic T cells might be capable of suppressing excessive Th17 and Th1 responses⁷⁷. Non-antigen-pulsed tolDCs might also induce regulatory populations that do not require an antigen. For instance, B cells can be converted into Bregs partly through the production of retinoic acid by the tolDC⁷⁸. However, if these non-antigen-pulsed tolDCs are able to take up antigen *in vivo*, one has to consider the safety of these tolDCs, since it is possible that the non-antigen-pulsed tolDCs also take up other antigens that should not be targeted.

Nonetheless, if tolDCs need to be loaded with antigen(s) prior to infusion, a remaining problem is the question of which antigen to use, and in what form. In many autoimmune diseases, including RA, the knowledge about the relevant autoantigen(s) involved is insufficient. Moreover, even if some of the relevant autoantigens are known, as is the case for multiple sclerosis (MS), the problem of HLA diversity remains⁷³. Some peptides (e.g. proteolipid protein) that have been shown to be involved in the pathogenesis of MS are restricted to a specific HLA-class (e.g. HLA-DQB1*0602), making it more difficult to standardize the peptides used for all MS patients⁷⁹. For RA, no universal autoantigen exists. Several candidate self-proteins have been described in relation to the pathogenesis of this disease. Epitopes from joint-derived antigens such as collagen type II (CII) and human cartilage-derived glycoprotein HCgp39 are presented by DCs and macrophages to T cells in inflamed joints of RA patients⁸⁰. Furthermore, the endoplasmic reticulum

(ER) stress-associated protein GRP78/BiP is described as a potential autoantigen. The ER stress response is increased in RA synovial tissue and fluid and the ER chaperone, GRP78, is important for synoviocyte proliferation and angiogenesis, which are substantial indicators of RA⁸¹.

Posttranslational modifications may also be important in generating novel epitopes that trigger autoimmunity. Anti-citrullinated peptide antibodies (ACPAs) are found in sera of 70-80% of RA patients⁸². To test if citrullinated antigens are good candidates for an immunomodulatory therapy, a phase I clinical trial was performed. In this study autologous *in vitro* generated tolDCs were exposed to citrullinated autoantigenic epitopes and administered intradermally into patients⁶⁹. The trial showed that the DC vaccination was safe and indicated an anti-inflammatory effect after DC administration. However, using citrullinated peptides has the consequence that therapy is limited to patients with HLA-DRB1 (*0101, *0401, *0404) and it is unknown if the reactivity in these patients is similar. A different approach was taken in the phase I safety trial in patients with rheumatoid and inflammatory arthritis⁷⁰. TolDCs were loaded with autologous synovial fluid; the rationale being that this fluid contains relevant joint-associated antigens. The downside of this approach is that it is not always possible to obtain sufficient synovial fluid from RA patients for tolDC loading. Furthermore, as the antigens are unknown, it is difficult to monitor changes in the antigen-specific T cell response after tolDC administration.

The use of surrogate autoantigens could be a preferred option for the loading of tolDCs. Possible candidates are heat shock proteins (HSPs). HSPs are typically intracellular proteins, with no peptide leader sequences that can target secretion. However, there is evidence that HSP can have access to the extracellular milieu, either by passive or active mechanisms. Both the endogenous upregulation of HSP with so-called HSP co-inducers and the exogenous administration of (recombinant) HSP have led to immunomodulatory effects in various models of experimental autoimmunity^{22,83,84}. Therefore, HSPs could be used as surrogate autoantigen not only for RA but also for other auto-immune diseases.

HSPs as surrogate autoantigens for autoimmunity

The main function of HSPs is to support folding and transport of a large variety of (misfolded) proteins as intracellular molecular chaperones. Their expression can be significantly upregulated under conditions of stress like fever, viral infection, nutritional deficiency, cold and exposure to the pro-inflammatory cytokines IFN- γ

and TNF⁸⁵⁻⁸⁷. Generally, HSPs can be classified into different families based on their monomeric molecular weight (HSP10, HSP20-30, HSP40, HSP60, HSP70, HSP90 and HSP100 families). Some HSP family members (e.g. HSP60 and HSP70) are highly conserved throughout evolution, resulting in immunological cross-recognition of certain mammalian and microbial HSP homologues.

Initial observations that ignited studies on the role of HSPs in autoimmunity were made in the mycobacteria-induced adjuvant arthritis model in rats. Generated mycobacteria-specific T cell lines were shown to have arthritogenic potential⁸⁸ and it was later discovered that HSP60 was the antigen recognized by the mycobacteria-specific T cell lines⁸⁹. Further studies followed showing that synovial fluid cells and peripheral blood mononuclear cells of chronic inflammatory arthritis patients could also respond to mycobacterial HSP60. In contrast, HSP60 responses were absent in control subjects⁹⁰. Moreover, monoclonal antibodies recognizing mammalian HSP60 were produced and it was found that HSP60 was expressed in synovial membranes of patients with chronic arthritis^{91,92}. Similar results were found for the HSP family members HSP40 and HSP70. Synovial fluid and peripheral blood T cells of RA patients could recognize a bacterial variant of HSP40, but healthy subjects or disease controls could not⁹³. In addition, the human homologues of HSP40 and HSP70 were found to be overexpressed in the synovial lining of the joints of RA patients^{24,25}.

Interestingly, numerous experimental animal models and even a few clinical trials have shown that treatment with (myco)bacterial HSPs can induce HSP-specific anti-inflammatory T cell responses. Experimental autoimmune disease models in both rat and mouse showed significantly reduced arthritis severity after prophylactic immunization with mycobacterial HSP60 or HSP70^{94,95}. Although the exact mechanism for disease amelioration is still not completely understood, suppression of arthritis is likely induced by IL-10 producing Tregs⁹⁵⁻⁹⁸. One possible explanation for the propagation and/or induction of a regulatory phenotype in HSP60/70-specific T cells lies in the high homology between the bacterial and mammalian variants of the HSP proteins. Even though HSPs are considered immunogenic - microbial HSP60, for example, has been known as the so-called 'common antigen of gram negatives' already before its molecular definition⁹⁹ - the highly conserved parts of the proteins could induce a tolerogenic response as these can be recognized as self-antigens by the body's own immune system¹⁰⁰. Moreover, since bacterial HSPs are mostly encountered in the tolerizing gut or lung mucosa, conserved and thus repeatedly encountered HSP antigens are more likely to obtain a regulatory phenotype. In addition to conservation and microbial-self cross-recognition, HSP70 family members are directly involved with antigen processing and consequently,

HSP70 fragments were found to be one of the most frequent cytosolic MHCII natural ligand sources¹⁰¹⁻¹⁰³. Presentation of HSP70 peptides may therefore be part of the earlier mentioned default tolerant state of the immune system, where MHCII presented HSP peptides are part of a continuous and credible target for Tregs. It is, however, important to keep in mind that in a dysregulated immune system like seen in patients with autoimmune diseases, antigens that would normally induce an anti-inflammatory immune response, could now potentially induce a pro-inflammatory response.

Since the HSPs used for the previous described experiments are from bacterial origin and can potentially induce an unwanted anti-inflammatory response towards these bacteria, a safer form of the HSPs is needed. One way to accomplish this is to use bacterial HSP-derived peptides that show high homology with the mammalian variant. The high homology to the self-antigen will prevent unwanted responses towards the bacteria and at the same time ensure cross-reactivity with the mammalian HSPs presented in the inflamed joint. Indeed, two of the three clinical trials using HSPs as therapy were performed with HSP-derived peptides. A pilot phase II trial using a HSP40-derived peptide, dnaJP1; which also contains the 'shared epitope'¹⁰⁴, was tested in juvenile idiopathic arthritis (JIA) patients. After oral administration of the dnaJP1, a change from a pro-inflammatory to a tolerogenic T cell response to dnaJP1 could be observed^{105,106}. In a second phase II trial, an HSP60-derived peptide, DiaPep277, was used to treat patients with type I diabetes. It was found that DiaPep277 was safe and showed a trend towards a greater preservation of beta-cell function as compared to controls^{107,108}. In a third recent trial, a mammalian HSP70 family member, BiP, was tested in RA patients. In this case, whole protein was administered intravenously. The results of this phase I/II safety trial showed no serious adverse drug reactions. Moreover, at the higher treatment doses disease remissions were seen in some cases¹⁰⁹.

As discussed earlier, one potential disadvantage of using peptides is HLA diversity in patients. Consequently, HSP peptides need to either 1) be able to bind multiple HLA-DR molecules, including the RA associated HLA-DRB1 *0101, *0401, *0404 molecules, or 2) a peptide pool of several HSP peptides able to bind one or more of the RA associated HLA-DR molecules needs to be administered. For HSP60 and HSP70 several pan-DR peptides have been discovered. Kamphuis *et al* used a computer algorithm to identify both self and bacterial HSP60 peptides able to bind a number of distinct HLA-DR haplotypes. They found several peptides that were able to bind the major RA/JIA-associated HLA-DR molecules and T cells from both JIA and RA patients were able to respond to five out of eight peptides^{110,111}.

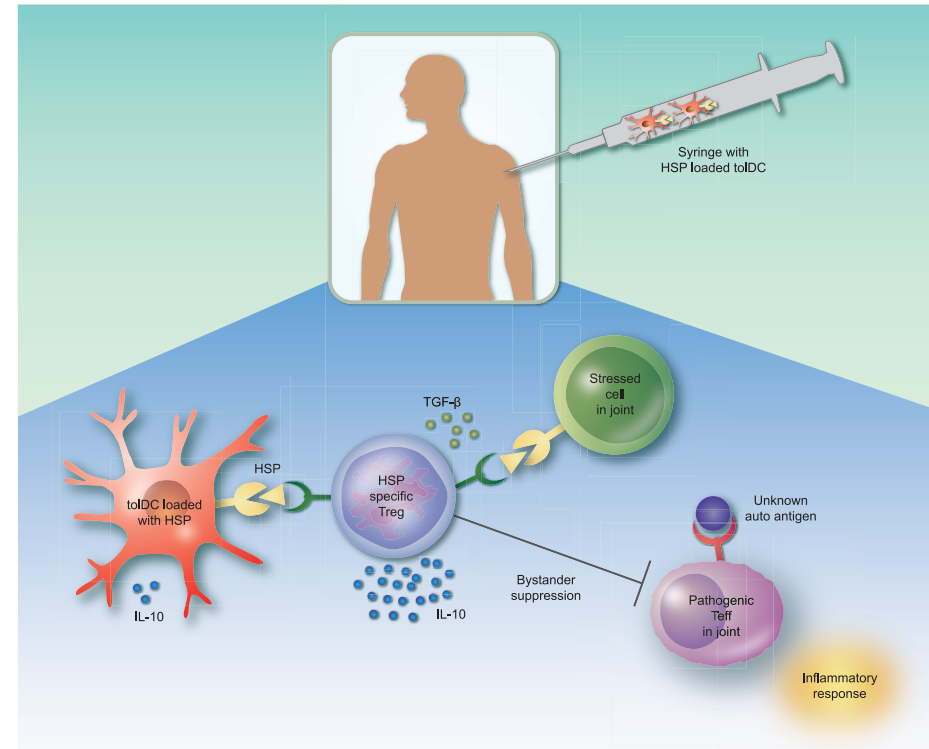


Figure 2. Heat-shock protein (HSP) loaded tolerogenic dendritic cell (toIDC) vaccination in rheumatoid arthritis (RA). This figure depicts the potential process that takes place in the patient's joint after injection with HSP loaded toIDCs. ToIDCs produce anti-inflammatory cytokines [e.g. interleukin-10 (IL-10)] and present epitopes of HSP to naive CD4⁺ T cells. These CD4⁺ T cells differentiate into HSP-specific regulatory T (Treg) cells and suppress stressed (HSP expressing) cells via immunomodulatory cytokines like IL-10 and transforming growth factor-β (TGF-β). Furthermore, bystander suppression could lead to suppression of pathogenic effector T (Teff) cells recognizing the unknown autoantigen, thereby inhibiting inflammatory symptoms. The presence of self HSP in the synovial fluid of RA patients might favor the selection of the generation of Tregs and their function.

In addition, de Wolf *et al* showed that an HSP70 peptide, B29, also binds multiple HLA-DR molecules. They concluded that more than 80% of human individuals can present B29 to their T cells (and among RA patients possibly even more due to high presence of HLA-DRB1 *0401). In subsequent cultures they showed that 10 out of 14 healthy individuals could respond to the peptide¹¹². The B29 peptide was earlier tested in a mouse model of arthritis and it was found that prophylactic intranasal administration of B29 could suppress disease. Moreover, CD4⁺CD25⁺T cells from B29 immunized mice could decrease disease severity in recipient arthritic mice, indicating that B29-specific Tregs are effective in diminishing autoimmune arthritis¹⁰³. Next

to the Treg inducing potential of B29, bone marrow derived dendritic cells pulsed with Mycobacterium tuberculosis (Mt) or mouse HSP70 induced IL-10 production in antigen-specific T cells and suppressed arthritis showing that HSP70 loading of DCs by itself is tolerizing¹¹³.

In order to make both tolDC therapy and HSP peptide treatment in autoimmune diseases (e.g. RA) as potent as possible, a combination therapy could be the solution. Pulsing tolDCs with HSP peptides could 1) solve the autoantigen problem and 2) the HSP peptides will be targeted to the HSP-specific T cells by DC with stable tolerogenic function, making sure a regulatory response towards the antigen is induced.

Outline and aim of this thesis

The research in this thesis explores therapeutic possibilities to treat RA. In **chapter 2** we describe the production of a T cell receptor (TCR) transgenic mouse to be able to study primary antigen (B29) specific CD4⁺ T cell responses both *in vitro* and *in vivo*. B29 is a peptide of heat shock protein 70 and a potential candidate for an alternative antigen in RA therapies since it has been described to have anti-inflammatory properties in a murine model for arthritis¹⁰³. In **chapter 3**, we investigate how tolerogenic dendritic cells loaded with B29 or human proteoglycan (hPG) influence the activation of CD4⁺ T cells. We show that tolDCs steer CD4⁺ T cells into an immune tolerant state and that these tolDCs, provided that they are stimulated with a maturation stimulus, are able to suppress arthritis in a murine arthritis model. Furthermore, in **chapter 4** we investigated the effects of human tolDCs on CD4⁺ T cells and the responsiveness of RA patients against HSP.

Next to tolDCs, we studied another potentially effective treatment for RA. As discussed, siRNA against TNF can be used to suppress excessive inflammation. However, the problem is delivering the siRNA across the cell membrane. In **chapter 5** we show that when encapsulating siRNA against TNF in lipid-polymer hybrid particles (LPNs) or stable nucleic acid lipidoid particles (SNALPs), the siRNA can be effectively delivered into macrophages. Furthermore, we tested these nanoparticles in the *in vivo* arthritis model to investigate if TNF siRNA encapsulated by LPNs or SNALPs suppress arthritic symptoms after local administration.

The research in **chapter 6** describes alternative routes of vaccine delivery. For most vaccines intramuscular administration is standard. However, for tolDCs the intradermal route might be a more suitable possibility. For nanoparticle

administration, next to local injections, tolerant routes (e.g. intranasal) could be an option. In order to know if these different routes of vaccination affect the outcome on immunization, we investigated which immune cells are involved after intranasal or intradermal administration of a model vaccine.

The results reported in this thesis are summarized and discussed in **chapter 7** in the context of current knowledge and future perspectives in the field of immune modulation and autoimmune diseases.

Part of this chapter is published in Immunology

Jansen MAA, Spiering R, Broere F, van Laar JM, Isaacs JD, van Eden W, Hilkens CMU. Targeting of tolerogenic dendritic cells towards heat-shock proteins: a novel therapeutic strategy for autoimmune diseases? *Immunology*. 2018 Jan;153(1):51-59. doi: 10.1111/imm.12811.



References

1. Cooper GS, Bynum ML, Somers EC. Recent insights in the epidemiology of autoimmune diseases: Improved prevalence estimates and understanding of clustering of diseases. *J Autoimmun.* 2009;33(3-4):197-207. doi: 10.1016/j.jaut.2009.09.008 [doi].
2. Lerner A, Jeremias P, Matthias T. The world incidence and prevalence of autoimmune diseases is increasing. *International Journal of Celiac Disease.* 2015;3:151-155.
3. Apostolou I, von Boehmer H. In vivo instruction of suppressor commitment in naive T cells. *J Exp Med.* 2004;199(10):1401-1408. doi: 10.1084/jem.20040249 [doi].
4. Fontenot JD, Gavin MA, Rudensky AY. Foxp3 programs the development and function of CD4+CD25+ regulatory T cells. *Nat Immunol.* 2003;4(4):330-336. doi: 10.1038/ni904 [doi].
5. Wing K, Onishi Y, Prieto-Martin P, et al. CTLA-4 control over Foxp3+ regulatory T cell function. *Science.* 2008;322(5899):271-275. doi: 10.1126/science.1160062 [doi].
6. Li MO, Wan YY, Flavell RA. T cell-produced transforming growth factor-beta1 controls T cell tolerance and regulates Th1- and Th17-cell differentiation. *Immunity.* 2007;26(5):579-591. doi: S1074-7613(07)00246-4 [pii].
7. Rubtsov YP, Rasmussen JP, Chi EY, et al. Regulatory T cell-derived interleukin-10 limits inflammation at environmental interfaces. *Immunity.* 2008;28(4):546-558. doi: 10.1016/j.immuni.2008.02.017 [doi].
8. Cao X, Cai SF, Fehniger TA, et al. Granzyme B and perforin are important for regulatory T cell-mediated suppression of tumor clearance. *Immunity.* 2007;27(4):635-646. doi: S1074-7613(07)00444-X [pii].
9. Lawson CA, Brown AK, Bejarano V, et al. Early rheumatoid arthritis is associated with a deficit in the CD4+CD25high regulatory T cell population in peripheral blood. *Rheumatology (Oxford).* 2006;45(10):1210-1217. doi: kel089 [pii].
10. Xiao H, Wang S, Miao R, Kan W. TRAIL is associated with impaired regulation of CD4+CD25- T cells by regulatory T cells in patients with rheumatoid arthritis. *J Clin Immunol.* 2011;31(6):1112-1119. doi: 10.1007/s10875-011-9559-x [doi].
11. Liu MF, Wang CR, Fung LL, Lin LH, Tsai CN. The presence of cytokine-suppressive CD4+CD25+ T cells in the peripheral blood and synovial fluid of patients with rheumatoid arthritis. *Scand J Immunol.* 2005;62(3):312-317. doi: SJI1656 [pii].
12. Wang T, Sun X, Zhao J, et al. Regulatory T cells in rheumatoid arthritis showed increased plasticity toward Th17 but retained suppressive function in peripheral blood. *Ann Rheum Dis.* 2015;74(6):1293-1301. doi: 10.1136/annrheumdis-2013-204228 [doi].
13. van Amelsfort JM, Jacobs KM, Bijlsma JW, Lafeber FP, Taams LS. CD4(+)/CD25(+) regulatory T cells in rheumatoid arthritis: Differences in the presence, phenotype, and function between peripheral blood and synovial fluid. *Arthritis Rheum.* 2004;50(9):2775-2785. doi: 10.1002/art.20499 [doi].
14. Ehrenstein MR, Evans JG, Singh A, et al. Compromised function of regulatory T cells in rheumatoid arthritis and reversal by anti-TNFalpha therapy. *J Exp Med.* 2004;200(3):277-285. doi: 10.1084/jem.20040165 [doi].
15. Herrath J, Muller M, Amoudruz P, et al. The inflammatory milieu in the rheumatic joint reduces regulatory T-cell function. *Eur J Immunol.* 2011;41(8):2279-2290. doi: 10.1002/eji.201041004 [doi].
16. van der Woude D, Rantapaa-Dahlqvist S, Ioan-Facsinay A, et al. Epitope spreading of the anti-citrullinated protein antibody response occurs before disease onset and is associated with the disease course of early arthritis. *Ann Rheum Dis.* 2010;69(8):1554-1561. doi: 10.1136/ard.2009.124537 [doi].
17. Sokolove J, Bromberg R, Deane KD, et al. Autoantibody epitope spreading in the pre-clinical phase predicts progression to rheumatoid arthritis. *PLoS One.* 2012;7(5):e35296. doi: 10.1371/journal.pone.0035296 [doi].
18. Feitsma AL, van der Voort EI, Franken KL, et al. Identification of citrullinated vimentin peptides as T cell epitopes in HLA-DR4-positive patients with rheumatoid arthritis. *Arthritis Rheum.* 2010;62(1):117-125. doi: 10.1002/art.25059 [doi].
19. von Delwig A, Locke J, Robinson JH, Ng WF. Response of Th17 cells to a citrullinated arthritogenic aggrecan peptide in patients with rheumatoid arthritis. *Arthritis Rheum.* 2010;62(1):143-149. doi: 10.1002/art.25064 [doi].
20. Snir O, Rieck M, Gebe JA, et al. Identification and functional characterization of T cells reactive to citrullinated vimentin in HLA-DRB1*0401-positive humanized mice and rheumatoid arthritis patients. *Arthritis Rheum.* 2011;63(10):2873-2883. doi: 10.1002/art.30445 [doi].
21. Scally SW, Petersen J, Law SC, et al. A molecular basis for the association of the HLA-DRB1 locus, citrullination, and rheumatoid arthritis. *J Exp Med.* 2013;210(12):2569-2582. doi: 10.1084/jem.20131241 [doi].
22. van Eden W, van Herwijnen M, Wagenaar J, van Kooten P, Broere F, van der Zee R. Stress proteins are used by the immune system for cognate interactions with anti-inflammatory regulatory T cells. *FEBS Lett.* 2013;587(13):1951-1958. doi: 10.1016/j.febslet.2013.05.024 [doi].
23. James EA, Rieck M, Pieper J, et al. Citrulline-specific Th1 cells are increased in rheumatoid arthritis and their frequency is influenced by disease duration and therapy. *Arthritis Rheumatol.* 2014;66(7):1712-1722. doi: 10.1002/art.38637 [doi].
24. Schett G, Redlich K, Xu Q, et al. Enhanced expression of heat shock protein 70 (hsp70) and heat shock factor 1 (HSF1) activation in rheumatoid arthritis synovial tissue. differential regulation of hsp70 expression and hsf1 activation in synovial fibroblasts by proinflammatory cytokines, shear stress, and antiinflammatory drugs. *J Clin Invest.* 1998;102(2):302-311. doi: 10.1172/JCI2465 [doi].
25. Kurzik-Dumke U, Schick C, Rzepka R, Melchers I. Overexpression of human homologs of the bacterial DnaJ chaperone in the synovial tissue of patients with rheumatoid arthritis. *Arthritis Rheum.* 1999;42(2):210-220. doi: 10.1002/1529-0131(199902)42:2<30.CO;2-U [doi].
26. Martin CA, Carsons SE, Kowalewski R, Bernstein D, Valentino M, Santiago-Schwarz F. Aberrant extracellular and dendritic cell (DC) surface expression of heat shock protein (hsp)70 in the rheumatoid joint: Possible mechanisms of hsp/DC-mediated cross-priming. *J Immunol.* 2003;171(11):5736-5742.
27. Padyukov L, Silva C, Stolt P, Alfredsson L, Klareskog L. A gene-environment interaction between smoking and shared epitope genes in HLA-DR provides a high risk of seropositive rheumatoid arthritis. *Arthritis Rheum.* 2004;50(10):3085-3092. doi: 10.1002/art.20553 [doi].
28. Di Giuseppe D, Discacciati A, Orsini N, Wolk A. Cigarette smoking and risk of rheumatoid arthritis: A dose-response meta-analysis. *Arthritis Res Ther.* 2014;16(2):R61. doi: 10.1186/ar4498 [doi].
29. Makrygiannakis D, Hermansson M, Ulfgren AK, et al. Smoking increases peptidylarginine deiminase 2 enzyme expression in human lungs and increases citrullination in BAL cells. *Ann Rheum Dis.* 2008;67(10):1488-1492. doi: 10.1136/ard.2007.075192 [doi].
30. Harre U, Georgess D, Bang H, et al. Induction of osteoclastogenesis and bone loss by human autoantibodies against citrullinated vimentin. *J Clin Invest.* 2012;122(5):1791-1802. doi: 10.1172/JCI60975 [doi].
31. Sokolove J, Zhao X, Chandra PE, Robinson WH. Immune complexes containing citrullinated fibrinogen costimulate macrophages via toll-like receptor 4 and fcgamma receptor. *Arthritis Rheum.* 2011;63(1):53-62. doi: 10.1002/art.30081 [doi].
32. Ospelt C, Pap T, Gay S. Synovial fibroblasts: Important players in the induction of inflammation and joint destruction. *Rheumatoid arthritis.* 2009:136-150.

33. Pap T, Muller-Ladner U, Gay RE, Gay S. Fibroblast biology. role of synovial fibroblasts in the pathogenesis of rheumatoid arthritis. *Arthritis Res*. 2000;2(5):361-367. doi: 10.1186/ar113 [doi].
34. Crofford LJ. Use of NSAIDs in treating patients with arthritis. *Arthritis Res Ther*. 2013;15 Suppl 3:S2. doi: 10.1186/ar4174 [doi].
35. Johnsen AK, Weinblatt ME. Methotrexate: The foundation of rheumatoid arthritis therapy. In: *Rheumatoid arthritis*. Philadelphia, USA: Mosby; 2009:307-314. <https://doi.org/10.1016/B978-032305475-1.50002-1>.
36. Curtis JR, Singh JA. Use of biologics in rheumatoid arthritis: Current and emerging paradigms of care. *Clin Ther*. 2011;33(6):679-707. doi: 10.1016/j.clinthera.2011.05.044 [doi].
37. Cun D, Jensen DK, Maltesen MJ, et al. High loading efficiency and sustained release of siRNA encapsulated in PLGA nanoparticles: Quality by design optimization and characterization. *Eur J Pharm Biopharm*. 2011;77(1):26-35. doi: 10.1016/j.ejpb.2010.11.008 [doi].
38. Keijzer C, Spiering R, Silva AL, et al. PLGA nanoparticles enhance the expression of retinaldehyde dehydrogenase enzymes in dendritic cells and induce FoxP3(+) T-cells in vitro. *J Control Release*. 2013;168(1):35-40. doi: 10.1016/j.jconrel.2013.02.027 [doi].
39. Keijzer C, Slutter B, van der Zee R, Jiskoot W, van Eden W, Broere F. PLGA, PLGA-TMC and TMC-TPP nanoparticles differentially modulate the outcome of nasal vaccination by inducing tolerance or enhancing humoral immunity. *PLoS One*. 2011;6(11):e26684. doi: 10.1371/journal.pone.0026684 [doi].
40. de Groot A, Thanki K, Gangloff M, et al. Immunogenicity testing of lipidoids *In Vitro* and *in silico*: Modulating lipidoid-mediated TLR4 activation by nanoparticle design. . 2018;11:159-169.
41. Zeng X, de Groot AM, Sijs AJ, et al. Surface coating of siRNA-peptidomimetic nano-self-assemblies with anionic lipid bilayers: Enhanced gene silencing and reduced adverse effects in vitro. *Nanoscale*. 2015;7(46):19687-19698. doi: 10.1039/c5nr04807a [doi].
42. Guillailliams M, Ginhoux F, Jakubzick C, et al. Dendritic cells, monocytes and macrophages: A unified nomenclature based on ontogeny. *Nat Rev Immunol*. 2014;14(8):571-578. doi: 10.1038/nri3712 [doi].
43. Collin M, Bigley V, Haniffa M, Hambleton S. Human dendritic cell deficiency: The missing ID? *Nat Rev Immunol*. 2011;11(9):575-583. doi: 10.1038/nri3046 [doi].
44. Steinman RM, Cohn ZA. Pillars article: Identification of a novel cell type in peripheral lymphoid organs of mice. I. morphology, quantitation, tissue distribution. *J. exp. med.*1973. 137: 1142-1162. *J Immunol*. 2007;178(1):5-25. doi: 178/1/5 [pii].
45. van der Kleij D, Latz E, Brouwers JF, et al. A novel host-parasite lipid cross-talk. schistosomal lysophosphatidylserine activates toll-like receptor 2 and affects immune polarization. *J Biol Chem*. 2002;277(50):48122-48129. doi: 10.1074/jbc.M206941200 [doi].
46. Steinbrink K, Jonuleit H, Muller G, Schuler G, Knop J, Enk AH. Interleukin-10-treated human dendritic cells induce a melanoma-antigen-specific anergy in CD8(+) T cells resulting in a failure to lyse tumor cells. *Blood*. 1999;93(5):1634-1642.
47. Sato K, Yamashita N, Yamashita N, Baba M, Matsuyama T. Regulatory dendritic cells protect mice from murine acute graft-versus-host disease and leukemia relapse. *Immunity*. 2003;18(3):367-379. doi: S1074-7613(03)00055-4 [pii].
48. Lan YY, Wang Z, Raimondi G, et al. "Alternatively activated" dendritic cells preferentially secrete IL-10, expand Foxp3+CD4+ T cells, and induce long-term organ allograft survival in combination with CTLA4-ig. *J Immunol*. 2006;177(9):5868-5877. doi: 177/9/5868 [pii].
49. Francisco LM, Sage PT, Sharpe AH. The PD-1 pathway in tolerance and autoimmunity. *Immunol Rev*. 2010;236:219-242. doi: 10.1111/j.1600-065X.2010.00923.x [doi].
50. Hammer GE, Ma A. Molecular control of steady-state dendritic cell maturation and immune homeostasis. *Annu Rev Immunol*. 2013;31:743-791. doi: 10.1146/annurev-immunol-020711-074929 [doi].
51. Nolting J, Daniel C, Reuter S, et al. Retinoic acid can enhance conversion of naive into regulatory T cells independently of secreted cytokines. *J Exp Med*. 2009;206(10):2131-2139. doi: 10.1084/jem.20090639 [doi].
52. Hilkens CM, Isaacs JD, Thomson AW. Development of dendritic cell-based immunotherapy for autoimmunity. *Int Rev Immunol*. 2010;29(2):156-183. doi: 10.3109/08830180903281193 [doi].
53. Pedersen AE, Gad M, Walter MR, Claesson MH. Induction of regulatory dendritic cells by dexamethasone and 1alpha,25-dihydroxyvitamin D(3). *Immunol Lett*. 2004;91(1):63-69. doi: S016524780300258X [pii].
54. Anderson AE, Sayers BL, Haniffa MA, et al. Differential regulation of naive and memory CD4+ T cells by alternatively activated dendritic cells. *J Leukoc Biol*. 2008;84(1):124-133. doi: 10.1189/jlb.1107744 [doi].
55. Anderson AE, Swan DJ, Sayers BL, et al. LPS activation is required for migratory activity and antigen presentation by tolerogenic dendritic cells. *J Leukoc Biol*. 2009;85(2):243-250. doi: 10.1189/jlb.0608374 [doi].
56. Harry RA, Anderson AE, Isaacs JD, Hilkens CM. Generation and characterisation of therapeutic tolerogenic dendritic cells for rheumatoid arthritis. *Ann Rheum Dis*. 2010;69(11):2042-2050. doi: 10.1136/ard.2009.126383 [doi].
57. Stoop JN, Harry RA, von Delwig A, Isaacs JD, Robinson JH, Hilkens CM. Therapeutic effect of tolerogenic dendritic cells in established collagen-induced arthritis is associated with a reduction in Th17 responses. *Arthritis Rheum*. 2010;62(12):3656-3665. doi: 10.1002/art.27756 [doi].
58. Mansilla MJ, Contreras-Cardone R, Navarro-Barriuso J, et al. Cryopreserved vitamin D3-tolerogenic dendritic cells pulsed with autoantigens as a potential therapy for multiple sclerosis patients. *J Neuroinflammation*. 2016;13(1):113-016-0584-9. doi: 10.1186/s12974-016-0584-9 [doi].
59. Giannoukakis N, Phillips B, Finegold D, Harnaha J, Trucco M. Phase I (safety) study of autologous tolerogenic dendritic cells in type 1 diabetic patients. *Diabetes Care*. 2011;34(9):2026-2032. doi: 10.2337/dc11-0472 [doi].
60. Thomson AW, Robbins PD. Tolerogenic dendritic cells for autoimmune disease and transplantation. *Ann Rheum Dis*. 2008;67 Suppl 3:iii90-6. doi: 10.1136/ard.2008.099176 [doi].
61. Boks MA, Kager-Groenland JR, Haasjes MS, Zwaginga JJ, van Ham SM, ten Brinke A. IL-10-generated tolerogenic dendritic cells are optimal for functional regulatory T cell induction--a comparative study of human clinical-applicable DC. *Clin Immunol*. 2012;142(3):332-342. doi: 10.1016/j.clim.2011.11.011 [doi].
62. Lutz MB. Therapeutic potential of semi-mature dendritic cells for tolerance induction. *Front Immunol*. 2012;3:123. doi: 10.3389/fimmu.2012.00123 [doi].
63. Zhang L, Fu J, Sheng K, et al. Bone marrow CD11b(+)F4/80(+) dendritic cells ameliorate collagen-induced arthritis through modulating the balance between treg and Th17. *Int Immunopharmacol*. 2015;25(1):96-105. doi: 10.1016/j.intimp.2015.01.014 [doi].
64. Park JE, Jang J, Choi JH, et al. DC-based immunotherapy combined with low-dose methotrexate effective in the treatment of advanced CIA in mice. *J Immunol Res*. 2015;2015:834085. doi: 10.1155/2015/834085 [doi].
65. Li X, Han Y, Zhou Q, et al. Apigenin, a potent suppressor of dendritic cell maturation and migration, protects against collagen-induced arthritis. *J Cell Mol Med*. 2016;20(1):170-180. doi: 10.1111/jcmm.12717 [doi].
66. Garcia-Gonzalez P, Morales R, Hoyos L, et al. A short protocol using dexamethasone and monophosphoryl lipid A generates tolerogenic dendritic cells that display a potent migratory capacity to lymphoid chemokines. *J Transl Med*. 2013;11:128-5876-11-128. doi: 10.1186/1479-5876-11-128 [doi].

67. Lord P, Spiering R, Aguilon JC, et al. Minimum information about tolerogenic antigen-presenting cells (MITAP): A first step towards reproducibility and standardisation of cellular therapies. *PeerJ*. 2016;4:e2300. doi: 10.7717/peerj.2300 [doi].
68. Jauregui-Amezaga A, Cabezon R, Ramirez-Morros A, et al. Intraperitoneal administration of autologous tolerogenic dendritic cells for refractory crohn's disease: A phase I study. *J Crohns Colitis*. 2015;9(12):1071-1078. doi: 10.1093/ecco-jcc/jjv144 [doi].
69. Benham H, Nel HJ, Law SC, et al. Citrullinated peptide dendritic cell immunotherapy in HLA risk genotype-positive rheumatoid arthritis patients. *Sci Transl Med*. 2015;7(290):290ra87. doi: 10.1126/scitranslmed.aaa9301 [doi].
70. Bell GM, Anderson AE, Diboll J, et al. Autologous tolerogenic dendritic cells for rheumatoid and inflammatory arthritis. *Ann Rheum Dis*. 2017;76(1):227-234. doi: 10.1136/annrheumdis-2015-208456 [doi].
71. Popov I, Li M, Zheng X, et al. Preventing autoimmune arthritis using antigen-specific immature dendritic cells: A novel tolerogenic vaccine. *Arthritis Res Ther*. 2006;8(5):R141. doi: ar2031 [pii].
72. van Duivenvoorde LM, Han WG, Bakker AM, et al. Immunomodulatory dendritic cells inhibit Th1 responses and arthritis via different mechanisms. *J Immunol*. 2007;179(3):1506-1515. doi: 179/3/1506 [pii].
73. Raiotach-Regue D, Grau-Lopez L, Naranjo-Gomez M, et al. Stable antigen-specific T-cell hyporesponsiveness induced by tolerogenic dendritic cells from multiple sclerosis patients. *Eur J Immunol*. 2012;42(3):771-782. doi: 10.1002/eji.201141835 [doi].
74. Mansilla MJ, Selles-Moreno C, Fabregas-Puig S, et al. Beneficial effect of tolerogenic dendritic cells pulsed with MOG autoantigen in experimental autoimmune encephalomyelitis. *CNS Neurosci Ther*. 2015;21(3):222-230. doi: 10.1111/cns.12342 [doi].
75. Charbonnier LM, van Duivenvoorde LM, Apparailly F, et al. Immature dendritic cells suppress collagen-induced arthritis by in vivo expansion of CD49b+ regulatory T cells. *J Immunol*. 2006;177(6):3806-3813. doi: 177/6/3806 [pii].
76. Creusot RJ, Chang P, Healey DG, Tcherepanova IY, Nicolette CA, Fathman CG. A short pulse of IL-4 delivered by DCs electroporated with modified mRNA can both prevent and treat autoimmune diabetes in NOD mice. *Mol Ther*. 2010;18(12):2112-2120. doi: 10.1038/mt.2010.146 [doi].
77. Maggi J, Schinnerling K, Pesce B, Hilkens CM, Catalan D, Aguilon JC. Dexamethasone and monophosphoryl lipid A-modulated dendritic cells promote antigen-specific tolerogenic properties on naive and memory CD4+ T cells. *Front Immunol*. 2016;7:359. doi: 10.3389/fimmu.2016.00359 [doi].
78. Di Caro V, Phillips B, Engman C, Harnaha J, Trucco M, Giannoukakis N. Retinoic acid-producing, ex-vivo-generated human tolerogenic dendritic cells induce the proliferation of immunosuppressive B lymphocytes. *Clin Exp Immunol*. 2013;174(2):302-317. doi: 10.1111/cei.12177 [doi].
79. Kaushansky N, Altmann DM, David CS, Lassmann H, Ben-Nun A. DQB1*0602 rather than DRB1*1501 confers susceptibility to multiple sclerosis-like disease induced by proteolipid protein (PLP). *J Neuroinflammation*. 2012;9:29-2094-9-29. doi: 10.1186/1742-2094-9-29 [doi].
80. Tsark EC, Wang W, Teng YC, Arkfeld D, Dodge GR, Kovats S. Differential MHC class II-mediated presentation of rheumatoid arthritis autoantigens by human dendritic cells and macrophages. *J Immunol*. 2002;169(11):6625-6633.
81. Yoo SA, You S, Yoon HJ, et al. A novel pathogenic role of the ER chaperone GRP78/BiP in rheumatoid arthritis. *J Exp Med*. 2012;209(4):871-886. doi: 10.1084/jem.20111783 [doi].
82. Kastbom A, Strandberg G, Lindroos A, Skogh T. Anti-CCP antibody test predicts the disease course during 3 years in early rheumatoid arthritis (the swedish TIRA project). *Ann Rheum Dis*. 2004;63(9):1085-1089. doi: 10.1136/ard.2003.016808 [doi].
83. Kolinski T, Marek-Trzonkowska N, Trzonkowski P, Siebert J. Heat shock proteins (HSPs) in the homeostasis of regulatory T cells (tregs). *Cent Eur J Immunol*. 2016;41(3):317-323. doi: 10.5114/ceji.2016.63133 [doi].
84. Wieten L, van der Zee R, Spiering R, et al. A novel heat-shock protein coinducer boosts stress protein Hsp70 to activate T cell regulation of inflammation in autoimmune arthritis. *Arthritis Rheum*. 2010;62(4):1026-1035. doi: 10.1002/art.27344 [doi].
85. Kaufmann SH. Heat shock proteins and the immune response. *Immunol Today*. 1990;11(4):129-136.
86. Fink AL. Chaperone-mediated protein folding. *Physiol Rev*. 1999;79(2):425-449.
87. Matz JM, Blake MJ, Tatelman HM, Lavoi KP, Holbrook NJ. Characterization and regulation of cold-induced heat shock protein expression in mouse brown adipose tissue. *Am J Physiol*. 1995;269(1 Pt 2):R38-47.
88. Holoshitz J, Naparstek Y, Ben-Nun A, Cohen IR. Lines of T lymphocytes induce or vaccinate against autoimmune arthritis. *Science*. 1983;219(4580):56-58.
89. van Eden W, Thole JE, van der Zee R, et al. Cloning of the mycobacterial epitope recognized by T lymphocytes in adjuvant arthritis. *Nature*. 1988;331(6152):171-173. doi: 10.1038/331171a0 [doi].
90. Res PC, Schaar CG, Breedveld FC, et al. Synovial fluid T cell reactivity against 65 kD heat shock protein of mycobacteria in early chronic arthritis. *Lancet*. 1988;2(8609):478-480. doi: S0140-6736(88)90123-7 [pii].
91. de Graeff-Meeder ER, Voorhorst M, van Eden W, et al. Antibodies to the mycobacterial 65-kd heat-shock protein are reactive with synovial tissue of adjuvant arthritic rats and patients with rheumatoid arthritis and osteoarthritis. *Am J Pathol*. 1990;137(5):1013-1017.
92. Boog CJ, de Graeff-Meeder ER, Lucassen MA, et al. Two monoclonal antibodies generated against human hsp60 show reactivity with synovial membranes of patients with juvenile chronic arthritis. *J Exp Med*. 1992;175(6):1805-1810.
93. Albani S, Keystone EC, Nelson JL, et al. Positive selection in autoimmunity: Abnormal immune responses to a bacterial dnaJ antigenic determinant in patients with early rheumatoid arthritis. *Nat Med*. 1995;1(5):448-452.
94. van Eden W, van der Zee R, Prakken B. Heat-shock proteins induce T-cell regulation of chronic inflammation. *Nat Rev Immunol*. 2005;5(4):318-330. doi: nri1593 [pii].
95. Wieten L, Berlo SE, Ten Brink CB, et al. IL-10 is critically involved in mycobacterial HSP70 induced suppression of proteoglycan-induced arthritis. *PLoS One*. 2009;4(1):e4186. doi: 10.1371/journal.pone.0004186 [doi].
96. Prakken BJ, Wendling U, van der Zee R, Rutten VP, Kuis W, van Eden W. Induction of IL-10 and inhibition of experimental arthritis are specific features of microbial heat shock proteins that are absent for other evolutionarily conserved immunodominant proteins. *J Immunol*. 2001;167(8):4147-4153.
97. Prakken BJ, Roord S, van Kooten PJ, et al. Inhibition of adjuvant-induced arthritis by interleukin-10-driven regulatory cells induced via nasal administration of a peptide analog of an arthritis-related heat-shock protein 60 T cell epitope. *Arthritis Rheum*. 2002;46(7):1937-1946. doi: 10.1002/art.10366 [doi].
98. Wendling U, Paul L, van der Zee R, Prakken B, Singh M, van Eden W. A conserved mycobacterial heat shock protein (hsp) 70 sequence prevents adjuvant arthritis upon nasal administration and induces IL-10-producing T cells that cross-react with the mammalian self-hsp70 homologue. *J Immunol*. 2000;164(5):2711-2717. doi: jj_v164n5p2711 [pii].
99. Shinnick TM, Vodkin MH, Williams JC. The mycobacterium tuberculosis 65-kilodalton antigen is a heat shock protein which corresponds to common antigen and to the escherichia coli GroEL protein. *Infect Immun*. 1988;56(2):446-451.
100. Hsieh CS, Lee HM, Lio CW. Selection of regulatory T cells in the thymus. *Nat Rev Immunol*. 2012;12(3):157-167. doi: 10.1038/nri3155 [doi].
101. Dengjel J, Schoor O, Fischer R, et al. Autophagy promotes MHC class II presentation of peptides from intracellular source proteins. *Proc Natl Acad Sci U S A*. 2005;102(22):7922-7927. doi: 0501190102 [pii].

102. Paludan C, Schmid D, Landthaler M, et al. Endogenous MHC class II processing of a viral nuclear antigen after autophagy. *Science*. 2005;307(5709):593-596. doi: 1104904 [pii].
103. van Herwijnen MJ, Wieten L, van der Zee R, et al. Regulatory T cells that recognize a ubiquitous stress-inducible self-antigen are long-lived suppressors of autoimmune arthritis. *Proc Natl Acad Sci U S A*. 2012;109(35):14134-14139. doi: 10.1073/pnas.1206803109 [doi].
104. La Cava A, Nelson JL, Ollier WE, et al. Genetic bias in immune responses to a cassette shared by different microorganisms in patients with rheumatoid arthritis. *J Clin Invest*. 1997;100(3):658-663. doi: 10.1172/JCI119577 [doi].
105. Prakken BJ, Samodal R, Le TD, et al. Epitope-specific immunotherapy induces immune deviation of proinflammatory T cells in rheumatoid arthritis. *Proc Natl Acad Sci U S A*. 2004;101(12):4228-4233. doi: 10.1073/pnas.0400061101 [doi].
106. Koffeman EC, Genovese M, Amox D, et al. Epitope-specific immunotherapy of rheumatoid arthritis: Clinical responsiveness occurs with immune deviation and relies on the expression of a cluster of molecules associated with T cell tolerance in a double-blind, placebo-controlled, pilot phase II trial. *Arthritis Rheum*. 2009;60(11):3207-3216. doi: 10.1002/art.24916 [doi].
107. Raz I, Elias D, Avron A, Tamir M, Metzger M, Cohen IR. Beta-cell function in new-onset type 1 diabetes and immunomodulation with a heat-shock protein peptide (DiaPep277): A randomised, double-blind, phase II trial. *Lancet*. 2001;358(9295):1749-1753. doi: S0140-6736(01)06801-5 [pii].
108. Raz I, Avron A, Tamir M, et al. Treatment of new-onset type 1 diabetes with peptide DiaPep277 is safe and associated with preserved beta-cell function: Extension of a randomized, double-blind, phase II trial. *Diabetes Metab Res Rev*. 2007;23(4):292-298. doi: 10.1002/dmrr.712 [doi].
109. Kirkham B, Chaabo K, Hall C, et al. Safety and patient response as indicated by biomarker changes to binding immunoglobulin protein in the phase I/IIA RAGULA clinical trial in rheumatoid arthritis. *Rheumatology (Oxford)*. 2016;55(11):1993-2000. doi: kew287 [pii].
110. Kamphuis S, Kuis W, de Jager W, et al. Tolerogenic immune responses to novel T-cell epitopes from heat-shock protein 60 in juvenile idiopathic arthritis. *Lancet*. 2005;366(9479):50-56. doi: S0140-6736(05)66827-4 [pii].
111. de Jong H, Lafeber FF, de Jager W, et al. Pan-DR-binding Hsp60 self epitopes induce an interleukin-10-mediated immune response in rheumatoid arthritis. *Arthritis Rheum*. 2009;60(7):1966-1976. doi: 10.1002/art.24656 [doi].
112. de Wolf C, van der Zee R, den Braber I, et al. An arthritis-suppressive and treg cell-inducing CD4+ T cell epitope is functional in the context of HLA-restricted T cell responses. *Arthritis Rheumatol*. 2016;68(3):639-647. doi: 10.1002/art.39444 [doi].
113. Spiering R, van der Zee R, Wagenaar J, van Eden W, Broere F. Mycobacterial and mouse HSP70 have immuno-modulatory effects on dendritic cells. *Cell Stress Chaperones*. 2013;18(4):439. doi: 10.1007/s12192-012-0397-4.





Chapter 2

Generation of the first TCR transgenic mouse with CD4⁺ T cells recognizing an anti-inflammatory regulatory T cell-inducing HSP70 peptide

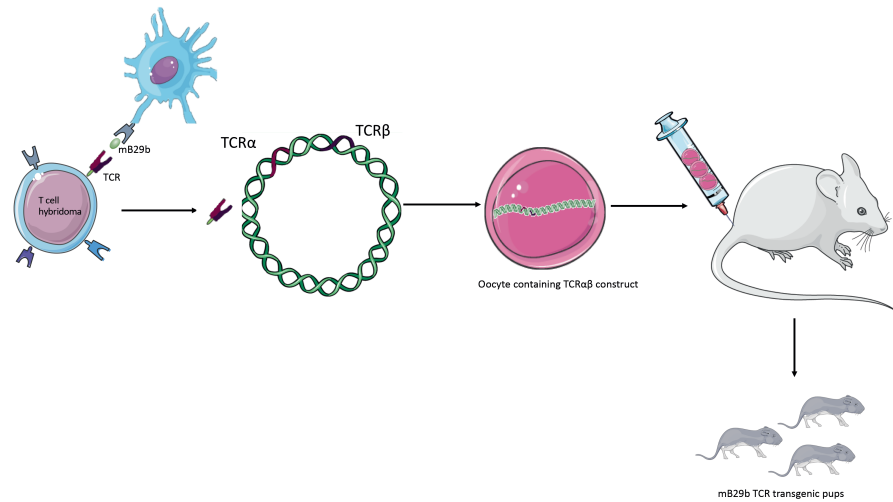
Manon AA Jansen^{1‡}, Martijn JC van Herwijnen^{1‡}, Peter JS van Kooten¹, Aad Hoek¹, Ruurd van der Zee¹, Willem van Eden¹, Femke Broere^{1*}

¹ Division of Immunology, Department of Infectious Diseases & Immunology, Utrecht University, Utrecht, the Netherlands

[‡] Contributed equally to this work

Frontiers in Immunology 2016 Mar 9;7:90.

Graphical abstract



Abstract

Antigen-specific regulatory T cells (Tregs) directed at self-antigens are difficult to study since suitable specific tools to isolate and characterize these cells are lacking. A T cell receptor (TCR)-transgenic mouse would generate possibilities to study such antigen-specific T cells. As was shown previously, immunization with the mycobacterial heat shock protein 70 derived peptide B29 and its mouse homologues mB29a and mB29b induced anti-inflammatory responses. Furthermore, B29 induced antigen-specific regulatory T cells (Tregs) *in vivo*. To study mB29b specific Tregs, we isolated the TCR from T cell hybridomas generated against mB29b and produced a TCR transgenic mouse that expresses a MHC-class II restricted mB29b-specific TCR. These TCR transgenic CD4⁺ T cells were found to cross react with the B29 epitope as identified with peptide induced proliferation and IL-2 production. Thus, we have successfully generated a novel mouse model with antigen-specific CD4⁺ T cells that recognize self and bacterial heat shock protein (HSP) 70 derived peptides. With this novel mouse model, it will be possible to study primary antigen specific T cells with specificity for a regulatory HSP70 T cell epitope. This will enable the isolation and characterization CD4⁺CD25⁺ Tregs with a proven specificity. This will provide useful knowledge of the induction, activation and mode of action of HSP70- specific Tregs, for instance during experimental arthritis.

Keywords: heat shock protein 70, transgenic mouse, autoimmunity, hybridoma, regulatory T cells

Introduction

Heat shock protein (HSP) 70 is a ubiquitously expressed protein and plays a role as chaperone in protein folding, either after protein synthesis or under conditions of cellular stress^{1,2}. HSP70 is evolutionary conserved and is expressed by many species, including bacteria and vertebrates. This is reflected by a high degree of homology of HSP between species. Interestingly, HSPs are also highly immunogenic, which might be explained by the fact that HSPs are found in bacteria that surround us. However, not only HSP derived peptides from bacteria are immunogenic, also peptides derived from self HSP can trigger immune responses^{3,4}. Peptides derived from endogenous HSP70 can not only be found in MHC class I molecules, but are also known to be present in MHC class II⁵⁻⁸. This indicates that HSP70 derived peptides can be recognized by immune cells in a MHC class II dependent manner. This is supported by experiments in which CD4⁺ T cell responses against HSP70 derived epitopes have been identified after immunization with bacterial HSP70⁷. Apart from presentation during cellular homeostasis, endogenous HSP can also be presented in MHC when it is upregulated during cellular stress such as heat shock^{8,9}. Due to the high degree of homology of HSP between species, cross reactive responses occur in which foreign HSP-peptide reactive T cells can recognize self-HSP peptides^{7,8,10,11}.

Interestingly, the administration of HSP70 can result in anti-inflammatory responses, which has been shown by the suppression of disease in animal models for chronic inflammation, due to activation of HSP70-specific regulatory T cells (Tregs) that are cross reactive with self-epitopes of HSP70^{4,7}. Tregs are a subset of specialized CD4⁺ T cells with high suppressive potential and are therefore important targets for immune modulation of inflammatory diseases¹². Therefore, activating these cells via HSP peptides is a growing field of interest, especially in inflammatory diseases in which the disease-inducing antigens are unknown.

Previously, we have shown that mycobacterial HSP70 peptide B29 is highly conserved and immunogenic. Immunization with, or intranasal administration of B29, activates B29-specific Treg *in vivo* which are potent suppressors of experimental arthritis⁷. Several tools, like T cell lines and T cell hybridomas, have been used to study HSP-specific T cell responses in the past. For instance, T cell lines generated from mycobacterial HSP60 immunized rats specific for a highly conserved sequence of HSP60 have been used to study the suppressive potential of HSP-specific T cells¹⁰. Similar results were obtained with T cell lines generated from mycobacterial HSP70 immunized rats: HSP70-specific T cells reduced the severity of arthritis in the experimental arthritis model¹³. However, none of these systems

allows the evaluation of primary T cell responses (*in vivo*), the behavior of HSP70-specific Tregs upon activation, nor the induction of particular T cell subsets like effector T cells and Tregs after administration of HSP70. Especially, antigen-specific Tregs are difficult to study since these cells comprise only a small fraction of the total T cell population and are difficult to culture and maintain *in vitro*¹⁴.

Therefore, we aimed to generate a mouse model to study primary and naive HSP70-specific CD4⁺ T cells in more detail. For that reason, we isolated the TCR- α and TCR- β chain genes from a T cell hybridoma generated against peptide mB29b, a mammalian homologue of B29 (Table 1). This hybridoma was found to cross react with B29 and another mammalian homologue: mB29a⁹. With the TCR- α and TCR- β chain genes, we generated a TCR transgenic mouse with HSP70 peptide-specific CD4⁺ T cells. We show that CD4⁺ T cells from the mB29b-TCR transgenic mouse undergo antigen-specific proliferation and produce IL-2 after restimulation with B29 or its mouse homologues. In future studies, primary CD4⁺ T cell responses directed against self and bacterial HSP70 peptides can be investigated *in vitro* and *in vivo*. Particularly, the activation and differentiation of antigen-specific CD4⁺ regulatory T cells can be studied with this model, which is not possible with long-term T cell lines or T cell hybridomas.

Table 1. Amino acid sequences of HSP70 peptides

The amino acid sequence and origin of the HSP70-derived peptides used in this study.

Peptide	Sequence	Protein	Origin
mB29a	VLRVINEPTAAALAY	HSPa9 (GRP75)	Mus musculus Homo sapiens
mB29b	VLRIINEPTAAAIAY	HSPa1a, HSPa8	Mus musculus Homo sapiens
a1a-long29	DAGVIAGLNVLRIINEPTAAAIAYGLDRTGK	HSPa1a (HSP72)	Mus musculus Homo sapiens
a8-long29	DAGTIAGLNVLRIINEPTAAAIAYGLDKK	HSPa8 (HSP70)	Mus musculus Homo sapiens
B29	VLRIINEPTAAALAY	DnaK (HSP70)	Mycobacterium tuberculosis

Materials & Methods

Mice, peptides and antibodies

Female Balb/c mice aged 8-12 weeks were purchased from Charles River and used as cell donors to create hybridomas and as source of APCs for co-culture assays. Animals were kept under standard conditions at the animal facility and all experiments were approved by the Animal Experiment Committee of Utrecht University. Mice strains used for the generation of the mB29b-TCR transgenic mouse were F1 of (CBA X C57BL/6) mice (Charles River). HSP70 derived peptides (mB29a, mB29b, B29) were identified previously⁷ and were obtained from GenScript Corporation. The amino acid sequences and origin of the peptides are shown in table 1. Anti-MHC-II (I-Ad/I-Ed) antibody (clone M5/114) 5 µg/ml; gift from Louis Boon from Bioceros B.V., Utrecht, The Netherlands) was used to block MHC-II-peptide TCR interactions in co-cultures. To stain mB29b specific cells, an APC labeled murine - mB29b specific tetramer composed of mB29b (VLRIINEPTAAAIAY linked to I-A(d)(BALB/c haplotype-matched MHC class II molecule)) was used for 90 minutes at 20 µg/ml. This tetramer is a gift from NIH Tetramer Core Facility (Emory University, Atlanta, GA, USA).

Generation of mB29b-TCR Hybridoma (LHEPs)

CD4⁺ T cell hybridomas (named LHEPs) were generated against HSP70 peptide mB29b in our laboratory as described previously⁹. Activation of specific hybridoma clones by mB29b was addressed by incubating hybridoma cells (2x10⁴/well) with irradiated (10.000 rad) A20 B lymphoma cells as APC (2x10⁴/well) loaded with HSP70 peptides in 96 wells flat bottom plates for 48 hours and pulsed with ³H-thymidine (0.4 µCi/ well) for an additional 16h to measure AICD.

As a positive control, hybridomas were stimulated with 2µg/ml ConA. After 48 hours co-culture, supernatants were harvested and frozen at -20°C. IL-2 production by hybridomas was studied by culturing the harvested supernatants with IL-2 responder CTLL-16 cells (cytotoxic T cell line; 5x10³/well) for 24 hours. The CTLL-16 cells were pulsed with ³H-thymidine (0.4 µCi/ well) for another 16h (Amersham Biosciences Europe GmbH, Roosendaal, the Netherlands). The 5/4E8 hybridoma specific for proteoglycan (PG) derived-peptide PG70-84¹⁵, was used as a control. RNA from the mB29b-TCR hybridoma was sequenced to determine the TCR usage. Sequencing revealed that the isolated mB29b TCR consisted of Vα 7 (TRAV-7.01-J26.01 in the IMGT nomenclature) and Vβ 8.2. The Vβ 8.2 is according to the NCBI nomenclature, this correlates with TRBV-13-2.01-D2.01-J2-7.01 in the IMGT nomenclature.

MHC restriction of T cell hybridomas

The MHC restriction of the peptide mB29b-specific hybridomas was determined using mouse anti-I-Ad (BD PharMingen) mAb. Hybridoma cells were cultured with A20 APCs in the presence of 0.5 µg/ml peptide mB29b and anti-I-Ad mAb (MKD6) at a concentration of 20µg/ml. The effect of mAb on IL-2 production was determined with the CTLL-16 bioassay as described above.

Cloning of the αβ TCR

Total RNA was isolated from the mB29b-TCR hybridoma cells by extraction with RNazol (Invitrogen). The oligo(dT)₁₂₋₁₈ primer from the Superscript Reverse Transcription kit (Invitrogen) was used for reverse transcription of the isolated RNA. To express the TCR mB29b genes in the transgenic mice, we cloned the Vα and Vβ genes into pTα and pTβ cassettes obtained from C. Benoist and D. Mathis¹⁶. Isolation of genomic DNA from the mB29b-TCR hybridoma was performed to obtain full length rearranged TCRα and TCRβ DNA, including leader and intron sequences. mB29b-TCR DNA was amplified by PCR using the primer for the Vα chain (Forw: TRAV7-1-XmaI: *TAATCCCGGGAGAATGAAGTCCTTGT GTGTTTCAC*, Rev; TRAJ26.01-NotI: *TAATGCGGGCCGACAGTAGACCTCAGGTCCCTCCAC*) and the Vβ chain (Forw: TRBV13-2.-1-XhoI: *TAATCTCGAGAAGATGGGCTCCAGGCTCTTC*; Rev: TRBJ2-7.01-SacII: *TAATCCCGGGCCTGGTCTACTCCAACTACTCC*). The PCR products of the two fragments were cloned using TA overhang into the pGEM-T easy vector (Promega). The constructs were subsequently introduced into *E. coli* DH5α. The XmaI and NotI- released DNA fragment, containing the TCRα chain, was cloned into the pTα cassette. The XhoI and SacII DNA fragment, containing the TCRβ chain, was cloned into the pTβ cassette. Both were transfected into XL10 gold cells (Stratagene) by electroporation.

In vitro expression of the αβ TCR

The pTα cassette, the pTβ cassette and the pcDNA3 plasmid (containing neomycin resistance gene) were electroporated into the mouse 58αβ⁻ T cell hybridoma which lacks functional TCR chains¹⁷. Transfected cells were cloned using limiting dilution in 96 wells plates using the FACS Vantage (BD) and cell lines were cultured in the presence of Geneticin 418 (0.8 mg/mL). PCR was used to validate DNA incorporation and transfected cells were tested for antigen-specificity in a similar manner as the hybridomas (described above).

Generation of the mB29b-TCR transgenic mouse

TCR transgenic mice were generated in our laboratory as described previously^{15, 17, 18}. The pT α mB29b-TCR and the pT β mB29b-TCR plasmids were linearized using *Sall* (pT α) and *Knpl* (pT β). Via pronuclear injection a mixture of the plasmids were introduced into fertilized eggs of F1 (CBA X C57BL/6) mice. Two mB29b-TCR transgenic founders were identified by PCR analysis of genomic DNA (same primers as described above). Founder 2 was mated with Balb/c mice (Balb/cBYJRj; Jackson laboratories) and offspring was tested for peptide specificity as described below.

Measurement of antigen-specific T cell responses from mB29b-TCR mice

Blood was taken from founders and depleted from erythrocytes with ACK lysis buffer (H₂O containing 150mM NH₄Cl, 10 mM KHCO₃ and 0.1 mM EDTA, pH 7.2-7.4). Blood cells (founder 1: 1x10⁵, founder 2: 5x10⁵, depending on cell yield after blood collection) were cultured for 96 h with 1x10⁶ irradiated A20 cells as APCs. Cells were stimulated with 2 μ g/ml or 20 μ g/ml B29 or with 5 μ g/ml ConA as a positive control. PBLs from founders were tested for antigen specific responses to 2 μ g/ml or 20 μ g/ml mB29a, mB29b or B29 peptides. Proliferation was determined by ³H-thymidine incorporation during the final 16 h of culture and IL-2 production was determined by Luminex. Splenocytes from offspring were screened for the expression of TCR α and TCR β chain. The mB29b-TCR positive splenocytes were also tested for antigen specificity.

Flow cytometric analysis

Single cell suspension of splenocytes, lymph node cells, or thymocytes were made and these were stained with antibodies CD3-APC (OKT-3, BD Biosciences), CD4-V450 (RM4-5, eBioscience), CD8-V500 (RPA-T8, BD Biosciences company), or V β 8-PE (F23.1, BD Biosciences) and incubated for 30 minutes at 4°C. Cells were washed 3 times with PBS containing 2% FCS. Cells were acquired on the FACS Canto II (BD) and analyzed with FlowJo 7 (Tree Star). For cell activation experiments, splenocytes from transgenic mice or littermates were cultured (1x10⁵ cells/well) for 24 h in the presence of 20 μ g/ml mB29b, in which the last 4 h was in the presence of 1 μ g/ml Brefeldin A.

Histology

For histology, thymus, spleen, inguinal lymph nodes (iLN; representative draining LNs) and liver were isolated from mB29b-TCR positive mice, or negative littermates. Tissues were fixed in 10% neutral buffered formalin, embedded in paraffin and 5 μ m sagittal sections were stained with hematoxylin and eosin (HE). Immunohistochemistry was performed to T cells and general proliferation in

lymphoid tissues. Briefly, cryosections (5 μ m) were fixed in ice-cold acetone and blocked against endogenous peroxidase with 0.3% hydrogen peroxide in methanol. Nonspecific staining was blocked with a 1% BSA solution and sections were incubated with primary antibodies against CD3 (BD Biosciences) or Ki-67 (BD Biosciences). Secondary staining was performed with an anti-rat HRP antibody (Millipore) and Peroxidase activity was developed using the DAB Peroxidase Substrate kit (Vector Laboratories). Sections were counterstained with hematoxylin and mounted with Aquatex (Merck, Darmstadt, Germany). Pictures were taken using an Olympus BX41 microscope and analyzed with Cellsens entry 1.9 software (Olympus Corporation).

Statistics

Unless stated otherwise, data are expressed as mean \pm standard deviation (SD). Statistical analyses were carried out using Student's t-test or the two-way ANOVA test using Prism software (Version 6.05). $p \leq 0.05$ was considered significantly different.

Results

MHC class II restricted recognition of HSP70 peptides mB29a, mB29b and B29 by mB29-TCR hybridoma LHEP4

T cell hybridomas specific for HSP70 peptide mB29b were generated by immunizing BALB/c mice with the peptide mB29b and fusing splenocytes from these mice with BW5147 cells followed by limiting dilution to obtain individual clones of the mB29b-TCR hybridomas. In order to test the TCR specificity of the generated hybridomas, which we named LHEPs, the cells were cultured in the presence of A20 cells as APCs and peptide mB29b, or its homologues mB29a and B29 (Figure 1). Activation induced cell death (AICD) and IL-2 production⁹, two characteristics of an activated hybridoma, were measured for seven LHEPs. The AICD was determined by ³H thymidine incorporation and the IL-2 production was measured by IL-2 dependent proliferation of the CTLL-16 cell line. Data of LHEP4 are depicted as a representative example in Figure 1. As seen in Figure 1, stimulation of LHEP4 with mB29a, mB29b and to some extent with B29 resulted in cell death and IL-2 production. To determine whether recognition of HSP70 peptides was MHC class II restricted, LHEPs were stimulated with peptide in the presence of an MHC class II blocking antibody. In this case, no AICD and a strongly reduced IL-2 production was seen upon stimulation with HSP70 peptides, indicating that peptide recognition of mB29b-TCR hybridomas was indeed MHC class II restricted (Figure 1A + B). The mB29b peptide was presented in the context of I-Ad molecules, since a mAb against I-Ad (MKD6) completely abrogated the mB29b-specific in vitro proliferation of the LHEP4 hybridoma (data not shown).

Screening of the obtained selected mB29b-specific T cell hybridomas revealed 7 LHEPs in total that were responsive to mB29b, of which 5 were cross-reactive to mB29a, and 4 that were cross-reactive to B29.

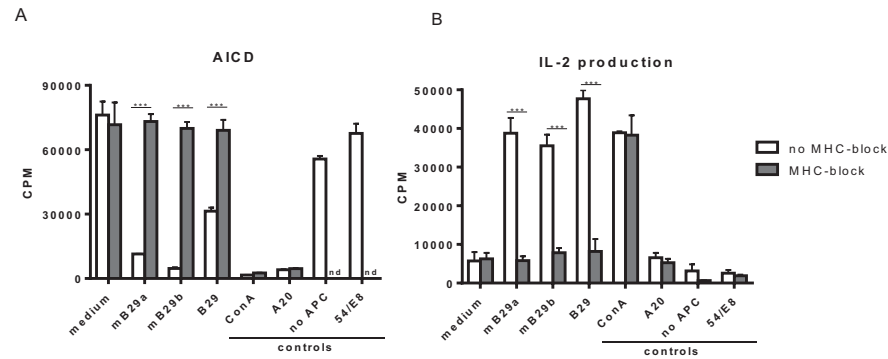


Figure 1. The hybridoma LHEP4 recognizes HSP70 peptides mB29a, mB29b and B29 in an MHC class II restricted way.

Splenocytes from BALB/c mice immunized with mB29b were fused with BW5147 cells which resulted in mB29b-specific CD4⁺ T cell hybridoma clones (LHEPs). (A) Activation induced cell death (AICD) is measured by reduced thymidine incorporation upon activation with mB29a, mB29b and B29. MHC-II blockage results abrogates AICD, which indicates that the mB29b-TCR hybridomas are MHC-II restricted. (B) IL-2 dependent CTLL-16 proliferation was measured to demonstrate that supernatant of activated hybridomas as depicted in A produce IL-2. As shown in B, IL-2 production is present after stimulation with mB29a, mB29b and B29. MHC-II blockage results in a diminished IL-2 production. As a positive control, cells were stimulated with ConA. As a negative control, LHEP4 hybridoma cells were cultured in medium only, in the presence of mB29b (no APC). Additional controls included A20 cells cultured with mB29b, or the 5/4E8 hybridoma cultured in the presence of mB29b peptide. ³H-thymidine incorporation is shown as mean of triplicate samples/well ± standard error of mean (s.e.m.). Data shown are representative of 3 independent experiments.

LHEPs respond to several length variants of the HSP70 peptide

We next determined a dose response of LHEP4 to the HSP70 peptides, as well as recognition of specific length extension variants of mB29b to assess the response to processed peptides. For this, LHEP4 was co-cultured with irradiated splenocytes in the presence of the extended HSPa8 (= Hsc70) or HSPa1a (=HSP72¹⁹) variants of the mB29b peptide, later referred to as a8-long29 and a1a-long29. CTLL-16 proliferation induced by IL-2 production from LHEP4 indicated that these length variants could be recognized (Figure 2A). Although IL-2 production decreased in cultures in which LHEP4 was stimulated with low amounts of mB29b or B29 (data not shown), CTLL-16 proliferation remained detectable, indicating that LHEP4 responds sensitively to presented HSP70 peptides (Figure 2A).

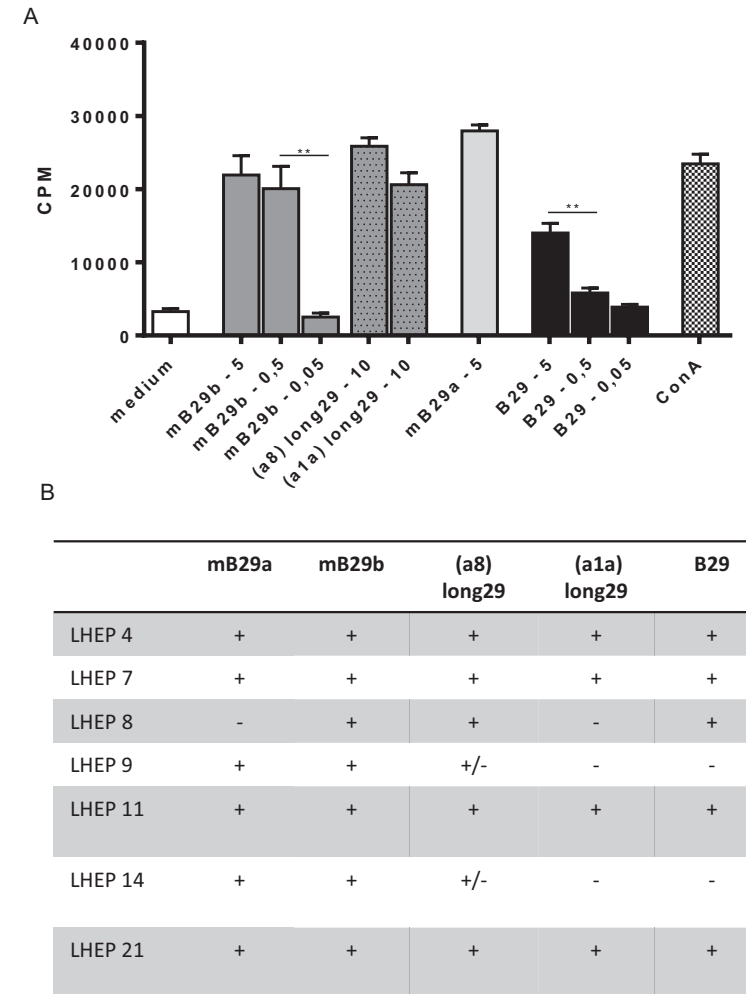


Figure 2. The mB29b-TCR hybridoma LHEP4 produces antigen-specific IL-2 upon co-culture with primary antigen presenting cells

(A) LHEP4 was co-cultured with irradiated splenocytes loaded with different concentrations (ranging from 5 µg/ml, 0,5 µg/ml to 0,05 µg/ml, as well as 10 µg/ml length variants of mB29b (HSPa8=Hsc70 or HSPa1a=HSP72(20))) of HSP70 peptides as indicated, after which supernatants were collected. CTLL-16 cell cultures were supplemented with supernatants from these stimulations to determine IL-2 dependent proliferation of CTLL-16 cells. As a control, co-cultured LHEP4 cells were unstimulated, or stimulated with ConA. ³H-thymidine incorporation is shown as mean of triplicate samples/well ± standard error of mean (s.e.m.). Data shown are representative of 3 independent experiments. (B) mB29-TCR hybridomas were stimulated with HSP70 peptides mB29a, mB29b or B29, as well as length variants of mB29b (HSPa8=Hsc70 or HSPa1a=HSP72(20)) as described in A). The + symbol (cpm > 15000) indicates AICD and IL-2 production upon co-culture with supernatants from peptide-stimulated LHEPs. Weak responses are depicted as +/- (on average the cpm = 4000). Medium stimulated samples show on average a cpm of 1500. Data shown summarize three independent experiments.

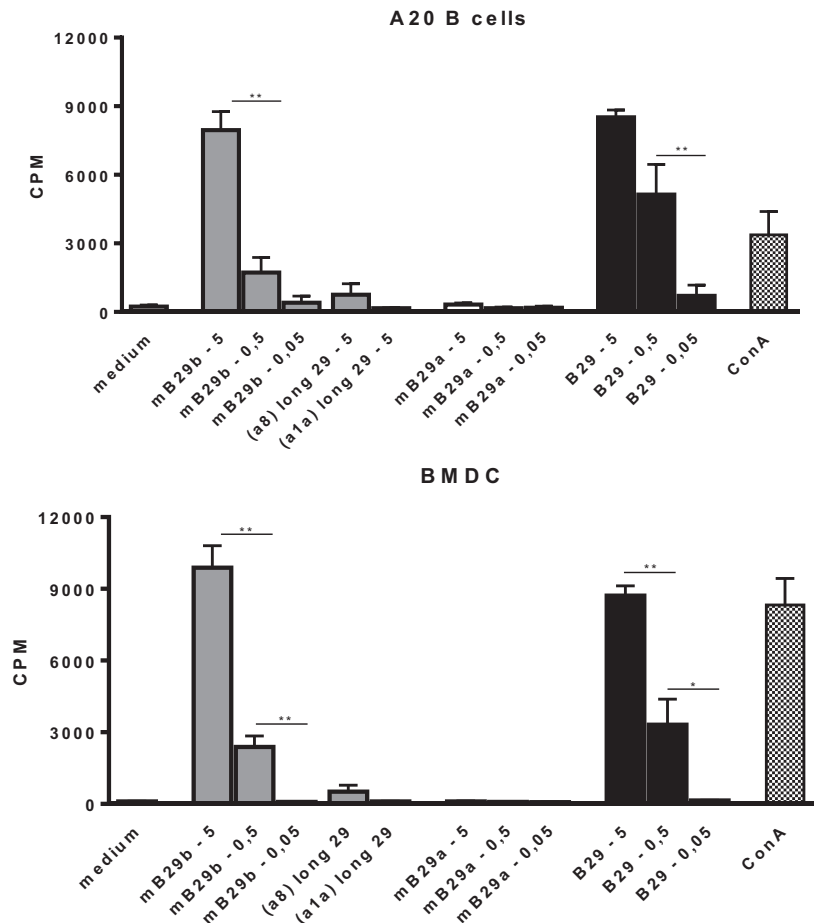


Figure 3. Cloning of the TCR α and TCR β chain from mB29b-TCR hybridoma LHEP4 into TCR cells results in HSP70 peptide-specific transfectants

Cloned transfected cells were co-cultured with A20 B cells (A) or BMDCs (B), which were loaded with 5 $\mu\text{g/ml}$, 0.5 $\mu\text{g/ml}$ or 0.05 $\mu\text{g/ml}$ HSP70 peptides. After stimulation with HSP70 peptides mB29a, mB29b or B29 as well as length variants of mB29b (a1a or a8), supernatants were added to CTLL-16 cells and IL-2 dependent proliferation was determined after 24h. The graph shows more IL-2 dependent proliferation of CTLL-16 cells when stimulated with a high concentration HSP70 peptide mB29b or B29. There is no response to stimulation with mB29a, and to a minor extent to the length variants of mB29b (a8 or a1a). Similar results were obtained with the BMDC co-culture (B). As a control, co-cultured LHEP4 cells were unstimulated, or stimulated with ConA (data not shown). ^3H -thymidine incorporation is shown as mean of triplicate samples/well \pm standard error of mean (s.e.m.). Data shown are representative of two independent experiments.

Apart from LHEP4, the previously selected T cell hybridomas were screened for the recognition of HSP70 peptide (length variants) (Figure 2B). All LHEPs responded to the mB29b peptide when presented by different primary APC, indicating that the mB29b-TCR hybridomas recognize HSP70 peptides presented by APCs from various sources (data not shown). As was previously seen (Figure 2B), not all LHEPs were cross-reactive to other peptides, including the length variants of mB29b (HSPa8 or HSPa1a). All mB29b-TCR hybridomas that recognize different length variants of mB29b provide a broad recognition spectrum.

Cloning of the TCR α and TCR β chain from mB29b-TCR hybridoma LHEP4 into TCR cells results in HSP70 peptide-specific transfectants

Based on the specificity and the strong cross reactive responses of LHEP4, the TCR α and TCR β chain of this mB29b-TCR hybridoma were cloned into TCR expression vectors which were transfected into cells lacking the TCR (TCR $^-$). The transfected cell line was co-cultured with BMDC or irradiated A20 B cells which were loaded with HSP70 peptides to confirm the antigen-specificity of the transfectant. Results showed a dose dependent response to mB29b and B29, but not to mB29a (Figure 3). Irradiated thymocytes and splenocytes were also used as APC, and gave similar proliferative responses (data not shown). Furthermore, addition of shorter variants of the mB29b peptide to LHEP4 and the transfected cells, failed to stimulate the mB29b specific hybridoma and cells indicating the specificity of the hybridoma and transfected cells (data not shown). Together, these data confirmed that the TCR α and TCR β chain were successfully cloned into TCR expression vectors and therefore we transferred the TCR α and TCR β chain constructs to mouse oocytes via pronuclear injection.

Antigen recognition of cells from mB29b-TCR transgenic mouse

After pronuclear injection of the DNA expressing TCR α and TCR β into the donor zygote, the zygote was injected in a foster mouse from which several pups were born that had incorporated the constructs. From these mice, two founders were positive for both constructs with PCR (data not shown). Peripheral blood lymphocytes (PBLs) from the two founders were stimulated with B29 in a co-culture with irradiated splenocytes. PBLs from one founder proliferated and produced IL-2 in response to B29 stimulation (Figure 4). Next, the positive founder was mated with Balb/c mice and F1 mice were screened for the expression of the TCR α and TCR β chain and splenocytes from mB29b-TCR positive offspring were tested for antigen specificity and compared to negative littermates. We observed responses to mB29b, B29 and mB29b length variant (a8) long29 (Figure 2B), while mB29b-TCR negative littermates showed no response to any of the peptides tested (data not shown). These data

show that we successfully generated mB29b-TCR transgenic mice with cells with a functional TCR that recognized HSP70 peptides.

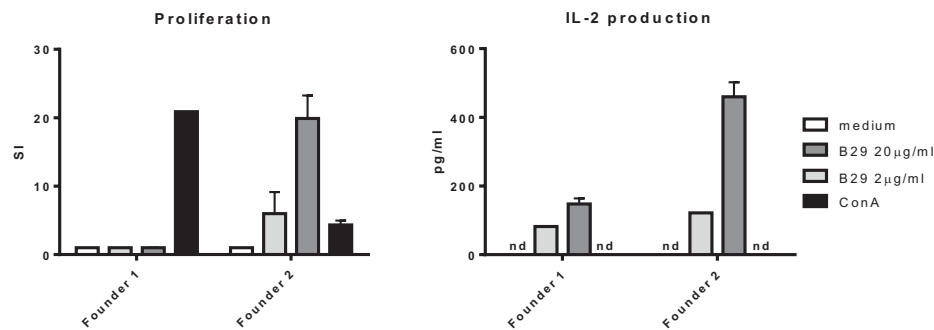


Figure 4. Antigen recognition by mB29b-TCR transgenic mouse

PBLs from two founders, positive for the TCR α and TCR β chain, were cultured for 96h with irradiated A20 B cells and stimulated with 2 μ g/ml or 20 μ g/ml B29, or 5 μ g/ml ConA as a positive control. PBLs from founder 2 proliferated in a dose-dependent response. The PBLs from founder 1 did not show any proliferation after B29 stimulation. The PBLs from both founders produced IL-2 but the PBLs from founder 2 produced higher amounts. Proliferation was determined by 3 H-thymidine incorporation during the final 16h of culture and IL-2 production was determined by Luminex. Data are from one experiment.

Flow cytometric analysis of mB29-TCR transgenic mouse tissues

Next, we examined the presence of CD3 $^+$, CD4 $^+$, CD8 $^+$ T cells in thymus of the mB29b-TCR transgenic mouse. Since the mB29b-TCR hybridoma was recognized by the antibody directed against V β 8, we also screened the thymus for V β 8 $^+$ T cells. The transgenic mice and littermates had a similar frequency of CD4 $^+$ cells, whereas the transgenic mouse had an increased percentage of V β 8 $^+$ T cells in the thymus and a decreased amount of CD8 $^+$ cells (Figure 5A). In the spleen, the same differences in CD4 $^+$ T cell and CD8 $^+$ T cell distribution (more CD4 $^+$ T cells compared to a wild type mouse) were observed, as well as an increased number of V β 8 $^+$ T cells were detected (Figure 5B). This resulted in changes in the CD4:CD8 ratio in both the thymus and spleen. The increased CD4:CD8 ratio became more evident in later generations. We observed a similar distribution and percentage of T cells in the LN (data not shown). To test the specificity of the CD4 $^+$ T cells in the mB29b-TCR Tg mouse, we stained splenocytes with an APC labeled murine - mB29b specific tetramer composed of mB29b (VLRINEPTAAAIAY linked to I-A(d)) and also cultured splenocytes in the presence of mB29b for 24 hrs. As shown in the lower part of figure 5B, the mB29b TCR Tg mouse contains more tetramer specific CD4 $^+$ T cells than the WT Balb/c and the negative littermate. Figure 5D demonstrates that after 24 hours of culture in the presence of mB29b, more CD4 $^+$ T cells are activated (IFN- γ and CD25 expression)

in the spleen of the transgenic mouse, in comparison with the negative littermate. Furthermore, also the CD4 $^+$ CD25 $^+$ FoxP3 $^+$ population is more pronounced in the mB29b TCR Tg mouse compared to the negative littermate; while in naïve mice, FoxP3 expression is lower in mB29b Tg mice (Figure 5C).

mB29b-TCR transgenic mice show an increase in naïve cells

To investigate cell distribution and activation, both histology and flow cytometry were used. Tissue sections from thymus, spleen, inguinal lymph nodes (iLN), and liver were made and stained for HE or CD3 (Figure 6). Based on the HE stained tissue slides, no apparent changes are observed in iLN, spleen, thymic or liver tissue architecture (data not shown). In addition, the distribution of CD3 $^+$ T cells in the different lymphoid tissues was comparable between the TCR transgenic mouse and the littermate (Figure 6A). However, we did find a difference in proliferative activity, as based on the Ki-67 expression in splenocytes (Figure 6B). The Ki-67 positive population is reduced in the mB29b TCR Tg mouse when compared to the wild type mice and negative littermates. This correlates with the enhanced non-proliferative naïve cell population (defined as CD62L $^{\text{hi}}$ CD44 $^{\text{low}}$) in naïve mB29b TCR Tg mice (Figure 6B). Overall, histological analysis revealed no major differences in T cell distribution or activation between the founder and control littermates in lymphoid organs, suggesting no development of gross pathology.

Discussion and conclusion

Investigating HSP-specific T cell responses *in vivo* and *in vitro* is of great interest to examine the effect of HSP administration on T cell activation and differentiation. Although there are HSP-specific cell lines that have been generated after long *in vitro* culture^{10, 20}, as well as HSP-specific T cell hybridomas⁹, these cells lack the properties of primary T cells. A huge disadvantage of these cells is that they lack the ability to differentiate from naïve cell to effector or regulatory T cell and can therefore only be used for qualitative analysis of HSP recognition. Several studies have shown that the immuno-modulatory effect of HSP administration (being immunization, intranasal administration or oral administration) is due to the activation of HSP-specific Tregs^{7, 21-23}. However, little is still known about the function of these cells. For instance, it is difficult to study Tregs *in vitro*, since these cells require more than peptide stimulation alone (e.g. growth factors like IL-2 and/or TGF- β) for their expansion and differentiation^{24, 25}, in comparison to immortalized T cell lines. Eventually, one would like to study primary antigen-specific T cells; however these are only a minor population within the total population of T cells. Therefore, a TCR-

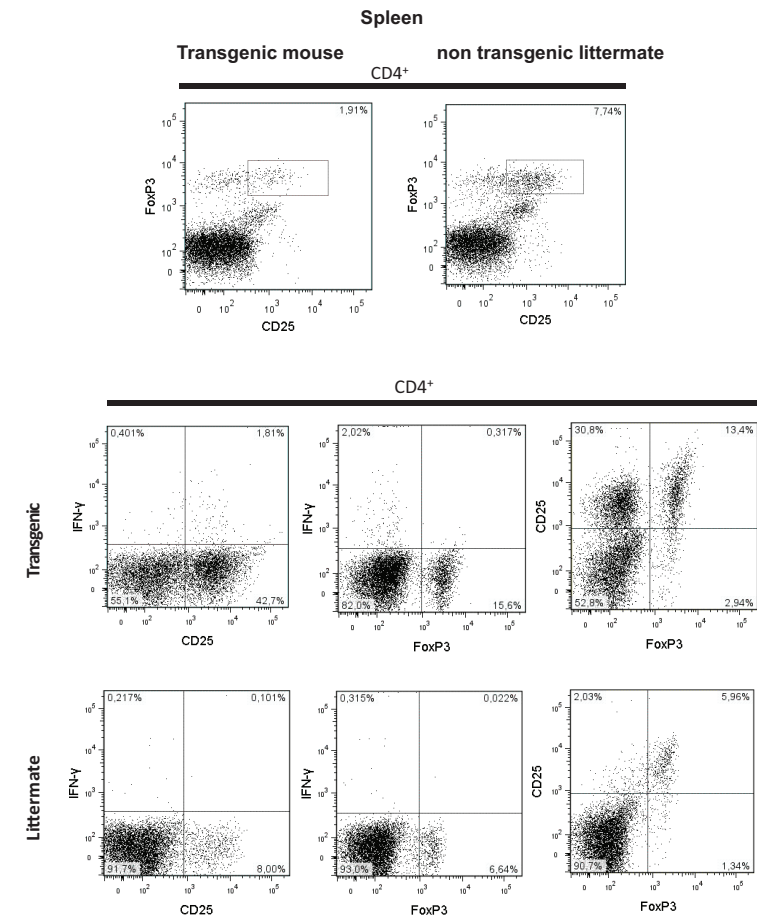
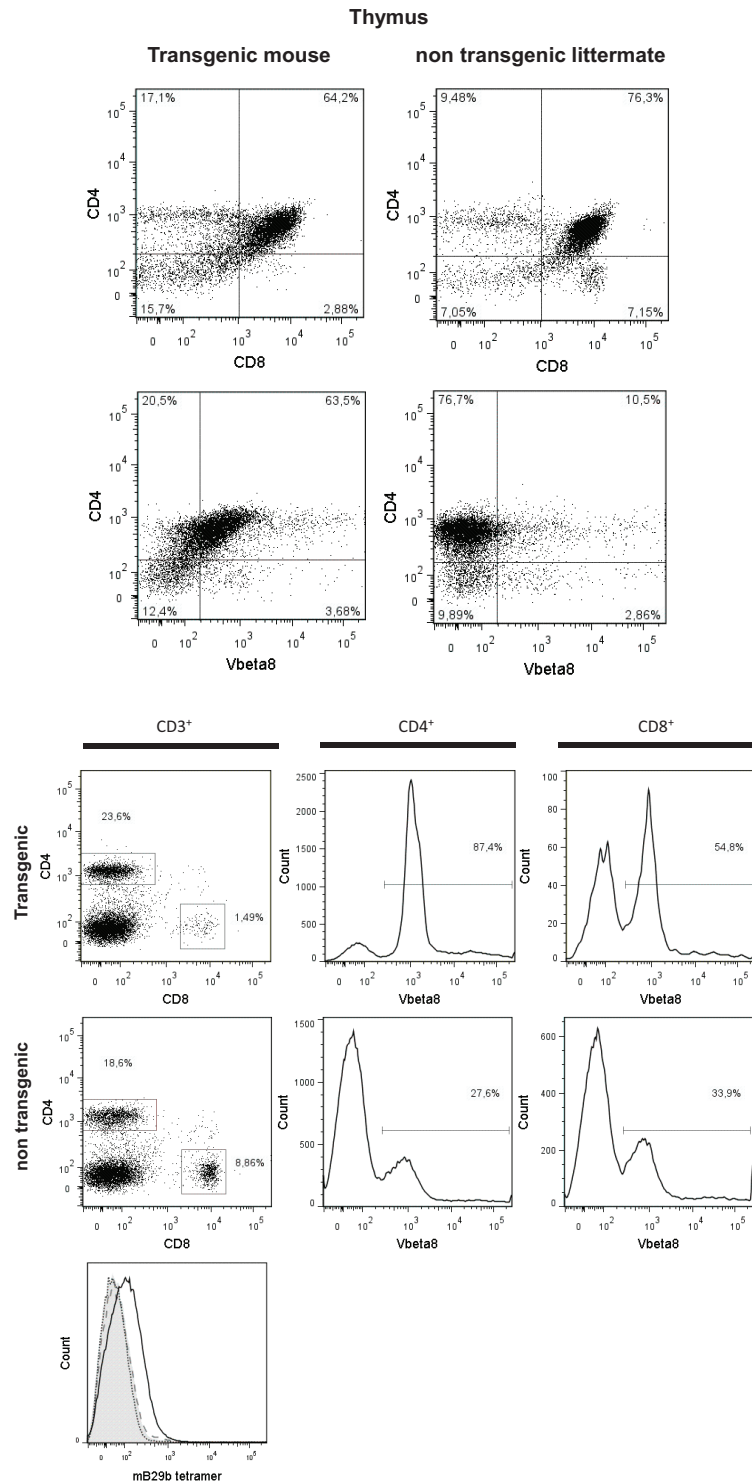


Figure 5. CD4⁺ and CD8⁺ T cell distribution in tissues of mB29b-TCR transgenic mouse

(A) Single cell suspensions were made from thymus of mB29b-TCR transgenic mice or negative littermates. Cells were stained for the expression of CD3, CD4, CD8 and V β 8. Live cells were gated on the forward scatter (FSC) and side scatter (SSC) and the percentage of CD4⁺ and CD8⁺ cells of the live cells are depicted in the upper panel of Figure 5 A. In the lower panel of Figure 5 A the percentage of CD4⁺V β 8⁺ of all live cells are shown. The different CD4⁺ and CD8⁺ T cell distribution of the mB29b-TCR transgenic mouse compared to non-transgenic littermates is due to the transgenic background, in which formation of T cells is changed. Plots shown are representatives of three independent experiments. (B) Distribution of CD4⁺ and CD8⁺ cells in the CD3⁺ cells (left row of graphs), histograms of CD4⁺ cells (middle row of graphs) and CD8⁺ cells (right row of graphs) of total CD3⁺ cells are depicted. The transgenic mouse shows an increase in CD8⁺V β 8⁺ and CD4⁺ V β 8⁺ T cells compared to the non-transgenic littermate. The overlay histogram at the bottom of figure 5B represents the amount of mB29b specific CD4⁺ T cells in a WT Balb/c (filled grey), a negative littermate (dashed line) and an mB29b TCR Tg mouse (black line). The dotted line shows splenocytes stained with a CLIP tetramer as negative control. Each line represents three different mice. (C) CD25 and FoxP3 expression measured within the CD4⁺ population of splenocytes derived from naïve mice. (D) CD25, IFN- γ and FoxP3 markers are measured by flow cytometry upon 24 hrs culture of splenocytes from both negative littermates and transgenic mouse in the presence of mB29b.

transgenic mouse is a valuable tool to obtain larger quantities of antigen-specific T cells. As a result, we set out to generate a TCR transgenic mouse with HSP70 peptide-specific T cells to establish a tool to study the activation, differentiation and suppressive capacity of HSP-specific T cells.

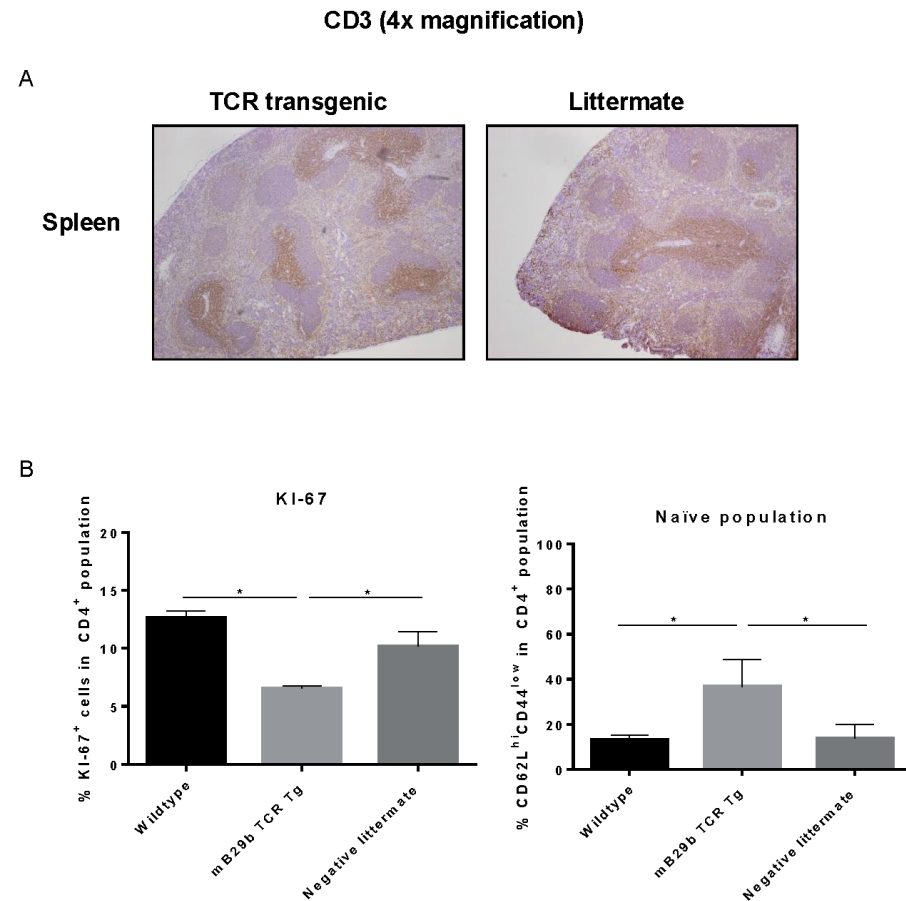


Figure 6. mB29b-TCR transgenic mouse shows no pathological changes in histology

(A) Thymus, inguinal lymph nodes (iLN) and liver (data not shown) were isolated from mB29b-TCR positive mice, or negative littermates. Figure 6A shows sections of the spleen in which no structural changes were observed between the mB29b-TCR transgenic mouse and the non-transgenic littermate. Immunohistochemistry was performed to T cells (α CD3) and general proliferation in lymphoid tissues. The distribution of CD3⁺ T cells in the mB29b-TCR transgenic mouse does not deviate from the non-transgenic littermate. Pictures show the spleen in a 4x magnification.

(B) Splenocytes were isolated from naïve wild type Balb/c, mB29b TCR Tg mice and negative littermates and CD4⁺ cells were stained for KI-67 or CD44 and CD62L. Data are obtained by flow cytometry. Data is shown as mean of triplicate samples/well \pm standard error of mean (s.e.m.). Data shown are representative of two independent experiments.

In this study, we have successfully cloned an mB29b-TCR hybridoma with specificity for the HSP70 peptide mB29b. Due to sequence homologies of HSP70 family members, this hybridoma can recognize self HSP peptides mB29a and mB29b, and the mycobacterial HSP70 peptide B29. Recognition was MHC class II dependent and all APCs tested were capable of activating the mB29b-TCR hybridoma (Figure 1 and Figure 2). Next, the TCR α and TCR β chain were isolated and cloned into TCR expression vectors which were electroporated into TCR⁻ T cells, which showed peptide-specific activation upon electroporation of the construct (Figure 3). Although the hybridomas did show a response to mB29a (Figure 1 and 2), the TCR⁻ cells in which the expression vectors from hybridoma LHEP4 were transfected showed little response to this peptide as measured by IL-2 production. This can be explained by the fact that hybridomas produce much larger amounts of IL-2 in response to antigen-specific stimulation compared to the TCR⁻ cells. In addition, the mB29a peptide was found to be a less strong agonist than the founding peptide mB29b when used to stimulate splenocytes from the mB29b TCR Tg mouse, most likely due to the two amino acids difference (table 1).

After linearization of the mB29b-TCR plasmids, the TCR α and TCR β chain were injected pronuclear into mouse oocytes. Two founders were born that carried both vectors. PBLs from one of the mB29b-TCR transgenic founders showed mB29b-specific activation, as well as cross recognition to the HSP70 peptide B29 (Figure 4). This founder (founder 2) was mated with Balb/c mice and offspring was screened for bearing the mB29b-TCR. Splenocytes were stimulated with HSP peptides and showed similar peptide recognition as the founder did. FACS analysis revealed that the distribution of CD4⁺ and CD8⁺ T cells in thymus and spleen of the mB29b-TCR transgenic were slightly different to that of littermates (Figure 5). Differences in CD4⁺ and CD8⁺ T cell distribution in TCR transgenic mice compared to non-transgenic littermates is due to the transgenic background in which formation of T cells is altered. This is considered normal for a TCR transgenic mouse^{26, 27}, since these mice will have selective development of $\alpha\beta$ TCR T cells in the thymus. The distribution of TCR transgenic cells could be seen in histology of the thymus (Figure 6). Although in general the T cell distribution in the tissue sections was comparable between the mice, a decreased CD4⁺CD25⁺FoxP3⁺ population was observed in naïve mB29b TCR transgenic mice by flow cytometry, comparable to several other TCR transgenic mice^{28, 29}. Furthermore, the amount of proliferated cells was altered in lymphoid tissues from the mB29b-TCR transgenic mouse compared to littermates. The mB29b-TCR Tg mice showed a decrease in KI-67⁺ cells, which might be due to the fact that mB29b is a self-peptide which causes self-regulation. The data do indicate that



tissue morphology is normal in the mB29b-TCR transgenic mouse. Furthermore, no spontaneous autoimmune disease was observed in these young TCR transgenic mice.

With this new TCR transgenic mouse, we are now able to study the properties of naïve T cells differentiating and proliferating into effector and regulatory T cells. Furthermore, we now hope to elucidate the mechanism of HSP70 mediated T cell regulation without prior HSP70 immunization and its associated non-specific immune activation.

Acknowledgements

We thank the workers at the animal facility for animal care. This work was supported by Innovation Oriented Program in Genomics Project Grants IGE3018 and IGE07004, European Union Grant Seventh Framework Program TOLERAGE: HEALTH-F4-2008-202156, and the Dutch Arthritis Foundation

Disclosures

The authors declare no conflict of interest.

Author contributions

MJ and MvH designed and performed experiments, analyzed data, wrote the paper and approved the submitted version. PvK designed and performed experiments, analyzed data and approved the submitted version; AH performed experiments, analyzed data and approved the submitted version; RvdZ designed experiments, analyzed data, commented on the manuscript at all stages and approved the submitted version; WvE commented on the manuscript at all stages and approved the submitted version; FB designed experiments, commented on the manuscript at all stages and approved the submitted version.

References

1. Bukau B, Horwich AL. The HSP70 and HSP60 chaperone machines. *Cell* (1998) 92:351-366. doi: S0092-8674(00)80928-9 [pii].
2. Hartl FU, Martin J, Neupert W. Protein folding in the cell: the role of molecular chaperones HSP70 and HSP60. *Annu Rev Biophys Biomol Struct* (1992) 21:293-322. doi: 10.1146/annurev.bb.21.060192.001453 [doi].
3. Naylor DJ, Hartl FU. Contribution of molecular chaperones to protein folding in the cytoplasm of prokaryotic and eukaryotic cells. *Biochem Soc Symp* (2001) (68):45-68.
4. van Eden W, van der Zee R, Prakken B. Heat-shock proteins induce T-cell regulation of chronic inflammation. *Nat Rev Immunol* (2005) 5:318-330. doi: nri1593 [pii].
5. Paludan C, Schmid D, Landthaler M, Vockerodt M, Kube D, Tuschl T, et al. Endogenous MHC class II processing of a viral nuclear antigen after autophagy. *Science* (2005) 307:593-596. doi: 1104904 [pii].
6. Dengjel J, Schoor O, Fischer R, Reich M, Kraus M, Muller M, et al. Autophagy promotes MHC class II presentation of peptides from intracellular source proteins. *Proc Natl Acad Sci U S A* (2005) 102:7922-7927. doi: 0501190102 [pii].
7. van Herwijnen MJ, Wieten L, van der Zee R, van Kooten PJ, Wagenaar-Hilbers JP, Hoek A, et al. Regulatory T cells that recognize a ubiquitous stress-inducible self-antigen are long-lived suppressors of autoimmune arthritis. *Proc Natl Acad Sci U S A* (2012) 109:14134-14139. doi: 10.1073/pnas.1206803109 [doi].
8. van Eden W, van Herwijnen M, Wagenaar J, van Kooten P, Broere F, van der Zee R. Stress proteins are used by the immune system for cognate interactions with anti-inflammatory regulatory T cells. *FEBS Lett* (2013) 587:1951-1958. doi: 10.1016/j.febslet.2013.05.024 [doi].
9. Wieten L, van der Zee R, Goedemans R, Sijtsma J, Serafini M, Lubsen NH, et al. HSP70 expression and induction as a readout for detection of immune modulatory components in food. *Cell Stress Chaperones* (2010) 15:25-37. doi: 10.1007/s12192-009-0119-8 [doi].
10. Anderton SM, van der Zee R, Prakken B, Noordzij A, van Eden W. Activation of T cells recognizing self 60-kD heat shock protein can protect against experimental arthritis. *J Exp Med* (1995) 181:943-952.
11. Durai M, Kim HR, Bala KK, Moudgil KD. T cells against the pathogenic and protective epitopes of heat-shock protein 65 are crossreactive and display functional similarity: novel aspect of regulation of autoimmune arthritis. *J Rheumatol* (2007) 34:2134-2143. doi: 07/13/1030 [pii].
12. Smigiel KS, Srivastava S, Stolley JM, Campbell DJ. Regulatory T-cell homeostasis: steady-state maintenance and modulation during inflammation. *Immunol Rev* (2014) 259:40-59. doi: 10.1111/imr.12170 [doi].
13. Prakken BJ, Wendling U, van der Zee R, Rutten VP, Kuis W, van Eden W. Induction of IL-10 and inhibition of experimental arthritis are specific features of microbial heat shock proteins that are absent for other evolutionarily conserved immunodominant proteins. *J Immunol* (2001) 167:4147-4153.
14. Shevach EM. Mechanisms of foxp3+ T regulatory cell-mediated suppression. *Immunity* (2009) 30:636-645. doi: 10.1016/j.immuni.2009.04.010 [doi].
15. Buzas EI, Brennan FR, Mikecz K, Garzo M, Negroiu G, Hollo K, et al. A proteoglycan (aggrecan)-specific T cell hybridoma induces arthritis in BALB/c mice. *J Immunol* (1995) 155:2679-2687.
16. Kouskoff V, Signorelli K, Benoist C, Mathis D. Cassette vectors directing expression of T cell receptor genes in transgenic mice. *J Immunol Methods* (1995) 180:273-280. doi: 002217599500002R [pii].
17. Schleicher U, Rollinghoff M, Gessner A. A stable marker for specific T-cells: a TCR alpha/green fluorescent protein (GFP) fusionprotein reconstitutes a functionally active TCR complex. *J Immunol Methods* (2000) 246:165-174. doi: S0022-1759(00)00298-2 [pii].

18. Berlo SE, van Kooten PJ, Ten Brink CB, Hauet-Broere F, Oosterwegel MA, Glant TT, et al. Naive transgenic T cells expressing cartilage proteoglycan-specific TCR induce arthritis upon in vivo activation. *J Autoimmun* (2005) 25:172-180. doi: 50896-8411(05)00125-3 [pii].
19. Kampinga HH, Hageman J, Vos MJ, Kubota H, Tanguay RM, Bruford EA, et al. Guidelines for the nomenclature of the human heat shock proteins. *Cell Stress Chaperones* (2009) 14:105-111. doi: 10.1007/s12192-008-0068-7 [doi].
20. van Eden W, Thole JE, van der Zee R, Noordzij A, van Embden JD, Hensen EJ, et al. Cloning of the mycobacterial epitope recognized by T lymphocytes in adjuvant arthritis. *Nature* (1988) 331:171-173. doi: 10.1038/331171a0 [doi].
21. Wieten L, Berlo SE, Ten Brink CB, van Kooten PJ, Singh M, van der Zee R, et al. IL-10 is critically involved in mycobacterial HSP70 induced suppression of proteoglycan-induced arthritis. *PLoS One* (2009) 4:e4186. doi: 10.1371/journal.pone.0004186 [doi].
22. Brownlie RJ, Myers LK, Wooley PH, Corrigan VM, Bodman-Smith MD, Panayi GS, et al. Treatment of murine collagen-induced arthritis by the stress protein BiP via interleukin-4-producing regulatory T cells: a novel function for an ancient protein. *Arthritis Rheum* (2006) 54:854-863. doi: 10.1002/art.21654 [doi].
23. Van Herwijnen MJ, Van Der Zee R, Van Eden W, Broere F. Heat shock proteins can be targets of regulatory T cells for therapeutic intervention in rheumatoid arthritis. *Int J Hyperthermia* (2013) 29:448-454. doi: 10.3109/02656736.2013.811546 [doi].
24. Curotto de Lafaille MA, Lafaille JJ. Natural and adaptive foxp3+ regulatory T cells: more of the same or a division of labor?. *Immunity* (2009) 30:626-635. doi: 10.1016/j.immuni.2009.05.002 [doi].
25. Kong N, Lan Q, Chen M, Wang J, Shi W, Horwitz DA, et al. Antigen-specific transforming growth factor beta-induced Treg cells, but not natural Treg cells, ameliorate autoimmune arthritis in mice by shifting the Th17/Treg cell balance from Th17 predominance to Treg cell predominance. *Arthritis Rheum* (2012) 64:2548-2558. doi: 10.1002/art.34513 [doi].
26. Kaye J, Hsu ML, Sauron ME, Jameson SC, Gascoigne NR, Hedrick SM. Selective development of CD4+ T cells in transgenic mice expressing a class II MHC-restricted antigen receptor. *Nature* (1989) 341:746-749. doi: 10.1038/341746a0 [doi].
27. DiPaolo RJ, Shevach EM. CD4+ T-cell development in a mouse expressing a transgenic TCR derived from a Treg. *Eur J Immunol* (2009) 39:234-240. doi: 10.1002/eji.200838772 [doi].
28. Picca CC, Larkin J, 3rd, Boesteanu A, Lerman MA, Rankin AL, Caton AJ. Role of TCR specificity in CD4+ CD25+ regulatory T-cell selection. *Immunol Rev* (2006) 212:74-85. doi: IMR416 [pii].
29. Apostolou I, Sarukhan A, Klein L, von Boehmer H. Origin of regulatory T cells with known specificity for antigen. *Nat Immunol* (2002) 3:756-763. doi: 10.1038/ni816 [doi].



Chapter 3

Matured tolerogenic dendritic cells modulate pre-activated and naïve CD4⁺ T cells and ameliorate proteoglycan induced arthritis in mice

Manon A.A. Jansen¹, Rachel Spiering^{2,3,4}, Irene S. Ludwig¹, Thomas Roodsant¹, Willem van Eden¹, Catharien M.U. Hilkens^{2,3,4}, Femke Broere^{1,5}

¹ Division of Immunology, Department of Infectious Diseases & Immunology, Utrecht University, Utrecht, The Netherlands

² Musculoskeletal Research Group, Institute of Cellular Medicine, Newcastle University, Newcastle upon Tyne

³ Arthritis Research UK Rheumatoid Arthritis Pathogenesis Centre of Excellence (RACE), UK

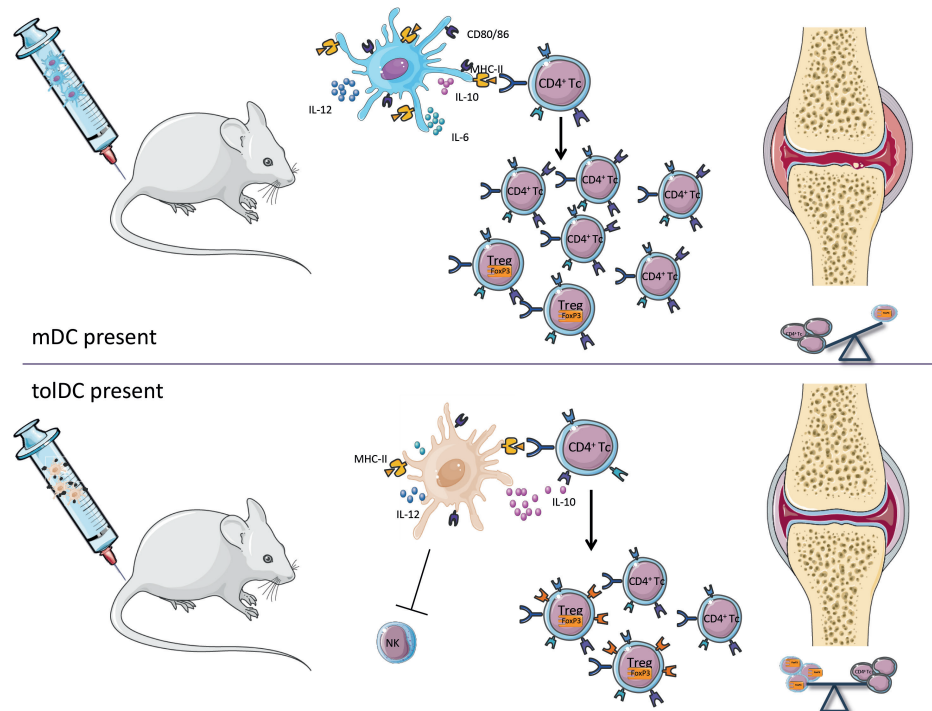
⁴ NIHR-Newcastle Biomedical Research Centre in Ageing and Long-Term Conditions, Newcastle upon Tyne Hospitals NHS Foundation Trust and Newcastle University, Newcastle upon Tyne, UK

⁵ Department of Clinical Sciences of Companion Animals, Faculty Veterinary Medicine, Utrecht University, Utrecht, The Netherlands

Submitted



Graphical abstract



Abstract

Tolerogenic dendritic cells (tolDCs) are a promising tool to restore immune tolerance in Rheumatoid arthritis. No cure is available yet, current medication is directed towards symptom suppression. In order to not only suppress disease but cure it, immune tolerance must be restored. To find out how tolDCs can restore tolerance we used murine tolDCs as a model. To be able to optimize tolDC vaccines in the future, we wanted to address the following questions: i) is a maturation stimulus needed for tolDCs to modulate CD4⁺ T cell responses *in vitro* and *in vivo*, ii) is antigen loading of tolDCs required to suppress arthritis. We co-cultured tolDCs, unstimulated or stimulated with a TLR4 agonist, with naïve CD4⁺ T cells. T cell characteristics were measured by flow cytometry and magpix. Next to this, we tested tolDC suppressive capabilities in an experimental arthritis model. We found that tolDCs modulate the CD4⁺ T cell response as shown by fewer proliferated and activated CD4⁺ T cells *in vitro* and *in vivo*. In addition, Tregs are multiplied in the proliferating cell population when in the presence of tolDCs. This indicates that CD4⁺ T cells are steered towards an immune-tolerant state. Furthermore, we show that when administering tolDCs pre-clinically they are capable to inhibit arthritis. However, a maturation stimulus is needed for tolDCs to manifest their tolerizing function in an inflammatory environment.

Keywords: Arthritis, tolDC, CD4⁺ T cell, immune modulation, immune tolerance



Introduction

Rheumatoid arthritis (RA) is an autoimmune disease characterized by chronic inflammation in the joints which causes cartilage and bone destruction¹. To date, there is no cure available and treatment is directed towards mitigating symptoms (NSAIDs) or dampening the immune response (DMARDs)^{2,3}. These therapies suppress the immune system non-specifically and thus are not completely effective and can cause many side effects. RA, as other chronic inflammatory diseases, is caused by a disbalance in the immune system. Immune tolerance is not maintained which means that autoreactive T cells can attack the body's own cells.

Regulatory T cells (Tregs), mainly CD4⁺ T cells, are able to restore immune tolerance by suppressing effector cells in an antigen-specific manner. In patients with autoimmune disease, it is thought that a subtle change in the function or presence of Tregs is involved in the pathogenesis of the disease. However, a lot of controversy exists in this area. Several studies show that the suppressive capacities of Tregs in synovial fluid of RA patients are diminished, while in peripheral blood these capacities are maintained⁴⁻⁶. Other studies indicate a decrease in Treg numbers^{7,8}, which could cause excessive inflammation in RA. Antigen specific Tregs are able to suppress this excessive inflammation by suppressing the immune cells that cause the pathological autoimmune response while leaving protective immunity intact.

As a tool to induce antigen specific Tregs, tolerogenic dendritic cells (toIDCs) can be used. ToIDCs are dendritic cells (DCs) that are modulated to become immune tolerance-inducing. Whether a DC is immune stimulatory or immune tolerant mainly depends on its maturation status. Additionally, the environmental cues the DCs receive determines if they become immunogenic or tolerogenic. By modulating DCs *in vitro*, they can be steered towards an immune tolerant status. Multiple approaches for inducing a tolerogenic function in antigen presenting cells *in vitro* have been described⁹⁻¹². We focus on the dexamethasone and 1 α ,25-dihydroxyvitamin D3 modulated DCs¹³⁻¹⁵.

The advantage of toIDCs is that they can be loaded with an antigen to specifically target autoreactive T cells without affecting other immune responses. Stoop *et al.* show that loading toIDCs with disease specific-antigen enhances their efficiency compared to unloaded toIDCs¹⁶. Some groups show that it is also possible to administer unloaded toIDCs¹⁷, but generating aspecific Tregs may give rise to general immune suppression thereby increasing the risk of infections. Furthermore, administering unloaded toIDCs might not actively induce Tregs but generate T

cell energy, which in turn can suppress excessive Th17 and Th1 responses¹⁸. Since the autoantigen that causes disease in RA is currently unknown, unloaded toIDC treatment could be an option.

However, since antigen loading is preferred in the case of RA, a surrogate antigen could be used when exploiting antigen loaded toIDC in this complex autoimmune disease. A possible candidate is one of the heat shock proteins (HSPs). HSPs are antigens that are upregulated during inflammation and ubiquitously expressed. Furthermore, due to their evolutionary conservation, multiple immune cells can recognize HSPs. Several studies have shown that HSPs can be used to induce tolerogenic responses in models for autoimmunity¹⁹⁻²¹.

Next to the issue of antigen loading, the stability of a toIDC is an important issue to address. Since DCs are essential for both tolerance and immunity they are the sentinels of the immune system. It is plausible that non-stimulated toIDCs change their phenotype when entering an immune stimulatory environment. Therefore, partial maturation with lipopolysaccharide (LPS)^{15,22}, monophosphoryl Lipid A (MPLA, lipid A portion of LPS)²³ or a cytokine cocktail²⁴ would be preferable. This potentially stabilizes the phenotype of the toIDC and improves antigen presentation and migration^{9,15}. A more complete understanding of the working mechanism of toIDCs will contribute to the development of toIDC treatment in the future. For that reason, we aimed to i) determine the role of maturation in murine dexamethasone and 1 α ,25-dihydroxyvitamin D3 induced toIDCs, ii) study if antigen loading of toIDCs is needed to modulate CD4⁺ T cell responses and suppress arthritis.

Materials and methods

Mice

Female Balb/cAnNCrl from 18-20 weeks old were purchased from Charles River laboratories for *in vivo* arthritis experiments. Male Balb/cAnNCrl from 10 weeks old were purchased from Charles River laboratories for co-transfer studies. mB29b T cell receptor (TCR) transgenic²⁵ and hPG TCR transgenic²⁶ mice were bred at the central animal laboratory of Utrecht University, the Netherlands. Both sexes were used as donor mice. Animals were kept under standard conditions of the animal facility and all experiments were approved by the Animal Experiment Committee of Utrecht University (project number AVD108002016467). Mice were randomly divided in control- or treatment groups and all animals were monitored and scored three times a week during the arthritis experiments.

BMDC culture

Bone marrow was isolated from the femur and tibia from Balb/cAnNCrI (both male and female) 10-20 weeks old mice and seeded 450,000 fresh cells/ml in 6 wells plates (Corning costar). As culture medium IMDM (Gibco) supplemented with 5% FCS (Bodinco), 100 units/ml penicillin, 100 µg/ml streptomycin and 5×10^{-5} M β-mercaptoethanol in the presence of 20 ng/ml GM-CSF (in house produced) was used. On day 2 an equal volume of fresh culture medium containing 20 ng/mL GM-CSF was added, and on day 4/5 20 ng/mL fresh GM-CSF was supplemented to the culture. Tolerogenicity was induced by adding 10^{-6} M dexamethasone (Invivogen) and 10^{-10} M 1α,25-dihydroxyvitamin D3 (Enzo Life sciences) to the BMDC culture on day 7. Simultaneously with the tolerogenic agents, peptide (hPG: ATEGRVRVNSAYQDK or B29: VLRIVNEPTAAALAY) and maturation stimuli (lipopolysaccharide (LPS); Sigma Aldrich and Monophosphoryl Lipid A (MPLA) from *Salmonella minnesota* R595; Invivogen) were added. After 8 days of culture at 37°C, 5% CO₂, the BMDCs or toIDCs were harvested for further experimentation. Before co-culture, BMDCs or toIDCs were replated into 24 wells plates (Corning costar). Before injection in co-transfer experiments, BMDCs or toIDCs were thoroughly washed with medium (2x) and PBS (1x) and kept on ice.

Co-cultures

For co-culture experiments, spleens from mB29b TCR transgenic mice were pooled and CD4⁺ cells were isolated using Dynal bead isolation (Invitrogen) by negatively selecting CD4⁺ T cells with a mixture of the following in house produced antibodies: anti-B220 (RA3-6B2), anti-CD11b (M1/70), anti-MHC-II (M5/114) and anti-CD8 (YTS169). To gain a naïve population, CD25⁺ and CD44⁺ cells were depleted by adding an anti-CD25 antibody (PC61, produced in house from hybridoma ATCC PC61 and purified from supernatants) and an anti-CD44 antibody (IM7.8, kindly provided by Tibor Glant) in predetermined optimal concentrations. The purified naïve CD4⁺ T cells were added to BMDCs in a 10:1 ratio.

Flow cytometry and antibodies

Flow cytometry was performed with FACS Canto II (BD) with monoclonal antibodies CD4-V500 (RM4-5, BD Biosciences), CD25-PerCP-Cy5.5 (PC61.5, ebioscience/Thermofisher), Thy1.1-PerCP-Cy5.5 (HIS51, ebioscience/Thermofisher), FoxP3-eFluor450 (FJK-16s, ebioscience/Thermofisher), CD62L PE (MEL-14, BD biosciences), NKp46 PE-Cy7 (29A1.4, ebioscience/Thermofisher) and CD3 APC (145-2C11, BD biosciences). Red blood cells were lysed with ACK (Ammonium-Chloride-Potassium) buffer. For BMDC phenotyping the following monoclonal antibodies were used:

I-A/I-E Horizon450 (M5/114.15.2, ebioscience/Thermofisher), CD11c APC (N418, ebioscience/Thermofisher), CD86 FITC (GL1, BD biosciences), PD-L1 PE (10F.9G2, Biolegend), IL12p40/70 PE (C15.6, BD biosciences). To identify dead cells the Zombie NIR fixable viability kit (Biolegend) was used.

Induction of PGIA

Human proteoglycan (hPG) was isolated from human articular cartilage as described²⁷. To induce arthritis, Balb/c mice were injected twice intraperitoneally with a mixture of 2 mg DDA and 250 µg human proteoglycan with a 21 day interval. Subsequently, mice were randomized among experimental groups, and arthritis scores were determined in a blinded fashion using a visual scoring system based on swelling and redness of paws as described²⁷. ToIDCs (1×10^6 cells in 200 µL PBS) were injected intravenously on day 17.

Co-transfers

Naïve CD4⁺ T cell co-transfer

CD4⁺CD25⁻CD44⁻ T cells were purified from spleens from hPG TCR transgenic Thy1.1⁺ mice by Dynal bead isolation (Invitrogen). The purified naïve CD4⁺ T cells were first labeled with 0.5 µM 5,6-carboxyfluorescein-succinimidyl-ester (CFSE, Invitrogen) and subsequently intravenously injected (max 10×10^6) in 200 µl PBS in acceptor mice (8-10 weeks old male Balb/cAnNCrI). On day one, 1×10^6 freshly cultured BMDCs or toIDCs were intravenously injected in the same acceptor mice. After 3 days, spleens from acceptor mice were harvested and transferred CD4⁺ T cells were tested on proliferation, activation and phenotype.

Activated CD4⁺ T cell co-transfer

On day -3 the donor hPG TCR transgenic Thy1.1⁺ mice were intra muscularly (left quadriceps) injected with 100 µg hPG peptide in 50 µl PBS. On day 0, CD4⁺ T cells were purified from spleens from hPG TCR transgenic Thy1.1⁺ mice by Dynal bead isolation (Invitrogen). The purified CD4⁺ T cells were first labeled with 0.5 µM 5,6-carboxyfluorescein-succinimidyl-ester (CFSE, Invitrogen) and subsequently intravenously injected in 200 µl PBS in acceptor mice (8-10 weeks old male Balb/cAnNCrI). On day one, 2×10^5 or 1×10^6 freshly cultured BMDCs (or toIDCs) were intravenously injected in the same acceptor mice. After 3 days, spleens from acceptor mice were harvested and transferred CD4⁺ T cells were tested on proliferation, activation and phenotype.

Cytokine analysis

Supernatants of *ex vivo* stimulations or co-cultures were used for multiplex cytokine

analysis of IL-10, IL-2, IL-6, IL-17, IFN- γ , IL-5 and IL-4, using the Magpix (Luminex XMAP) system according to manufacturer's instructions. Briefly, supernatant together with magnetic capture beads for the respective cytokines were added to polystyrene, black, 96 flat bottom plates, (Greiner bio-one, 655096). Subsequently, biotin-conjugated detection antibodies and Streptavidin-PE (BD Bioscience) were added and incubated together. The antibody pairs used:

Cytokine	Coating	Detecting
IL-2	JES6-1A12	JES6-5H4
IL-4	BVD-1D11	BVD6-24G2
IL-5	TRFK5	TRFK4
IL-6	MP5-20F3	MP5-32C11
IL-10	JES5-2A5	SXC-1
IL-17A	TC11-18H10	TC11-8H4.1
IFN- γ	AN-18	XMG1.2

The concentrations of cytokines in the tested samples were calculated using standard curves and the MFI data was analyzed using a 5-parameter logistic method (xPONENT software, Luminex, Austin, USA).

ELISpot

Multiscreen IP filter plate plates (Milipore) were activated with 70% Ethanol and coated with a rat anti-mouse anti-IFN- γ antibody (clone AN-18, in house produced) or anti-IL-10 antibody (JES5-2A5, in house produced) at 2 μ g/ml in PBS and then blocked with IMDM medium supplemented with 5% FCS. Subsequently, single cell suspensions of spleen from co-transferred acceptor mice were cultured in 200 μ l complete medium for 48 hours in 96-wells flat bottom plates (Corning) at 5x10⁶ cells/ml. Medium or 20 μ g/ml hPG peptide were added as restimulation. After culture, the plates were washed and the IFN- γ or IL-10 producing cells were detected using the rat anti-mouse biotin-anti-IFN- γ antibody (clone XMG1.2, BD biosciences) or rat anti-mouse biotin-anti-IL-10 antibody (clone SXC-1, BD biosciences) respectively. Streptavidin-alkaline phosphatase (Sigma, S2890) and BCIP/NPT solution (Roche) were used to visualize the spots according to manufacturer's instructions. Counting of the IFN- γ or IL-10 producing cells was done by the Automated ELISpot Assay Video Analysis System (A.EL.VIS GmbH).

Statistical analyses

The following statistical analyses were performed using Prism 7.04: repeated measures analysis of variance (ANOVA) with Dunnett or Bonferroni correction for comparisons between multiple groups, paired Student t-test for comparisons between two groups.

Results

ToIDCs exhibit a semi-mature phenotype

First, we investigated the change in phenotype of (to)DCs after stimulation with a TLR4 agonist and their stability *in vitro*. DCs were generated from bone marrow and treated with dexamethasone and the active form of vitamin D3 to develop toIDCs. Untreated bone marrow derived dendritic cells (BMDCs) were used as controls. To compare the phenotype of BMDCs and toIDCs, both cell types were measured unstimulated or after stimulation with the lipid A portion of LPS: MPLA. The toIDCs exhibited a semi-mature phenotype, consisting of a lower expression of MHC-II, CD86 and a higher PD-L1/CD86 ratio compared to control BMDCs (Figure 1b). Furthermore, the toIDCs produced a lower amount of pro-inflammatory cytokines IL-12 and IL-6, and a trend towards more anti-inflammatory IL-10 (Figure 1c) which is important since cytokine signaling is one of the mechanisms of DCs to communicate. Considering the toIDCs were generated for *in vivo* use, the stability of the toIDCs was tested by challenging them with a pro-inflammatory cytokine mix (IL-1 β , GM-CSF, IL-6, TNF and IFN- γ). After a 24h challenge, the pro-inflammatory milieu did not significantly increase the IL-12p70, MHC-II or PD-L1/CD86 ratio (Figure 1d).

Peptide pulsed toIDCs hamper CD4⁺ T cell activation *in vitro*

To study their function, unstimulated (itoIDCs) or MPLA stimulated toIDCs (mtolDCs) were co-cultured with naïve CD4⁺ T cells from an mB29b-TCR transgenic mouse²⁵. mB29b is a peptide of mammalian HSP70²⁸. BMDCs were used as controls. After three days of co-culture with toIDCs, either immature or mature, fewer CD4⁺ T cells expressed the activation marker CD25. Additionally, more CD4⁺ T cells expressed CD62L (L-selectin) compared to the controls (Figure 2a). Next to this, there was a trend towards more CD4⁺FoxP3⁺ cells after co-culturing with toIDCs (Figure 2a). To address CD4⁺ T cell activation and differentiation status, as indicated by cytokine profile, culture supernatants were analyzed by Magpix. The results shown in figure 2b show that toIDCs impair pro-inflammatory cytokine production of the CD4⁺ T cells by two to twenty fold compared to CD4⁺ T cells stimulated by control DC. Only the anti-inflammatory cytokine IL-10 was produced in higher amounts by the CD4⁺ T cells that were in co-culture with toIDCs, indicating that these T cells contain a more regulatory character. Thus, toIDCs modulate CD4⁺ T cell activation and drives them towards an immune tolerant state. In these experiments, maturation of the toIDCs did not influence their effect on CD4⁺ T cells.



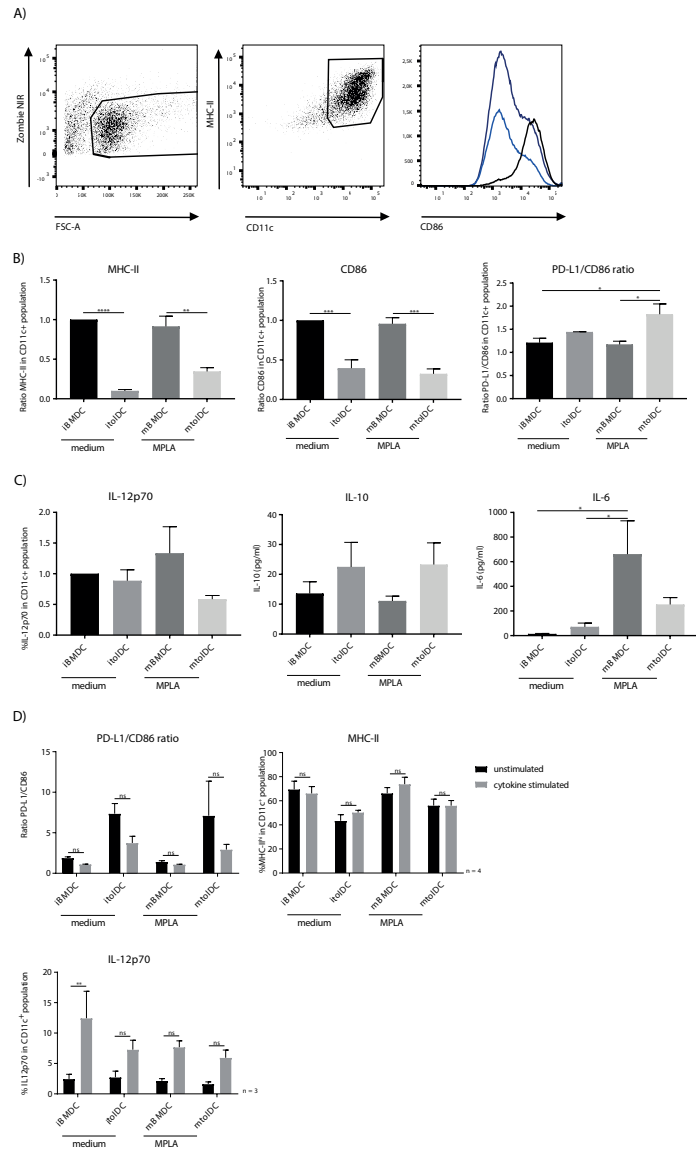


Figure 1. ToIDCs exhibit a semi-mature phenotype and remain stable after challenge *in vitro*.

ToIDCs were generated by adding dexamethasone and 1,25-dihydroxyvitamin D3 and stimulated with MPLA or medium as control. Phenotype was measured by flow cytometry. In the histogram, mBMDCs (black line), itoIDCs (light blue) and mtolDCs (dark blue) representatives are shown (A). The ratio to immature BMDC was used to determine the difference in expression of MHC-II, CD86 and PD-L1 (B). Cytokine production (C) was measured in the supernatant by Magpix (IL-10, IL-6, GM-CSF) or intracellular by flow cytometry (IL-12p70). To test the stability of toIDCs *in vitro*, toIDCs were stimulated for 24 hrs with a pro-inflammatory cytokine mix (IL-1 β , GM-CSF, IL-6, TNF and IFN- γ). After 24 hrs, the phenotype of the (to)IDCs was measured by flow cytometry (D). Two-tailed paired student T-test was used. * $p \leq 0.05$, ** $p \leq 0.01$, *** $p \leq 0.001$. N = 4

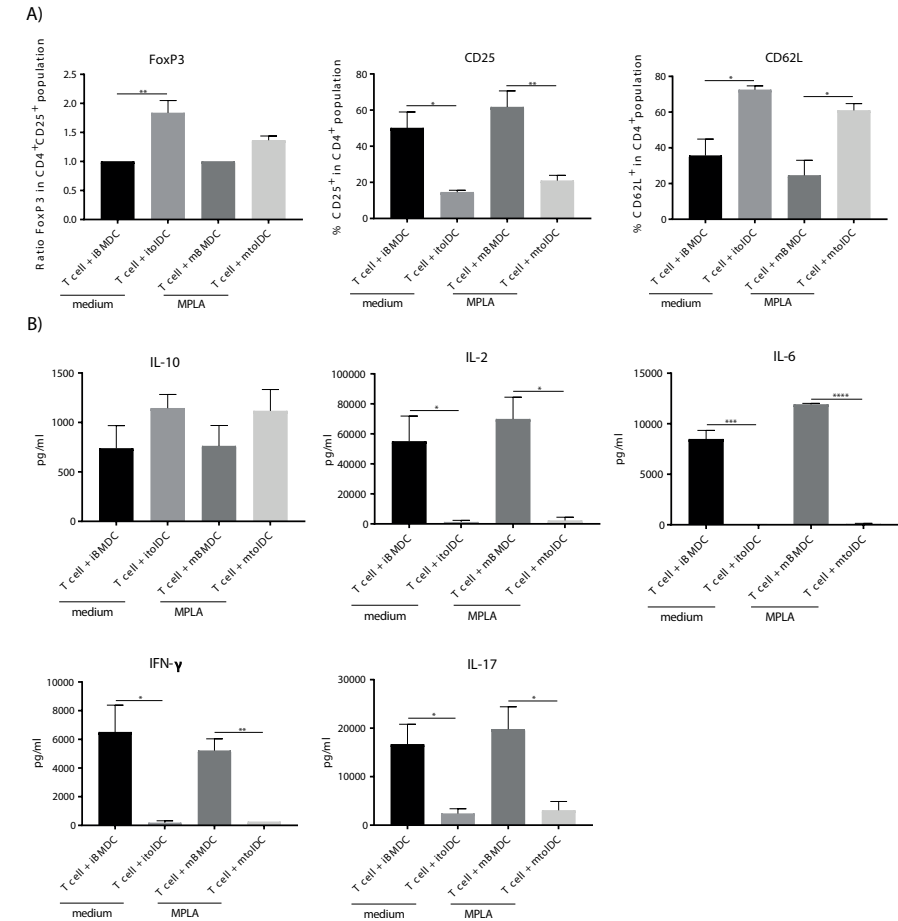


Figure 2. ToIDCs hamper the activation of CD4⁺ T cells antigen specifically *in vitro*.

BMDCs, itoIDCs or (MPLA stimulated) mtolDCs were pulsed with B29 and co-cultured for three days with naïve (CD25⁺ and CD44⁺ depleted) CD4⁺ T cells from a mB29b-TCR transgenic mouse. On day 3, phenotype of the CD4⁺ T cells was determined by flow cytometry (A). For FoxP3, the ratio to CD4⁺ T cells that were in co-culture with BMDCs was used to compare the difference when co-culturing with toIDCs. As markers for activation status of the CD4⁺ T cell, CD25 and CD62L (L-selectin) were measured. Cytokine production was measured after co-culture in the supernatant by Magpix (B). Two-tailed paired student T-test was used. * $p \leq 0.05$, ** $p \leq 0.01$, *** $p \leq 0.001$. N = 4

ToIDCs restrict the activation of naïve antigen specific CD4⁺ T cells *in vivo*

To determine if toIDCs modulate CD4⁺ T cells *in vivo* as suggested by the *in vitro* experiments (Figure 2), we performed co-transfer experiments. First, we transferred naïve hPG-TCR transgenic CD4⁺ T cells and subsequently (one day later) itoIDCs or mtolDCs pulsed with hPG peptide into a naïve acceptor mouse. As a control, LPS matured BMDCs (mBMDCs) loaded with hPG peptide were transferred with naïve CD4⁺ T cells instead of toIDCs. The CD4⁺ T cells that were co-transferred with mBMDCs proliferated nearly 100%, while the CD4⁺ T cells that were co-transferred with itoIDCs or mtolDCs proliferated respectively 45% and 75% (Figure 3a). At the same time, the CD25 expression was lower on the CD4⁺ T cells and the CD62L expression was higher on CD4⁺ T cells compared to the control (Figure 3a+b). This indicates that next to *in vitro* modulation, both toIDC types can also modulate the CD4⁺ T cell response *in vivo*. In addition, the percentage CD4⁺FoxP3⁺ in the total transferred cells was not significantly increased when toIDCs were co-transferred. However, in the proliferating cells we observe a trend towards a higher percentage CD4⁺FoxP3⁺ cells when toIDCs were present (Figure 3c).

To further define the phenotype of the CD4⁺ T cells *ex vivo*, IL-10 and IFN- γ secreting cells were measured by ELISpot. The amount of IL-10 producing antigen specific CD4⁺ T cells was similar when toIDCs or mBMDCs were present *in vivo*, but the amount of IFN- γ producing cells was lower when mice were co-transferred with toIDCs (Figure 3d). In addition, splenocytes were antigen specifically restimulated for 72 hrs. Next, cytokine production by these cells was measured. The cytokine measurements show a similar image as the ELISpot: pro-inflammatory cytokines IL-5, IL-4, IL-6, IL-17A, TNF and IFN- γ are produced less by cells from mice that were co-transferred with toIDCs compared to mBMDCs (Supplemental figure 3). Moreover, the IL-2 production by *ex vivo* stimulated splenocytes is increased when mice received toIDCs. These results confirm that CD4⁺ T cell activation is constrained after encountering toIDCs *in vivo*.

ToIDCs are capable of modifying activated CD4⁺ T cells

Since toIDCs are intended to be used as therapeutic agents under inflammatory conditions, restraining the activation of naïve CD4⁺ T cells alone is not sufficient. Therefore, we performed co-transfer studies with activated CD4⁺ T cells to establish if toIDCs are capable to modify such proinflammatory T cells. We co-transferred toIDCs or mBMDCs pulsed with peptide and activated peptide-specific CD4⁺ T cells into a naïve acceptor Balb/c mouse. Both itoIDCs and mtolDCs inhibited proliferation and further activation of the peptide-specific CD4⁺ T cells *in vivo* (Figure 4a), similar as was seen when naïve CD4⁺ T cells were injected. Next to this, in mice that were injected

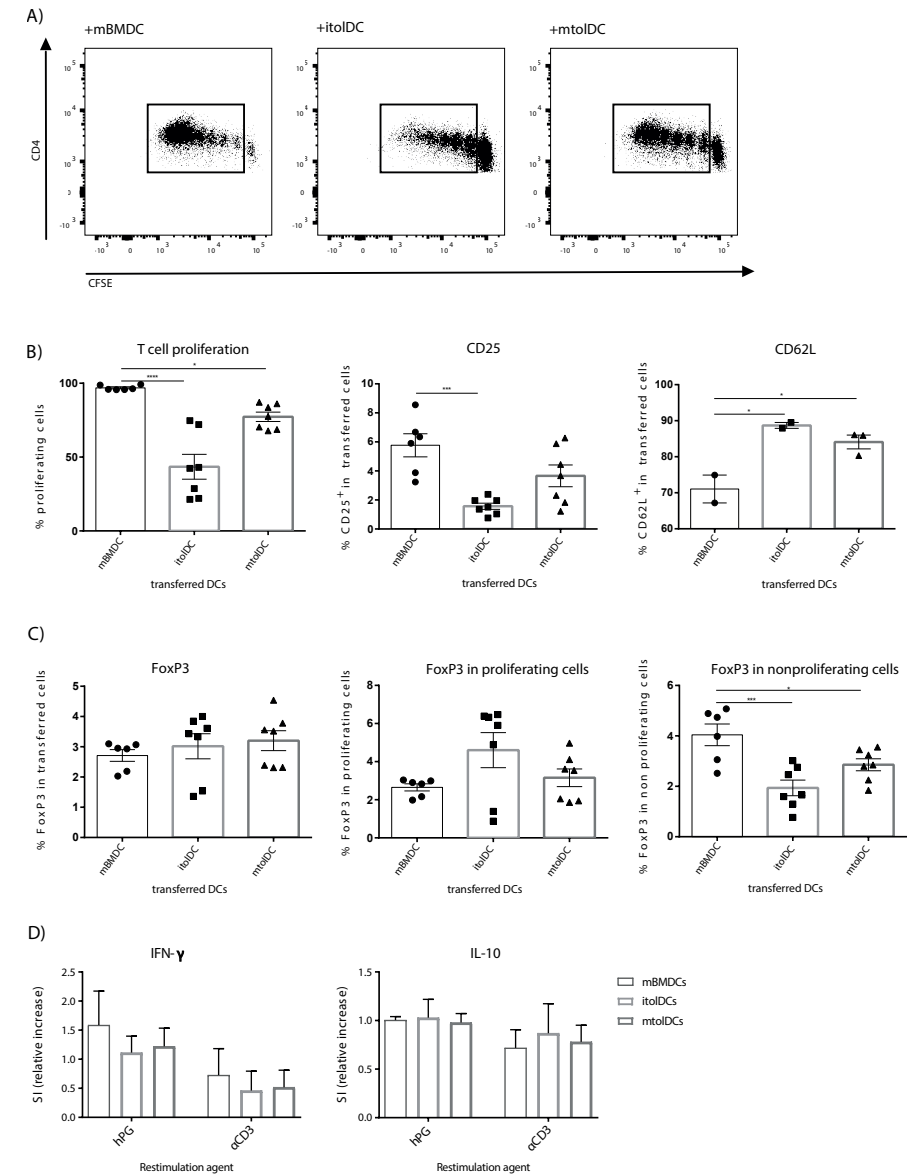


Figure 3. ToIDCs restrict the activation of naïve antigen specific CD4⁺ T cell *in vivo*.

(Im)mature toIDCs or mature BMDCs were pulsed with hPG peptide and transferred (1E6 cells/injection) one day after the naïve CFSE labeled hPG TCR transgenic CD4⁺ T cells. Proliferation (A) and phenotype from the transferred CD4⁺ T cells was measured by flow cytometry (B/C). Each symbol represents an individual mouse. To further examine the activation status of the transferred CD4⁺ T cells, splenocytes were stimulated with hPG (antigen specific) or soluble aCD3 (general). After three days, IFN γ and IL-10 producing cells were measured by ELISpot (D). One way ANOVA (Dunnett) was used. *p \leq 0.05, **p \leq 0.01, ***p \leq 0.001.

with toIDCs, not only more Tregs (CD4⁺CD25⁺FoxP3⁺) were measured, but these Tregs were also more activated when compared to mice that received mBMDCs (Figure 4b). In addition, the spleens of toIDC treated mice contained more naïve CD4⁺ T cells as shown by the CD62L positive cells (Figure 4a). These results indicate that toIDCs are not only able to modulate naïve CD4⁺ T cells but also activated CD4⁺ T cells *in vivo*. Mice in which activated CD4⁺ T cells were co-transferred with toIDCs or mBMDCs pulsed with an irrelevant peptide did not show any proliferation or activation of the peptide-specific CD4⁺ T cells, showing that they are antigen dependent (data not shown). Together with the transfer of CD4⁺ T cells, NK cells were transferred since the purity of CD4⁺ T cells is not 100%. When analyzing the state and amount of NK cells after co-transfer with mBMDCs or toIDCs, we noticed that when NK cells were co-transferred with toIDCs, the amount of donor NK cells was lower compared to the mBMDC co-transferred NK cells (Supplemental figure 5).

Besides investigating the ability of toIDCs to modulate active CD4⁺ T cells, we tested if the effect of the toIDCs is dose dependent. In addition to the 1 x 10⁶ mBMDCs or toIDCs, we injected mice with a five times lower dose (2 x 10⁵). The striking result was that even at such a low dose, the toIDCs retained their effects on the CD4⁺ T cells. Activated CD4⁺ T cells that were co-transferred with toIDCs, both immature as MPLA matured, show a decrease in activation and an increase in activated Tregs (Supplemental figure 4). This shows that even if the toIDC dosage is lowered, toIDCs are capable of reducing antigen specific CD4⁺ T cell activation.

ToIDCs ameliorate proteoglycan induced arthritis

To establish if toIDCs are able to affect arthritic symptoms, we performed *in vivo* arthritis studies in the PGIA model. Female Balb/c mice were injected with hPG protein and dimethyl-dioctadecylammonium (DDA) two times intraperitoneal with a three week interval to induce arthritis. Unloaded toIDCs or toIDCs loaded with a non-disease inducing antigen (B29 peptide) or hPG peptide were injected intravenously in the pre-clinical phase of disease. As pre-clinical phase is considered the stage in which the mice received the first immunization with hPG protein and DDA and thus develop antibodies against hPG but do not experience symptoms yet²⁹. Mice treated with immature unstimulated toIDCs (itoIDCs) showed equal arthritis scores compared to the PBS animals (Figure 5a). Treatment with mtolDCs unloaded or loaded with hPG resulted in a reduced and delayed development of arthritis (Figure 5b). The mice that were injected with mtolDCs pulsed with the non-disease inducing antigen showed a trend towards a decrease in PGIA score. No significant difference was observed between mice that were injected with unloaded mtolDCs or mtolDCs loaded with hPG peptide. These results indicate that toIDCs

need a maturation stimulus to execute their function *in vivo*. Taking the day of onset and maximum arthritis score into account (table 1, data combined from two independent *in vivo* studies), the mice that were treated with mtolDCs do not only experience significantly decreased arthritis but develop symptoms at a later time point than PBS mice.

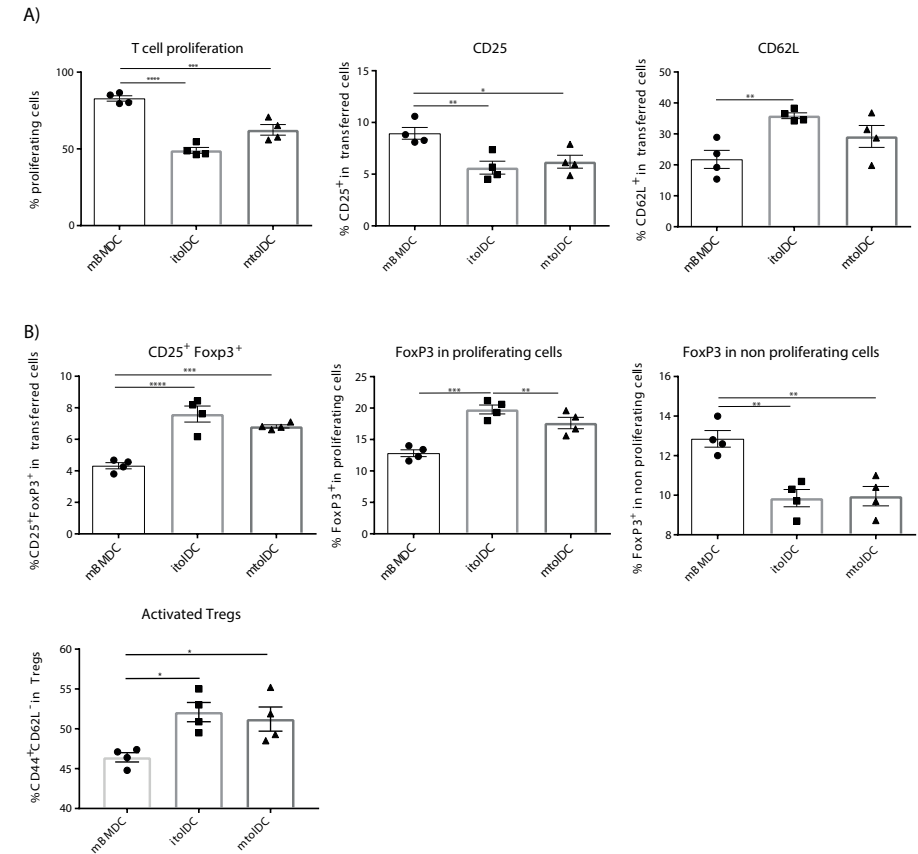


Figure 4. ToIDCs pulsed with peptide inhibit further activation of CD4⁺ T cells *in vivo*.

First, hPG TCR transgenic CD4⁺ T cells were activated *in vivo* by injecting hPG peptide i.m. into the transgenic mice. After three days, CD4⁺ TCR transgenic T cells were isolated and transferred into a naïve Balb/c acceptor mouse. One day later, hPG pulsed (im)mature toIDCs or mature BMDCs were injected into the acceptor mice. After three days, phenotype and proliferation of the transferred CD4⁺ T cells was measured by flow cytometry (A/B). One way ANOVA (Dunnett) was used. *p<0.05, **p<0.01, ***p<0.001.

Ex vivo analyses of spleen and draining lymph nodes (popliteal lymph nodes) show that Tregs (defined as CD4⁺CD25⁺FoxP3⁺ cells) are present in lower quantities in the spleen (Figure 5c) in antigen-pulsed mtolDC treated mice, while in the popliteal lymph node there are more Tregs present in mice that received antigen-pulsed mtolDCs (Figure 5c). The arthritis experiments described show that toIDC treatment can be effective if toIDCs are stimulated prior to infusion with MPLA.

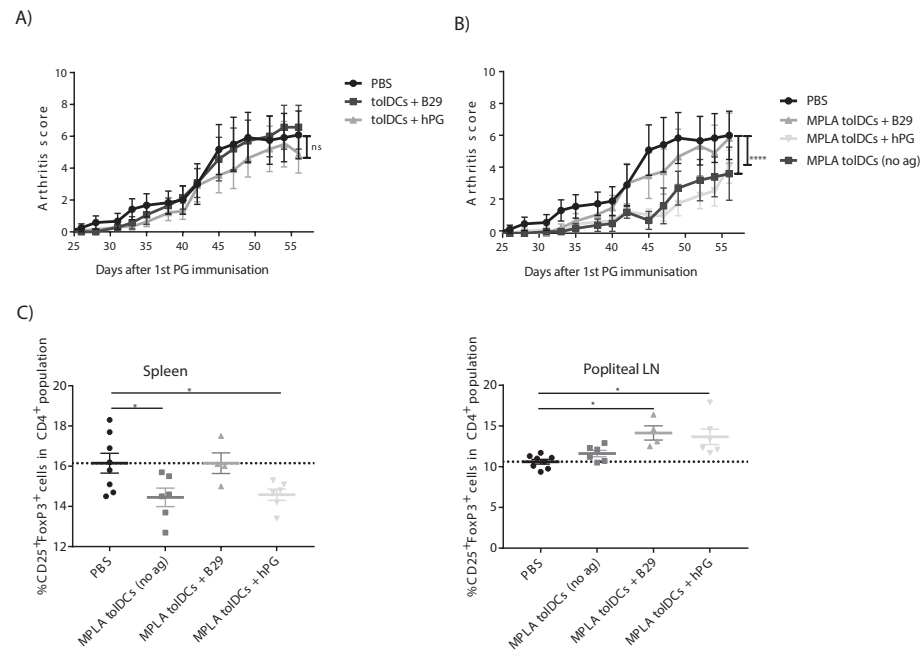


Figure 5. ToIDCs matured with MPLA ameliorate PGIA in an antigen independent fashion.

Arthritis was induced by injecting the mice two times with hPG protein and DDA. After the second injection, the mice developed arthritic symptoms. ToIDCs (1×10^6 cells in 200 μ L PBS) were administered intravenously on day 17, before the second hPG/DDA injection. Mice were scored three times a week for arthritis. The arthritis scores are based on a visual scoring system. Mice received either immature toIDCs (A) pulsed with disease specific antigen (hPG) or an inflammatory mediated disease irrelevant peptide (B29), or MPLA matured toIDCs (B) unloaded or pulsed with the same peptides. (C) The percentage Tregs (CD4⁺CD25⁺FoxP3⁺) was analysed *ex vivo* in the spleen and popliteal lymph nodes by flow cytometry. Two way ANOVA (Dunnnett) was used. * $p \leq 0.05$, ** $p \leq 0.01$, *** $p \leq 0.001$.

Table 1. MPLA toIDCs ameliorate PGIA and delay the onset of disease.

Group	Day of onset	Maximum arthritis score
PBS	35,36 \pm 8,0	5,82 \pm 3,52
MPLA toIDCs (no ag)	41,27 \pm 7,45	3,36 \pm 3,44
MPLA toIDCs + B29	40,4 \pm 5,68	4,85 \pm 3,80
MPLA toIDCs + hPG	41,85 \pm 7,49	3,269 \pm 2,48

MPLA stabilized toIDCs reduce arthritis scores (maximum arthritis scores) and delay the onset of PGIA (day of onset) when compared to the PBS group. As day of onset is considered the first day that a mouse has a score of 1.

Discussion

ToIDCs are a potential tool to restore immune tolerance in rheumatoid arthritis. In this study we addressed two questions. The first question was to establish if toIDCs need maturation to influence CD4⁺ T cells *in vitro* and *in vivo*. To answer the second question, we investigated if maturation and antigen loading of toIDCs is necessary to induce tolerance in an experimental arthritis model.

The matter of stability of toIDCs is an important issue to address. Immature toIDCs could be unstable and thus differentiate into an immunogenic DC under inflammatory conditions^{30,31}. Therefore, we tested the stability of immature and matured toIDCs in *in vitro* experiments. After stimulation with a mixture of pro-inflammatory cytokines no significant increase in toIDC markers were observed, indicating that toIDCs were stable as also shown by others^{22,23,32}. Despite these results it does not provide an insight in the stability of toIDCs *in vivo*. However, a study performed by Griffin *et al* in 2001 shows that toIDCs induced with 1 α ,25-dihydroxyvitamin D3 are also stable *in vivo*. Since maturation of toIDCs might not only be required for stability but also for function of toIDCs^{9,15}, we tested LPS stimulated toIDCs next to unstimulated and MPLA stimulated toIDCs. LPS stimulation gave similar similar results (Supplemental figure 1 and 2). To assess the, possibly antigen-specific, effects of toIDCs on CD4⁺ T cells, we made use of a CD4⁺ TCR transgenic mouse. When naïve CD4⁺ T cells were in co-culture with toIDCs loaded with B29, their phenotype was modulated into an immune-regulatory state (Figure 2). Unloaded toIDCs were not able to alter the CD4⁺ T cells, which implies that the interaction is antigen specific (data not shown).



In vivo, toIDCs hampered the activation and proliferation of both naïve as pre-activated CD4⁺ T cells (Figure 3 and 4). These toIDC effects on CD4⁺ T cells are antigen dependent: only peptide-specific toIDCs and not toIDCs pulsed with an irrelevant peptide were able to modulate the antigen specific CD4⁺ T cells (data not shown). Remarkably, the toIDC dose did not affect the ability of toIDCs to restrain CD4⁺ T cell activation; both dosages of toIDCs (1×10^6 and 2×10^5) were successful (Figure 4 and supplemental figure 4). Since lowering the toIDC dose five times did not affect the outcome, it is interesting to determine if the dosage could be lowered even further.

Consequently, the itoIDCs and mtolDCs (MPLA stimulated) were tested in the *in vivo* arthritis model. As shown in Figure 5, toIDCs need stimulation with MPLA to exert their function in the arthritis model. However, itoIDCs were also efficient in modulating the CD4⁺ T cell response *in vitro* or in the co-transfer studies. We hypothesize that this difference is caused by the proinflammatory milieu in the arthritis experiments, which is not present *in vitro* or in the *in vivo* co-transfer experiments. itoIDCs are able to modulate CD4⁺ T cells in these 'neutral' environments, but when a proinflammatory milieu is present they are not potent enough to induce tolerance and/or disease suppressing responses. Maturation induces metabolic changes in the DC which are essential for stabilization, cell survival and function^{32,33}.

The analysis of local and systemic Treg presence *ex vivo* (Figure 5c) implies that the Tregs that are present migrate to the site of inflammation under the influence of mtolDCs. Furthermore, antigen loading of toIDCs did not significantly enhance the efficacy of therapy. Both the unloaded mtolDC as the hPG loaded mtolDC injections caused reduced and delayed arthritis symptoms in the treated mice. However, this antigen-independence might be evoked by the fact that the mtolDCs were administered before the second injection with hPG/DDA. A possible explanation for the reduction of arthritis by unloaded toIDCs is that they took up hPG *in vivo* since by injecting hPG/DDA, a depot is formed. Thereby, unloaded toIDCs could inhibit arthritis in an antigen-specific manner.

Next to this, we preliminary studies have shown that if we add supernatant from cultured toIDCs to antigen presenting cells in the presence of CD4⁺ T cells *in vitro*, the proliferation of the CD4⁺ T cells is abrogated (unpublished observations), indicating that the toIDCs exert their function, at least partly, via soluble mediators such as cytokines.

Another possible explanation for the efficiency of unloaded mtolDCs is the dose. Possibly, if the injected mtolDC dose is lowered, the antigen does play a role since there are fewer general anti-inflammatory signals present. Besides the mtolDC dose, the route of administration could influence the working mechanism of the mtolDCs. After intravenous injection, DCs mainly travel to the lungs, liver and spleen where they encounter other immune cells^{34,35}. To develop a toIDC therapy, the injection frequency must also be optimized. In this study, we show that one mtolDC injection provides significant healthier mice in the groups that were treated with unloaded toIDCs or hPG loaded toIDCs. However, for the toIDCs loaded with irrelevant peptide, the mice only showed significantly less arthritic symptoms after two dosages of toIDCs (data not shown). For this reason the longevity of a toIDC injection has to be investigated in future research. Next to optimizing the dose, frequency and route of administration, a follow-up study should also include therapeutic injections with toIDCs.

Based on the *in vitro* co-cultures and the *in vivo* co-transfers, we hypothesize that toIDCs provide immune-tolerant signals to other immune cells, like CD4⁺ T cells as investigated in this study, and steer those immune cells towards an immune modulatory state. The observation in our study that toIDCs also influence the presence of NK cells (Supplemental figure 5) shows that toIDCs also influence other immune cells besides T cells. It might also be possible that toIDCs transfer their tolerogenicity to other APCs, thereby spreading tolerance. The effects on CD4⁺ T cells seem antigen dependent but the spreading of tolerance could also be elicited by anti-inflammatory cytokines or extracellular vesicles carrying immune-modulating molecules derived from the toIDC.

Acknowledgements

The authors would like to thank Peter van Kooten for technical assistance and breeding the transgenic mice. This research was supported by the Dutch arthritis foundation (projects 13-3-303 and 14-3-301). This project has received funding from the European Union's Horizon 2020 research and innovation programme under the Marie Skłodowska-Curie grant agreement no 654882.

This work was supported by a grant from the European Cooperation in Science and Technology (COST) for the AFACTT project (Action to Focus and Accelerate Cell-based Tolerance-inducing Therapies; BM1305). COST is part of the EU Framework Programme Horizon 2020.

Conflict of interest

WvE has shares in Trajectum Pharma Inc., a SME that develops HSP peptides for immunotherapy.

References

1. Aletaha D, Neogi T, Silman AJ, et al. 2010 rheumatoid arthritis classification criteria: An american college of rheumatology/european league against rheumatism collaborative initiative. *Ann Rheum Dis*. 2010;69(9):1580-1588. doi: 10.1136/ard.2010.138461 [doi].
2. Crofford LJ. Use of NSAIDs in treating patients with arthritis. *Arthritis Res Ther*. 2013;15 Suppl 3:S2. doi: 10.1186/ar4174 [doi].
3. Johnsen AK, Weinblatt ME. Methotrexate: The foundation of rheumatoid arthritis therapy. In: *Rheumatoid arthritis*. Philadelphia, USA: Mosby; 2009:307-314. <https://doi.org/10.1016/B978-032305475-1.50002-1>.
4. van Amelsfort JM, Jacobs KM, Bijlsma JW, Lafeber FP, Taams LS. CD4(+)CD25(+) regulatory T cells in rheumatoid arthritis: Differences in the presence, phenotype, and function between peripheral blood and synovial fluid. *Arthritis Rheum*. 2004;50(9):2775-2785. doi: 10.1002/art.20499 [doi].
5. Herrath J, Muller M, Amoudruz P, et al. The inflammatory milieu in the rheumatic joint reduces regulatory T-cell function. *Eur J Immunol*. 2011;41(8):2279-2290. doi: 10.1002/eji.201041004 [doi].
6. Wang T, Sun X, Zhao J, et al. Regulatory T cells in rheumatoid arthritis showed increased plasticity toward Th17 but retained suppressive function in peripheral blood. *Ann Rheum Dis*. 2015;74(6):1293-1301. doi: 10.1136/annrheumdis-2013-204228 [doi].
7. Lawson CA, Brown AK, Bejarano V, et al. Early rheumatoid arthritis is associated with a deficit in the CD4+CD25high regulatory T cell population in peripheral blood. *Rheumatology (Oxford)*. 2006;45(10):1210-1217. doi: kel089 [pii].
8. Xiao H, Wang S, Miao R, Kan W. TRAIL is associated with impaired regulation of CD4+CD25- T cells by regulatory T cells in patients with rheumatoid arthritis. *J Clin Immunol*. 2011;31(6):1112-1119. doi: 10.1007/s10875-011-9559-x [doi].
9. Boks MA, Kager-Groenland JR, Haasjes MS, Zwaginga JJ, van Ham SM, ten Brinke A. IL-10-generated tolerogenic dendritic cells are optimal for functional regulatory T cell induction--a comparative study of human clinical-applicable DC. *Clin Immunol*. 2012;142(3):332-342. doi: 10.1016/j.clim.2011.11.011 [doi].
10. Tan PH, Yates JB, Xue SA, et al. Creation of tolerogenic human dendritic cells via intracellular CTLA4: A novel strategy with potential in clinical immunosuppression. *Blood*. 2005;106(9):2936-2943. doi: 2005-05-1826 [pii].
11. Kim SH, Kim S, Oligino TJ, Robbins PD. Effective treatment of established mouse collagen-induced arthritis by systemic administration of dendritic cells genetically modified to express FasL. *Mol Ther*. 2002;6(5):584-590. doi: S1525001602907124 [pii].
12. Zheng J, Jiang HY, Li J, et al. MicroRNA-23b promotes tolerogenic properties of dendritic cells in vitro through inhibiting Notch1/NF-kappaB signalling pathways. *Allergy*. 2012;67(3):362-370. doi: 10.1111/j.1398-9995.2011.02776.x [doi].
13. Pedersen AE, Gad M, Walter MR, Claesson MH. Induction of regulatory dendritic cells by dexamethasone and 1alpha,25-dihydroxyvitamin D(3). *Immunol Lett*. 2004;91(1):63-69. doi: S016524780300258X [pii].
14. Anderson AE, Sayers BL, Haniffa MA, et al. Differential regulation of naive and memory CD4+ T cells by alternatively activated dendritic cells. *J Leukoc Biol*. 2008;84(1):124-133. doi: 10.1189/jlb.1107744 [doi].
15. Anderson AE, Swan DJ, Sayers BL, et al. LPS activation is required for migratory activity and antigen presentation by tolerogenic dendritic cells. *J Leukoc Biol*. 2009;85(2):243-250. doi: 10.1189/jlb.0608374 [doi].

16. Stoop JN, Harry RA, von Delwig A, Isaacs JD, Robinson JH, Hilkens CM. Therapeutic effect of tolerogenic dendritic cells in established collagen-induced arthritis is associated with a reduction in Th17 responses. *Arthritis Rheum.* 2010;62(12):3656-3665. doi: 10.1002/art.27756 [doi].
17. Funda DP, Golias J, Hudcovic T, Kozakova H, Spisek R, Palova-Jelinkova L. Antigen loading (e.g., glutamic acid decarboxylase 65) of tolerogenic DCs (tolDCs) reduces their capacity to prevent diabetes in the non-obese diabetes (NOD)-severe combined immunodeficiency model of adoptive cotransfer of diabetes as well as in NOD mice. *Front Immunol.* 2018;9:290. doi: 10.3389/fimmu.2018.00290 [doi].
18. Maggi J, Schinnerling K, Pesce B, Hilkens CM, Catalan D, Aguillon JC. Dexamethasone and monophosphoryl lipid A-modulated dendritic cells promote antigen-specific tolerogenic properties on naive and memory CD4⁺ T cells. *Front Immunol.* 2016;7:359. doi: 10.3389/fimmu.2016.00359 [doi].
19. Wieten L, van der Zee R, Spiering R, et al. A novel heat-shock protein coinducer boosts stress protein Hsp70 to activate T cell regulation of inflammation in autoimmune arthritis. *Arthritis Rheum.* 2010;62(4):1026-1035. doi: 10.1002/art.27344 [doi].
20. van Herwijnen MJ, Wieten L, van der Zee R, et al. Regulatory T cells that recognize a ubiquitous stress-inducible self-antigen are long-lived suppressors of autoimmune arthritis. *Proc Natl Acad Sci U S A.* 2012;109(35):14134-14139. doi: 10.1073/pnas.1206803109 [doi].
21. Kolinski T, Marek-Trzonkowska N, Trzonkowski P, Siebert J. Heat shock proteins (HSPs) in the homeostasis of regulatory T cells (tregs). *Cent Eur J Immunol.* 2016;41(3):317-323. doi: 10.5114/ceji.2016.63133 [doi].
22. Unger WW, Laban S, Kleijwegt FS, van der Slik AR, Roep BO. Induction of treg by monocyte-derived DC modulated by vitamin D3 or dexamethasone: Differential role for PD-L1. *Eur J Immunol.* 2009;39(11):3147-3159. doi: 10.1002/eji.200839103 [doi].
23. Harry RA, Anderson AE, Isaacs JD, Hilkens CM. Generation and characterisation of therapeutic tolerogenic dendritic cells for rheumatoid arthritis. *Ann Rheum Dis.* 2010;69(11):2042-2050. doi: 10.1136/ard.2009.126383 [doi].
24. Raich-Regue D, Naranjo-Gomez M, Grau-Lopez L, et al. Differential effects of monophosphoryl lipid A and cytokine cocktail as maturation stimuli of immunogenic and tolerogenic dendritic cells for immunotherapy. *Vaccine.* 2012;30(2):378-387. doi: 10.1016/j.vaccine.2011.10.081 [doi].
25. Jansen MA, van Herwijnen MJ, van Kooten PJ, et al. Generation of the first TCR transgenic mouse with CD4(+) T cells recognizing an anti-inflammatory regulatory T cell-inducing Hsp70 peptide. *Front Immunol.* 2016;7:90. doi: 10.3389/fimmu.2016.00090 [doi].
26. Berlo SE, van Kooten PJ, Ten Brink CB, et al. Naive transgenic T cells expressing cartilage proteoglycan-specific TCR induce arthritis upon in vivo activation. *J Autoimmun.* 2005;25(3):172-180. doi: S0896-8411(05)00125-3 [pii].
27. Hanyecz A, Berlo SE, Szanto S, Broeren CP, Mikecz K, Glant TT. Achievement of a synergistic adjuvant effect on arthritis induction by activation of innate immunity and forcing the immune response toward the Th1 phenotype. *Arthritis Rheum.* 2004;50(5):1665-1676. doi: 10.1002/art.20180 [doi].
28. van Eden W, van Herwijnen M, Wagenaar J, van Kooten P, Broere F, van der Zee R. Stress proteins are used by the immune system for cognate interactions with anti-inflammatory regulatory T cells. *FEBS Lett.* 2013;587(13):1951-1958. doi: 10.1016/j.febslet.2013.05.024 [doi].
29. Glant TT, Radacs M, Nagyeri G, et al. Proteoglycan-induced arthritis and recombinant human proteoglycan aggrecan G1 domain-induced arthritis in BALB/c mice resembling two subtypes of rheumatoid arthritis. *Arthritis Rheum.* 2011;63(5):1312-1321. doi: 10.1002/art.30261 [doi].
30. Kryczanowsky F, Raker V, Graulich E, Domogalla MP, Steinbrink K. IL-10-modulated human dendritic cells for clinical use: Identification of a stable and migratory subset with improved tolerogenic activity. *J Immunol.* 2016;197(9):3607-3617. doi: jimmunol.1501769 [pii].
31. Tureci O, Bian H, Nestle FO, et al. Cascades of transcriptional induction during dendritic cell maturation revealed by genome-wide expression analysis. *FASEB J.* 2003;17(8):836-847. doi: 10.1096/fj.02-0724com [doi].
32. Ferreira GB, Vanherwegen AS, Eelen G, et al. Vitamin D3 induces tolerance in human dendritic cells by activation of intracellular metabolic pathways. *Cell Rep.* 2015. doi: S2211-1247(15)00026-1 [pii].
33. Danova K, Klapetkova A, Kayserova J, Sediva A, Spisek R, Jelinkova LP. NF-kappaB, p38 MAPK, ERK1/2, mTOR, STAT3 and increased glycolysis regulate stability of paricalcitol/dexamethasone-generated tolerogenic dendritic cells in the inflammatory environment. *Oncotarget.* 2015;6(16):14123-14138. doi: 4234 [pii].
34. Mansilla MJ, Selles-Moreno C, Fabregas-Puig S, et al. Beneficial effect of tolerogenic dendritic cells pulsed with MOG autoantigen in experimental autoimmune encephalomyelitis. *CNS Neurosci Ther.* 2015;21(3):222-230. doi: 10.1111/cns.12342 [doi].
35. Lappin MB, Weiss JM, Delattre V, et al. Analysis of mouse dendritic cell migration in vivo upon subcutaneous and intravenous injection. *Immunology.* 1999;98(2):181-188. doi: imm850 [pii].



Supplementary information

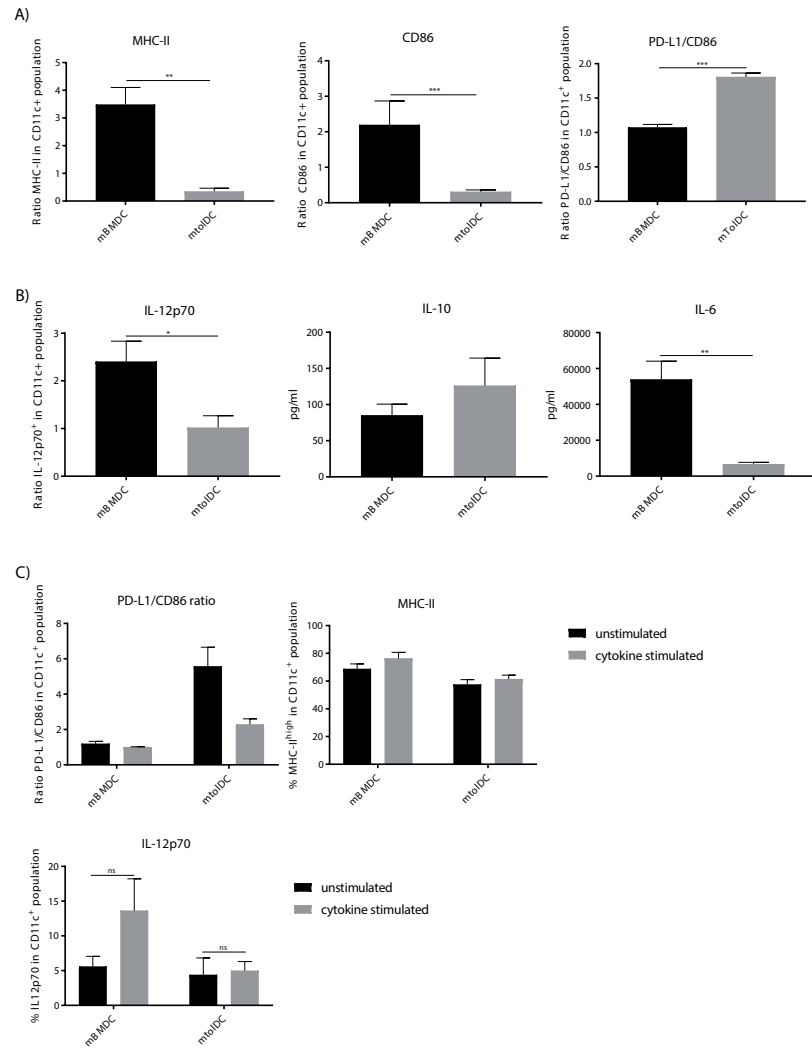


Figure S1. LPS stimulated tolDCs show similar semi-mature phenotype and stability *in vitro*.

TolDCs were generated by adding dexamethasone and 1,25-dihydroxyvitamin D3 and stimulated with LPS. Phenotype was measured by flow cytometry (A) and the ratio to immature BMDC was used to determine the difference in expression of MHC-II, CD86 and PD-L1. Cytokine production (B) was measured in the supernatant by Magpix (IL-10, IL-6, GM-CSF) or intracellular by flow cytometry (IL-12p70). To test the stability of tolDCs *in vitro*, tolDCs were stimulated for 24 hrs with a pro-inflammatory cytokine mix (IL-1 β , GM-CSF, IL-6, TNF and IFN- γ). After 24 hrs, the phenotype of the (tol)DCs was measured by flow cytometry (C). Two-tailed paired student T-test was used. *p \leq 0.05, **p \leq 0.01, ***p \leq 0.001. N = 4

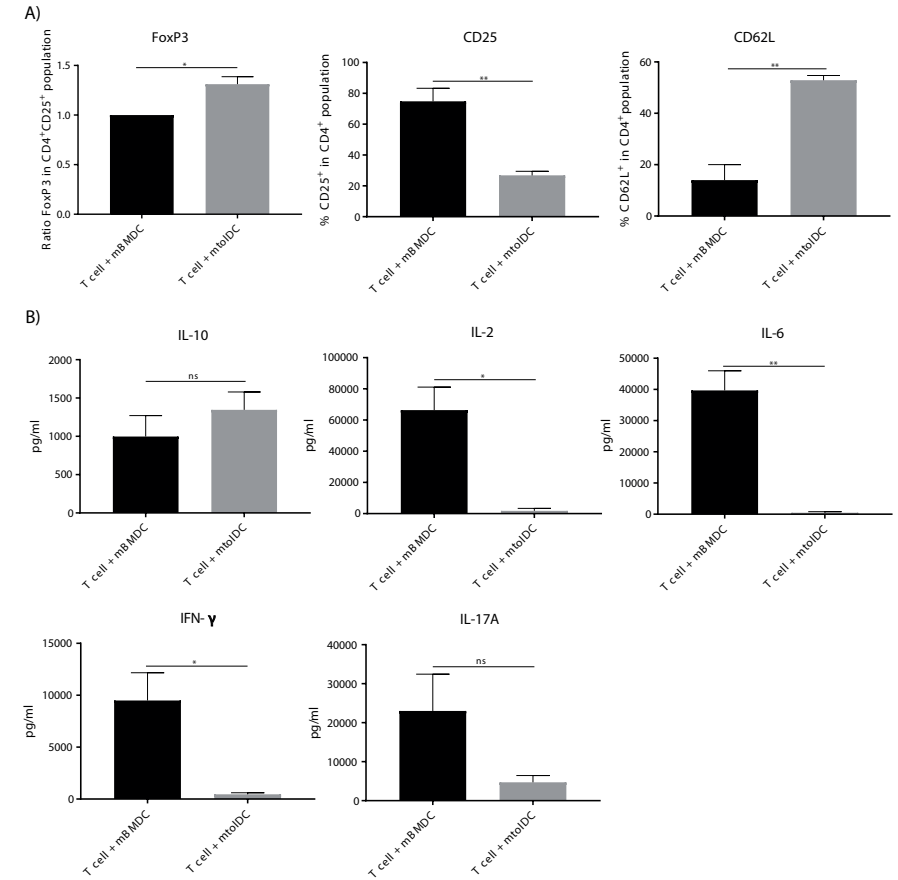


Figure S2. LPS stimulated tolDCs show similar effects on CD4⁺ T cells *in vitro*.

BMDCs or (LPS stimulated) mtolDCs were pulsed with B29 and co-cultured for three days with naive (CD25⁺ and CD44⁺ depleted) CD4⁺ T cells from a mb29b-TCR transgenic mouse. On day 3, phenotype of the CD4⁺ T cells was determined by flow cytometry (A). For FoxP3, the ratio to CD4⁺ T cells that were in co-culture with BMDCs was used to compare the difference when co-culturing with tolDCs. As markers for activation status of the CD4⁺ T cell, CD25 and CD62L (L-selectin) were measured. Cytokine production was measured after co-culture in the supernatant by Magpix (B). Two-tailed paired student T-test was used. *p \leq 0.05, **p \leq 0.01, ***p \leq 0.001. N = 4

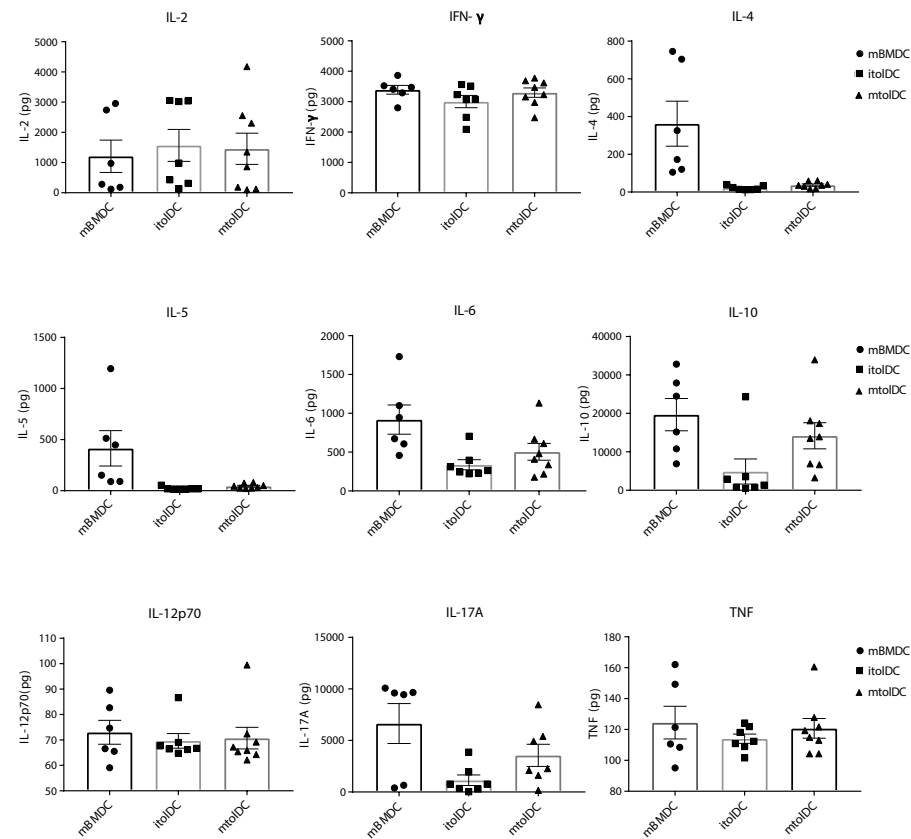


Figure S3. Ex vivo cytokine production by hPG stimulated splenocytes from mice that received a co-transfer from DCs and naïve CD4⁺ T cells.

Activation status of transferred CD4⁺ T cells was measured by cytokine release in the supernatant after hPG restimulation (72 hrs) *ex vivo*. Cytokine amounts were determined by Magpix.

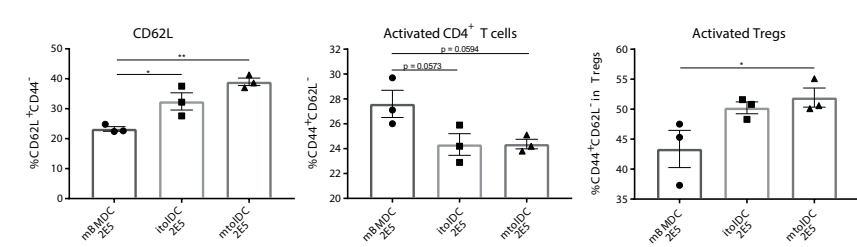


Figure S4. Lowering the toIDC dose 5 times does not affect toIDC efficiency.

(Im)mature toIDCs or mature BMDCs were pulsed with hPG peptide and transferred (2×10^5 cells/injection) one day after the naïve CFSE labeled hPG TCR transgenic CD4⁺ T cells. Proliferation and phenotype from the transferred CD4⁺ T cells was measured by flow cytometry (A/B). Each symbol represents an individual mouse. * $p \leq 0.05$, ** $p \leq 0.01$

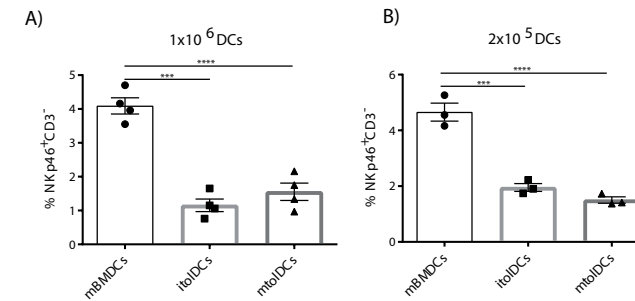


Figure S5. Percentage of transferred NK cells lower after toIDC co-transfer.

First, hPG TCR transgenic CD4⁺ T cells were activated *in vivo* by injecting hPG peptide i.m. into the transgenic mice. After three days, CD4⁺ TCR transgenic T cells were isolated and transferred into a naïve Balb/c acceptor mouse. One day later, hPG pulsed (im)mature toIDCs or mature BMDCs (1×10^6) were injected into the acceptor mice. However, purity of the CD4⁺ T cells is not 100% thus other cell types are also transferred. After three days, the percentage NK cells (CD3⁺NKp46⁺) was measured by flow cytometry (A). When the amount of transferred toIDCs is lowered to 2×10^5 cells, the effect on the percentage NK cells remains (B). One way ANOVA (Dunnett) was used. * $p \leq 0.05$, ** $p \leq 0.01$, *** $p \leq 0.001$.





Chapter 4

Targeting of tolerogenic dendritic cells to heat-shock proteins in inflammatory arthritis

Rachel Spiering^{1,2,3}, Manon A.A. Jansen⁴, Matthew J. Wood^{1,2,3}, Anshorulloh A. Fath^{1,2,3}, Oliver Eltherington^{1,2,3}, Amy E. Anderson^{1,2,3}, Arthur G. Pratt^{1,2,3}, Willem van Eden⁴, John D. Isaacs^{1,2,3}, Femke Broere^{4,5}, Catharien M.U. Hilkens^{1,2,3}

¹ Musculoskeletal Research Group, Institute of Cellular Medicine, Newcastle University, Newcastle upon Tyne, UK

² Arthritis Research UK Rheumatoid Arthritis Pathogenesis Centre of Excellence (RACE), UK

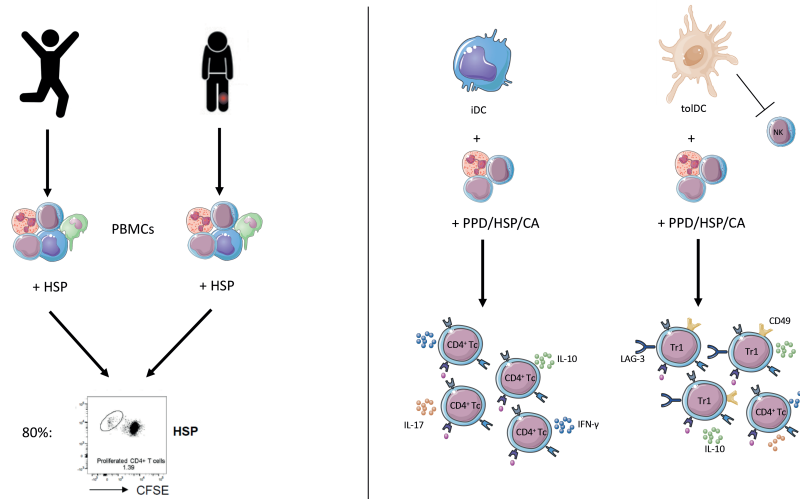
³ NIHR-Newcastle Biomedical Research Centre in Ageing and Long-Term Conditions, Newcastle upon Tyne Hospitals NHS Foundation Trust and Newcastle University, Newcastle upon Tyne, UK

⁴ Division of Immunology, Department of Infectious Diseases and Immunology, Utrecht University, Utrecht, the Netherlands

⁵ Department of Clinical Sciences of Companion Animals, Faculty Veterinary Medicine, Utrecht University, Utrecht, The Netherlands

Submitted

Graphical abstract



Abstract

Objectives: Autologous tolerogenic dendritic cells (tolDC) are a safe and well-tolerated therapeutic strategy in rheumatoid arthritis (RA). Outstanding priorities for clinical development include (I) identification of optimal (auto)antigen(s) for tolDC loading, and (II) characterisation of functional biomarkers of T cell modulation by tolDCs to confirm therapeutic activity. Here, we investigated tolDC-targeting of heat shock proteins (HSPs) that are known to be abundant in inflamed synovia.

Methods: Cell proliferation dye-labelled human peripheral blood mononuclear cells of RA patients, psoriatic arthritis (PsA) patients or healthy donors were cultured with antigen (HSP40-, HSP60- and HSP70-derived peptides, or as controls purified protein derivative (PPD) or *Candida albicans* (CA)) in the presence or absence of tolDC or immature DC (imDC) for nine days. Functional characteristics of proliferated antigen-specific T cells were measured using flow cytometry, NanoString and Meso Scale Discovery immunoassays.

Results: All test groups showed a robust CD4⁺ T cell response towards one or more HSP-derived peptides (stimulation index > 2; healthy: 78%, RA: 73%, PsA: 90%). These HSP-specific T cells produced significant amounts of pro-inflammatory cytokines. Addition of tolDC but not imDC induced a type 1 regulatory (Tr1) phenotype in HSP-specific CD4⁺ T cells. TolDC-induced Tr1 cells were identified by their upregulated levels of LAG3, CD49b and IL-10. Furthermore, tolDC inhibited bystander NK cell activation.

Conclusions: Pro-inflammatory HSP-specific CD4⁺ T cells are detectable in the majority of donors. These can be converted into LAG3⁺, CD49b⁺, IL-10⁺ Tr1 cells by tolDC. HSP-loaded tolDC are a promising tool for directing Tr1 cells to inflamed synovia.

Keywords: inflammatory arthritis, HSP, tolDCs, Tr1 cells, therapy

Introduction

Rheumatoid arthritis (RA) arises from a breakdown in self-tolerance leading to aberrant immune responses to autoantigens. Current treatments involve chronic immunosuppression in a non-antigen specific manner. Although these treatments can be effective at alleviating symptoms they do not provide a cure and the associated general immunosuppression can cause unwanted side effects (e.g. increased susceptibility to infection and cancer). An alternative approach are treatments that reinstate self-tolerance, leading to long-term remission whilst leaving protective immunity intact.

An emerging tolerogenic strategy is the administration of tolerogenic dendritic cells (tolDC). These cells act by inhibiting T cell mediated pathology, for example through the induction of regulatory T cells (Treg)^{1,2}. We recently conducted a clinical trial of autologous tolDC treatment in both RA and psoriatic arthritis (PsA) patients, confirming the safety and feasibility of this approach³. However, two critical and related issues were highlighted. The first relates to identification of the optimal target (auto)antigen(s). Because definitive arthritogenic autoantigens have not been identified, we pragmatically 'loaded' tolDC with autologous synovial fluid in that study, based on data suggesting a content of relevant patient-specific autoantigens⁴. However, without knowledge of the targeted antigen(s)' identity it was not possible to measure modulation of the antigen-specific T cell response. The second issue is the lack of suitable biomarkers. Because tolDC act in a highly targeted manner, it is imperative to monitor changes in antigen-specific T cells, rather than measuring systemic immune markers. Loading of tolDC with known antigens will enable immune monitoring in a highly specific manner, for example through the use of specific MHC II-peptide tetramers to identify the relevant antigen-specific T cells. Thus, future therapeutic studies with tolDC can be greatly improved by loading tolDC with relevant and known antigens, facilitating immune monitoring at the antigen-specific level and defining biomarkers of tolDC-effectiveness.

We recently suggested to load tolDC with the surrogate self-antigens heat shock proteins (HSPs)⁵. HSPs are molecular chaperone proteins highly expressed in inflamed tissue. Indeed, the expression of HSP40, HSP60 and HSP70 family members is upregulated in the synovial tissue of RA patients⁶⁻⁹ and in the inflamed tissues of patients with other autoimmune diseases like multiple sclerosis, atherosclerosis, (juvenile dermato-) myositis and juvenile idiopathic arthritis¹⁰⁻¹⁴. Furthermore, adoptive transfer of HSP-specific Treg effectively suppressed established disease in a murine autoimmune arthritis model. Subsequent deletion of these donor HSP-

specific Tregs completely reversed disease progress, indicating disease suppression was induced by HSP-specific Tregs and not via bystander suppression¹⁵. Thus, it is likely that directing a regulatory T cell response to a non-disease inducing antigen present in the diseased tissue is sufficient to dampen down pathogenic autoimmune responses.

To this aim, we 1) assessed the presence and phenotype of HSP-specific T cells in RA and PsA patients and healthy donors; 2) investigated the ability of tolDC to induce a regulatory phenotype in HSP-specific T cells, and 3) identified suitable biomarkers for the identification of tolDC-modulated T cells that can be used for imminent clinical trials.

Materials and methods

A complete description of experimental and bioinformatics approaches is given in the online supplementary text.

The minimum information about the tolerogenic antigen presenting cells (APC) (MITAP) checklist was followed for the preparation of this paper¹⁶.

Peptides and Antigens

HSP40 peptide: DnaJP1: QKRAAYDQYGHAAFE, HSP60 peptides: p1: GEALSTLVVNKIRGT and p3: PYILLVSSKVSTVKD, HSP70 peptide: B29: VLRIVNEPTAAALAY and a negative control peptide A5: RQAILTLQTSSEPR (Genscript). Whole antigens that were used were purified protein derivative (PPD; Statens Serum Institut) and *Candida albicans* (CA; Soluprick; Alk).

Isolation of cells

Human blood samples were obtained from healthy controls (HC) and treatment-naïve patients with recent onset arthritis (PsA and RA). Samples were collected with informed consent and following a favourable ethical opinion from South West 3 Research Ethics Committee. Peripheral blood mononuclear cells (PBMC; from 40 ml EDTA blood per donor) were isolated according to Anderson et al. 2017¹⁷. Monocytes were positively selected from PBMC using anti-CD14 microbeads (Miltenyi Biotec) according to manufacturer's protocol with one minor change: 10µl instead of 20µl anti-CD14 beads per 1x10⁷ cells was used for cell isolation. CD14⁺ PBMC were collected from the column flow through and stored for one week at -80°C in FCS (Gibco) with 10% DMSO (Sigma).

Establishment of DC

CD14⁺ Monocytes were cultured in CellGenix DC medium (CellGenix) in the presence of GM-CSF (50 ng/ml; Immunotools), IL-4 (50 ng/ml; Immunotools), dexamethasone (1 μ M; Sigma), 1,25-dihydroxyvitamin D3 (Calcitriol; 0.1 nM; Tocris) and monophosphoryl lipid A (MPLA) (1.0 μ g/ml; Invivogen) to generate tolDC (¹⁸ and supplementary text).

HSP assay

CD14-depleted PBMC were thawed, washed and labelled with 0.2 μ M carboxyfluorescein succinimidyl ester (CFSE; eBioscience) or 0.2 μ M cell proliferation dye eFluor-450 (CTV; eBioscience) in PBS for ten minutes at 37°C. CFSE/CTV was quenched with 10% human serum (HS; Sigma) in HBSS (Lonza). Cells were resuspended at 2x10⁶ cells/ml in X-VIVO-15 medium (Lonza) supplemented with 4% HS (final concentration 2%) and plated at 2x10⁵ cells per well (96 wells; round bottom; Corning). For each peptide eight wells were prepared. Peptides were added at 10 μ g/ml. Cells were cultured for nine days at 37°C with 5% CO₂. At the end of the culture, supernatants were collected for cytokine determination. As CD14 cells were needed for the preparation of tol- and imDC and unfractionated PBMC and CD14-depleted PBMC gave similar results (data not shown), CD14-depleted PBMC in 'results' and 'discussion' section are named 'PBMC'.

Co-cultures

CFSE or CTV-labelled CD14-depleted PBMC were resuspended at 4x10⁶ cells/ml in X-VIVO-15 medium (Lonza) supplemented with 8% HS (final concentration 2%) and plated at 2x10⁵ cells per well (96 wells; round bottom; Corning). DC were added in a 1:10 ratio (i.e. 2x10⁴/well). For PPD-DC and CA-DC assays, 1 μ g/ml PPD or 1 μ l/ml CA in X-VIVO-15 medium was added to the wells. For HSP-DC assays, 4 μ g/ml of each of the peptides in X-VIVO-15 medium was added to the wells. Cells were cultured for six (IL-10 secretion) or nine days (all other) at 37°C with 5% CO₂. TGF- β RI (ALK5) inhibitor (SB-505124; 1 μ M; Sigma) was added where indicated. At the end of the culture, supernatants were collected for cytokine determination.

Flow cytometry

For complete description of experimental methods see supplementary text. For antibodies and live/dead dyes used see table 1. Data were collected on an LSRfortessa X20 (BD Biosciences) and analysed using FlowJo (Tree Star Inc).

Table 1. List of reagents used for flow cytometry analysis.

Marker	Fluorochrome	Clone	Supplier
<i>Antibodies</i>			
CD3	BUV395	UCHT1	BD Biosciences
CD4	AF700	SK3	Biolegend
CD4	APC eFluor 780	SK3	eBioscience
CD4	BV786	SK3	BD Biosciences
CD8b	eFluor 660	SID18BEE	eBioscience
CD19	BV421	HIB19	Biolegend
CD56	PE Dazzle 594	HCD56	Biolegend
CD49b	APC	P1E6-C5	Biolegend
CD86	BV711	IT2.2	Biolegend
IFN γ	AF700	B27	BD Biosciences
IL-10	PE	JES3-19F1	Miltenyi
IL-17A	APC-Cy7	BL168	Biolegend
GM-CSF	PerCP-Cy5.5	BVD2-21C11	Biolegend
LAG3	PerCP eFluor 710	3DS223H	eBioscience
PD-1	PE	EH12.2H7	Biolegend
TIM-3	BV650	7D3	BD Biosciences
<i>Live/dead dyes</i>			
DAPI	-	-	Life technologies
Zombie aqua	-	-	Biolegend

RNA isolation and NanoString analysis

Cells from PPD co-cultures were harvested and a total of 100,000 CFSE:CD4⁺DAPI cells per sample were sorted into RLT buffer (Qiagen) supplemented with 1% β -mercaptoethanol (Sigma) using a FACSaria-fusion sorter (BD Biosciences). Lysates were stored for up to four months at -80°C before isolation of RNA. RNA was isolated using an RNeasy Micro Kit (Qiagen; including DNase step) according to the manufacturer's protocol. A total of 100 ng of RNA was used for NanoString analysis (Human Immunology Panel). Nanostring was performed according to the manufacturer's protocol: https://www.nanostring.com/application/files/2315/0818/2175/MAN-10023-11_nCounter_XT_Assay_User_Manual.pdf.

IL-10 secretion

Cells from PPD co-cultures were harvested and a minimum of 25,000 cells per sample sorted into X-VIVO-15 with 20% HS. For immature DC (imDC)-PPD cultures and non-monocyte-derived DC-PPD cultures, CFSE⁺CD4⁺ cells were sorted. For tolDC-PPD cultures, CFSE⁺CD4⁺LAG3⁺CD49b⁺ cells were sorted. Sorted cells were rested for two days in X-VIVO-15 supplemented with 2% HS and 10 IU/ml of IL-2 (Proleukin; 25,000 cells/well; 96-well round-bottom). Cells were subsequently washed and restimulated with 10 µg/ml platebound anti-CD3 (OKT3; Biolegend) and 1 µg/ml soluble anti-CD28 (CD28.2; Biolegend) in X-VIVO-15 supplemented with 2% HS (total 100 µl; 96-well flat-bottom). Supernatants were collected after 72 hours for cytokine determination.

Cytokine secretion

Cytokine production was determined in supernatants by Meso Scale Discovery (MSD; U-Plex (IL-10, IFN γ , IL-4, IL-17A, GM-CSF) or by sandwich ELISA from BD (IL-10).

Statistical analysis

The following statistical analyses were performed using Prism 5: repeated measures analysis of variance (ANOVA) with bonferroni correction for comparisons between multiple groups, paired Student t-test for comparisons between two groups.

Results

Pro-inflammatory HSP-specific T cells are present in IA patients

Our initial studies investigated whether immunodominant pan-DR-binding peptides from bacterial HSP40 (dnaJP1), mycobacterial (myc)-HSP60 (p1 and p3) and myc-HSP70 (B29)^{10,15,19} could be recognised by peripheral blood CD4⁺ T cells of healthy donors and RA and PsA patients (table 2). We tested both RA and PsA patients as both patient groups were used for the phase I/II safety trial.

PBMC were labelled with a proliferation dye and cultured with HSP peptides, medium alone or peptide control. After nine days, proliferation of CD4⁺ T cells was analysed (figure 1a). As shown in figure 1b, 78% of healthy donors, 73% of RA patients and 90% of PsA patients responded to one or more of the HSP peptides tested (figure 1b). Most donors responded to one HSP and the least to all four HSP peptides tested (supplementary figure 1).

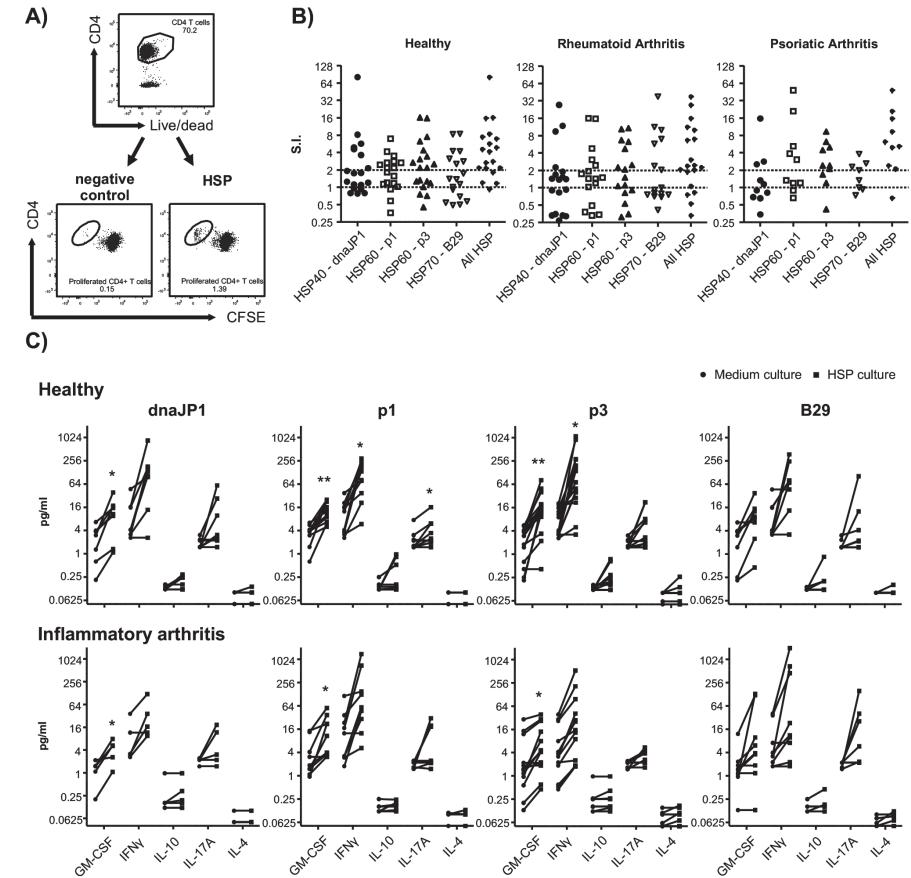


Figure 1. Inflammatory arthritis (IA) patients have pro-inflammatory HSP-specific CD4⁺ T cells. Cell proliferation dye (CFSE/CTV)-labelled PBMC of healthy controls and IA patients were cultured with pan-DR-binding HSP peptides: DnaJP1, HSP60p1, HSP60p2 and B29 for nine days. (A/B) Percentage of CFSE/CTV-negative live CD4⁺ T cells was measured using flow cytometry. Gating example (A) and graphs with stimulation index (S.I.) (B) are shown. S.I. was measured by dividing the percentage of CFSE/CTV⁻ CD4⁺ T cells of HSP culture by the percentage of CFSE/CTV⁻ CD4⁺ T cells negative control culture. S.I. > 2 was considered as increased above background proliferation. All HSP indicates best HSP response per donor. (C) Cytokine secretion in culture supernatants was measured using MSD immunoassay. Left circle indicates cytokine concentration in medium control, right square indicates cytokines concentration in HSP culture. Two-tailed paired student T-test was used. *p≤0.05, **p≤0.01.

To study the inflammatory nature of HSP-specific T cell responses, we measured the secretion of the pro-inflammatory cytokines IFN γ , GM-CSF, IL-17A and IL-4 and the anti-inflammatory cytokine IL-10 in the supernatants of the HSP cultures. PBMC from both healthy donors and RA/PsA patients produced significant levels of pro-inflammatory cytokines in response to HSP (Figure 1c).



Table 2. Characteristics of RA and PsA patients and healthy donors

	RA (n=19)	PsA (n=10)	Healthy (n=19)
Age, years	66 (60-70)	50 (34-56)	45 (29-52)
Sex, % females	68	50	63
duration of symptoms, weeks	12 (7-40)	17 (8-37)	-
CRP, gm/liter	27 (9-53)	6 (5-19)	-

Except where indicated otherwise, values are the median (interquartile range). CRP: C-reactive protein.

ToIDC induce a Tr1 phenotype in antigen-specific T cells

The T cell modulatory effects of human toIDC are usually studied in (tol)DC/T cell co-culture models. However, because toIDC need to be able to regulate T cell responses in the context of other immune cells, we assessed whether toIDC could regulate autologous CD4⁺ T cells in the antigen-specific PBMC culture system described above. To this aim, we initially used the recall antigen PPD. T cell responses to PPD were assessed in the absence or presence of toIDC. As a control, we used another DC population with known, but unstable, tolerogenic function – immature monocyte-derived DC (imDC). Mature DCs (matDC) as control were also considered, but matDC showed extremely high non-antigen-specific CD4, CD8 and NK cell proliferation (data not shown). We compared the immune-related gene-expression profile of PPD-specific T cells activated in the absence or presence of toIDC or imDC by NanoString. The gene expression profiles of the differentially activated PPD-specific T cell groups clustered well together, indicating clear differences between treatment groups at the mRNA level (figure 2a). We identified 82 differentially expressed genes (DEGs) from a total of 579 genes in PPD-specific T cells activated in the presence of toIDC (toIDC-PPD T cells) as compared to PPD-specific T cells activated in the absence of monocyte-derived DC (control PPD T cells) (Benjamini-Hochberg false discovery rate 10%). Of these 82 genes, 25 DEGs were also found in toIDC-PPD T cells as compared to PPD-specific T cells activated in the presence of imDC (imDC-PPD T cells). Nine additional DEGs could be identified in toIDC-PPD T cells as compared to imDC-PPD T cells (figure 2b and supplementary table 1).

Among the toIDC-PPD versus control PPD T cell identified DEGs, 20 genes could either be identified as type 1 regulatory T cells (Tr1)-specific genes or genes that have been described as inducers of Tr1-specific genes (figure 2c). Recently, Gagliani et al, described two surface antigens, LAG3 and CD49b, as being highly and stably expressed on Tr1 cells. Moreover, co-expression of only these two surface proteins

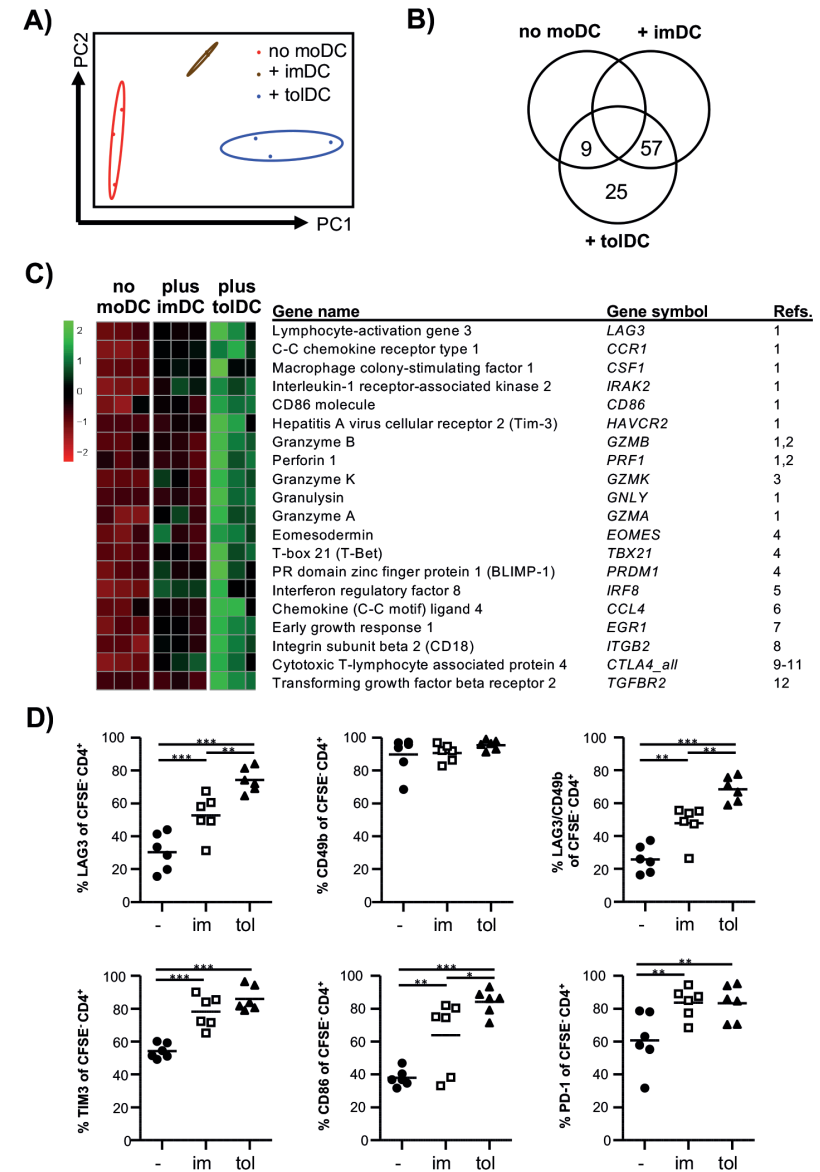


Figure 2. ToIDC induce a Tr1 phenotype in PPD-specific T cells. Cell proliferation dye (CFSE/CTV)-labelled PBMC of healthy controls were cultured with PPD and toIDC (tol), imDC (im) or without moDC (-) for nine days. (A-C) 100.000 CFSE/CTV- life CD4⁺ T cells were sorted by FACS. Cell were then lysed and mRNA was analysed by NanoString. (A) Gating strategy of sort. (B) Principal component analysis (PCA) plot showing clustering of the different groups. (C) Heat map of gene expression levels that were significantly (BH P ≤ 0.1) differentially expressed with at least a 1.5-fold change in toIDC compared to non-moDC. (D) Percentages of LAG3, CD49b, TIM3, CD86 and PD-1 in CFSE/CTV- live CD4⁺ T cells were measured using flow cytometry. Repeated measures analysis of variance was used. *p<0.05, **p<0.01, ***p<0.001

allowed for the identification of Tr1 cells²⁰. To confirm that tolDC induce a Tr1 phenotype in PPD-specific T cells, we therefore measured the co-expression of LAG3 and CD49b and several other Tr1-specific proteins identified in the NanoString analysis, by flow cytometry. TolDC induced significant upregulation of the LAG3, TIM3, CD86 and PD-1 proteins as compared to control PPD cultures and the combined expression of LAG3 and CD49b could identify tolDC-induced PPD-specific Tr1 cells (figure 2d).

A hallmark of Tr1 cells is the high secretion of IL-10²⁰⁻²³. As shown in figure 3a, significantly higher levels of IL-10 were produced in the tolDC-PPD cultures as compared to the imDC-PPD or control PPD cultures. Since it could not be excluded that IL-10 was (partly) tolDC-derived, proliferated PPD-specific CD4⁺ T cells (imDC-PPD T cells and control PPD-T cells) or proliferated PPD-specific LAG3⁺CD49b⁺CD4⁺ T cells (tolDC-PPD T cells) were sorted (figure 3b), rested for two days and subsequently restimulated with monoclonal antibodies to CD3 and CD28 for three days. tolDC-PPD T cells produced significantly higher levels of IL-10, but not IL-4, IL-17A or IFN γ as compared to non-moDC-PPD T cells (figure 3c).

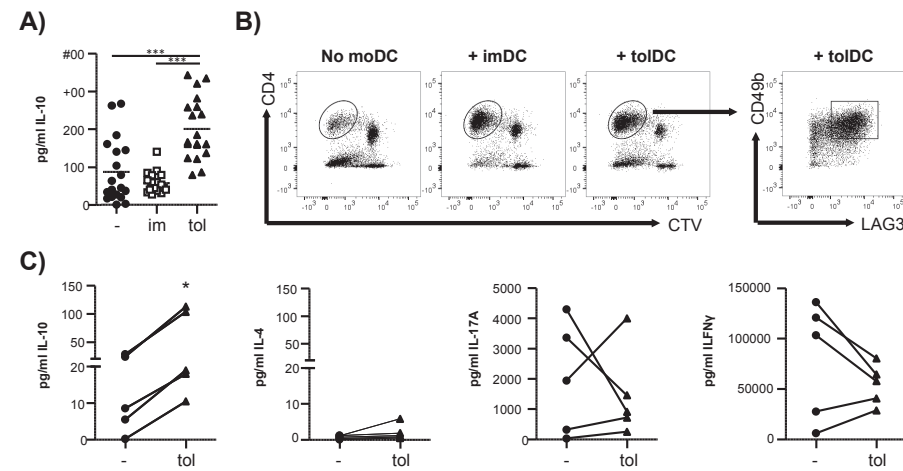


Figure 3. TolDC induce functional IL-10-producing PPD-specific Tr1 cells. Cell proliferation dye (CFSE/CTV)-labelled PBMC of healthy controls were cultured with PPD and tolDC (tol), imDC (im) or without moDC (-) for nine (A) or six (B/C) days. (A) Cytokine secretion in culture supernatants was measured using ELISA. Repeated measures ANOVA was used. (B/C) A minimum of 25,000 CFSE/CTV live CD4⁺ T cells were sorted for non-moDC and imDC cultures. A minimum of 25,000 CFSE/CTV live CD4⁺LAG3⁺CD49b⁺ T cells was sorted for tolDC cultures. Cell were then rested with 10 IU/ml of IL-2 for two days and restimulated by plate bound anti-CD3 (10 μ g/ml) and soluble anti-CD28 (1 μ g/ml) for three days. (B) Gating strategy sort. (C) Cytokine secretion in culture supernatants was measured using MSD immunoassay. One-tailed paired student T-test was used. * $p \leq 0.05$, ** $p \leq 0.01$, *** $p \leq 0.001$.

Overall, these data clearly indicate that tolDC induce a Tr1 phenotype in autologous antigen (PPD)-specific CD4⁺ T cells.

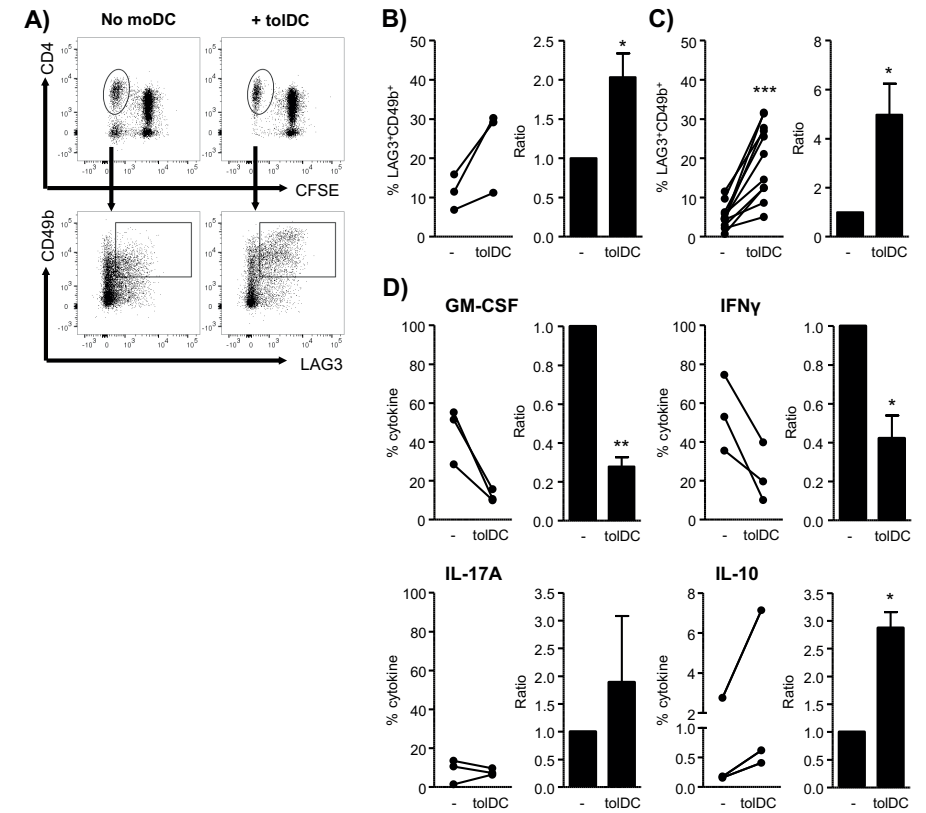


Figure 4. TolDC can tolerate the HSP-specific T cell response.

Cell proliferation dye (CFSE/CTV)-labelled PBMC of IA patients were cultured with an HSP-peptide pool (HSP60p1, HSP60p2 and B29; 4 μ g/ml per peptide) (A/B/D) or CA (1:1000) (C) and tolDC (tolDC) or without moDC (-) for nine days. (A-C) Percentages and ratios of LAG3 and CD49b in CFSE/CTV life CD4⁺ T cells were measured using flow cytometry. Gating strategy (A) HSP-peptide graphs (B) and CA graphs (C) are shown. Ratios were measured by dividing the percentage of CFSE/CTV CD4⁺ T cells of tolDC cultures by the percentage of CFSE/CTV CD4⁺ T cells of non-moDC cultures. (D) Percentages of GM-CSF, IFN γ , IL-17A and IL-10 in CFSE/CTV life CD4⁺ T cells were measured after stimulation with PMA (50 ng/ml) ionomycin (1 μ g/ml) and brefeldin A (1 μ g/ml for 5 hours by using flow cytometry. One-tailed (IL-10 and LAG3/CD49b) or two-tailed (all other) paired student T-test was used. * $p \leq 0.05$, ** $p \leq 0.01$, *** $p \leq 0.001$.



ToIDC induce a Tr1 phenotype in HSP-specific T cells of RA patients

Since we established that HSP-specific T cells are pro-inflammatory in both patients and healthy controls, and that the co-expression of LAG3 and CD49b can be used to identify toIDC-activated antigen-specific Tr1 cells, we used these markers to study whether toIDC induced a Tr1 phenotype in HSP-specific T cells of RA/PsA patients. toIDC-activated HSP T cells had significantly higher levels of LAG3/CD49b, coinciding with decreased levels of GM-CSF and IFN γ and increased IL-10 production as compared to control PPD T cells (figure 4a, b and d). In addition, toIDC also induced a Tr1 phenotype in response to a third (control) antigen, *Candida albicans* (CA; figure 4c). Thus, toIDC are capable of inducing Tr1 responses in autologous antigen-specific CD4⁺ T cells, irrespective of the antigen.

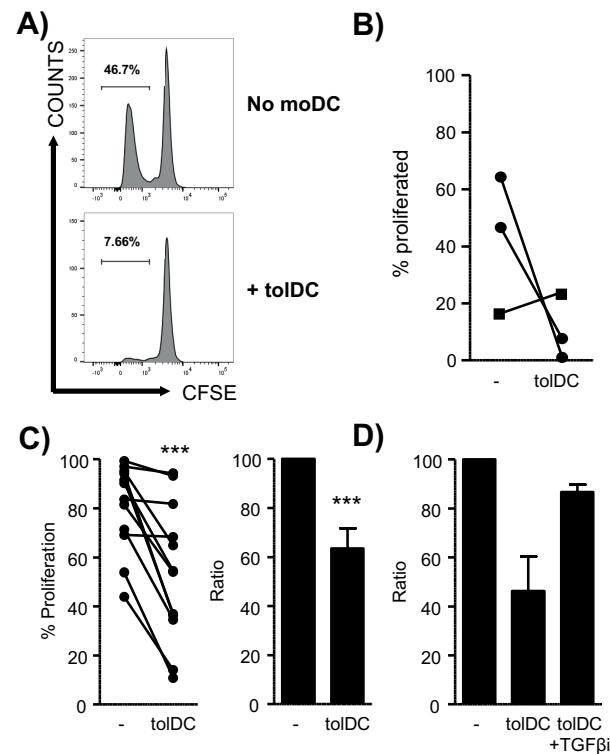


Figure 5. ToIDC can inhibit bystander NK cell proliferation. Cell proliferation dye (CFSE/CTV)-labelled PBMC of IA patients were cultured with an HSP-peptide pool (HSP60p1, HSP60p2 and B29; 4 μ g/ml per peptide) (A/B) or CA (1:1000) (C/D) and toIDC (toIDC) or without moDC (-) for nine days. (A-D) Percentages of CFSE/CTV⁻ NK cells were measured using flow cytometry. Gating strategy (A) HSP-peptide graph (B) and CA graphs (C/D) are shown. (D) TGF- β RI (ALK5) inhibitor (SB-505124) was added at 1 μ M. (N=2). Ratios were measured by dividing the percentage of CFSE/CTV⁻ CD4⁺ T cells of toIDC cultures by the percentage of CFSE/CTV⁻ CD4⁺ T cells of moDC cultures. Two-tailed paired student T-test was used. ***p \leq 0.001.

As our antigen-specific T cell activation model using PBMC allowed us to check the behaviour of other types of immune cells, we had observed high levels of NK cell proliferation. Interestingly, bystander NK cell proliferation was largely inhibited by toIDC in HSP-cultures (figure 5a and b) and CA-cultures (figure 5c). We have previously shown that toIDC produce high amounts of TGF β ¹⁷. It is known that TGF β can hamper NK cell proliferation and activation^{24,25} and we therefore investigated whether blocking of the TGF β -receptor could reverse the toIDC-induced suppression of NK cell activation. Indeed, addition of SB-505124, a small molecule inhibitor of TGF- β RI, restored NK cell proliferation in toIDC-CA cultures (figure 5d).

Altogether, our findings demonstrate that toIDC can convert pro-inflammatory antigen-specific CD4⁺ T cells in RA and PsA patients into anti-inflammatory Tr1 cells, which are characterised by expression of LAG3/CD49b and enhanced IL-10 production. In addition, toIDC-derived TGF β blocks bystander NK cell activation.

Discussion

This study focused on two key questions that require elucidation before further toIDC clinical trials in RA can commence. First, as the idea behind toIDC therapy is to dampen the autoreactive T cell response, toIDC will need 'loading' with an appropriate disease-relevant antigen. Second, as toIDC act in a highly targeted manner, it is necessary to have suitable biomarkers that reflect modification of antigen-specific CD4⁺ T cell responses in order to monitor toIDC efficiency in clinical trials.

There has been debate over the last few years about the need for loading of toIDC with a disease-relevant antigen for treatment in autoimmune diseases. Several animal studies have shown that disease remission can be achieved by treatment with unpulsed toIDC^{26,27}, suggesting that toIDC may be able to pick up the relevant antigens *in vivo*. Indeed, phase I/II safety trials with unloaded toIDC have been completed for diabetes and Crohn's disease^{28,29}. The risk, however, with using non-antigen-pulsed toIDC *in vivo*, is that i) it is uncertain whether toIDC pick up and present appropriate antigen(s) and ii) the identity of the presented antigen is unknown. Thus, if it is unknown which antigens are presented by toIDC, monitoring the antigen-specific T cells response is not possible. In addition, other animal studies have shown that loading of toIDC is crucial for their therapeutic potential. For example, we and others have shown that loading of toIDC with type II collagen was required for disease remission in the collagen-induced arthritis model³⁰⁻³². The same is true for a mouse model of multiple sclerosis. Myelin oligodendrocyte glycoprotein-pulsed toIDC performed significantly



better than unpulsed tolDC^{33,34}. We and others have therefore used autoantigen-pulsed tolDC for our phase I/II clinical safety trials^{3,35}.

However, the search for a common antigen to load tolDC for treatment of autoimmune diseases, like RA, has been a challenge. Here, we describe the use of HSPs as surrogate self-antigens to load tolDC. Since HSPs are highly expressed in the inflamed tissues of patients with numerous autoimmune diseases⁶⁻¹⁴, they would be ideal antigens to load, not only tolDC for RA therapy, but also other autoimmune diseases. Expression of the HSP antigens only at the sites of inflammation, will assure suppression by tolDC will occur only locally. We found that nearly 80% of both healthy individuals and RA/PsA patients have CD4⁺ T cell-reactivity to the HSP peptides tested, indicating the promiscuity of the HSP peptides tested. For this study, we used microbial HSP variants that were highly homologous to human HSP epitopes. The rationale for this approach is that previous animal studies have shown that immunization with microbial HSP leads to the activation and expansion of T cells that cross-react with self-HSPs (reviewed in³⁶). Furthermore, Tregs specific for the microbial HSP peptide B29 were shown to effectively ameliorate disease in the proteoglycan arthritis model¹⁵. Thus, the idea behind this study is that loading tolDC with microbial HSP peptides will lead to the induction and expansion of self-reactive T cells with regulatory function.

The next step was to identify how tolDC alter the antigen-specific CD4⁺ T cell response. As with all novel therapeutic approaches, suitable biomarkers are vital for the measurement of treatment efficiency. Using several antigens, including the HSP peptides, we showed that tolDC induce a clear Tr1 phenotype in antigen-specific CD4⁺ T cells, with high expression of the Tr1 molecules LAG3 and CD49b and the anti-inflammatory cytokine IL-10^{20,37}. With these findings, future immune monitoring could significantly be improved by measuring the Tr1 markers LAG3/CD49b on HSP-specific – or other disease-relevant antigen-specific – MHC II tetramer⁺ CD4⁺ T cells.

An important additional finding we report here is the striking reduction of bystander NK cell proliferation in tolDC-HSP and tolDC-CA cultures. The synovial fluid of RA patients contains high levels of NK cells and they have been shown to aggravate cytokine imbalance and inflammation in rheumatic joints³⁸⁻⁴¹. NK cell proliferation is mainly dependent on the cytokines IL-2, IL-7 and IL-15^{42,43} and can be hampered by factors like H₂O₂, soluble CD25 and TGFβ. We found that tolDC did not inhibit NK cell proliferation via IL-2, IL-15, soluble CD25 or H₂O₂, (data not shown), but found that NK cell proliferation could be restored by blocking TGFβ receptor signalling. This finding supports our previous notion that enhanced production of TGFβ is

important for tolDC function¹⁷ and that the tolerogenic role of tolDC *in vivo* might not be limited to their effect on the CD4⁺ T cell population. Instead, tolDC could have a direct anti-inflammatory effect on the pathogenic immune cells present in the arthritic joints.

In conclusion, tolDC induce a Tr1 phenotype in antigen-specific T cells of both healthy individuals and RA/PsA patients. The normally pro-inflammatory HSP-specific CD4⁺ T cells of IA patients can be converted into anti-inflammatory Tr1 cells and bystander NK cell proliferation is hampered due to high levels of tolDC-derived TGFβ. Thus, HSP-pulsed tolDC may be a promising tool for the restoration of immune tolerance in IA patients. Indeed, a phase I/II trial with HSP70 peptide B29-pulsed tolDC is currently underway.

Acknowledgements

We thank Ms. Anastasia Resteu (Newcastle NanoString Facility, Newcastle University) for processing the samples on the NanoString nCounter platform. This project has received funding from the European Union's Horizon 2020 research and innovation programme under the Marie Skłodowska-Curie grant agreement no 654882. The research was supported by the National Institute for Health Research Newcastle Biomedical Research Center based at Newcastle Hospitals NHS Foundation Trust and Newcastle University. This work was supported by a grant from the European Cooperation in Science and Technology (COST) for the AFACTT project (Action to Focus and Accelerate Cell-based Tolerance-inducing Therapies; BM1305). COST is part of the EU Framework Programme Horizon 2020.

We acknowledge the Flow Cytometry Core Facility at Newcastle University for their expert help.

References

1. Hilkens CM, Isaacs JD, Thomson AW. Development of dendritic cell-based immunotherapy for autoimmunity. *Int Rev Immunol*. 2010;29(2):156-183. doi: 10.3109/08830180903281193 [doi].
2. Domogalla MP, Rostan PV, Raker VK, Steinbrink K. Tolerance through education: How tolerogenic dendritic cells shape immunity. *Front Immunol*. 2017;8:1764. doi: 10.3389/fimmu.2017.01764 [doi].
3. Bell GM, Anderson AE, Diboll J, et al. Autologous tolerogenic dendritic cells for rheumatoid and inflammatory arthritis. *Ann Rheum Dis*. 2017;76(1):227-234. doi: 10.1136/annrheumdis-2015-208456 [doi].
4. Tsark EC, Wang W, Teng YC, Arkfeld D, Dodge GR, Kovats S. Differential MHC class II-mediated presentation of rheumatoid arthritis autoantigens by human dendritic cells and macrophages. *J Immunol*. 2002;169(11):6625-6633.
5. Jansen MAA, Spiering R, Broere F, et al. Targeting of tolerogenic dendritic cells towards heat-shock proteins: A novel therapeutic strategy for autoimmune diseases? *Immunology*. 2018;153(1):51-59. doi: 10.1111/imm.12811 [doi].
6. de Graeff-Meeder ER, Voorhorst M, van Eden W, et al. Antibodies to the mycobacterial 65-kd heat-shock protein are reactive with synovial tissue of adjuvant arthritic rats and patients with rheumatoid arthritis and osteoarthritis. *Am J Pathol*. 1990;137(5):1013-1017.
7. Boog CJ, de Graeff-Meeder ER, Lucassen MA, et al. Two monoclonal antibodies generated against human hsp60 show reactivity with synovial membranes of patients with juvenile chronic arthritis. *J Exp Med*. 1992;175(6):1805-1810.
8. Kurzik-Dumke U, Schick C, Rzepka R, Melchers I. Overexpression of human homologs of the bacterial DnaJ chaperone in the synovial tissue of patients with rheumatoid arthritis. *Arthritis Rheum*. 1999;42(2):210-220. doi: 10.1002/1529-0131(199902)42:23.0.CO;2-U [doi].
9. Schett G, Redlich K, Xu Q, et al. Enhanced expression of heat shock protein 70 (hsp70) and heat shock factor 1 (HSF1) activation in rheumatoid arthritis synovial tissue. differential regulation of hsp70 expression and hsf1 activation in synovial fibroblasts by proinflammatory cytokines, shear stress, and antiinflammatory drugs. *J Clin Invest*. 1998;102(2):302-311. doi: 10.1172/JCI2465 [doi].
10. Kamphuis S, Kuis W, de Jager W, et al. Tolerogenic immune responses to novel T cell epitopes from heat-shock protein 60 in juvenile idiopathic arthritis. *Lancet*. 2005;366(9479):50-56. doi: S0140-6736(05)66827-4 [pii].
11. Brosnan C,F, Battistini, Luca, Selmaj, Krzysztof. Heat shock proteins in multiple sclerosis. .
12. Xu Q. Role of heat shock proteins in atherosclerosis. *Arterioscler Thromb Vasc Biol*. 2002;22(10):1547-1559.
13. Hohlfeld R, Engel AG. Expression of 65-kd heat shock proteins in the inflammatory myopathies. *Ann Neurol*. 1992;32(6):821-823. doi: 10.1002/ana.410320619 [doi].
14. Tezak Z, Hoffman EP, Lutz JL, et al. Gene expression profiling in DQA1*0501+ children with untreated dermatomyositis: A novel model of pathogenesis. *J Immunol*. 2002;168(8):4154-4163.
15. van Herwijnen MJ, Wieten L, van der Zee R, et al. Regulatory T cells that recognize a ubiquitous stress-inducible self-antigen are long-lived suppressors of autoimmune arthritis. *Proc Natl Acad Sci U S A*. 2012;109(35):14134-14139. doi: 10.1073/pnas.1206803109 [doi].
16. Lord P, Spiering R, Aguilon JC, et al. Minimum information about tolerogenic antigen-presenting cells (MITAP): A first step towards reproducibility and standardisation of cellular therapies. *PeerJ*. 2016;4:e2300. doi: 10.7717/peerj.2300 [doi].
17. Anderson AE, Swan DJ, Wong OY, et al. Tolerogenic dendritic cells generated with dexamethasone and vitamin D3 regulate rheumatoid arthritis CD4(+) T cells partly via transforming growth factor-beta1. *Clin Exp Immunol*. 2017;187(1):113-123. doi: 10.1111/cei.12870 [doi].
18. Harry RA, Anderson AE, Isaacs JD, Hilkens CM. Generation and characterisation of therapeutic tolerogenic dendritic cells for rheumatoid arthritis. *Ann Rheum Dis*. 2010;69(11):2042-2050. doi: 10.1136/ard.2009.126383 [doi].
19. Prakken BJ, Samodal R, Le TD, et al. Epitope-specific immunotherapy induces immune deviation of proinflammatory T cells in rheumatoid arthritis. *Proc Natl Acad Sci U S A*. 2004;101(12):4228-4233. doi: 10.1073/pnas.0400061101 [doi].
20. Gagliani N, Magnani CF, Huber S, et al. Coexpression of CD49b and LAG-3 identifies human and mouse T regulatory type 1 cells. *Nat Med*. 2013;19(6):739-746. doi: 10.1038/nm.3179 [doi].
21. Bacchetta R, Bigler M, Touraine JL, et al. High levels of interleukin 10 production in vivo are associated with tolerance in SCID patients transplanted with HLA mismatched hematopoietic stem cells. *J Exp Med*. 1994;179(2):493-502.
22. Bacchetta R, de Waal Malefijt R, Yssel H, et al. Host-reactive CD4+ and CD8+ T cell clones isolated from a human chimera produce IL-5, IL-2, IFN-gamma and granulocyte/macrophage-colony-stimulating factor but not IL-4. *J Immunol*. 1990;144(3):902-908.
23. Groux H, O'Garra A, Bigler M, et al. A CD4+ T cell subset inhibits antigen-specific T cell responses and prevents colitis. *Nature*. 1997;389(6652):737-742. doi: 10.1038/39614 [doi].
24. Wilson EB, El-Jawhari JJ, Neilson AL, et al. Human tumour immune evasion via TGF-beta blocks NK cell activation but not survival allowing therapeutic restoration of anti-tumour activity. *PLoS One*. 2011;6(9):e22842. doi: 10.1371/journal.pone.0022842 [doi].
25. Viel S, Marcais A, Guimaraes FS, et al. TGF-beta inhibits the activation and functions of NK cells by repressing the mTOR pathway. *Sci Signal*. 2016;9(415):ra19. doi: 10.1126/scisignal.aad1884 [doi].
26. Charbonnier LM, van Duivenvoorde LM, Apparailly F, et al. Immature dendritic cells suppress collagen-induced arthritis by in vivo expansion of CD49b+ regulatory T cells. *J Immunol*. 2006;177(6):3806-3813. doi: 177/6/3806 [pii].
27. Creusot RJ, Chang P, Healey DG, Tcherepanova IY, Nicolette CA, Fathman CG. A short pulse of IL-4 delivered by DCs electroporated with modified mRNA can both prevent and treat autoimmune diabetes in NOD mice. *Mol Ther*. 2010;18(12):2112-2120. doi: 10.1038/mt.2010.146 [doi].
28. Giannoukakis N, Phillips B, Finegold D, Harnaha J, Trucco M. Phase I (safety) study of autologous tolerogenic dendritic cells in type 1 diabetic patients. *Diabetes Care*. 2011;34(9):2026-2032. doi: 10.2337/dc11-0472 [doi].
29. Jauregui-Amezaga A, Cabezon R, Ramirez-Morros A, et al. Intraperitoneal administration of autologous tolerogenic dendritic cells for refractory crohn's disease: A phase I study. *J Crohns Colitis*. 2015;9(12):1071-1078. doi: 10.1093/ecco-jcc/jjv144 [doi].
30. Stoop JN, Harry RA, von Delwig A, Isaacs JD, Robinson JH, Hilkens CM. Therapeutic effect of tolerogenic dendritic cells in established collagen-induced arthritis is associated with a reduction in Th17 responses. *Arthritis Rheum*. 2010;62(12):3656-3665. doi: 10.1002/art.27756 [doi].
31. Popov I, Li M, Zheng X, et al. Preventing autoimmune arthritis using antigen-specific immature dendritic cells: A novel tolerogenic vaccine. *Arthritis Res Ther*. 2006;8(5):R141. doi: ar2031 [pii].
32. van Duivenvoorde LM, Han WG, Bakker AM, et al. Immunomodulatory dendritic cells inhibit Th1 responses and arthritis via different mechanisms. *J Immunol*. 2007;179(3):1506-1515. doi: 179/3/1506 [pii].
33. Raiotach-Regue D, Grau-Lopez L, Naranjo-Gomez M, et al. Stable antigen-specific T cell hyporesponsiveness induced by tolerogenic dendritic cells from multiple sclerosis patients. *Eur J Immunol*. 2012;42(3):771-782. doi: 10.1002/eji.201141835 [doi].

34. Mansilla MJ, Selles-Moreno C, Fabregas-Puig S, et al. Beneficial effect of tolerogenic dendritic cells pulsed with MOG autoantigen in experimental autoimmune encephalomyelitis. *CNS Neurosci Ther.* 2015;21(3):222-230. doi: 10.1111/cns.12342 [doi].
35. Benham H, Nel HJ, Law SC, et al. Citrullinated peptide dendritic cell immunotherapy in HLA risk genotype-positive rheumatoid arthritis patients. *Sci Transl Med.* 2015;7(290):290ra87. doi: 10.1126/scitranslmed.aaa9301 [doi].
36. van Eden W, van der Zee R, Prakken B. Heat-shock proteins induce T cell regulation of chronic inflammation. *Nat Rev Immunol.* 2005;5(4):318-330. doi: nri1593 [pii].
37. Zeng H, Zhang R, Jin B, Chen L. Type 1 regulatory T cells: A new mechanism of peripheral immune tolerance. *Cell Mol Immunol.* 2015;12(5):566-571. doi: 10.1038/cmi.2015.44 [doi].
38. Conigliaro P, Scrivero R, Valesini G, Perricone R. Emerging role for NK cells in the pathogenesis of inflammatory arthropathies. *Autoimmun Rev.* 2011;10(10):577-581. doi: 10.1016/j.autrev.2011.04.017 [doi].
39. Soderstrom K, Stein E, Colmenero P, et al. Natural killer cells trigger osteoclastogenesis and bone destruction in arthritis. *Proc Natl Acad Sci U S A.* 2010;107(29):13028-13033. doi: 10.1073/pnas.1000546107 [doi].
40. Dalbeth N, Callan MF. A subset of natural killer cells is greatly expanded within inflamed joints. *Arthritis Rheum.* 2002;46(7):1763-1772. doi: 10.1002/art.10410 [doi].
41. Dalbeth N, Gundle R, Davies RJ, Lee YC, McMichael AJ, Callan MF. CD56bright NK cells are enriched at inflammatory sites and can engage with monocytes in a reciprocal program of activation. *J Immunol.* 2004;173(10):6418-6426. doi: 173/10/6418 [pii].
42. Dunne J, Lynch S, O'Farrelly C, et al. Selective expansion and partial activation of human NK cells and NK receptor-positive T cells by IL-2 and IL-15. *J Immunol.* 2001;167(6):3129-3138.
43. Ma A, Koka R, Burkett P. Diverse functions of IL-2, IL-15, and IL-7 in lymphoid homeostasis. *Annu Rev Immunol.* 2006;24:657-679. doi: 10.1146/annurev.immunol.24.021605.090727 [doi].

Supplementary text

Establishment of DC

Immediately after isolation, monocytes were cultured in 24 wells plates (Corning) at 0.5×10^6 cells/ml (total 1 ml/well) for seven days in CellGenix DC medium (CellGenix) containing penicillin (100 U/ml), streptomycin (100 µg/ml), GM-CSF (50 ng/ml; Immunotools) and IL-4 (50 ng/ml; Immunotools). During this period cells were kept at 37°C with 5% CO₂. On day three, half of the medium was substituted by fresh (warm) medium containing GM-CSF (100 ng/ml) and IL-4 (100 ng/ml). For the generation of tolDC, dexamethasone (1 µM; Sigma) was added on days three and six and 1,25-dihydroxyvitamin D3 (Calcitriol; 0.1 nM; Tocris) and monophosphoryllipid A (MPLA) (1.0 µg/ml; Invivogen) were added only on day six. Immature DC (imDC) were cultured in the presence of GM-CSF (50 ng/ml) and IL-4 (50 ng/ml). On day seven, 24 hours after the last treatment, DC were harvested and washed extensively before functional assays were performed. DC were then resuspended at 4×10^5 cells/ml in X-VIVO-15. DC phenotype was checked using flow cytometry and was consistent with tolDC exhibiting a semi-mature phenotype, expressing low levels of CD83, intermediate levels of CD86 and high levels of human leucocyte antigen D-related (HLA-DR) and toll-like receptor 2 (TLR2; data not shown).

Flow cytometry

For cell surface staining: cells were washed in flow cytometry buffer (PBS (Lonza) supplemented with 3% fetal calf serum (FCS; Gibco), 1 mM EDTA (Fisher Scientific) and 0.01% sodium azide (Sigma)) before incubating them for 30 min on ice in flow cytometry buffer containing antibodies and 4 µg/ml human immunoglobulin (Ig) G (Grifols). Cells were washed and resuspended in flow cytometry buffer before analysis. For intracellular cytokine staining (ICS): cells were first stimulated with PMA (50 ng/ml) and ionomycin (1 µg/ml) for 5 hours in the presence of brefeldin A (1 µg/ml; all from Sigma Aldrich) at 37°C, 5% CO₂. Cells were then surface stained as described before, washed in flow cytometry buffer and fixed/permeabilised using cytofix/cytoperm buffer (BD Biosciences) for 30 min on ice. Cells were washed twice in 1x perm wash buffer (BD Biosciences) and stained for 30 min in 1x perm wash buffer containing antibodies and 8% mouse serum. Cells were washed once in 1x perm wash buffer and once in flow cytometry buffer before resuspending them in flow cytometry buffer.



Chapter 5

Lipidoid-polymer hybrid nanoparticles loaded with TNF siRNA suppress inflammation after intra-articular administration in a murine experimental arthritis model

Manon A.A. Jansen,^{†,‡} Lasse H. Klausen,^{#,‡} Kaushik Thanki,[§] Jeppe Lyngsø,^{#,||} Jan Skov Pedersen,^{#,||} Henrik Franzyk,^Δ Hanne M. Nielsen,[§] Willem van Eden,[†] Mingdong Dong,[#] Femke Broere,^{†,±} Camilla Foged,^{§,*} Xianghui Zeng^{§,*}

[†] Division of Immunology, Department of Infectious diseases & Immunology, Utrecht University, Utrecht, the Netherlands

[#] Interdisciplinary Nanoscience Center, Aarhus University, Gustav Wieds Vej 14, DK-8000 Aarhus C, Denmark

[§] Department of Pharmacy, Faculty of Health and Medical Sciences, University of Copenhagen, Universitetsparken 2, DK-2100 Copenhagen Ø, Denmark

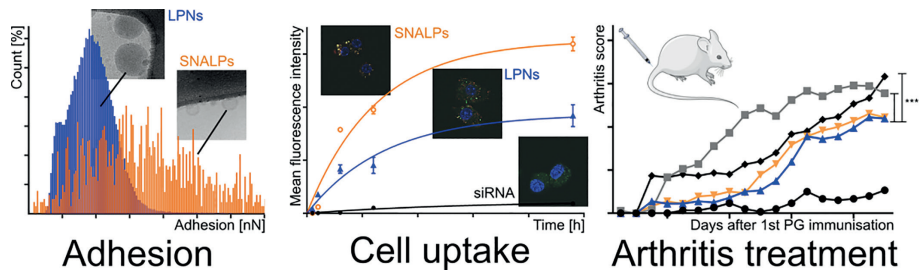
^{||} Department of Chemistry, Aarhus University, Gustav Wieds Vej 14, DK-8000 Aarhus C, Denmark

^Δ Department of Drug Design and Pharmacology, Faculty of Health and Medical Sciences, University of Copenhagen, Jagtvej 162, DK-2100 Copenhagen Ø, Denmark

[±] Department of Clinical Sciences of Companion Animals, Faculty Veterinary Medicine, Utrecht University, Utrecht, The Netherlands

Submitted

Graphical abstract



Abstract

Rheumatoid arthritis (RA) is an autoimmune disease, which is characterized by chronic inflammation in the joints, and novel safe and efficacious treatments are urgently needed. RNA interference (RNAi) therapy based on small interfering RNA (siRNA) is a promising approach for silencing specific genes involved in inflammation. However, delivery of siRNA to the target site, *i.e.* the cytosol of immune cells, is a challenge. We recently designed siRNA-loaded lipid-polymer hybrid nanoparticles (LPNs) composed of lipidoid and poly (DL-lactic-co-glycolic acid) and demonstrated their unprecedented ability to deliver a model cargo siRNA intracellularly. Here, we compared the delivery of a therapeutic cargo siRNA directed against tumor necrosis factor (TNF) mediated by LPNs and reference lipidoid-based stable nucleic acid lipid particles (SNALPs) *in vitro* and *in vivo*. Cryogenic transmission electron microscopy, atomic force microscopy and small-angle X-ray scattering revealed that the mode of loading of siRNA in lamellar structures differs between the two formulations. siRNA was tightly packed in LPNs, and LPNs displayed lower adhesion than SNALPs. LPNs mediated a higher TNF silencing effect *in vitro* than SNALPs in the RAW 264.7 macrophage cell line activated with lipopolysaccharide. For both types of delivery systems, macropinocytosis was involved in cellular uptake. In addition, SNALPs were taken up via clathrin-mediated endocytosis. LPNs loaded with TNF siRNA mediated sequence-specific suppression of inflammation in a murine experimental arthritis model upon intra-articular administration. Hence, this study demonstrates that LPN-mediated TNF knockdown may constitute a promising approach for arthritis therapy of TNF-mediated chronic inflammatory conditions.

Keywords: siRNA delivery; lipidoid; nanoparticles; vesicles; macrophage; TNF; arthritis.

Introduction

Rheumatoid arthritis (RA) is an autoimmune disease characterized by chronic synovial inflammation, leading to cartilage and bone destruction in the joints¹. In RA, the regulation of the inflammatory process is deficient, and immune responses against self-antigens are triggered. Currently, medication is directed towards relief of symptoms by the use of disease-modifying anti-rheumatic drugs (DMARDs). These drugs target the immune inflammatory response in a non-specific way, and undesired side effects are frequently experienced by RA patients. Hence, there is a need for novel and more specific treatments, which are efficacious and safe. The pro-inflammatory cytokine tumor necrosis factor (TNF), which is produced by monocytes and macrophages among other cell types, plays a key role in the progression of a wide variety of chronic inflammatory disorders, *e.g.*, RA. It is found in high concentrations in the serum and synovial fluid of patients with RA². TNF does not only induce other pro-inflammatory cytokines, but also the secretion of matrix-degrading proteases produced by fibroblasts, eventually resulting in destruction of cartilage. Currently, patients with RA are treated with anti-TNF biopharmaceuticals, which consist of monoclonal anti-TNF antibodies and soluble TNF receptors. Infliximab (monoclonal TNF antibody) and etanercept (soluble TNF receptor) are the most commonly used anti-TNF biopharmaceuticals. In combination with methotrexate, they are relatively efficacious in inducing disease remission^{3,4}. However, one of the disadvantages of this treatment strategy is that infliximab and etanercept may induce antibodies, which can result in response failure⁵. RNA interference (RNAi) therapy can be used to suppress disease-associated exacerbated inflammation and inhibiting TNF overexpression with small interfering RNA (siRNA) can prevent the problem of antibody formation.

However, a drug delivery system is needed to deliver siRNA intracellularly to target the RNAi pathway in the cytosol, because siRNA cannot permeate cellular membranes. A vast number of different cationic lipids and helper lipids have been intensively studied for delivery of exogenous nucleic acids into cells⁶. Cationic lipids form lipoplexes with nucleic acids by complexation with polyanionic nucleic acids via attractive electrostatic interactions. Owing to their fusogenic properties and ability to undergo structural changes from bilayer to hexagonal structures, certain cationic lipids or helper lipids can improve the transfection efficiency⁶. However, lipoplexes are highly unstable in serum-containing physiological media, eventually resulting in poor *in vivo* performance⁷.

A solution to this problem is to combine a polymeric core with a cationic lipid shell layer to form colloiddally more stable lipid-polymer hybrid nanoparticles (LPNs) for nucleic acid delivery⁸. We have demonstrated that LPNs composed of poly(DL-lactic-co-glycolic acid) (PLGA) and the cationic lipid 1,2-dioleoyl-3-trimethylammonium propane (DOTAP) efficiently deliver siRNA to cells and mediate high transfection efficiency^{9,10}. However, a main challenge is the toxicity of many cationic lipids. Therefore, replacement of the toxicity-associated cationic lipids with alternative and more transfection-competent lipids as the lipid component of LPNs might enable more efficient gene silencing. This would allow for dose reduction, thus improving the overall safety and efficacy of the delivery system. The so-called lipidoids are examples of such compounds that constitute a novel class of lipid-like components based on an alkylated tetraamine backbone¹¹. Depending on the alkylation degree, different subtypes are obtained *e.g.*, the penta-substituted lipidoid (*i.e.* L₅ which appears as an isomeric mixture) and the hexa-substituted lipidoid (*i.e.* L₆ being a single fully acylated entity)^{11,12}. We recently showed that if siRNA is encapsulated in LPNs based on PLGA and lipidoids, the intracellular delivery of siRNA is enhanced^{12,13}. Nevertheless, it is of major concern that bulk lipidoids are able to activate Toll-like receptor (TLR) 4¹³. However, inclusion of lipidoid into the LPNs structure was shown to abrogate TLR4 activation *in vitro*¹³.

To date, we have limited knowledge about the capability of lipidoid-based LPNs to deliver a therapeutic siRNA cargo and ensuing transfection efficiency *in vitro* and *in vivo*. Hence, we investigated the potential of LPNs for intracellular delivery of TNF siRNA resulting in TNF silencing in the murine macrophage cell line RAW 264.7 activated with lipopolysaccharide (LPS). For comparison, we prepared and characterized a reference formulation of TNF siRNA-loaded stable nucleic acid lipid particles (SNALPs) using lipidoid as the cationic lipid component, and investigated how the particle structure and surface properties of these two systems differentially affected the siRNA delivery to activated macrophages *in vitro*. Furthermore, their therapeutic capacities were tested *in vivo* in a murine experimental arthritis model.

Materials and methods

Materials

L₅ was synthesized, purified and characterized as previously reported¹¹. 2'-O-methyl modified dicer substrate asymmetric siRNA duplexes directed against TNF (TNF siRNA), negative control siRNA and Alexa647-labeled siRNA were kindly provided by GlaxoSmithKline (Stevenage, UK) as dried, purified and desalted duplexes



(Supplementary data, Table S2). Primers were purchased from TAG Copenhagen (Frederiksberg, Denmark). PLGA (lactide:glycolide molar ratio 75:25, Mw: 20 kDa) was purchased from Wako Pure Chemical Industries (Osaka, Japan). Polyvinylalcohol (PVA) 403 with an 80.0% degree of hydrolysis was provided by Kuraray (Osaka, Japan). Cholesterol and C₁₆ PEG₂₀₀₀ ceramide were purchased from Avanti Polar Lipids (Alabaster, AL, USA). Quant-iT™ RiboGreen® RNA Reagent and Tris-EDTA buffer were acquired from Molecular Probes Invitrogen (Paisley, UK). RNase-free diethyl pyrocarbonate (DEPC)-treated Milli-Q water was used for all buffers and dilutions. Additional chemicals were obtained commercially at analytical grade (Sigma-Aldrich, St Louis, MO, USA).

Preparation and physicochemical characterization of LPNs and SNALPs

The PLGA nanoparticles (NPs), the non-loaded LPNs and the siRNA-loaded LPNs were prepared using a double emulsion solvent evaporation method as previously reported⁹. Briefly, a volume of 125 µL of Tris-EDTA buffer or 66.7 mM TNF siRNA solution (w_1) was emulsified in 250 µL of a 15 mg PLGA in CH₂Cl₂ or 2.25 mg lipidoid/12.75 mg PLGA binary mixture in CH₂Cl₂ (o) by sonication to form a primary emulsion, which was dispersed in 2% (w/v) PVA aqueous solution (w_2), resulting in the formation of a water-in-oil-in-water ($w_1/o/w_2$) double emulsion. With the evaporation of CH₂Cl₂, the emulsion droplets were gradually solidified as LPNs. The LPNs were washed and freeze-dried as previously reported. L₅-based SNALPs loaded with TNF siRNA were prepared using the ethanol destabilization method as previously reported^{11,12}. For the Alexa647-labeled particles, TNF siRNA was replaced with the corresponding Alexa647-labeled siRNA.

The intensity-weighted average hydrodynamic diameter (z-average) and polydispersity index (PDI) of the NPs were determined by DLS using the photon correlation spectroscopy technique as previously described¹². Laser-Doppler electrophoresis was used to determine the zeta-potential of the NPs as previously described¹². The RiboGreen® RNA reagent was used to determine the siRNA encapsulation efficiency and practical loading as previously described⁹.

Cryo-transmission electron microscopy (cryo-TEM)

Morphological analysis was carried out by cryo-TEM using a Tecnai G2 20 TWIN transmission electron microscope (FEI, Hillsboro, OR, USA) as previously described⁹. In brief, samples for cryo-TEM were prepared using a FEI Vitrobot Mark IV. A small droplet was deposited onto a Pelco Lacey carbon-film grid and spread carefully; excess liquid was removed, resulting in the formation of a thin sample film. The samples were immediately plunged into liquid ethane and kept at -180 °C. The

vitrified samples were subsequently transferred in liquid nitrogen to an Oxford CT3500 cryo holder connected to the electron microscope. The sample temperature was continuously kept below -180 °C. All observations were made in bright field mode at an acceleration voltage of 120 kV. Digital images were recorded with a Gatan Imaging Filter 100 CCD camera (Gatan, Pleasanton, CA, USA).

Atomic force microscopy (AFM)

LPN dispersions were added to freshly cleaved muscovite mica and air-dried before characterization using a MultiMode 8 microscope (Bruker, Santa Barbara, CA, USA) operated in PeakForce QNM mode. TAP525A cantilevers (nominal spring constant 200 N/m, nominal tip radius 8 nm) (Bruker AFM Probes, Camarillo, CA, USA) were calibrated before and after characterization of each sample using an absolute method. Full force distance data was acquired and post processed using the Nano Scope Analysis v 1.80 (Santa Barbara, CA, USA). A nominal force of 100 nN was applied to indent the sample and the Young's Modulus was determined using the Hertz indentation model, while the maximum step height between the baseline and the minimum value of the curve was used to determine adhesion¹⁴.

Small-angle X-ray scattering (SAXS)

SAXS data were recorded using a modified flux-optimized NanoSTAR SAXS instrument (Bruker AXS) at Aarhus University with a rotating Cu source ($\lambda = 1.54\text{\AA}$),¹⁵ a two-pinhole setup with a home-built scatterless slit/pinhole in front of the sample, a semi-transparent beamstop, and a thermostated sample cell (Anton Paar GmbH, Graz, Austria). A home-built flow-through quartz capillary sample cell ($\phi = 2\text{mm}$) was used for the measurement. Data were recorded with a VÅNTEC-500 2D-area detector (Bruker AXS). LPNs (10 mg/mL) or SNALPs (1 mg/mL) were exposed for 900 s and Milli-Q water was subtracted as buffer background and used for absolute scale calibration. Data analysis was performed with the program package SUPERSAXS developed in-house (Oliveira, C. L. P.; Pedersen, J. S., unpublished).

Cell culture

The murine macrophage cell line RAW 264.7 was purchased from the American Type Culture Collection (TIP71, Manassas, VA, USA). The cells were maintained in Dulbecco's Modified Eagle's Medium (DMEM, Fisher Scientific Biotech Line, Slangerup, Denmark) and supplemented with 100 U/mL penicillin, 100 µg/mL streptomycin, 2 mM glutamine (all from Sigma-Aldrich) and 10% (v/v) fetal bovine serum (FBS, PAA Laboratories, Pasching, Austria). The cells were grown in an atmosphere of 5% CO₂/95% O₂ at 37 °C, the growth medium was renewed every second day, and the cells were sub-cultured twice a week by detaching them from the culture flask by scraping.



Determination of silencing efficiency *in vitro*

Silencing of TNF expression in activated RAW 264.7 cells was determined essentially as previously described^{10,16}. In brief, cells were seeded in 24-well tissue culture plates (Sigma) at a density of 1.0×10^5 cells per well and incubated overnight. Subsequently, nanoparticle suspensions were added to each well in triplicates, resulting in a final siRNA concentration of 100 nM, and then the cells were incubated for 21 h. To each well, 5 ng/mL (final concentration) LPS (Sigma-Aldrich) was added, and the cells were incubated for additional 3 h. Untreated cells were incubated with PBS, negative control cells received LPS but not siRNA or particles, and cells dosed with LPS and TNF siRNA complexed with Trans-IT TKO (Mirus Corp, Madison, WI, USA) served as the positive control. In addition, cells transfected with NPs loaded with scrambled siRNA were used as negative control. RNA was isolated and purified using the RNA Stat-60 (AMS Biotechnology, Abingdon, UK), and reverse transcription of RNA was performed by applying the iScript cDNA synthesis kit (Bio-Rad Laboratories, Hercules, CA, USA). The PCR reactions were conducted in duplicates using a LightCycler[®] 480 (Roche, Basel, Switzerland) and the SYBR Green[®] Master mix (Roche). The reference genes β -actin (ACT) and β -glucuronidase (GUS) were used for normalization. The LightCycler[®] 480 software v.1.5.0 (Roche) was used for crossing point (CP) analysis, followed by quantification relative to the LPS-treated cells using the comparative $\Delta\Delta CP$ method as previously described^{10,16}. The concentrations corresponding to 50% TNF silencing (IC_{50} values) for the dose-response curves were calculated using curve fitting algorithms (GraphPad Prism, La Jolla, CA, USA).

Viability assay

The effect of LPNs and SNALPs on the viability of RAW 264.7 cells was determined using the 3-(4,5-dimethylthiazol-2-yl)-2,5-diphenyltetrazolium bromide (MTT) assay. RAW 264.7 cells were seeded at a density of 10,000 cells per well in 96-well plates and cultured for 24 h. The cells were incubated with dispersions of LPNs or SNALPs in medium at different TNF siRNA concentrations for 24 h at 37 °C. Cells incubated with lipofectamine2000 (Invitrogen) were used as positive control, while untreated cells were used as negative control. After incubation, the cells were washed with PBS, and 100 μ L of freshly prepared MTT reagent in HBSS buffer was added to each well followed by incubation at 37 °C for 4 h. The cell viability was determined by measuring the absorbance of the formed formazan at 595 nm.

Cell apoptosis and necrosis analysis

Cell apoptosis and necrosis were determined essentially as described previously^{10,16}. RAW 264.7 cells were seeded in 24-well culture plates (Sigma) at a concentration of 4.0×10^5 cells per well. The apoptosis of cells, exposed to LPNs and SNALPs (at

TNF siRNA concentrations of 100, 200, 400, and 800 nM) for 24 h, was determined. After treatment, cells were collected, washed with PBS, and stained with FITC-labeled Annexin V and propidium iodide (Life Technologies, Carlsbad, CA, USA) following the manufacturer's instructions. The numbers of cells undergoing necrosis (positive for propidium iodide), early apoptosis (positive for Annexin V), and late apoptosis (double-positive for Annexin V and propidium iodide) were quantified by flow cytometry using a Gallios flow cytometer (Beckman Coulter, Brea, CA, USA) as previously described^{10,16}.

Cell uptake

Cellular association of siRNA was quantified by using flow cytometry. RAW 264.7 cells were seeded in 24-well plates (2.0×10^5 cells per well) 24 h before the experiment, which was initiated by incubating the cells with nanoparticles at a concentration of 100 nM Alexa647-labelled siRNA in medium at 37 °C for 0.5, 1, 3, 6 and 24 h. Cells were rinsed twice with PBS, scraped and diluted with medium. After washing and centrifugation, the cell pellet was resuspended in 200 μ L PBS and analyzed by flow cytometry using a Gallios flow cytometer (Beckman Coulter) as previously described¹⁷. Data were analyzed using FlowJo 7.6.5 (Three Star, Ashland, OR, USA).

In the uptake experiments conducted at 4 °C, RAW 264.7 cells were preincubated in medium at 4 °C for 10 min before NP suspensions were added, and the cells were incubated for 3 h either at 37 or 4 °C. For the endocytic inhibition assays, RAW 264.7 cells were washed with PBS, and fresh medium was added containing endocytosis inhibitors as previously described¹⁸. The cells were treated with NPs in the absence or presence of endocytosis inhibitors including nystatin (20 μ g/mL, Sigma) chlorpromazine (5 μ g/mL, Sigma), cytochalasin D (2 μ g/mL, Sigma), amiloride (100 μ g/mL, Sigma) and dynasore (26 μ g/mL, Sigma). The compounds were added to the cell culture medium 0.5 h prior to addition of the LPN or SNALP suspensions. The concentration of Alexa647 siRNA in the cell culture medium was 100 nM in all the experiments. The fluorescence level in the cells was determined after 3 h.

Cellular siRNA distribution

Confocal laser scanning microscopy was used to visualize uptake of Alexa647 siRNA in RAW 264.7 cells¹⁷. Cells were seeded in 12-well tissue culture plates containing a cover slip at a density of 4.0×10^5 cells per well. The cell culture medium was aspirated and replaced with fresh culture medium. Cells were incubated with NPs at a concentration equivalent to 100 nM of Alexa647 siRNA for 3 h at 37 °C. After incubation, the cells were washed three times with PBS and incubated for additional 1 h with LysoTracker DND99 (200 nM, Molecular Probes) to stain late

endosomes and lysosomes. After washing with PBS, the cells were fixed with fresh 3% (v/v) paraformaldehyde, and the cells were incubated with 4', 6-diamidino-2-phenylindole (DAPI, 0.2 µg/ mL, Invitrogen) for 5 min to stain the nuclei. After washing, the cover slips were placed on a slide using the Vectashield® mounting medium (Vector Laboratories, Peterborough, UK). The cells were imaged by confocal microscopy using a Zeiss LSM 710 confocal microscope (Carl Zeiss, Jena, Germany). The obtained images were processed using the Zeiss Zen black 2012 software.

Mice

Female Balb/cAnNCrI mice, 18-20 weeks old were purchased from Charles River laboratories (Sulzfeld, Germany). Animals were fed *ad libitum*, housed in groups of six mice per cage and kept under standard conditions of the animal facility. All experiments were approved by the Animal Experiment Committee of Utrecht University (AVD108002016467).

Induction of PGIA

Human proteoglycan (hPG) was isolated from human articular cartilage as previously described¹⁹. To induce arthritis, Balb/c mice were injected twice intraperitoneally with a mixture of 2 mg dimethyldioctadecylammonium (DDA) (Sigma Aldrich) and 250 µg human proteoglycan with a 21 day interval²⁰. Subsequently, mice were randomized among the experimental groups, and arthritis scores (0-4 per ankle, maximum score per mouse is 16, but the humane end point is 12) were determined three times a week in a blinded fashion using a visual scoring system based on swelling and redness of paws as previously described¹⁹. NP dispersions (10 µL/ mouse) were administered twice by intra-articular injection in the left ankle joint with 29G insulin syringes (1 mL, BD Medical, Le Pont de Claix Cedex, France) at day 25 and 27. The positive control group received three times a week an intraperitoneal injection with 125 µg dexamethasone in 100 µL PBS.

hPG ELISA

Blood was sampled from the submandibular vein of the mice by a cheek puncture on day 27 and 46. Serum was separated by centrifuging the blood at 10.000 g for 10 minutes. The hPG specific antibodies in serum were measured by enzyme-linked immunosorbent assay (ELISA). The hPG-specific IgG1 and IgG2a Ab levels were compared with a standard of pooled sera from arthritic mice. Flat-bottom Costar assay 96-well plates (Corning, Kennebunk, USA) were coated with hPG (5 µg/mL), and the free binding sites were blocked with 1% BSA (Sigma Aldrich, St Louis, USA) in PBS (Lonza, Maastricht, The Netherlands). Sera were applied in increasing dilutions, and levels of both total hPG-IgG and hPG-IgG2a were determined using

horse radish peroxidase conjugated goat anti-mouse IgG2a (Southern biotech, Birmingham, USA). For detection, 2,2'-Azinobis [3-ethylbenzothiazoline-6-sulfonic acid]-diammonium salt (ABTS, Roche, Woerden, The Netherlands) was used. Optical density was measured at 405 nm with a microplate reader (Bio-rad, 550 model).

Statistics

Experiments were performed in triplicate, and data are presented as mean values ± SD. The difference of experimental data between two groups was assessed using the two-tailed Student's *t* test, and one-way analysis of variance (ANOVA) followed by a Tukey's post hoc test was used to analyze the mean difference among groups. The statistical significance level was set to $p < 0.05$.

Results and discussion

Preparation of lipidoid-polymer hybrid nanoparticles (LPNs)

A double emulsion solvent evaporation method was applied to prepare non-loaded and TNF siRNA-loaded, L₅-modified LPNs, as previously reported¹². The mean hydrodynamic diameter (z-averages) of the resulting nanoparticles was approximately 210 nm and the polydispersity index (PDI) was approximately 0.11, inferring relatively narrow size distributions (Table 1). We used the previously reported ethanol destabilization method to prepare L₅-based SNALPs¹¹. Dynamic light scattering (DLS) results indicated that the average size of the siRNA-loaded SNALPs (74 ± 8 nm) was significantly smaller ($p < 0.001$) than the size of the LPNs (Table 1). The size distribution of the SNALPs was relatively narrow (PDI = 0.09 ± 0.01). The LPNs had a positive zeta potential (12.5 ± 6.5 mV), while the SNALPs displayed an almost neutral zeta potential (-1.3 ± 4.4 mV). The siRNA encapsulation efficiencies of the LPNs and SNALPs were 93.3 ± 5.7 % and 84.9 ± 1.5 %, respectively, indicating high siRNA entrapment efficiency for both types of nanoparticles (Table 1). An important observation is that the encapsulation efficiency measured for the TNF siRNA (93 %) is higher than the encapsulation efficiency we previously reported for an siRNA targeting enhanced green fluorescent protein (EGFP), as the latter LPNs displayed an encapsulation efficiency in the range of 60–80%¹². We speculate that the encapsulation efficiency is sequence-specific and may depend, among other factors, on the chemical modification pattern of the bases, which influences the hydrophobicity and hence the siRNA encapsulation during emulsification. The practical siRNA loading was approximately 10 times higher for the SNALPs than for the LPNs, as previously reported¹².

Table 1. Physicochemical properties of nanoparticles (NPs). Data represent mean values \pm standard deviation (SD, n = 3).

Formulation	Z-average (nm)	PDI	Zeta potential (mV)	Encapsulation efficiency (%)	siRNA loading ($\mu\text{g}/\text{mg}$ NPs)
PLGA NPs	195.6 \pm 1.9	0.08 \pm 0.01	-17.6 \pm 1.1		
Non-loaded LPNs ^{a)}	174.7 \pm 2.2	0.09 \pm 0.01	19.5 \pm 1.4		
LPNs ^{a,b)}	210.2 \pm 9.1	0.11 \pm 0.01	12.5 \pm 6.5	93.3 \pm 5.7	9.1 \pm 0.6
SNALPs ^{c)}	73.6 \pm 8.2	0.09 \pm 0.01	-1.3 \pm 4.4	84.9 \pm 1.5	98.9 \pm 1.9

^{a)} lipidoid:LPNs weight ratio 15%; ^{b)} siRNA:lipidoid weight ratio 1:15; ^{c)} siRNA:total lipids weight ratio 1:7.5.

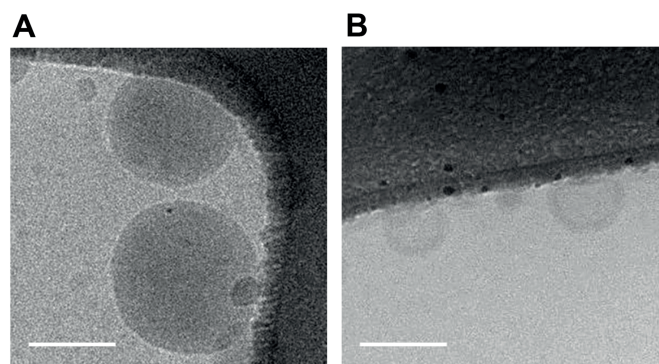


Figure 1. Representative cryo-TEM images of siRNA-loaded LPNs (A) and SNALPs (B). Scale bars = 100 nm.

The shape, morphology and size of LPNs and SNALPs loaded with TNF siRNA were examined by cryo-TEM (Figure 1). The LPNs were spherical (Figure 1A), and the particle sizes corresponded to the size distributions and PDIs measured by dynamic light scattering (Table 1). We observed a pronounced structural difference between LPNs and SNALPs (Figure 1 A and B). The electron density profile across the lipid layer structure observed for the SNALPs demonstrates that SNALPs are multilamellar vesicles (Figure 1B). In contrast, no lamellar structures were observable in the cryo-TEM images for the LPNs, and no visual difference was evident between the appearance of the non-loaded LPNs and the corresponding nanocarriers loaded with siRNA cargo. A similar morphology was demonstrated in our recently reported cryo-TEM studies of lipidoid-modified LPNs¹². Interestingly, previous SAXS studies indicated that lamellar lipid structures are present on the surface of DOTAP-modified LPNs⁹. The multilamellar vesicle model was proposed for the self-assembled SNALPs based on studies showing that the outer shell layer is composed of helper lipid and cationic lipid, while the nucleic acid cargo is localized between the onion-like lipid

bilayers^{21,22}. However, a nanostructure core model and a homogeneous core-shell model have also been proposed for such self-assembled lipid nanoparticles^{23,24}. It must be noted that the preparation method, the specific type of lipids, the formulation parameters, and the specific RNA cargo significantly contribute to the cargo loading, the particle volume and the resulting particle structure.

Nanomechanical characterization of nanoparticle stiffness and adhesion

The structure and stability of LPNs are important for their ability to efficiently deliver siRNA. The stiffness of nanoparticles can affect their cellular uptake²⁵. Hence, we examined the effect of L₅ and siRNA loading on the stiffness and adhesion of LPNs using quantitative nanomechanical mapping (QNM), which is an atomic force microscopy (AFM)-based method²⁶. The stiffness of the non-loaded PLGA particles was found to be 5.90 \pm 1.44 GPa (mean value \pm SD of the normal distribution, Figure 2A), corresponding to the stiffness reported for the bulk material²⁷. Inclusion of L₅ in the particle structure resulted in a significantly decreased particle stiffness of 2.16 \pm 0.57 GPa, whereas loading of siRNA resulted in an increased stiffness of 3.48 \pm 0.92 GPa. This indicates that both L₅ and siRNA interact with the PLGA matrix of the LPNs. The opposite zeta potential of the LPNs with L₅ incorporated as compared to that of unmodified PLGA NPs (Table 1), shows that the cationic L₅ is located on the surface of the LPNs. However, the adhesion force measured between the silicon AFM probe and the PLGA NPs was not affected by the incorporation of L₅ and loading of siRNA (Table S1). This could indicate that the main part of L₅ and siRNA are integrated within the bulk of the PLGA NPs, accounting for the lack of internal structure observed by cryo-TEM. The nanomechanical stiffness could not be accurately determined for the SNALPs due to their small size and strong adhesion. Compared to LPNs, a significantly stronger and more variable adhesion of SNALPs was observed (Figure 2B), which is most likely caused by a different surface composition and morphology of SNALPs.

SAXS characterization of L₅ and siRNA loading in LPNs

To further investigate the packing of L₅ and siRNA, we characterized the LPNs by SAXS. The SAXS data of the LPNs, displayed as intensity as a function of the modulus of the scattering vector, q , showed strong scattering at low $-q$ values originating from the overall particle size in the nano range (Figure 2C, cyan, red and black curves). The smaller-sized SNALPs showed a distinctly different signal indicative of vesicular structures, where a low $-q$ upturn, originating from the overall shape, was observed along with a characteristic broad bilayer core-shell cross-section bump

in the medium q range (Figure 2C, blue curve). No Bragg-like peaks were observed for the unmodified PLGA NPs (Figure 2C, cyan curve), indicating that there is no ordered structural organization of the PLGA polymer on the nanometer length scale, in agreement with previously published results⁸. Inclusion of L_5 resulted in the appearance of peaks at q -values of approximately 0.0455 and 0.091 \AA^{-1} , respectively (red curve). Using Bragg's law, these peaks can be assigned to structures with d spacings of approximately 138 \AA and 69 \AA , respectively (Figure 2C, red curve, red arrows). Considering the amphiphilic structure of L_5 , these peaks were identified as the characteristic first and second order reflection of a lamellar phase with a periodicity of approximately 69 \AA . Lamellar L_5 structures have not previously been studied, but for dispersions of bulk L_5 , we observed a periodic structure of approximately 50 \AA (results not shown). Loading of siRNA into the LPNs resulted in the appearance of an additional broad peak at a q -value of 0.125 \AA^{-1} , corresponding to a d spacing of 50 \AA (blue arrow). The first and (less visible) second order peaks of L_5 were also present with d spacings of approximately 135 \AA and 69 \AA , respectively (Figure 2C, black curve, red arrows). Therefore, these data suggest that L_5 forms a bilayer structure when included in the PLGA NPs. However, in the absence of counter charges, *e.g.*, provided by the siRNA, this structure has a significantly larger d spacing than the native bilayer, probably as a result of interbilayer repulsive electrostatic interactions between the cationic groups. Hence, the siRNA is integrated with the L_5 in the PLGA NPs, where bilayers of similar thickness as the native L_5 bilayers are formed. This is in agreement with our previous results, where it was observed that increased loading with siRNA resulted in a decreased thickness of the DOTAP bilayers in the LPNs⁹. The weak peak at a d spacing of approximately 69 \AA could indicate the coexistence of non-complexed L_5 . Further experiments are needed to elucidate the structural properties of L_5 in greater detail, as the molecule displays four amine functionalities and five hydrocarbon chains that could result in alternative structures in addition to the observed bilayer structure.

The SAXS data for the SNALPs (Figure 2C, blue curve) were simplistically modeled by using a single-layered polydisperse vesicle model to obtain information about the particle morphology and the bilayer cross-section structure. The fit suggested a vesicle diameter of approximately 76 nm, correlating well with the hydrodynamic diameter measured by DLS (Table 1), and a bilayer cross-section thickness of approximately 10 nm, which is in the same range as the width of the electron density distribution measured using cryoTEM (Figure 1B).

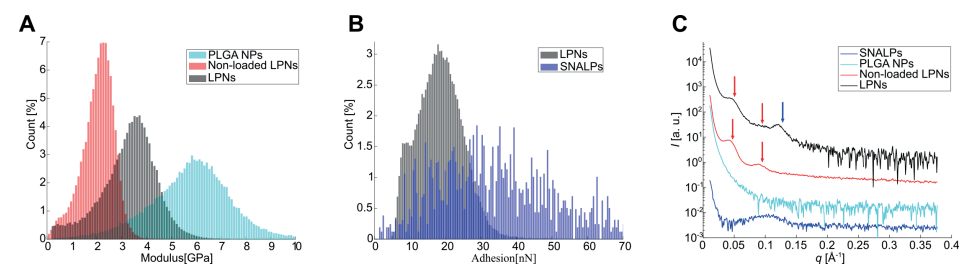


Figure 2. (A) AFM-based nanomechanical stiffness characterization of unmodified PLGA NPs (cyan), non-loaded LPNs (red) and siRNA-loaded LPNs (black). (B) Adhesion of LPNs (black) and SNALPs (blue). (C) SAXS diffraction patterns for SNALPs (blue), PLGA NPs (cyan), non-loaded LPNs (red) and siRNA-loaded LPNs (black). Red and blue arrows, respectively, indicate the Bragg-like peaks corresponding to lamellar structures.

siRNA-loaded LPNs mediate dose-dependent TNF mRNA silencing

The ability of siRNA-loaded LPNs and SNALPs to mediate RNAi *in vitro* was evaluated in LPS-activated RAW 264.7 cells by real-time reverse transcription (RT) PCR as previously described^{10,16}. The TNF silencing mediated by LPNs and SNALPs was dose-dependent (Figure 3A). The half-maximal inhibitory concentration (IC_{50}) of LPNs (21.5 ± 2.2 nM) was significantly lower ($p < 0.05$) than the IC_{50} value of SNALPs (38.1 ± 5.3 nM). Negative control LPNs loaded with scrambled siRNA did not induce any silencing of TNF expression, whereas the commercial siRNA transfection reagent TKO induced TNF silencing in a dose-dependent manner (Figure S1). These results indicate siRNA-dependent induction of RNAi mediated by LPNs and SNALPs. Our previous study showed that the IC_{50} value for the transfection efficiency of LPNs loaded with EGFP siRNA was in the range of 4 – 10 nM in the human non-small cell lung carcinoma cell line H1299 stably transfected with EGFP¹². This discrepancy may be a result of cell line-dependent differences in transfection efficiency.

Subsequently, the cell viability was examined in order to exclude that the observed TNF silencing effect was influenced by NP-induced toxicity. Cell viability measurements using the MTT assay showed that neither LPNs nor SNALPs caused any significant toxicity *in vitro* in RAW 264.7 cells in the tested concentration range (Figure S2). Potential apoptotic and necrotic effects of the particles, which may not be apparent from the MTT assay, were investigated by flow cytometry using a combination of fluorescein isothiocyanate (FITC)-labeled annexin V and propidium iodide. Compared with the negative control (PBS), no significant apoptosis or necrosis was observed for LPNs and SNALPs at siRNA concentrations of 100 nM and 200 nM, respectively (Figure 3B). At the highest siRNA concentration tested (400 nM),

both types of particles induced low levels of apoptosis (<10%). In addition, a significant increase in induced apoptosis/necrosis was observed for SNALPs as compared to that found for LPNs at an siRNA concentration of up to 800 nM ($p < 0.01$). Induction of apoptosis or necrosis at such high concentrations could be attributed to the undesired side effects mediated by the cationic lipidoid component of the LPNs¹³.

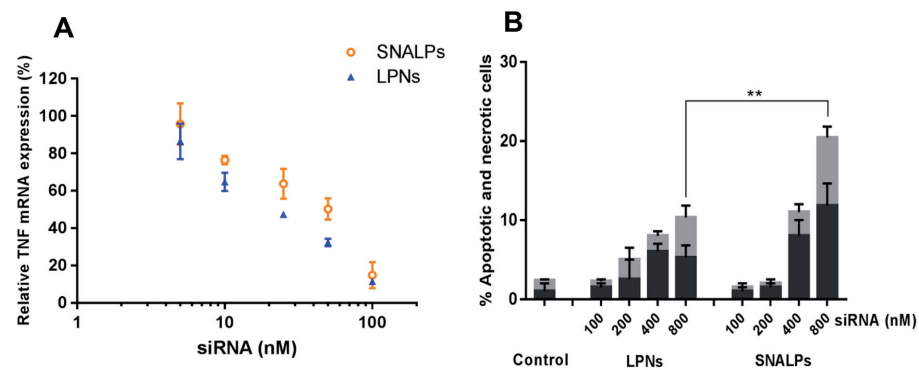


Figure 3. (A) TNF mRNA silencing in RAW 264.7 cells incubated with LPNs (blue triangles) or SNALPs (orange circles). Results are normalized to non-transfected, LPS-treated cells (100%). (B) Comparison of apoptotic (black) and necrotic (gray) cells for RAW 264.7 cells incubated with LPNs and SNALPs for 24 h, respectively, measured relative (in percentage) to the values for untreated RAW 264.7 cells (control). Data represent mean values \pm SD ($n = 3$). $**p < 0.01$.

RAW 264.7 cells internalize siRNA more efficiently when encapsulated in LPNs and SNALPs, and the NP-mediated uptake is energy-dependent

To quantitatively investigate cellular uptake in RAW 264.7 cells, Alexa647-labelled siRNA was loaded in LPNs and SNALPs, respectively, and the uptake in cultured living cells was compared to the uptake of unloaded Alexa647-labelled siRNA by measuring the Alexa647 fluorescence intensity after incubation for 0.5, 1, 3, 6 and 24 h (Figure 4A). After a relatively short incubation period (0.5 and 1 h), the levels of cellular siRNA delivered by LPNs appeared to be higher than the levels delivered by SNALPs. However, the cellular levels of siRNA were significantly higher in the case of SNALPs after continued treatment in new culture medium for 3, 6 or 24 h. The uptake data were analyzed using pseudo-first and pseudo-second order kinetics, which have been employed to characterize uptake profiles²⁸. The LPNs and SNALPs tended to exhibit pseudo-first order uptake characteristics (Figure 4A). For pseudo-first order model, the fraction of intracellular siRNA delivered by LPNs and SNALPs increases exponentially as a function of incubation time, and the uptake efficiency is dependent on the specific type of NPs. In addition, the r^2 values of fits for both

models for the unloaded siRNA were found to be less than 0.9, indicating that the uptake of unloaded siRNA neither follows pseudo-first order nor pseudo-second order kinetics. In contrast, very little unloaded siRNA was taken up by RAW 264.7 cells, which is consistent with the hypothesis that large biomolecules like siRNA are hardly endocytosed by cells²⁹. To investigate the energy dependency of the cellular internalization, the uptake of the particles was compared at 4 and 37 °C. Endocytosis is an energy-dependent process that is inhibited at low temperatures³⁰. There was a remarkable reduction of intracellular siRNA accumulation at 4 °C, which was 88% for LPNs and 98% for SNALPs, respectively, as compared to the experiments performed at 37 °C (Figure 4B). These findings indicate that both LPNs and SNALPs are internalized via energy-dependent processes.

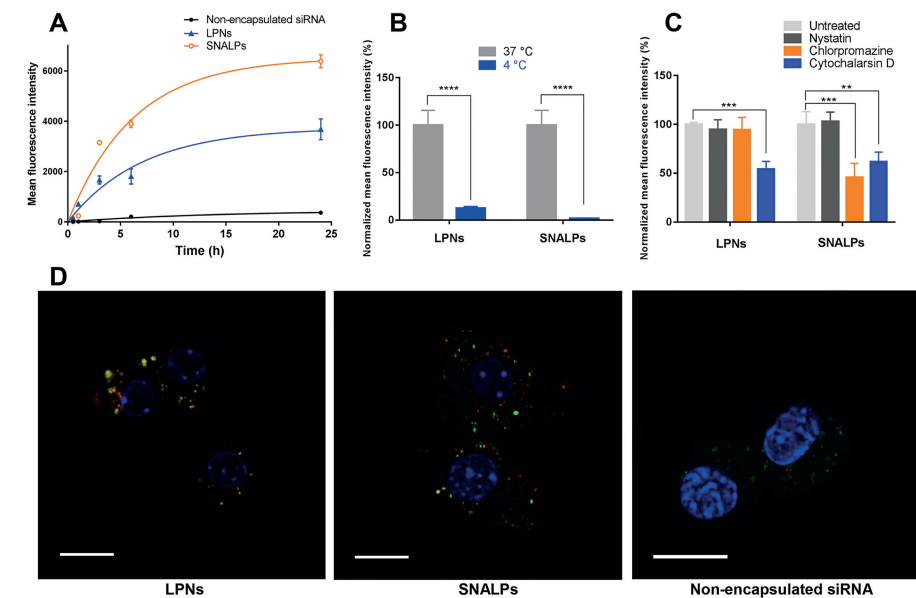


Figure 4. (A) Intracellular Alexa647 siRNA level in RAW 264.7 cells exposed to non-encapsulated Alexa647 siRNA, LPNs and SNALPs, respectively for 0.5, 1, 3, 6 and 24 h at 37 °C, and plot of the data with nonlinear regression fits (full lines). (B) Endocytosis of NPs loaded with Alexa647 siRNA at 4 °C. Cells were pretreated at 4 °C for 10 min prior to subsequent incubation of NPs at 4 °C for 3 h. $***p < 0.0001$ when compared with cells incubated at 37 °C. (C) RAW 264.7 cells were pre-incubated with inhibitors for 0.5 h, and they were subsequently cultured in medium containing NPs. The concentration of Alexa647 siRNA in the cell culture medium was 100 nM in all the experiments. The fluorescence level of Alexa647 siRNA was determined at 3 h. $**p < 0.01$, $***p < 0.001$, as compared to untreated cells. Data represent mean \pm SD ($n = 3$). (D) Representative confocal microscopy images of RAW 264.7 cells (blue: nuclei) transfected with LPNs, SNALPs and non-encapsulated Alexa647 siRNA, respectively. In all experiments a concentration of 100 nM Alexa647 siRNA was used. The co-localization patterns (yellow) of siRNA (red) with LysoTracker (late endosome/lysosome marker, green) 3 h after treatment with NPs show different intracellular siRNA distribution patterns. Scale bars = 20 μ m.

Macropinocytosis and clathrin-mediated endocytosis are possible mechanisms involved in the uptake of LPNs and SNALPs

A considerable difference between the siRNA uptake profiles of the LPNs and SNALPs was noted, indicating that the siRNA delivery mediated by these two types of nanoparticles is likely to involve different endocytic pathways. Hence, we performed selective inhibition assays to elucidate which endocytic pathways that are involved in the cellular internalization of lipidoid-based nanoparticles¹⁸. We studied the effects of selective inhibitors of macropinosome-mediated endocytosis (*i.e.*, cytochalasin D), clathrin-mediated endocytosis (*i.e.*, chlorpromazine), or caveolae-mediated endocytosis (*i.e.*, nystatin) on the uptake of Alexa647-labeled siRNA-loaded LPNs and SNALPs in RAW 264.7 cells (Figure 4C). In comparison to cell-associated fluorescence in the absence of inhibitors, treatment with cytochalasin D led to reduced siRNA uptake, suggesting that the cellular uptake pathway for LPNs and SNALPs may be macropinocytosis (Figure 4C). Furthermore, a significant decrease in SNALP-associated fluorescence was observed for cells treated with chlorpromazine (Figure 4C). Therefore, clathrin-mediated endocytosis may also be involved in the uptake of SNALPs in RAW 264.7 cells. In contrast, incubation with nystatin did not influence cellular internalization, which suggests that caveolae-mediated endocytosis is not involved in uptake. The effects of amiloride (an inhibitor of macropinosome-mediated endocytosis) and dynasore (an inhibitor of clathrin-mediated endocytosis) treatment on the uptake of nanoparticles in RAW 264.7 cells were also studied. The obtained results demonstrated the comparable endocytic pathways for LPNs and SNALPs (Figure S3). The experimental results indicate that macropinocytosis appears to be the primary endocytic mechanism for uptake of both LPNs and SNALPs in RAW 264.7 cells. This is probably a result of the unique phagocytic capacity of macrophages, which generally serve as scavengers by engulfing foreign particles³⁰. In addition, the particle size is a major parameter affecting endocytosis of NPs³¹. Clathrin-coated vesicles have a general diameter of approximately 150 nm³¹. Since the diameter of SNALPs is in the range of 60-80 nm, it is likely that clathrin-coated vesicles may also be involved in the intracellular trafficking of SNALPs. Likewise, lipid NPs with an average diameter of approximately 60 nm have been shown to enter cells via clathrin-mediated endocytosis, as well as micropinocytosis³². Apart from inhibitors, endocytic markers and endogenous protein knock-out cell lines may also be employed to verify or exclude specific endocytic pathways for nanomedicines³³. The mechanisms of LPN uptake in cell culture remain to a large extent unknown, and further studies are needed to elucidate the exact endocytosis mechanisms.

To examine further how LPNs and SNALPs are taken up by antigen-presenting cells, we used confocal microscopy to investigate qualitatively their distribution and extent of cellular accumulation in RAW 264.7 cells upon incubation for 3 hours at concentrations corresponding to 100 nM Alexa647 siRNA (Figure 4D). A strong red fluorescence signal from Alexa647 siRNA was observed in RAW 264.7 cells incubated with both types of nanoparticles (Figure 4D), indicating that both LPNs and SNALPs mediate intracellular delivery of a considerable amount of siRNA. In contrast, only a weak fluorescence signal was present in cells treated with non-encapsulated siRNA, which confirms that the use of a delivery system is important for siRNA transfection. In order to obtain more details on the intracellular trafficking of the particles, we performed co-localization studies using lysotracker to distinguish labeled siRNA present in endosomes and lysosomes. Co-localization of the fluorescence signals (yellow color) from Alexa647 siRNA and lysotracker demonstrate that both LPNs and SNALPs may be transported to late endosomes and lysosomes following endocytosis in RAW 264.7 cells (Figure 4D). In addition, red fluorescence signals from Alexa647 siRNA were observed in cells treated with LPNs and SNALPs, which indicates that siRNA escapes from the lysosomes into the cytosol.

LPNs and SNALPs loaded with TNF siRNA reduce experimental arthritis *in vivo* after intra-articular administration

To test the effect of TNF siRNA-loaded LPNs and SNALPs on arthritis progression, we made use of the proteoglycan-induced arthritis (PGIA) model²⁰. Arthritis was induced by intraperitoneal injection (i.p.) of a mixture of hPG and DDA. After two injections with hPG/DDA (on day 0 and day 21), the mice were dosed (on day 25 and day 27) with LPNs or SNALPs loaded with TNF siRNA or scrambled siRNA, and non-encapsulated siRNA was used as control (Figure 5). Local administration was performed via intra-articular injections, where a dose volume of 10 μ L of the nanoparticle dispersions or non-encapsulated siRNA was injected, respectively. As positive control, mice were injected three times a week with dexamethasone, which is an immune-suppressing drug used for RA treatment. From day 23 onwards, mice were scored three times a week for arthritic symptoms to monitor disease progression.

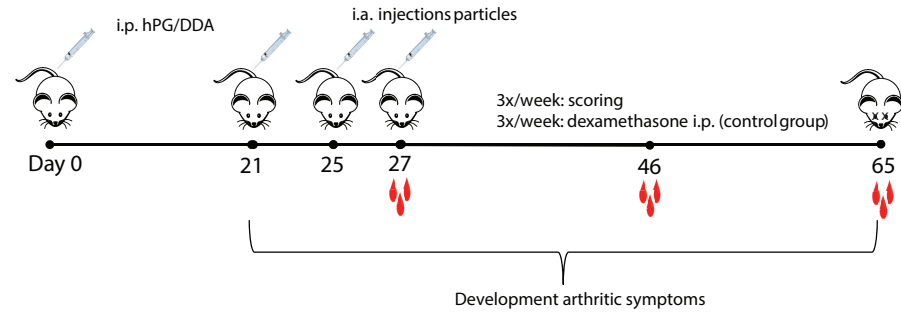


Figure 5. Experimental scheme. Mice were immunized twice intraperitoneally (i.p.) with a mixture of 250 μ g hPG and 2 mg DDA at day 0 and day 21. The mice were dosed twice at day 25 and day 27 with the different treatments. From day 21, the animals were scored three times a week for arthritis symptoms. As positive control, animals were dosed i.p. three times a week with 125 μ g dexamethasone from day 21. Blood samples were collected at day 27 and 46 for measurement of hPG-specific antibodies. Animals were euthanized at day 65, and hPG-specific antibodies were measured in the blood.

Mice that were dosed with LPNs or SNALPs (loaded with 1 μ g TNF siRNA) showed significantly less arthritic symptoms than the control groups (Figures 6A and B). In contrast, mice that were dosed with TNF siRNA loaded in DOTAP-modified PLGA NPs did not show reduced arthritis (Figure S4). Although non-encapsulated TNF siRNA alone also reduced arthritic symptoms (Figure 6C), it should be noted that the dose of the non-encapsulated TNF siRNA was ten times higher than the siRNA dose of the administered NP dispersions (10 μ g vs 1 μ g). These results show that L₅-modified LPNs loaded with siRNA deliver their cargo efficiently *in vivo*.

Furthermore, mice that were treated with TNF siRNA encapsulated in SNALPs or LPNs did not only show a reduced disease severity (as shown by the maximum arthritis score) but also a delayed onset of arthritis (Table 2). Mice that were injected with non-encapsulated TNF siRNA experienced the first arthritic symptoms at a similar time point as the control groups treated with scrambled non-encapsulated siRNA. This indicates that loading of siRNA in NPs enhances the delivery of the siRNA also *in vivo*. In contrast, mice that received a higher dose of NPs, corresponding to 10 μ g siRNA, showed inflammatory symptoms immediately after injection (data not shown), indicating that this dose induces immune activation. Since the results showed a systemic effect of the NPs (when the arthritis score from the injected paw was subtracted, the mice that received LPNs and SNALPs containing TNF siRNA remained significantly less sick than the control groups), systemic administration of the cargo would be an option in future experiments³⁴.

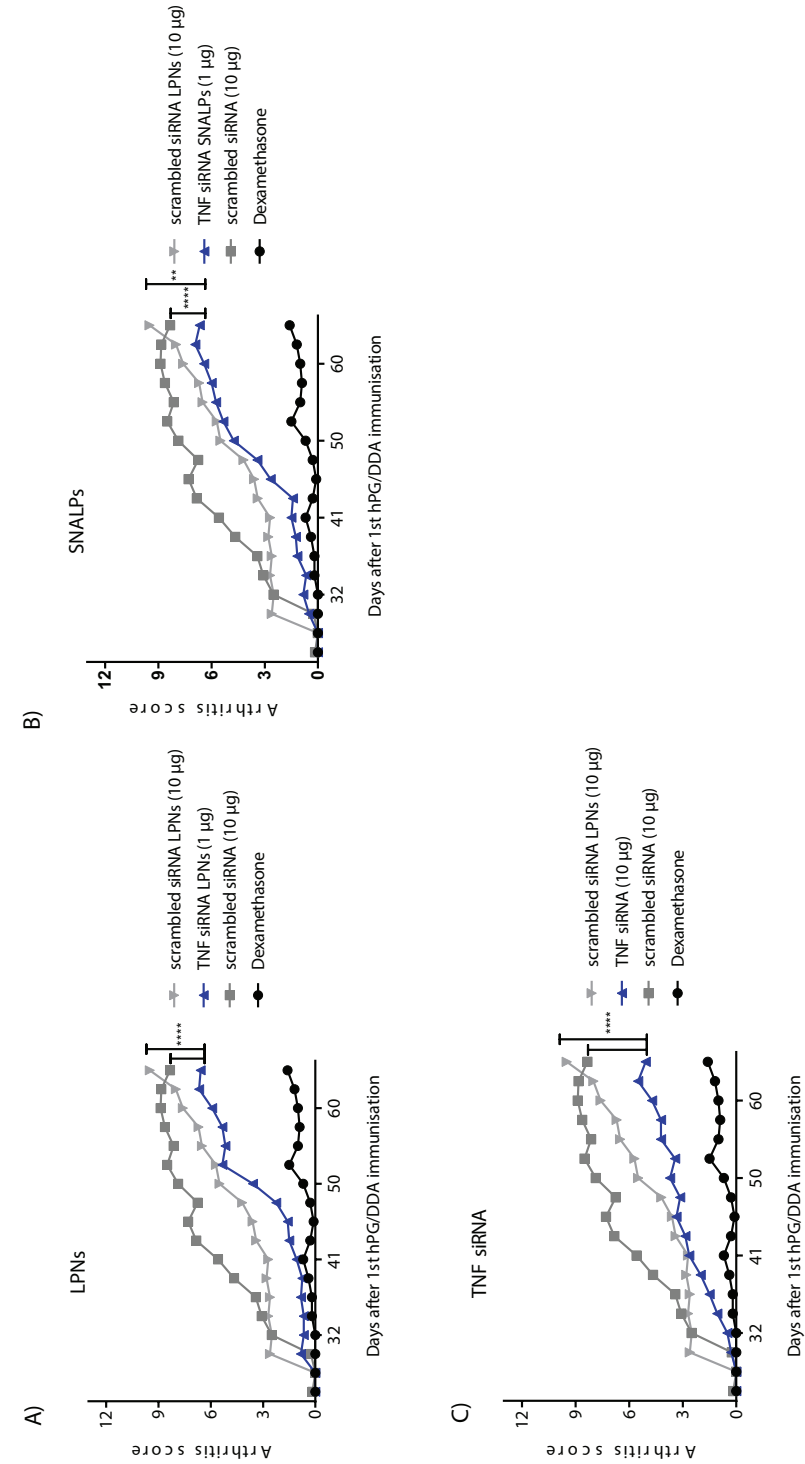


Figure 6. Therapeutic effect of TNF siRNA-loaded LPNs and SNALPs *in vivo*, shown as the arthritis score as a function of the number of days after the first hPG/DDA immunization. Two intra-articular injections were given in the left ankle joint of the mice at day 25 and 27 of (A) LPNs (1 μ g siRNA, blue triangles), (B) SNALPs (1 μ g siRNA, blue triangles) and (C) non-encapsulated TNF siRNA (10 μ g siRNA, blue triangles); this reduced arthritis compared to the control groups treated with scrambled siRNA (10 μ g siRNA, grey squares) and LPNs loaded with scrambled siRNA (10 μ g siRNA, grey inverted triangles). As positive control, animals were treated three times a week with dexamethasone (125 μ g in 100 μ L PBS, black circles). The control groups are shown in all plots. Statistical analysis at day 65: two-way analysis of variance (ANOVA) and Tukey's post hoc test. Data represent mean values, n = 6. * p < 0.05, ** p < 0.01, and **** p < 0.0001.



Table 2. Maximum arthritis score and day of onset of disease.

Group	Maximum arthritis score	Day of onset
Dexamethasone	1.7 ± 0.9	50.0 ± 6.6
TNF siRNA SNALPs (1 µg)	7.4 ± 3.2	43.2 ± 7.8
TNF siRNA LPNs (1 µg)	7.4 ± 2.7	46.3 ± 9.4
TNF siRNA (10 µg)	6.1 ± 3.9	35.3 ± 5.4
Scrambled siRNA LPNs (10 µg)	10.0 ± 2.4	33.0 ± 8.0
Scrambled siRNA (10 µg)	10.9 ± 1.6	35.3 ± 4.9

Data represent mean values ± SD (n = 6). As day of onset of disease is considered the first day on which a mouse has a score of 1 or more at one of the paws or toes. The maximum arthritis score is the maximum arthritis score during the entire experiment (not at day of euthanization).

SNALPs reduce the Th1-mediated immune response

Besides the disease-suppressing effects, we tested whether TNF siRNA loaded in LPNs and SNALPs, respectively, could modify the adaptive immune response. To determine whether TNF siRNA treatment had an effect on antibody production, we compared serum antibody levels at three different time points (t = 27, 46, and 65 days, Figure 7). Disease inducing antigen hPG-specific IgG2a antibodies were measured for all groups and time points. At the last time point (t = 65 days), the mice that were dosed with TNF siRNA loaded in SNALPs showed a significantly decreased level of hPG-specific IgG2a antibodies similar to the positive control group treated with dexamethasone. Treatment with non-encapsulated TNF siRNA or LPNs loaded with TNF siRNA did not reduce the hPG-specific IgG2a antibody levels in serum, as compared to the antibody levels measured for the control group treated with scrambled, non-encapsulated siRNA. In the applied PGIA model, mice that accommodate a response against autologous proteoglycan, and thus develop arthritic symptoms, have been shown to exhibit an increase in Th1-supported IgG2a antibodies³⁵. As shown by the measurements in serum, SNALPs but not LPNs influence the production of hPG-specific-IgG2a antibodies (Figure 7). Since IgG2a antibodies are driven by the Th1 cytokine interferon γ (IFN- γ), it is possible that SNALPs inhibit the production or neutralize this cytokine, whereas non-encapsulated TNF siRNA and LPNs containing TNF siRNA do not affect IFN- γ ³⁶. Furthermore, no differences in the levels of hPG-specific IgG1 antibodies were observed (data not shown), which indicates that non-encapsulated TNF siRNA, TNF siRNA-loaded LPNs, and TNF siRNA-loaded SNALPs do not affect the Th2 response.

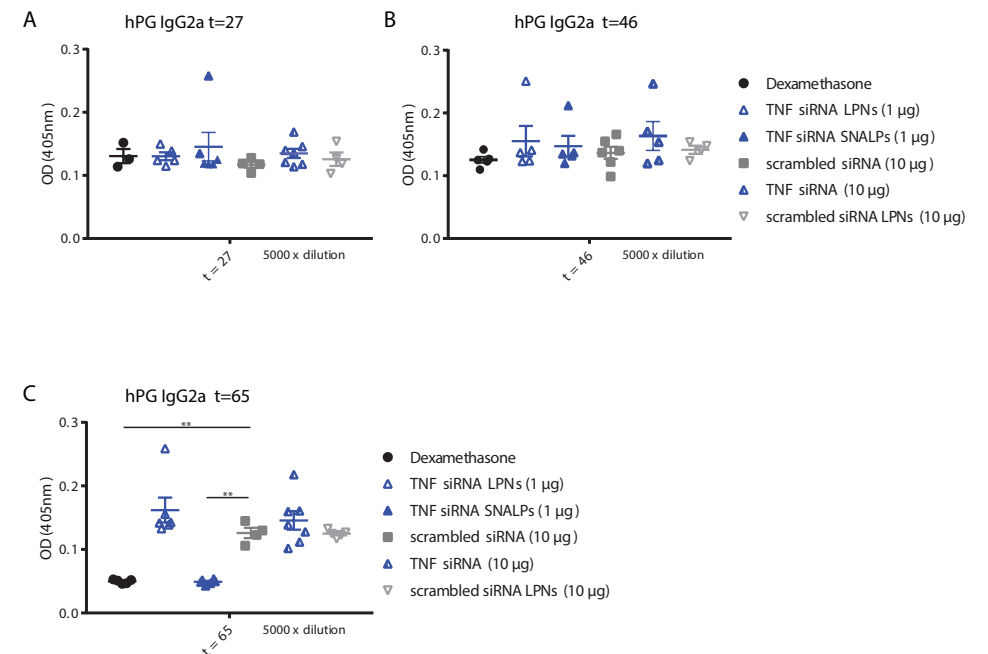


Figure 7. Treatment with SNALPs loaded with TNF siRNA reduces the levels of hPG-specific IgG2a antibodies. hPG-specific IgG2a antibodies were measured in serum at day 27, 46 and 65. At the first two time points (A and B), there was no statistically significant differences in the hPG IgG2a antibody levels between the groups. However, on day 65 (C), the mice treated with TNF siRNA encapsulated in SNALPs (filled upward triangles) showed antibody levels comparable to the positive control group (dexamethasone, filled circles), which were significantly lower than the levels measured for the group treated with scrambled non-encapsulated siRNA (filled squares). Optical density (OD) was measured at 405 nm. Statistical analysis: two-way analysis of variance (ANOVA) and Tukey's post hoc test. Bars represent mean values ± SD, n = 6. ***p* < 0.01.

Conclusions

In conclusion, we have designed a new type of lipidoid-based LPNs, for which the siRNA delivery efficiency was compared to that of canonical SNALP nanoparticles. LPNs were larger in size and more stable than SNALPs, and siRNA was incorporated into the particle matrix as opposed to being displayed mainly on the surface of SNALPs, as seen from cryo-TEM and validated by AFM and SAXS experiments. The *in vitro* experiments show that both LPNs and SNALPs are efficient delivery systems for TNF siRNA, as evident by their ability to reduce the expression of TNF in LPS-activated macrophages. Both particle types were taken up via macropinocytosis, while only SNALPs could be taken up via clathrin-mediated endocytosis. *In vivo* results indicate that LPNs and SNALPs can efficiently suppress inflammation in

an experimental arthritis model by using a relatively low TNF siRNA dose (1 µg). Furthermore, treatment with SNALPs lead to a reduced Th1 response. These findings may guide future rational design of lipidoid-based nanocarriers for siRNA delivery in chronic inflammatory disorders and autoimmune diseases.

Notes

XZ, KT, HF, HMN and CF are inventors of a patent application relating to the cationic lipid structure (European PCT application number 57590PC01). All rights have been assigned to University of Copenhagen. All other authors report no potential conflicts.

Acknowledgements

We gratefully acknowledge the support from the Danish Council for Independent Research and FP7 Marie Curie Actions – COFUND (grant number DFF-4093-00292), the Lundbeck Foundation - Denmark (grant numbers R181-2014-3793 and R219-2016-908), Hørslev-Fonden – Denmark, the Carlsberg Foundation – Denmark and the Novo Nordisk Foundation – Denmark (grant number NNF17OC0026526). We are also thankful to the Innovative Medicines Initiative Joint Undertaking under grant agreement no. 115363 resources which are composed of the financial contribution from the European Union's Seventh Framework Programme (FP7/2007-2013) and EFPIA companies' in kind contributions. LHK acknowledges support from the Carlsberg Foundation Internationalization fellowships (CF16-0757). This project has received funding from the European Union's Seventh Framework Programme for research, technological development and demonstration under grant agreement no. 600207. We acknowledge the Core Facility for Integrated Microscopy, Faculty of Health and Medical Sciences, University of Copenhagen and the skilled technical assistance of Klaus Qvortrup. We are grateful to Emily Falkenberg for synthesizing and purifying L₅. Furthermore, we thank Dr. Irene Ludwig for technical assistance during the *in vivo* experiments and the Dutch Arthritis foundation for financial support.

References

1. Aletaha D, Neogi T, Silman AJ, et al. 2010 rheumatoid arthritis classification criteria: An american college of rheumatology/european league against rheumatism collaborative initiative. *Ann Rheum Dis.* 2010;69(9):1580-1588. doi: 10.1136/ard.2010.138461 [doi].
2. Tetta C, Camussi G, Modena V, Di Vittorio C, Baglioni C. Tumour necrosis factor in serum and synovial fluid of patients with active and severe rheumatoid arthritis. *Ann Rheum Dis.* 1990;49(9):665-667.
3. van der Kooij SM, le Cessie S, Goekoop-Ruiterman YP, et al. Clinical and radiological efficacy of initial vs delayed treatment with infliximab plus methotrexate in patients with early rheumatoid arthritis. *Ann Rheum Dis.* 2009;68(7):1153-1158. doi: 10.1136/ard.2008.093294 [doi].
4. Weinblatt ME, Bathon JM, Kremer JM, et al. Safety and efficacy of etanercept beyond 10 years of therapy in north american patients with early and longstanding rheumatoid arthritis. *Arthritis Care Res (Hoboken).* 2011;63(3):373-382. doi: 10.1002/acr.20372 [doi].
5. Wolbink GJ, Vis M, Lems W, et al. Development of antiinfliximab antibodies and relationship to clinical response in patients with rheumatoid arthritis. *Arthritis Rheum.* 2006;54(3):711-715. doi: 10.1002/art.21671 [doi].
6. Sparks J, Slobodkin G, Matar M, et al. Versatile cationic lipids for siRNA delivery. *J Control Release.* 2012;158(2):269-276. doi: 10.1016/j.jconrel.2011.11.006 [doi].
7. Buyens K, De Smedt SC, Braeckmans K, et al. Liposome based systems for systemic siRNA delivery: Stability in blood sets the requirements for optimal carrier design. *J Control Release.* 2012;158(3):362-370. doi: 10.1016/j.jconrel.2011.10.009 [doi].
8. Bruno K. Using drug-excipient interactions for siRNA delivery. *Adv Drug Deliv Rev.* 2011;63(13):1210-1226. doi: 10.1016/j.addr.2011.09.003 [doi].
9. Colombo S, Cun D, Remaut K, et al. Mechanistic profiling of the siRNA delivery dynamics of lipid-polymer hybrid nanoparticles. *J Control Release.* 2015;201:22-31. doi: 10.1016/j.jconrel.2014.12.026 [doi].
10. te Boekhorst BC, Jensen LB, Colombo S, et al. MRI-assessed therapeutic effects of locally administered PLGA nanoparticles loaded with anti-inflammatory siRNA in a murine arthritis model. *J Control Release.* 2012;161(3):772-780. doi: 10.1016/j.jconrel.2012.05.004 [doi].
11. Akinc A, Zumbuehl A, Goldberg M, et al. A combinatorial library of lipid-like materials for delivery of RNAi therapeutics. *Nat Biotechnol.* 2008;26(5):561-569. doi: 10.1038/nbt1402 [doi].
12. Thanki K, Zeng X, Justesen S, et al. Engineering of small interfering RNA-loaded lipidoid-poly(DL-lactic-co-glycolic acid) hybrid nanoparticles for highly efficient and safe gene silencing: A quality by design-based approach. *Eur J Pharm Biopharm.* 2017;120:22-33. doi: S0939-6411(17)30565-9 [pii].
13. de Groot A, Thanki K, Gangloff M, et al. Immunogenicity testing of lipidoids *In Vitro* and *in silico*: Modulating lipidoid-mediated TLR4 activation by nanoparticle design. . 2018;11:159-169.
14. Adamcik J, Berquand A, Mezzenga R. Single-step direct measurement of amyloid fibrils stiffness by peak force quantitative nanomechanical atomic force microscopy. *Appl Phys Lett.* 2011;98:193701-193703.
15. Pedersen JS. A flux- and background-optimized version of the NanoSTAR small-angle x-ray scattering camera for solution scattering. *J Appl Crystallogr.* 2004;37:369-380.
16. Jensen LB, Griger J, Naeye B, et al. Comparison of polymeric siRNA nanocarriers in a murine LPS-activated macrophage cell line: Gene silencing, toxicity and off-target gene expression. *Pharm Res.* 2012;29(3):669-682. doi: 10.1007/s11095-011-0589-0 [doi].
17. Zeng X, de Groot AM, Sijts AJ, et al. Surface coating of siRNA-peptidomimetic nano-self-assemblies with anionic lipid bilayers: Enhanced gene silencing and reduced adverse effects in vitro. *Nanoscale.* 2015;7(46):19687-19698. doi: 10.1039/c5nr04807a [doi].



18. Zeng X, Zhang Y, Nystrom AM. Endocytic uptake and intracellular trafficking of bis-MPA-based hyperbranched copolymer micelles in breast cancer cells. *Biomacromolecules*. 2012;13(11):3814-3822. doi: 10.1021/bm301281k [doi].
19. Hanyecz A, Berlo SE, Szanto S, Broeren CP, Mikecz K, Glant TT. Achievement of a synergistic adjuvant effect on arthritis induction by activation of innate immunity and forcing the immune response toward the Th1 phenotype. *Arthritis Rheum*. 2004;50(5):1665-1676. doi: 10.1002/art.20180 [doi].
20. van Herwijnen MJ, Wieten L, van der Zee R, et al. Regulatory T cells that recognize a ubiquitous stress-inducible self-antigen are long-lived suppressors of autoimmune arthritis. *Proc Natl Acad Sci U S A*. 2012;109(35):14134-14139. doi: 10.1073/pnas.1206803109 [doi].
21. Maurer N, Wong KF, Stark H, et al. Spontaneous entrapment of polynucleotides upon electrostatic interaction with ethanol-destabilized cationic liposomes. *Biophys J*. 2001;80(5):2310-2326. doi: S0006-3495(01)76202-9 [pii].
22. Crawford R, Dogdas B, Keough E, et al. Analysis of lipid nanoparticles by cryo-EM for characterizing siRNA delivery vehicles. *Int J Pharm*. 2011;403(1-2):237-244. doi: 10.1016/j.ijpharm.2010.10.025 [doi].
23. Viger-Gravel J, Schantz A, Pinon AC, Rossini AJ, Schantz S, Emsley L. Structure of lipid nanoparticles containing siRNA or mRNA by dynamic nuclear polarization-enhanced NMR spectroscopy. *J Phys Chem B*. 2018;122(7):2073-2081. doi: 10.1021/acs.jpbc.7b10795 [doi].
24. Yanez Arteta M, Kjellman T, Bartesaghi S, et al. Successful reprogramming of cellular protein production through mRNA delivered by functionalized lipid nanoparticles. *Proc Natl Acad Sci U S A*. 2018;115(15):E3351-E3360. doi: 10.1073/pnas.1720542115 [doi].
25. Zhang L, Feng Q, Wang J, et al. Microfluidic synthesis of hybrid nanoparticles with controlled lipid layers: Understanding flexibility-regulated cell-nanoparticle interaction. *ACS Nano*. 2015;9(10):9912-9921. doi: 10.1021/acs.nano.5b05792 [doi].
26. Zhang S, Aslan H, Besenbacher F, Dong M. Quantitative biomolecular imaging by dynamic nanomechanical mapping. *Chem Soc Rev*. 2014;43(21):7412-7429. doi: 10.1039/c4cs00176a [doi].
27. Gentile P, Chiono V, Carmagnola I, Hatton PV. An overview of poly(lactic-co-glycolic) acid (PLGA)-based biomaterials for bone tissue engineering. *Int J Mol Sci*. 2014;15(3):3640-3659. doi: 10.3390/ijms15033640 [doi].
28. Hermann G, Heffeter P, Falta T, Berger W, Hann S, Koellensperger G. In vitro studies on cisplatin focusing on kinetic aspects of intracellular chemistry by LC-ICP-MS. *Metallomics*. 2013;5(6):636-647. doi: 10.1039/c3mt20251h [doi].
29. Yin H, Kanasty RL, Eltoukhy AA, Vegas AJ, Dorkin JR, Anderson DG. Non-viral vectors for gene-based therapy. *Nat Rev Genet*. 2014;15(8):541-555. doi: 10.1038/nrg3763 [doi].
30. Conner SD, Schmid SL. Regulated portals of entry into the cell. *Nature*. 2003;422(6927):37-44. doi: 10.1038/nature01451 [doi].
31. Petros RA, DeSimone JM. Strategies in the design of nanoparticles for therapeutic applications. *Nat Rev Drug Discov*. 2010;9(8):615-627. doi: 10.1038/nrd2591 [doi].
32. Gilleron J, Querbes W, Zeigerer A, et al. Image-based analysis of lipid nanoparticle-mediated siRNA delivery, intracellular trafficking and endosomal escape. *Nat Biotechnol*. 2013;31(7):638-646. doi: 10.1038/nbt.2612 [doi].
33. Iversen TG, Skotland T, Sandvig K. Endocytosis and intracellular transport of nanoparticles: Present knowledge and need for future studies. *Nanotoday*. 2011;6:176-185.
34. Ursic-Bedoya R, Mire CE, Robbins M, et al. Protection against lethal marburg virus infection mediated by lipid encapsulated small interfering RNA. *J Infect Dis*. 2014;209(4):562-570. doi: 10.1093/infdis/jit465 [doi].
35. Hollo K, Glant TT, Garzo M, Finnegan A, Mikecz K, Buzas E. Complex pattern of Th1 and Th2 activation with a preferential increase of autoreactive Th1 cells in BALB/c mice with proteoglycan (aggrecan)-induced arthritis. *Clin Exp Immunol*. 2000;120(1):167-173. doi: ce11174 [pii].
36. Kaplan C, Valdez JC, Chandrasekaran R, et al. Th1 and Th2 cytokines regulate proteoglycan-specific autoantibody isotypes and arthritis. *Arthritis Res*. 2002;4(1):54-58. doi: 10.1186/ar383 [doi].

Supplemental data

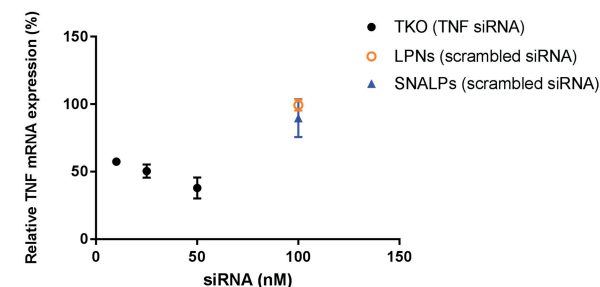


Figure S1. TNF silencing in RAW 264.7 cells incubated with nanoparticles. Results are normalized to non-transfected, LPS-treated cells (100%). The samples of TKO group were tested at TNF siRNA concentrations of 25, 50 and 100 nM, and the samples of LPNs and SNALPs were tested at a scrambled siRNA concentration of 100 nM. Data represent mean \pm SD (n = 3).

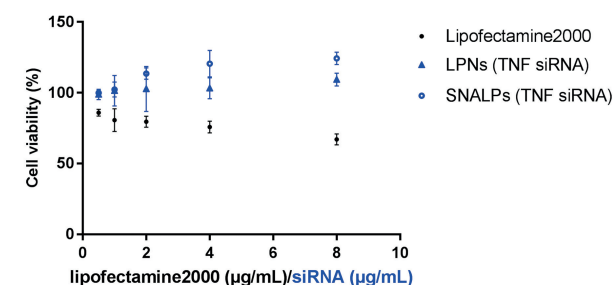


Figure S2. Cell viability values obtained after 24 h of incubation for RAW 264.7 cells. Data represent mean \pm SD (n = 3).

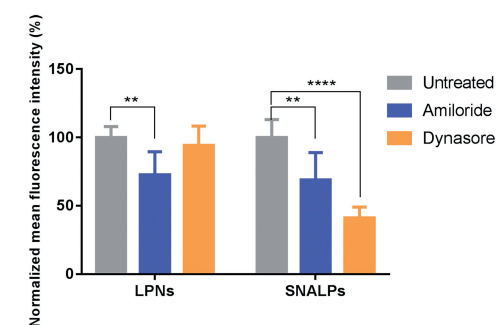


Figure S3. RAW 264.7 cells were pre-incubated with inhibitors for 0.5 h, and they were subsequently cultured in medium containing nanoparticles. The concentration of Alexa 647 siRNA in the cell culture medium was 100 nM in all the experiments. The fluorescence level of Alexa647 siRNA was determined at 3 h. **p < 0.01, ****p < 0.0001, as compared to untreated cells. Data represent mean \pm SD (n = 3).

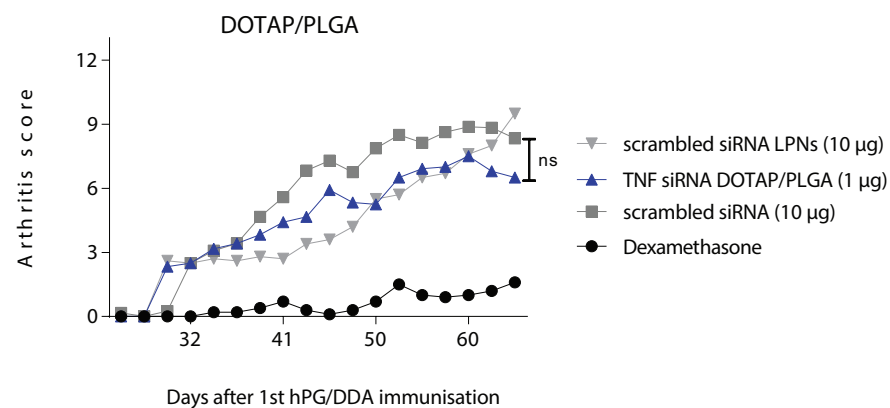


Figure S4. Therapeutic effects of TNF siRNA loaded DOTAP/PLGA *in vivo*. Injection with DOTAP/PLGA NPs containing TNF siRNA did not inhibit arthritis.

Table S1. Nanomechanical properties of LPN and SNALPs.

Formulation	Stiffness [GPa]	Adhesion [nN]
PLGA NPs	5.90 ± 1.44	17.29 ± 9.55
Non-loaded LPNs	2.16 ± 0.57	18.79 ± 5.06
TNF siRNA LPNs	3.48 ± 0.92	16.93 ± 5.23
TNF siRNA SNALPs		49.90 ± 18.14

Table S2. siRNA and primer sequences and modification patterns. Lower case letters represent deoxyribonucleotides, underlined capital letters represent 2'-O-methylribonucleotides and p phosphate residues.

Name	Sense sequence / forward primer	Antisense sequence / Reverse primer
siRNA-TNF	5'- pGUCUCAGCCUCUUCUCAUUCUGct-3'	5'- AGCAGGA <u>U</u> GAGAGAGGCUGAGACAU-3'
siRNA-Scrambled	5'-AU <u>C</u> GU <u>A</u> CGU <u>A</u> CCGU <u>C</u> GU <u>A</u> Utt-3'	5'-AU <u>A</u> CG <u>A</u> CGGU <u>A</u> CGU <u>A</u> CGAUtt-3'
Primer TNF	5'-tgctatgtctcagctcttc-3'	5'-ggtctggccatagaactga-3'
Primer ACT	5'-cagctctttgagctcctt-3'	5'-cacgatggagggaatacag-3'
Primer GUS	5'-agttgtgtgggtgaatggga-3'	5'-ggaagggtatgaggggtcag-3'





Chapter 6

Routing dependent immune responses after experimental R848-adjuvated vaccination

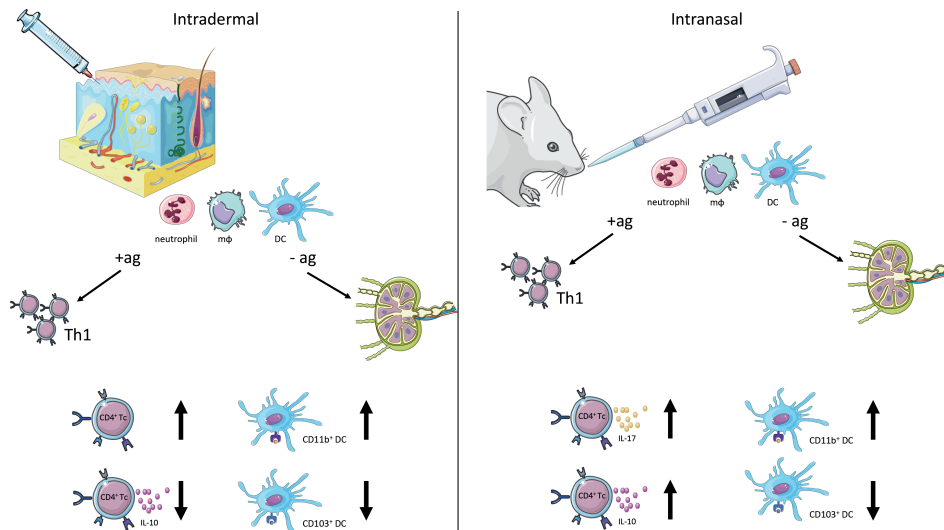
Susan van Aalst¹, Manon A.A. Jansen^{1*}, Irene S. Ludwig^{1*}, Ruurd van der Zee¹, Willem van Eden¹, Femke Broere¹

¹ Division of Immunology, Department of Infectious diseases & Immunology, Utrecht University, Utrecht, the Netherlands

* contributed equally to this work

Vaccine, 2018 Mar 36; 1405–1413

Graphical abstract



Abstract

Most traditional vaccines are administered via the intramuscular route. Other routes of administration however, can induce equal or improved protective memory responses and might provide practical advantages such as needle-free immunization, dose sparing and induction of tissue-specific (mucosal) immunity. Here we explored the differences in immunological outcome after immunization with model antigens via two promising immunization routes (intradermal and intranasal) with or without the experimental adjuvant and TLR7/8-agonist R848. Because the adaptive immune response is largely determined by the local innate cells at the site of immunization, the effect of R848-adjuvation on local cellular recruitment, antigenic uptake by antigen-presenting cells and the initiation of the adaptive response were analyzed for the two routes of administration. We show a general immune-stimulating effect of R848 irrespective of the route of administration. This includes influx of neutrophils, macrophages and dendritic cells to the respective draining lymph nodes and an increase in antigen-positive antigen-presenting cells which leads for both intradermal and intranasal immunization to a mainly T_H1 response. Furthermore, both intranasal and intradermal R848-adjuvanted immunization induces a local shift in DC subsets; frequencies of CD11b⁺DC increase whereas CD103⁺DC decrease in relative abundance in the draining lymph node. In spite of these similarities, the outcome of immune responses differs for the respective immunization routes in both magnitude and cytokine profile. Via the intradermal route, the induced T-cell response is higher compared to that after intranasal immunization, which corresponds with the local higher uptake of antigen by antigen-presenting cells after intradermal immunization. Furthermore, R848-adjuvation enhances *ex vivo* IL-10 and IL-17 production after intranasal, but not intradermal, T-cell activation. Quite the opposite, intradermal immunization leads to a decrease in IL-10 production by the vaccine induced T-cells. This knowledge may lead to a more rational development of novel adjuvanted vaccines administered via non-traditional routes.

Keywords: R848, adjuvant, route of administration, intranasal, intradermal, vaccine



Introduction

Vaccines play an essential role in prevention of many live-threatening infectious diseases¹. Nowadays, most vaccines are administered via the intramuscular route, but other routes of administration show equal or improved immunological effectiveness²⁻⁵ and provide practical advantages e.g. needle-free administration and dose-sparing^{6,7}. Local antigen-presenting cells (APC), most importantly dendritic cells (DC), take up antigen, mature and transport antigen to local draining lymph nodes where they prime naïve T-cells⁸, thus determining the type and magnitude of the adaptive response^{9,10}. Therefore, vaccination strategies may improve by choosing a distinct route of administration.

With its high numbers of APC, efficient drainage and easy access, the skin is an attractive location for immunization¹¹. Cutaneous APC, the epidermal-based Langerhans cells (LC), dermal DC (CD11b⁺ or CD103⁺ migrating DC), macrophages and migrating LC^{11,12} are well equipped to initiate a protective immune response. Animal experiments^{13,14} and e.g. rabies- and Fluzone Intradermal[®]-vaccinations^{15,16} show successful vaccine-responses after intradermal immunization. Another promising route of administration is intranasal immunization for its ease in administration and enrichment of classical DC in the nasopharynx¹⁷. Phenotype and function of nasal APC were recently described¹⁸. A minor CD103⁺DC- and a major CD11b⁺DC-population were found in the nose-associated lymphoid tissue (NALT), next to macrophages and B-cells. In addition to one FDA-approved intranasal vaccine (FluMist[®], a live attenuated influenza vaccine that conveys protection in healthy adults¹⁹), animal experiments also demonstrate the potential of intranasal immunization^{14,20}.

Skin and mucosal immune cells are exposed to environmental antigens and have well-developed tolerance mechanisms. To induce an immune response to vaccine-antigens and overcome tolerance, adjuvants are often required. Synthetic mimics of pathogen-associated molecular patterns, a novel class of adjuvants^{8,21}, efficiently stimulate pattern recognition receptors on innate cells, most importantly Toll-like receptors (TLR; reviewed in²²). TLR-agonists preferentially induce advantageous T_H1 responses, supporting cellular immunity, important in protective vaccine-responses^{23,24}. Resiquimod (R848) is an imidazoquinoline and a TLR7/8-agonist. Its less potent equivalent Imiquimod is already FDA-approved for topical administration in anti-viral cream and TLR7/8-agonists are being studied in clinical trials for their adjuvanticity²⁵. R848 was shown to activate local innate cells, to induce pro-inflammatory cytokines^{26,27} and to affect APC-maturation²⁷⁻²⁹ which, when co-

delivered with vaccine-antigens, predominantly leads to T_H1-responses after both intranasal and intradermal immunization in animal models^{14,30}.

With increasing interest in new routes of administration, it becomes evident that immunization with identical antigenic components via different routes influences responses and even the effect of adjuvant may depend on the route^{2,14}. The exact mechanisms of these differences are, however, not (completely) known. Here we explored differences in immunological outcome after immunization with model antigens, with or without R848, via two promising immunization routes (intranasal and intradermal). Effects on APC-recruitment and antigen-uptake as well as initiation of adaptive responses were studied. A similar local cellular influx after R848-adjuvation was found for both routes of administration, consisting of neutrophils, macrophages, and also DC. Furthermore, R848-adjuvation induced *in vivo* DC maturation, expansion of CD11b⁺ DC and a decline of CD103⁺ DC-subset after both intradermal and intranasal immunization. However, intradermal immunization resulted in more antigen-uptake by local APC compared to intranasal immunization, resulting in heightened T-cell response. R848 enhanced T-cell proliferation for both routes, but (T-cell-) cytokine production differed; most importantly IL-10, which was, compared to non-adjuvated vaccinations, upregulated after intranasal, but downregulated after intradermal immunization. In conclusion, we show a general immune-stimulating effect for R848 but different outcomes of immune responses for intradermal and intranasal immunization when presented with the same model-vaccine.

Material and Methods

Mice

BALB/c wildtype mice (8-10 weeks) were obtained from Charles River Laboratories and human proteoglycan specific Thy1.1⁺TCR-5/4E8-transgenic mice^{31,32} were bred at the Central Animal Laboratory of Utrecht University, The Netherlands. Mice were kept under standard conditions and received water and food *ad libitum*. Experiments were approved by the Utrecht University Animal Experiments Committee.

Immunizations

Wild type mice were immunized intradermally (pinnae of the ear;³³) or via the intranasal route³⁴. Intradermal and intranasal treatment consisted of antigen in PBS±R848 (Invivogen, 25 µg) (in 10 µl or 20 µl respectively). The contralateral ear was left untreated and used as control. Antigens were human proteoglycan

peptide, the cognate antigen of Thy1.1⁺TCR-5/4E8-CD4⁺ T-cells, (hPGp; 100 µg, ⁷⁰ATEGRVRVNSAYQDK⁸⁴; GenScript), Ovalbumin-peptide₃₂₃₋₃₃₉ (pOVA; 250 µg; GenScript,) or DQ-Ovalbumin (DQ-OVA; 50 µg; Thermo Fisher).

Single cell suspensions

Twenty-four hours after intradermal immunization, immune cells from both ears were isolated as described³⁵. Twenty-four hours after intranasal immunization, NALT was isolated as described³⁶. Also, spleens and draining lymph nodes were collected. Draining lymph nodes were the auricular lymph node, cervical lymph node and deep cervical lymph node (intranasal immunization) or the auricular lymph node (intradermal immunization). Single cell suspensions from spleens, lymph node and NALT were prepared as described³².

Co-cultures

Co-culture with TCR-5/4E8-Tg CD4⁺ T-cells

Single cell suspensions from spleens of Thy1.1⁺TCR-5/4E8-Tg donor mice were CD4⁺ T-cell enriched and CD25-depleted (PC61) and labeled with 5,6-carboxy-succinimidyl-fluoresceine-ester (CFSE) (protocol adapted from³⁷). The purity of the CD4⁺ T cells used in co-cultures was between 83 and 85%. After CD25 depletion, 0.4% (intranasal experiment) and 0.7% (intradermal experiment) of the CD4⁺ T cells still expressed CD25. Immune cells from ear and lymph node harvested 24 hours post immunization (hpi) with hPGp were labeled with CellTrace Violet (Invitrogen) with 5 µM CellTrace Violet in PBS according to manufacturer's instructions.

CFSE-labeled TCR-5/4E8-Tg CD4⁺ T-cells were co-cultured with CellTrace-labeled cells ('APC') isolated from ear, auricular or cervical lymph node at a 1:2 ratio (T-cell:APC) with or without hPGp (10 µg/ml) for 72 h at 37 °C, 5% CO₂ in IMDM containing FBS (Lonza, 5%), β-mercaptoethanol (Gibco; 5 x10⁻⁵M), penicillin (Gibco; 100 units/ml) and streptomycin (Gibco; 100 µg/ml). Cells from the deep cervical lymph node or NALT were co-cultured in a 2:1 ratio, since cell yield in these organs was not sufficient for the 1:2 ratio. Cells were cultured. Subsequently, supernatants were collected for cytokine assays.

Co-culture with hybridoma DO11.10-GFP CD4⁺ T-cell

DO11.10-GFP hybridoma cells³⁸ were grown under geneticin selection (0.5 mg/ml; Invivogen) and, to distinguish from other cells, stained with CellTrace Violet as described above. Immune cells from ear, NALT and lymph node ('APC') harvested 24h after pOVA immunization, were co-cultured in Opti-MEM (Gibco) containing FBS (10%), β-mercaptoethanol (5 x10⁻⁵ M), penicillin (100 units/ml) and streptomycin

(100 µg/ml) for 18 h at 37 °C, 5% CO₂ with the CellTrace⁺DO11.10 cells in a 5:1 (APC: T-cell) ratio with or without pOVA (0.2 µg/ml).

In vivo transfer studies

One day before hPGp immunization, acceptor wild type mice received 3 x10⁶ CFSE-labeled CD4⁺-enriched T-cells from Thy1.1⁺TCR-5/4E8-Tg donor mice intravenously in 200µl PBS. The purity of the transferred CD4⁺ T cells was 68% and 70% for the intranasal and intradermal experiment respectively. Four days post immunization (dpi), ears, NALT, draining lymph node and spleen were harvested. Cells were directly used for flow cytometric analysis or stimulated (2 x10⁵ cells/well; 200 µl) with hPGp (10 µg/ml) for 72h at 37 °C, 5% CO₂ for supernatants for cytokine assays.

Standardization of experiments

Paired intradermal and intranasal experiments were performed within the same timeslot (< 1-4 days) and experimental conditions were kept as stable as possible: (1) immunized mice were from the same cohort and randomly divided in 4 groups before paired experiments (intranasal PBS, intranasal R848, intradermal PBS or intradermal R848), (2) Immunizations were performed by the same researcher, (3) both the FACS antibody mix and the CD4⁺ T cell enrichment antibody mix for individual experiments was prepared as one mix and kept cool and in the dark to prevent reduction in quality, (4) FACS and Magpix settings were kept the same and (5) the CD4⁺ T cell donor mice were from the same cohort and randomly divided in 2 groups before experiments (intranasal or intradermal).

Cytokine analysis

Supernatants were used for multiplex cytokine analysis of IFN-γ, IL-2, IL-6, IL-10 and IL-17, using the Magpix (Luminex XMAP) system according the manufacturer's instructions and as described³⁹. The antibody pairs (coat:detect) were AN-18:XMG1.2, JES6-1A12:JES6-5H4, MP5-20F3:MP5-32C11, JES5-2A5:SCC-1 and TC11-18H10:TC11-8H4.1 for IFN-γ, IL-2, IL-6, IL-10 and IL-17 respectively. The concentrations of cytokines in the tested samples were calculated using standard curves and the MFI data was analyzed using a 5-parameter logistic method (xPONENT software, Luminex, Austin, USA).

Flowcytometry analysis

Cells were stained in PBS supplemented with 2% FBS with the monoclonal antibodies F4/80-FITC/Pe-Cy7 (BM8), CD45-APC-H7 (2D1), Ly6C-PE (HK1.4), Ly6G-BV510 (1A8) (Biolegend), I-A/I-E-HorizonV450/FITC (M5/114.15.2), CD11b-PerCPCy5.5 (M1/70), CD11c-APC (N418), CD3-eFluor450 (17A2), CD69-APC (H1.2F3), Thy1.1-PerCPCy5.5



(HIS51) (eBioscience) and/or CD4-APC/eFLuorV510 (RM4-5), CD24-V450/Pe-Cy7 (M1/69), CD86-FITC (GL1), CD40-PE (3/23), CD103-BV510 (M290), CD19-APC-H7 (1D3) (BDBiosciences).

Subsequently, cells were measured on a FACSCanto II Flowcytometer (BDBiosciences). Analysis was performed with FlowJo v10 (Tree Star). Representative dot plots, including gating strategies, can be found in the supplemental figures 1-3.

Statistical analysis

Unpaired, two-tailed t-tests with Welch correction were performed using Prism v6.05 (Graphpad). Differences were considered significant at $p < 0.05$ and indicated as * $p < 0.05$, ** $p < 0.01$, *** $p < 0.001$.

Results

R848-adjuvation changes local cellular environment and antigen-uptake after intradermal and Intranasal immunization

Initiation of vaccine-responses start with uptake of vaccine-antigen by local innate cells. Therefore, we determined the cellular composition at local sites 24h after intranasal or intradermal immunization with model-antigen hPGp, adjuvated or not with R848. Furthermore, antigen-uptake was determined by immunization with DQ-OVA that fluoresces after intracellular processing.

Twenty-four hours post intranasal immunization with hPGp+R848, frequencies of neutrophils, macrophages, and DC but not inflammatory monocytes were increased in cervical lymph node, compared to hPGp only (Fig. 1a). R848-adjuvation led to higher expression of CD40 (Fig. 1b) and CD86 (56% vs 91%; not shown) on DC and relatively more CD11b⁺DC, but less CD103⁺DC were observed (Fig. 1c). In auricular lymph node and deep cervical lymph node, R848-adjuvation induced similar changes in cell composition and DC phenotypes as in the cervical lymph node (not shown). In NALT a potential increase in %MHCII⁺-cells could be seen, whereas frequencies of macrophages and inflammatory monocytes appeared to decrease (not shown). After intranasal immunization, DQ-OVA was taken up and processed by only a small number of cells and this tended to be increased by R848-adjuvation only in DC and B-cells in the cervical lymph node (Fig. 1d).

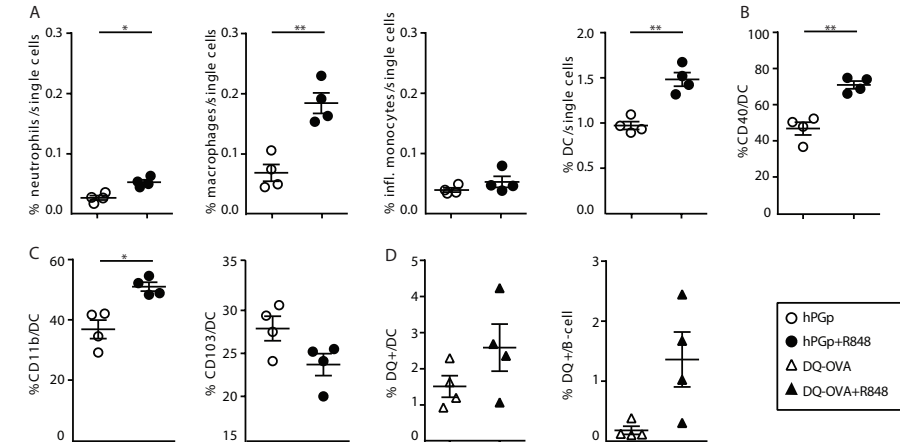


Figure 1. Addition of adjuvant R848 to intranasal immunization changes local cellular composition and antigenic uptake. Mice were intranasally immunized with hPGp±R848 (A-C) or DQ-OVA±R848 (D) and 24hpi cellular composition and uptake of DQ-OVA in the cervical lymph node was analyzed. Flow cytometric analysis of (A) neutrophils (CD11b⁺Ly-6G⁺), macrophages (CD11b⁺F4/80⁺Ly-6G⁺), inflammatory monocytes (CD11b⁺Ly-6C⁺F4/80⁺Ly-6G⁺) and DC (CD11c⁺MHCII⁺) and (B) the expression of markers CD40 and (C) CD11b and CD103 on DC. Cell populations are indicated as % cells in the live single cell gate. In (D) the % B-cells (CD19⁺MHCII⁺) and DC that have taken up and processed DQ-OVA is shown. Each symbol represents an individual animal and mean±SEM are indicated. N=4/group.

R848-adjuvation of intradermal immunization also affected cellular composition and DQ-OVA uptake in skin. Frequencies of macrophages and inflammatory monocytes went down with hPGp+R848 compared to hPGp only, but had no obvious effect on neutrophil-, DC- or LC-frequency (Fig. 2a). Skin-DC expressed more CD40 (Fig. 2b) and took up DQ-OVA. However, DQ-OVA was mainly processed by skin-neutrophils in the presence of R848 (Fig. 2c); over 90% of neutrophils contained processed DQ-OVA. In auricular lymph node, frequencies of mostly neutrophils, macrophages, inflammatory monocytes and DC increased by R848-adjuvation (Fig. 2d). Similar to intranasal immunization, intradermal hPGp+R848 immunization led to higher expression of CD40 (Fig. 2e) and CD86 (56% vs 91%; not shown) on DC, and increasing CD11b⁺DC- but decreasing CD103⁺DC-frequencies in draining lymph nodes (Fig. 2f). Twenty-four hours after intradermal immunization, neutrophils and DC, and to a smaller extent B-cells, had taken up and processed DQ-OVA and R848-adjuvation increased this significantly (Fig 2g).



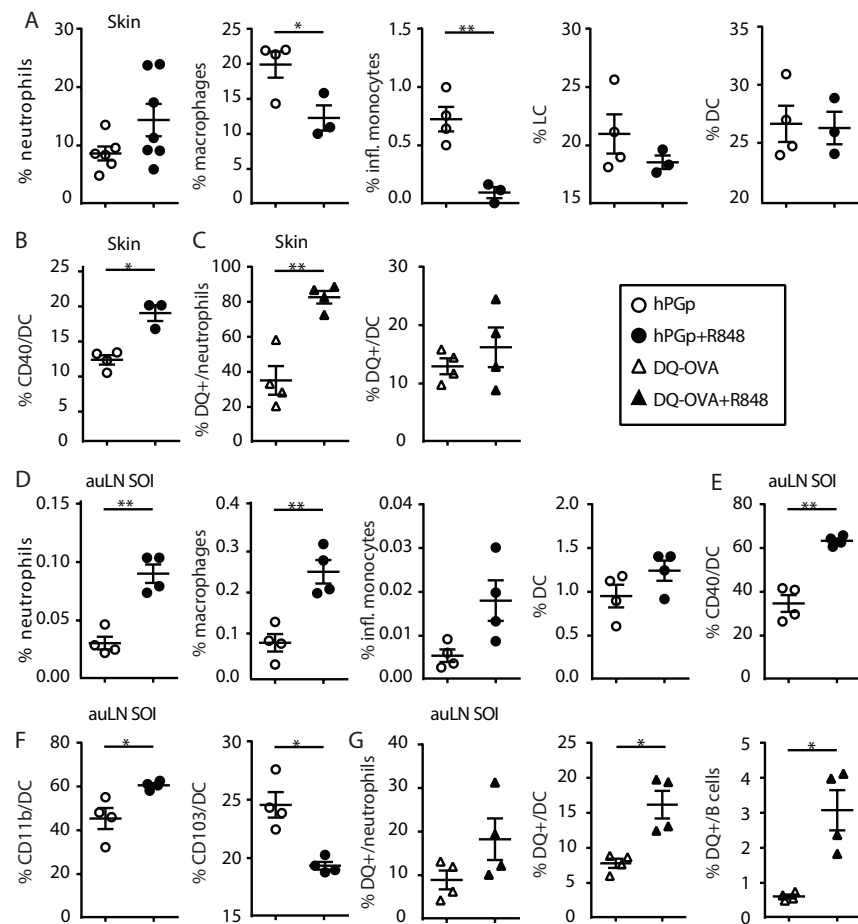


Figure 2. Addition of adjuvant R848 to intradermal immunization changes local cellular composition and antigenic uptake. Mice were intradermally immunized with hPGp±R848 (A,B, D-F) or DQ-OVA±R848 (C,G) and 24hpi cellular composition of the skin (A-B) and auricular lymph nodes (D-E) and uptake of DQ-OVA in the ear skin (C) and auricular lymph nodes (G) at the site of injection were analyzed. Flow cytometric analysis of (A) neutrophils (CD11b⁺Ly-6G⁺), macrophages (CD11b⁺F4/80⁺Ly-6G⁺CD11c⁻), inflammatory monocytes (CD11b⁺Ly-6C⁺F4/80⁺Ly-6G⁺CD11c⁻), LC (MHCII⁺CD24⁺CD11b⁺) and DC (CD11c⁺MHCII⁺) and (B) the expression of marker CD40 on DC in skin. In skin, cell numbers are indicated as % cells in the live, CD45⁺, single cell gate. In (D) neutrophils, macrophages, inflammatory monocytes and DC are shown in the auricular lymph node. In (E) the expression of markers CD40 and (F) CD11b and CD103 on DC in auricular lymph node are shown. In the auricular lymph node, cell populations were gated as described in Figure 1 legend. In (C,G) the % neutrophils and DC in skin (C) and neutrophils, B-cells and DC in the auricular lymph node (G) that have taken up and processed DQ-OVA are shown. Graphical representation as described for Fig 1. N=4-7/group. Abbreviations: auLN: auricular lymph node, SOI: site of injection.

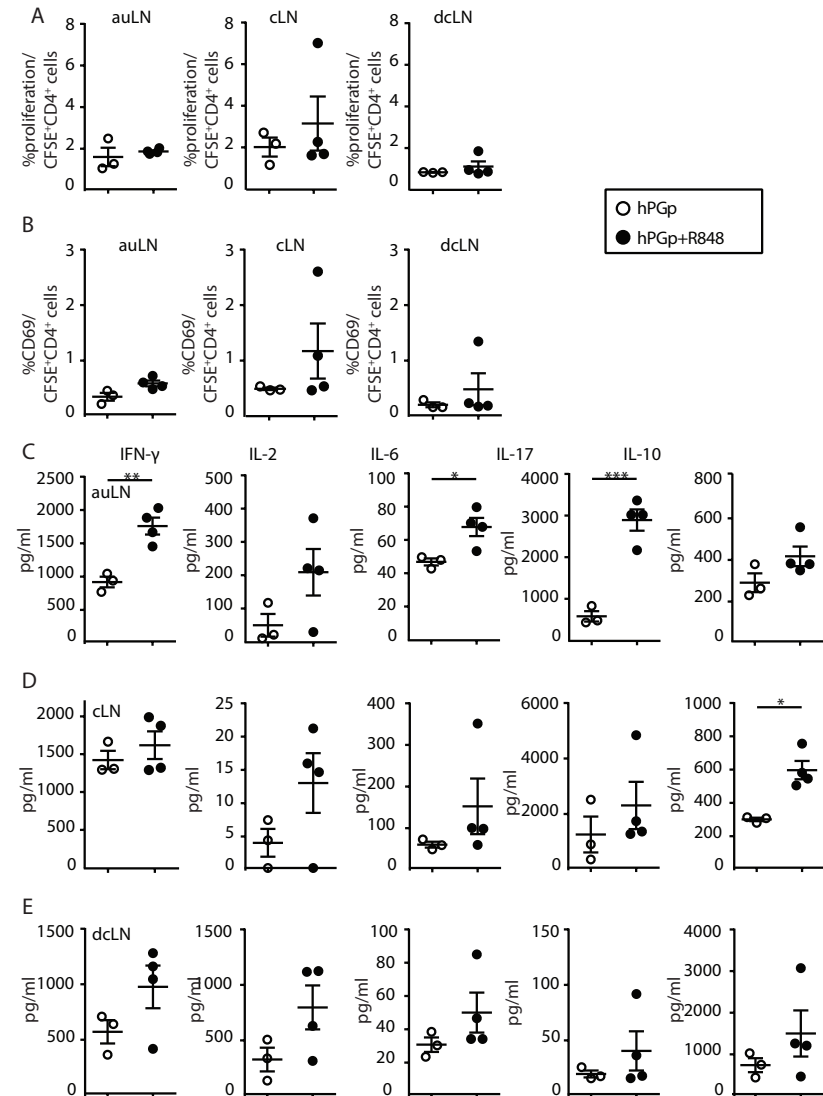


Figure 3. Addition of adjuvant R848 to intranasal immunization has no effect on *ex vivo* proliferation or activation of cognate CD4⁺ T-cells, but does change their cytokine production. Mice were intranasally immunized with hPGp±R848 and after 24h auricular lymph nodes, cervical lymph nodes and deep cervical lymph nodes were harvested and co-cultured with CFSE-labeled hPGp-specific CD4⁺ T-cells for 3 days. Proliferation of (A) and CD69 expression on (B) CFSE-labeled hPGp-specific CD4⁺ T-cells. Proliferation is defined as %divided CFSE⁺CD4⁺ cells. (C-E) Net cytokine concentrations (pg/ml) for IFN-γ, IL-2, IL-6, IL-17 and IL-10 in supernatant of co-cultures with (C) auricular lymph nodes, (D) cervical lymph nodes and (E) deep cervical lymph nodes are shown. Net cytokine concentration: cytokine production_{hPGp restimulated} - cytokine production_{medium}. Graphical representation as described for Fig 1. N=3-4/group. Abbreviations: auLN: auricular lymph node, cLN: cervical lymph node, dcLN: deep cervical lymph node.

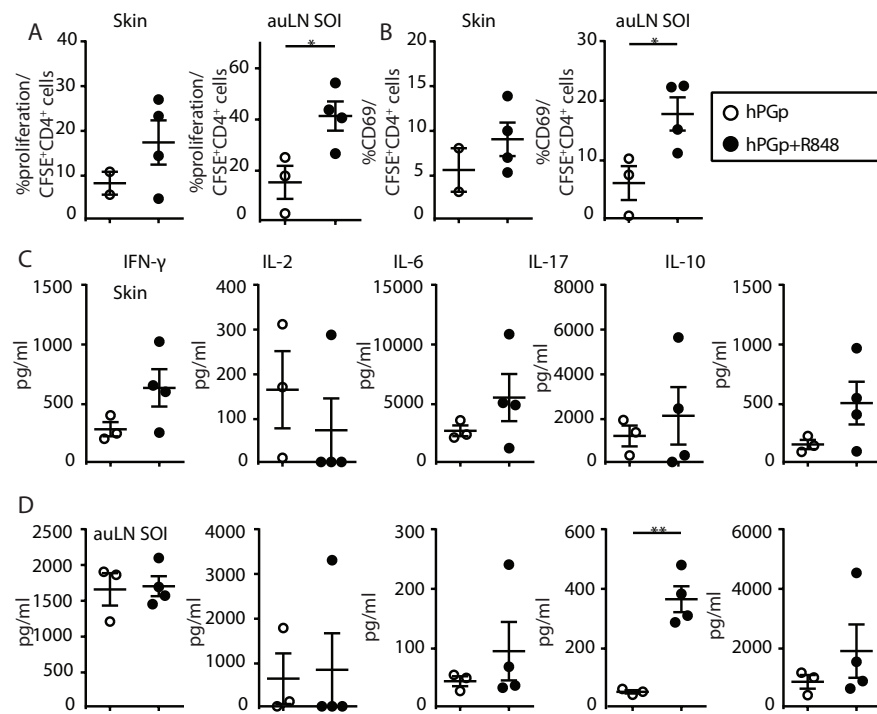


Figure 4. Addition of adjuvant R848 to intradermal immunization enhances *ex vivo* proliferation and activation of cognate CD4⁺ T-cells, and changes their cytokine production. Mice were intradermally immunized with hPGp±R848 and after 24h, skin and auricular lymph nodes from the site of injection were harvested and co-cultured with CFSE-labeled hPGp-specific CD4⁺ T-cells for 3 days. (A) Proliferation of and (B) CD69 expression on CFSE-labeled hPGp-specific CD4⁺ T-cells. (C-E) Net cytokine concentrations (pg/ml) for IFN- γ , IL-2, IL-6, IL-17 and IL-10 in supernatant for co-cultures with (C) skin or (D) auricular lymph node cells. Proliferation and cytokine production was determined as in Fig 3. Graphical representation as described for Fig 1. N=3-4/group. Abbreviations: auLN: auricular lymph node, SOI: site of injection.

Intradermal immunization with R848, but not intranasal immunization, enhances *ex vivo* antigen-presenting capacities of local APC

To assess effects of routing and R848-adjuvation on antigen-presenting capacities of APC, we measured the initiation of adaptive responses. Cells from skin and/or draining lymph nodes from mice injected 24h prior with hPGp±R848 either via the intradermal or intranasal route, were co-cultured with hPGp-specific CD4⁺ T-cells.

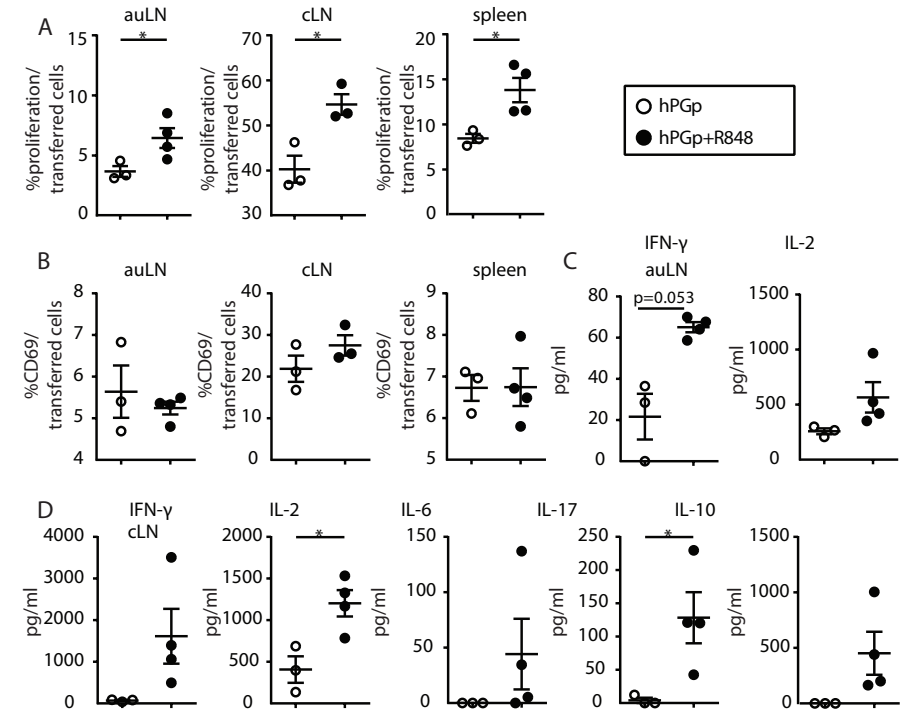


Figure 5. Addition of adjuvant R848 to intranasal immunization enhances local and systemic *in vivo* proliferation of transferred cognate CD4⁺ T-cells, and changes their *ex vivo* cytokine production. Mice received an intravenous transfer of CFSE-labeled hPGp specific CD4⁺ T-cells 1d prior to intranasal immunization with hPGp±R848. (A) Proliferation of and (B) CD69 expression on transferred CFSE-labeled hPGp-specific CD4⁺ T-cells 4dpi in auricular lymph node and spleen. (C-D) Net cytokine concentrations (pg/ml) for IFN- γ , IL-2, IL-6, IL-17 and IL-10 in supernatant after 72h of stimulation with hPGp (10 μ g/ml) in (C) auricular lymph nodes (IFN- γ , IL-2 only) and (D) cervical lymph nodes. Proliferation and cytokine production was determined as in Fig. 3. Graphical representation as described for Fig 1. N=3-4/group. Abbreviations: auLN: auricular lymph node, cLN: cervical lymph node.

APC from auricular lymph node, cervical lymph node or deep cervical lymph node of intranasal immunized mice did not induce proliferation of, or CD69-upregulation on the hPGp-specific CD4⁺ T-cells (Fig. 3a,b). Supplementation of hPGp in culture, however, did result in proliferation and enhanced CD69-expression (not shown) irrespective of adjuvation, indicating that T-cells could proliferate. Although no effect of R848 on proliferation was observed, hPGp-stimulated T-cells showed higher IFN- γ , IL-6, IL-17 and IL-10 production when the APC were derived after R848-adjuvation (Fig. 3c,d,e), suggesting a stimulating effect of R848.



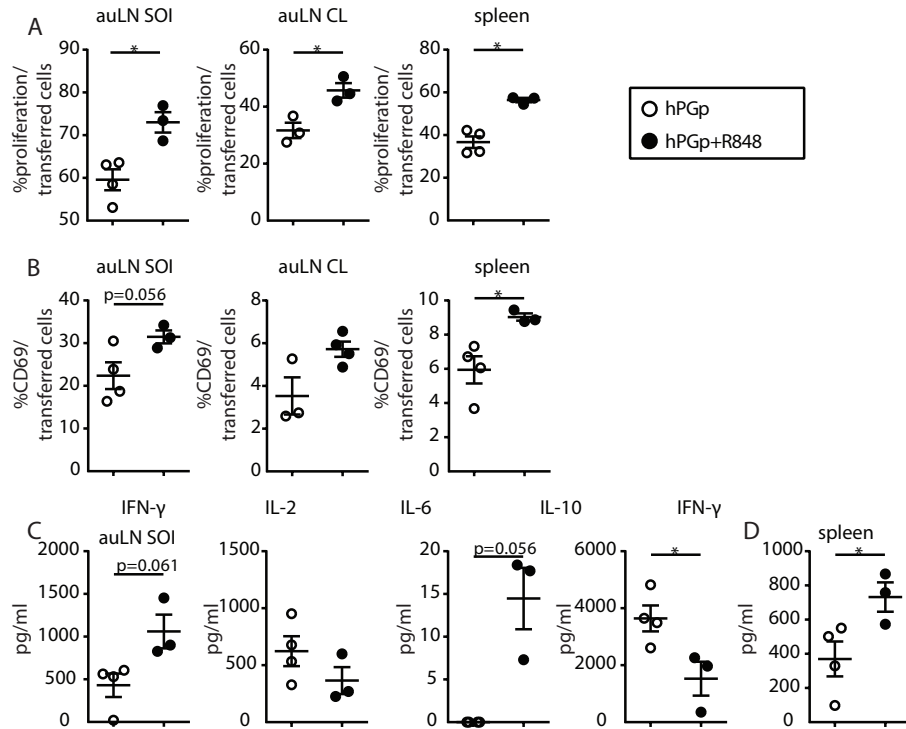


Figure 6. Addition of adjuvant R848 to intradermal immunization enhances local and systemic *in vivo* proliferation of transferred cognate CD4⁺ T-cells, and changes their *ex vivo* cytokine production. Mice received an i.v. transfer of CFSE-labeled hPGp specific CD4⁺ T-cells 1d prior to intradermal immunization with hPGp±R848. (A) Proliferation of and (B) CD69 expression on transferred CFSE-labeled hPGp-specific CD4⁺ T-cells 4dpi in auricular lymph nodes at the site of injection and contralateral and spleen. (C-D) Net cytokine concentrations (pg/ml) for IFN-γ, IL-2, IL-6 and IL-10 in supernatant after 72h of stimulation with hPGp (10μg/ml) in (C) auricular lymph node at the site of injection and (D) spleen (IFN-γ only). Proliferation and cytokine production was determined as in Fig. 3. Graphical representation as described for Fig 1. N=3-4/group. Abbreviations: auLN: auricular lymph node, SOI: site of injection, CL: contralateral.

Co-cultures containing skin or auricular lymph node cells derived from hPGp-intradermally immunized mice led to proliferation of the hPGp-specific CD4⁺ T-cells, and R848-adjuvation further enhanced this, in particular for auricular lymph node cells (Fig. 4a). Co-culture with skin and auricular lymph node cells also increased CD69-expression on CD4⁺ T-cells when immunizations were R848-adjuvated (Fig. 4b). Stimulation of the cultures with *in vitro* added hPGp, led to substantial cytokine production, but differences between groups were minor. Though not significant, in skin-T-cell co-cultures IFN-γ, IL-6 and IL-10 production appeared higher when skin

cells were derived from hPGp+R848-immunized mice, compared to hPGp (Fig. 4c). This was not the case in auricular lymph node-T-cell co-cultures. There, only IL-17 cytokine production was significantly higher when the immunization contained R848 (Fig. 4d), albeit much lower than after intranasal hPGp+R848-immunization.

To confirm the difference in *ex vivo* antigen-presentation after intranasal and intradermal immunization, we made use of pOVA-specific hybridoma cells. These MHC-II-restricted cells become GFP-fluorescent when activated and were co-cultured with cells from mice intranasally or intradermally immunized with pOVA. In accordance with what we observed in the hPGp-co-cultures, no obvious T-cell activation was observed after co-culture with cells derived from intranasally pOVA-immunized mice (Table S1a). A similar experiment with cells from intradermally pOVA-immunized mice did lead to T-cell activation, which was further increased by R848 with skin and auricular lymph node derived cells (Table S1b).

R848-supplementation enhances *in vivo* proliferation of transferred cognate CD4⁺ T-cells, and changes their *ex vivo* cytokine production

To compare the immunization routes in an *in vivo* setup we transferred hPGp-specific T-cells 1d prior to intranasal or intradermal immunization with hPGp±R848. Four days after intranasal immunization, T-cells had proliferated in the auricular lymph node, cervical lymph node, and spleen, and this was significantly increased with R848 (Fig. 5a). In the cervical lymph node, transferred T-cells upregulated CD69 after R848-adjuvation (Fig. 5b; trend) concurring with high proliferation. *Ex vivo* hPGp-restimulation resulted in IFN-γ and IL-2 production by auricular lymph node and cervical lymph node cells, which was increased with R848-adjuvation (Fig. 5c,d). Furthermore, hPGp+R848-injected mice showed IL-6, IL-17 and IL-10 production in the cervical lymph node. This in contrast to hPGp-injection only, where production was mostly below detection limit (Fig. 5d).

After intradermal immunization transferred T-cells had proliferated in both auricular lymph node (site of injection and contralateral) and spleen, and R848 significantly increased proliferation and CD69-expression (Fig. 6a,b). In ear skin, no (transferred) T-cells could be detected. hPGp-restimulation induced (limited) cytokine production in auricular lymph node at the site of injection (Fig. 6c) and spleen (Fig. 6d), but hardly any in the contralateral (not shown). IFN-γ production was enhanced when R848 was included in both auricular lymph node and spleen as was IL-6 in auricular lymph node. In auricular lymph node, IL-10 production was significantly lower after intradermal hPGp+R848-immunization compared to hPGp only, in contrast with responses after intranasal immunization.



Discussion

Improved initiation of vaccine-responses is a potential means to strengthen vaccine-efficacy and properly combined with adjuvant, might steer adaptive responses suited for protective immunity. Here we explored the potential differential effects of R848-adjuvant upon different routes of administration; intranasal and intradermal immunization. We show that, when using an identical model-vaccine, intranasal and intradermal immunization lead to differences in magnitude and type of adaptive responses and that R848-adjuvant enhances local and systemic responses via both routes to a different extent.

First, we compared local cellular compositions shortly after immunization (Fig. 1 and 2). Surprisingly, in skin and NALT, the effects of R848-adjuvation were similar in that macrophages and inflammatory monocytes went down in frequency (skin: Fig. 2a and NALT-data not shown), possibly indicating an efflux to draining lymph nodes since macrophage, inflammatory monocytes and DC frequencies went up in draining lymph nodes after both routes of administration (Fig. 1a, 2d). Furthermore, R848-supplemented intradermal immunization slightly increased neutrophil frequency in skin (Fig. 2a). Neutrophil-influx was also observed after laser-assisted intradermal immunization⁴⁰ and intradermal immunization in pig-skin¹³ already 6hpi, corresponding with neutrophil's function as first responders⁴¹. In the relevant draining lymph node, neutrophil frequencies were significantly increased for both routes of administration (Fig. 1a, 2d). Additionally, after intradermal immunization, in particular in skin (Fig. 2c) and to a lesser extent in draining lymph node (Fig. 2g), mainly neutrophils contained processed antigen similar to other studies^{18,42}. After intranasal immunization only limited numbers of neutrophils processed antigen (not shown) in contrast with other reports^{18,43}. Besides neutrophils, DC and B-cells were the main antigen⁺ cells in draining lymph nodes for both routes of administration, although also in these cells at this particular time point, intradermal immunization ensured higher antigen-uptake than intranasal immunization (Fig. 1d, 2c,g). Irrespective of route of administration, addition of R848 induced more mature DC (Fig. 1b, 2b,e), corresponding with other observations²⁷⁻²⁹.

To assess effects of routing and R848-adjuvation on antigen-presenting capacities of APC, we measured initiation of adaptive responses by means of *ex vivo* co-cultures. In line with the higher antigen-uptake after intradermal immunization compared to intranasal immunization, APC in skin and draining lymph nodes of intradermally immunized animals induced *ex vivo* activation and proliferation of naïve CD4⁺ T-cells (Fig. 4A,B), confirming that APC *in vivo* took up antigen and

received maturation signals. This in contrast with APC from intranasally immunized animals, that did not induce significant proliferation in co-culture (Fig. 3A,B). A possible explanation for this might be the existing disagreement of the actual draining lymph node after intranasal immunization. Both mediastinal lymph node⁴³⁻⁴⁵ and cervical lymph node^{18,46} have been described as draining lymph node after intranasal immunization. The draining lymph node of mice intranasally immunized under anesthesia is the mediastinal lymph node⁴⁷. However, we have immunized superficially breathing conscious mice and thus the nasal cavity is the main priming site which is drained by the cervical lymph node¹⁸. Of course this does not exclude other draining lymph nodes involved during the course of an intranasal immune response as is also demonstrated by the observed effects in the auricular lymph node after intranasal immunization (Fig. 5A,C). However, in¹⁸ it was shown that 24h after intranasal immunization antigen⁺DC are significantly increased in cervical lymph node indicating that we analyzed the correct draining lymph node and at the right time for this route of administration. Nonetheless, the time point might explain differences between the success of the two routes since routes may differ in time at which antigen-carrying, mature APC arrive in the respective draining lymph nodes. This was demonstrated by² where the peak of antigen⁺APC in the draining lymph node arrived at different times after intraperitoneally and intramuscular immunization and even DC-subsets arrive differently in the draining lymph node for the routes of administration tested².

To compare routes of administration and effects of R848-adjuvation in an *in vivo* setup, we performed CD4⁺ T-cell-transfers prior to immunization. Both intradermal and, surprisingly also intranasal immunization, despite its associated low antigen-uptake (Fig. 1d) and lack of *ex vivo* induction of T-cell proliferation in co-culture (Fig. 3a, Table S1a), led to *in vivo* proliferation of naïve T-cells (Fig. 5a, 6a). For both routes of administration, the effect was systemic and R848-adjuvation enhanced responses significantly both in draining lymph nodes and in spleen. However, responses were much higher after intradermal immunization, in line with high antigen-uptake by APC (Fig. 2c,g) and co-cultures (Fig 4, Table S1b). IFN- γ production by vaccine-specific CD4⁺ T-cells was observed after both routes of administration without R848, albeit higher after intradermal immunization, and was increased by R848-adjuvation (Fig. 5d, 6c), in line with R848's T_H1-profile²⁹. Furthermore, although IL-17 production was generally below detection limits in the non-adjuvated situations, R848-adjuvation induces significant IL-17 production by the intranasal, but not intradermal route. In addition, IL-10 production is also route-dependent. Non-adjuvated, intradermal, but not intranasal, immunization induces IL-10, which is decreased when R848 is supplemented, as expected with R848's

pro-inflammatory profile²⁹. However, IL-10 increases after intranasal immunization if R848-supplemented. In our setup it is unclear if R848 directly acts on T-cells, as was found *in vitro* for human effector memory CD4⁺ T-cells⁴⁸, or on surrounding cells. The increase in IL-10 after intranasal R848-adjuvation might result from higher proliferation and represent the contracting-phase of immune responses. Similarly, IL-10 is high after intradermal immunization, where significant proliferation is observed and restoration of homeostasis via IL-10 might be required.

Differences in magnitude and cytokine-profiles after different routes of administration likely follow from differences in priming, in particular the DC-subsets involved^{10,12}. We distinguished two subsets of DC, CD11b⁺DC, likely a mixture of DC and macrophages, and good primers of CD4⁺ T-cells¹⁷ and the subset CD103⁺DC, known for their migratory and cross-presenting capacities and potential in tolerance induction^{17,49}. However, after intranasal and intradermal immunization, relative frequencies of CD11b⁺DC and CD103⁺DC are similar in the respective draining lymph node, but R848-adjuvation ensures an increase in CD11b⁺DC parallel to a decrease in CD103⁺DC irrespective of routes of administration (Fig 1c, 2f). TLR-7/8-agonists in mice are topic of debate since in mice TLR-8 might not be functional and R848 thus signals via TLR-7²⁶ which is not expressed on all APC, but mainly on CD8⁺DC or pDC and macrophages/monocytes²⁶. To pinpoint the cause of the differential responses for the respective routes of administration and R848-adjuvation, a more thorough DC-subset analysis is required, in particular now it becomes clear that multiple distinct DC-subsets are important for coordinated T_H1 responses⁵⁰. This was, however, outside the scope of our research.

In both routes of administration, R848-adjuvation results in enhanced immune responses as was demonstrated by an increase in cell influx, proliferation and more pronounced T_H1 responses. However, the final R848-induced response differs for the intradermal and intranasal route of administration. Our results demonstrate the necessity for more research on different route of administration, which can aid in the development of more effective vaccines.

Acknowledgements

This work was part of the BioVacSafe project. The BioVacSafe project has received support from the Innovative Medicines Initiative Joint Undertaking under grant agreement n° 115308, resources of which are composed of financial contribution from the European Union's Seventh Framework Programme (FP7/2007-2013) and EFPIA companies' in kind contribution. Furthermore, the authors would like to thank Peter van Kooten for his excellent work with the breeding of transgenic mice.

Conflict of interest

None



References

- 1 Rappuoli R, Pizza M, Del Giudice G, De Gregorio E. Vaccines, new opportunities for a new society. *Proceedings of the National Academy of Sciences* 2014;111(34):12288-93.
- 2 Schmidt ST, Khadke S, Korsholm KS, Perrie Y, Rades T, Andersen P et al. The administration route is decisive for the ability of the vaccine adjuvant CAF09 to induce antigen-specific CD8+ T-cell responses: The immunological consequences of the biodistribution profile. *J Control Release* 2016;239:107-17.
- 3 Wang T, Yin H, Li Y, Zhao L, Sun X, Cong H. Vaccination with recombinant adenovirus expressing multi-stage antigens of *Toxoplasma gondii* by the mucosal route induces higher systemic cellular and local mucosal immune responses than with other vaccination routes. *Parasite* 2017;24.
- 4 Wang J, Li P, Wu MX. Natural STING Agonist as an "Ideal" Adjuvant for Cutaneous Vaccination. *J Invest Dermatol* 2016;136(11):2183-91.
- 5 Levin Y, Kochba E, Shukarev G, Rusch S, Herrera-Taracena G, van Damme P. A phase 1, open-label, randomized study to compare the immunogenicity and safety of different administration routes and doses of virosomal influenza vaccine in elderly. *Vaccine* 2016;34(44):5262-72.
- 6 Seaman MS, Wilck MB, Baden LR, Walsh SR, Grandpre LE, Devoy C et al. Effect of vaccination with modified vaccinia ankara (ACAM3000) on subsequent challenge with Dryvax. *J Infect Dis* 2010;201(9):1353-60.
- 7 Wilck MB, Seaman MS, Baden LR, Walsh SR, Grandpre LE, Devoy C et al. Safety and immunogenicity of modified vaccinia ankara (ACAM3000): Effect of dose and route of administration. *J Infect Dis* 2010;201(9):1361-70.
- 8 Coffman RL, Sher A, Seder RA. Vaccine Adjuvants: Putting Innate Immunity to Work. *Immunity* 2010;33(4):492-503.
- 9 Walsh KP, Mills KHG. Dendritic cells and other innate determinants of T helper cell polarisation. *Trends Immunol* 2013;34(11):521-30.
- 10 Chow KV, Lew AM, Sutherland RM, Zhan Y. Monocyte-derived dendritic cells promote Th polarization, whereas conventional dendritic cells promote th proliferation. *J Immunol* 2016;196(2):624-36.
- 11 Engelke L, Winter G, Hook S, Engert J. Recent insights into cutaneous immunization: How to vaccinate via the skin. *Vaccine* 2015;33(37):4663-74.
- 12 Igyártó B, Haley K, Ortner D, Bobr A, Gerami-Nejad M, Edelson B et al. Skin-Resident Murine Dendritic Cell Subsets Promote Distinct and Opposing Antigen-Specific T Helper Cell Responses. *Immunity* 2011;35(2):260-72.
- 13 Le Ludec J-, Debeer S, Piras F, Andréoni C, Boudet F, Laurent P et al. Intradermal vaccination with un-adjuvanted sub-unit vaccines triggers skin innate immunity and confers protective respiratory immunity in domestic swine. *Vaccine* 2016;34(7):914-22.
- 14 McKay PF, King DFL, Mann JFS, Barinaga G, Carter D, Shattock RJ. TLR4 and TLR7/8 adjuvant combinations generate different vaccine antigen-specific immune outcomes in minipigs when administered via the ID or in routes. *PLoS ONE* 2016;11(2).
- 15 Robertson CA, Tsang P, Landolfi VA, Greenberg DP. Fluzone® Intradermal Quadrivalent Influenza Vaccine. *Expert Rev Vaccines* 2016;15(10):1245-53.
- 16 Vescovo P, Rettby N, Ramaniraka N, Liberman J, Hart K, Cachemaille A et al. Safety, tolerability and efficacy of intradermal rabies immunization with DebioJect™. *Vaccine* 2017;35(14):1782-8.
- 17 Merad M, Sathe P, Helft J, Miller J, Mortha A. The dendritic cell lineage: Ontogeny and function of dendritic cells and their subsets in the steady state and the inflamed setting. *Annu Rev Immunol* 2013;31:563-604.
- 18 Lee H, Ruane D, Law K, Ho Y, Garg A, Rahman A et al. Phenotype and function of nasal dendritic cells. *Mucosal Immunol* 2015;8(5):1083-98.
- 19 Amorij J-, Hinrichs WLJ, Frijlink HW, Wilschut JC, Huckriede A. Needle-free influenza vaccination. *Lancet Infect Dis* 2010;10(10):699-711.
- 20 Morabito KM, Ruckwardt TR, Redwood AJ, Moin SM, Price DA, Graham BS. Intranasal administration of RSV antigen-expressing MCMV elicits robust tissue-resident effector and effector memory CD8+ T cells in the lung. *Mucosal Immunol* 2017;10(2):545-54.
- 21 Reed S.G., Orr M.T., Fox C.B. Key roles of adjuvants in modern vaccines. *Nat Med* 2013;19(12):1597-608.
- 22 Kumar H., Kawai T., Akira S. Pathogen recognition by the innate immune system. *Int Rev Immunol* 2011;30(1):16-34.
- 23 Swain SL, McKinstry KK, Strutt TM. Expanding roles for CD4 + T cells in immunity to viruses. *Nat Rev Immunol* 2012;12(2):136-48.
- 24 Martins KAO, Cooper CL, Stronsky SM, Norris SLW, Kwilas SA, Steffens JT et al. Adjuvant-enhanced CD4T Cell Responses are Critical to Durable Vaccine Immunity. *EBioMedicine* 2016;3:67-78.
- 25 ClinicalTrials. Website overview of current worldwide clinical trials. 2017;2017(4/26/2017).
- 26 Tomai MA, Vasilakos JP. TLR7/8 agonists as vaccine adjuvants. In: Anonymous Novel Immune Potentiators and Delivery Technologies for Next Generation Vaccines. , 2013: 3-18.
- 27 Hemmi H, Kaisho T, Takeuchi O, Sato S, Sanjo H, Hoshino K et al. Small-antiviral compounds activate immune cells via the TLR7 MyD88-dependent signaling pathway. *Nat Immunol* 2002;3(2):196-200.
- 28 Kwissa M, Nakaya HI, Oluoch H, Pulendran B. Distinct TLR adjuvants differentially stimulate systemic and local innate immune responses in nonhuman primates. *Blood* 2012;119(9):2044-55.
- 29 Ahonen CL, Gibson SJ, Smith RM, Pederson LK, Lindh JM, Tomai MA et al. Dendritic Cell Maturation and Subsequent Enhanced T-Cell Stimulation Induced with the Novel Synthetic Immune Response Modifier R-848. *Cellular Immunology* 1999;197(1):62-72.
- 30 Otero M, Calarota SA, Felber B, Laddy D, Pavlakis G, Boyer JD et al. Resiquimod is a modest adjuvant for HIV-1 gag-based genetic immunization in a mouse model. *Vaccine* 2004;22(13-14):1782-90.
- 31 Berlo SE, van Kooten PJ, ten Brink CB, Hauet-Broere F, Oosterwegel MA, Glant TT et al. Naive transgenic T cells expressing cartilage proteoglycan-specific TCR induce arthritis upon in vivo activation. *J Autoimmun* 2005;25(3):172-80.
- 32 van Aalst S, Ludwig IS, van der Zee R, van Eden W, Broere F. Bystander activation of irrelevant CD4+ T cells following antigen-specific vaccination occurs in the presence and absence of adjuvant. *PLOS ONE* 2017(5):e0177365.
- 33 Li JL, Goh CC, Keeble JL, Qin JS, Roediger B, Jain R et al. Intravital multiphoton imaging of immune responses in the mouse ear skin. *Nat Protoc* 2012;7(2):221-34.
- 34 Machholz E, Mulder G, Ruiz C, Corning BF, Pritchett-Corning KR. Manual restraint and common compound administration routes in mice and rats. *J Visualized Exp* 2012(67).
- 35 Malosse C, Henri S. Isolation of mouse dendritic cell subsets and macrophages from the skin. *Methods Mol Biol* 2016;1423:129-37.
- 36 Cisney ED, Fernandez S, Hall SI, Krietz GA, Ulrich RG. Examining the Role of Nasopharyngeal-associated Lymphoreticular Tissue (NALT) in Mouse Responses to Vaccines. 2012(66):e3960.
- 37 Broere F, Wieten L, Klein Koerkamp EI, Van Roon JAG, Guichelaar T, Lafeber FPJG et al. Oral or nasal antigen induces regulatory T cells that suppress arthritis and proliferation of arthritogenic T cells in joint draining lymph nodes. *J Immunol* 2008;181(2):899-906.
- 38 Underhill DM, Bassetti M, Rudensky A, Aderem A. Dynamic interactions of macrophages with T cells during antigen presentation. *J Exp Med* 1999;190(12):1909-14.
- 39 van Aalst S, Ludwig IS, van Kooten PJS, van der Zee R, van Eden W, Broere F. Dynamics of APC recruitment at the site of injection following injection of vaccine adjuvants. *Vaccine* 2017;35(12):1622-9.

- 40 Terhorst D, Fossum E, Baranska A, Tamoutounour S, Malosse C, Garbani M et al. Laser-assisted intradermal delivery of adjuvant-free vaccines targeting XCR1⁺ dendritic cells induces potent antitumoral responses. *J Immunol* 2015;194(12):5895-902.
- 41 Kruger P, Saffarzadeh M, Weber ANR, Rieber N, Radsak M, von Bernuth H et al. Neutrophils: Between Host Defence, Immune Modulation, and Tissue Injury. *PLoS Pathogen* 2015;11(3).
- 42 Salabert N, Todorova B, Martinon F, Boisgard R, Zurawski G, Zurawski S et al. Intradermal injection of an anti-Langerin-HIVGag fusion vaccine targets epidermal Langerhans cells in non-human primates and can be tracked in vivo. *Eur J Immunol* 2015;n/a,n/a.
- 43 Fougieron D, Van Maele L, Songhet P, Cayet D, Hot D, Van Rooijen N et al. Indirect Toll-like receptor 5-mediated activation of conventional dendritic cells promotes the mucosal adjuvant activity of flagellin in the respiratory tract. *Vaccine* 2015;33(29):3331-41.
- 44 Ciabattini A, Pettini E, Fiorino F, Prota G, Pozzi G, Medagliani D. Distribution of primed T cells and antigen-loaded antigen presenting cells following intranasal immunization in mice. *PLoS ONE* 2011;6(4).
- 45 Vendetti S, Riccomi A, Negri DRM, Veglia F, Sciaraffia E, De Magistris MT. Development of antigen-specific T cells in mediastinal lymph nodes after intranasal immunization. *Methods* 2009;49(4):334-9.
- 46 Duverger A, Jackson RJ, Van Ginkel FW, Fischer R, Tafaro A, Leppla SH et al. Bacillus anthracis edema toxin acts as an adjuvant for mucosal immune responses to nasally administered vaccine antigens. *J Immunol* 2006;176(3):1776-83.
- 47 Willart MAM, Deswarte K, Pouliot P, Braun H, Beyaert R, Lambrecht BN et al. Interleukin-1a controls allergic sensitization to inhaled house dust mite via the epithelial release of GM-CSF and IL-33. *J Exp Med* 2012;209(8):1505-17.
- 48 Caron G, Duluc D, Frémaux I, Jeannin P, David C, Gascan H et al. Direct stimulation of human T cells via TLR5 and TLR7/8: Flagellin and R-848 up-regulate proliferation and IFN- γ production by memory CD4⁺ T cells. *J Immunol* 2005;175(3):1551-7.
- 49 Semmrich M, Plantinga M, Svensson-Frej M, Uronen-Hansson H, Gustafsson T, Mowat AM et al. Directed antigen targeting in vivo identifies a role for CD103⁺ dendritic cells in both tolerogenic and immunogenic T-cell responses. *Mucosal Immunol* 2012;5(2):150-60.
- 50 Kastenmüller K, Wille-Reece U, Lindsay RWB, Trager LR, Darrah PA, Flynn BJ et al. Protective T cell immunity in mice following protein-TLR7/8 agonist-conjugate immunization requires aggregation, type I IFN, and multiple DC subsets. *J Clin Invest* 2011;121(5):1782-96.

Supplementary Data

Table S1. GFP expression of pOVA-specific CD4⁺ T hybridoma cells after co-culture.

A

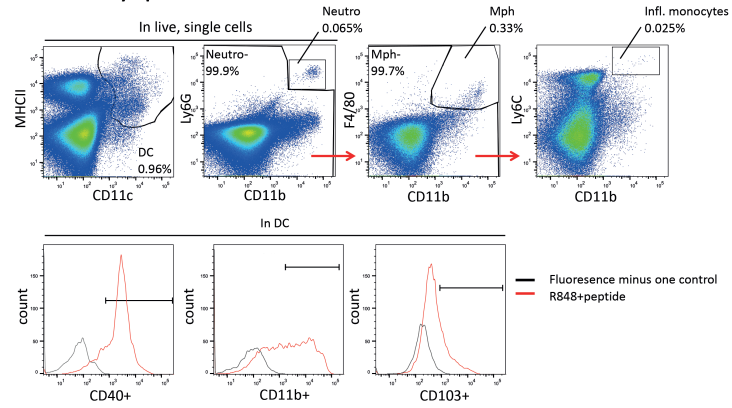
GFP-expression of pOVA-specific CD4 ⁺ T-cells			
<i>ID immunization</i>			
organ	treatment	av(%)	stdev(%)
Skin SOI	pOVA	7.79	2.83
	pOVA+R848	14.67	4.77
Skin CL	pOVA	3.99	1.18
	pOVA+R848	4.55	0.63
auLN SOI	pOVA	1.85	0.24
	pOVA+R848	5.55	2.42
auLN CL	pOVA	0.59	0.06
	pOVA+R848	0.83	0.09

GFP-expression of pOVA-specific CD4 ⁺ T-cells			
<i>IN immunisation</i>			
organ	treatment	av (%)	Stdv(%)
auLN	pOVA	1.77	0.11
	pOVA+R848	1.90	0.07
cLN	pOVA	2.48	0.28
	pOVA+R848	2.38	0.25
dcLN	pOVA	1.61	0.14
	pOVA+R848	1.68	0.21

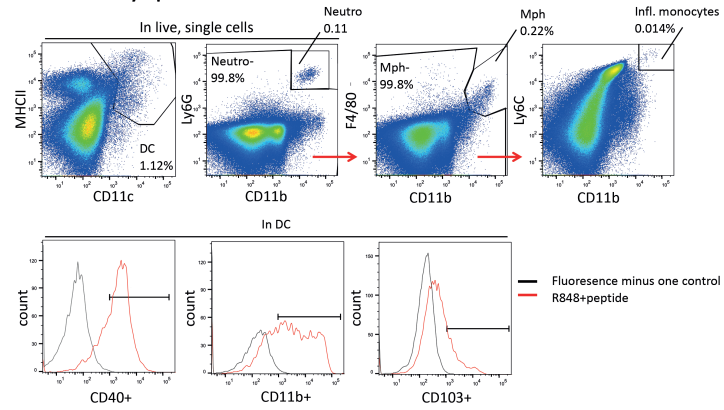
Mice were (A) IN or (B) ID immunized with 250 μ g pOVA \pm R848 and after 24h skin and draining LN were harvested and co-cultured with pOVA-specific CD4⁺ hybridoma cells for 18h. GFP expression of pOVA-specific CD4⁺ hybridoma cells was determined by flow cytometry. Indicated are the average and standard deviation per group per organ after the respective immunizations and N=4 per group. SOI: site of injection, CL: contralateral, auLN: auricular LN, cLN: cervical LN, dcLN: deep cervical LN.



S1A: Cervical lymph node after intranasal immunization



S1B: Auricular lymph node after intradermal immunization



S1C: Skin after intradermal immunization

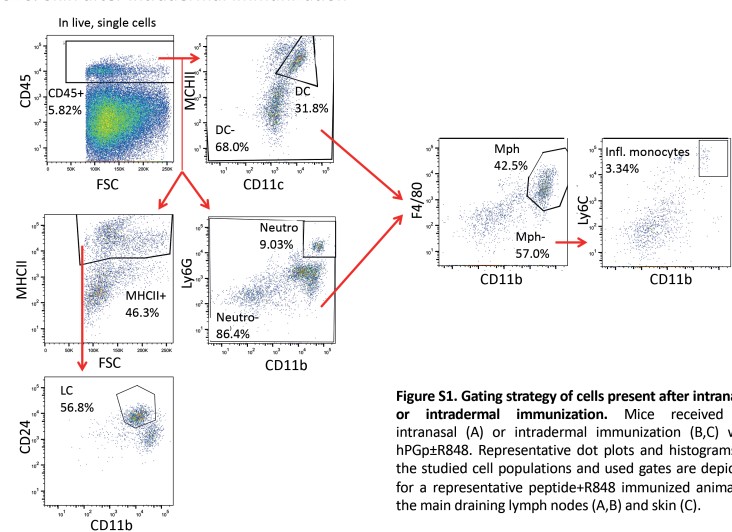
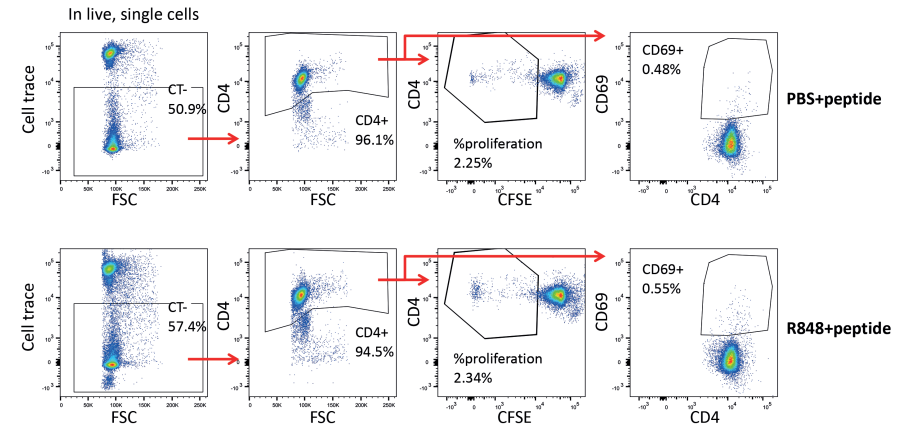


Figure S1. Gating strategy of cells present after intranasal or intradermal immunization. Mice received an intranasal (A) or intradermal immunization (B,C) with hPGp±R848. Representative dot plots and histograms of the studied cell populations and used gates are depicted for a representative peptide+R848 immunized animal in the main draining lymph nodes (A,B) and skin (C).

S2A: Cervical lymph node after intranasal immunization



S2B: Auricular lymph node after intradermal immunization

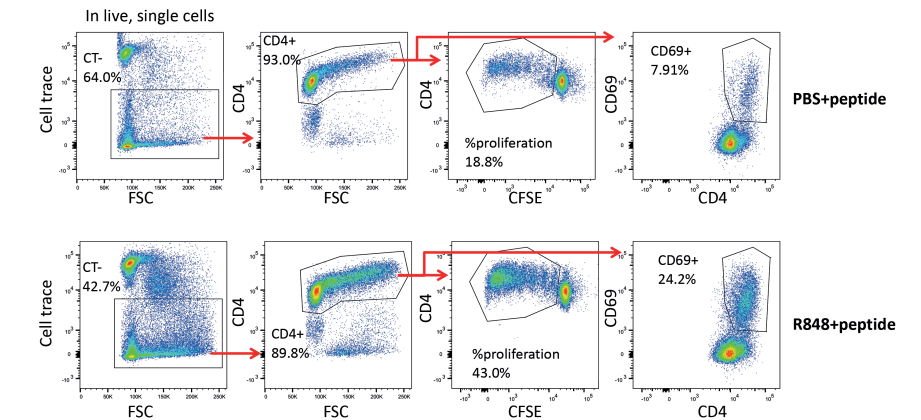
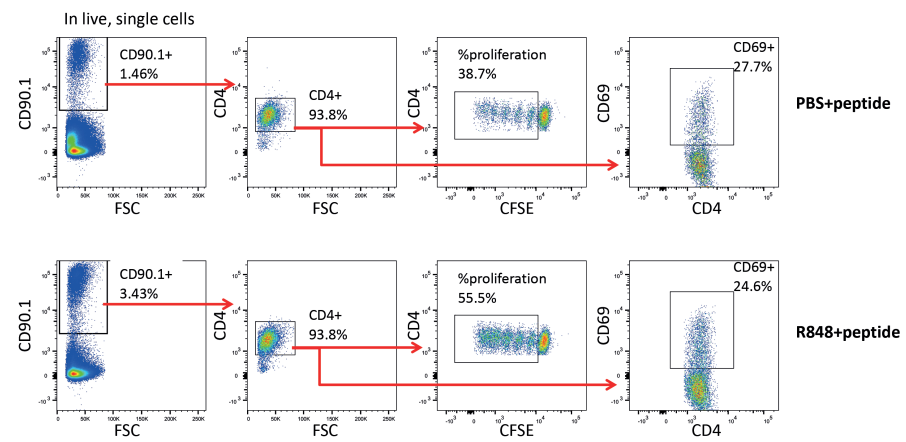


Figure S2. Gating strategy of proliferation and activation of co-cultured CD4⁺T cells. Mice received an intranasal (A) or intradermal immunization (B) with hPGp±R848. Representative dot plots are depicted for peptide±R848 immunized animals in the main draining lymph node. Proliferation and activation in the control culture (with naïve APC and CD4⁺ T cells) were 1.7% and 0.15% after intranasal immunization and 2.9% and 0.45% after intradermal immunization respectively.



S3A: Cervical lymph node after intranasal immunization



S3B: Auricular lymph node after intradermal immunization

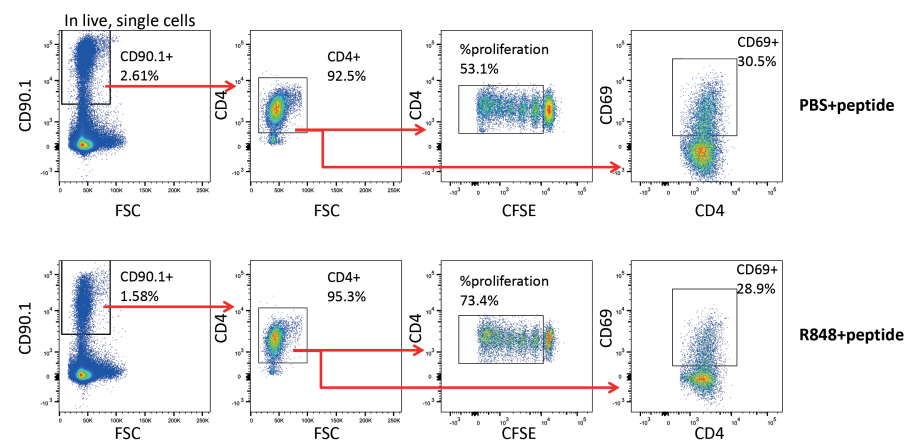


Figure S3. Gating strategy of proliferation and activation of transferred CD4⁺ T cells. Mice received an i.v. transfer of CFSE-labeled hPGp specific CD4⁺ T-cells 1d prior to intranasal (A) or intradermal immunization (B) with hPGp±R848. Representative dot plots are depicted for peptide±R848 immunized animals in the main draining lymph node. Proliferation and activation of a mock-injected animal were 5.5% and 7.5% after intranasal immunization and 8.6% and 3% after intradermal immunization respectively.





Chapter 7

Summarizing discussion



Tuning tolerance in autoimmunity

Autoimmune diseases are in general multi-etiological diseases in which genetic predisposition and environmental factors, together with a dysregulation in immune responses lead to pathology. In healthy individuals, peripheral immune tolerance is an important mechanism to maintain immune homeostasis and to keep self-recognizing lymphocytes that escaped the thymus from becoming activated. Failure of immune regulation or an imbalance in anti- and pro-inflammatory responses could lead towards autoimmune diseases. However, the initial trigger that causes faulty immune regulation is often unknown.

Rheumatoid arthritis (RA) is an example of an autoimmune disease in which current medication is directed towards relief of symptoms and mainly based on general immune suppression (**Chapter 1**). These general therapies can cause unwanted side effects such as a greater risk of infections. To relief patients of symptoms and effectively cure autoimmunity, restoration of long-term immune tolerance is needed. Several approaches can be taken to achieve this. Since the auto-aggressive effector T cell population has escaped elimination from the central and peripheral tolerance mechanisms, antibody treatment could be used to delete all effector T cells, including autoreactive T cells. Mainly CD4 and CD8 monoclonal antibodies were applied but this initiated various side-effects¹⁻³. Next to this, administration of the self-antigen via a tolerogenic route (e.g. orally) could be used to establish tolerance⁴. The major disadvantage of this approach is however that for most autoimmune diseases, the self-antigen causing the disease is unknown. Besides eradicating pathogenic cells, the regulatory immune response can also be antigen-specifically stimulated to suppress disease. This way autoreactive cells can be inhibited while leaving other immune responses intact.

To achieve immune tolerance, several approaches can be considered. In this thesis we investigated two possible approaches: tolerogenic dendritic cells (**Chapter 3 and 4**) and nanoparticles containing TNF siRNA (**Chapter 5**). Since the route of administration also determines the immunological responses that are initiated, we explored and compared two vaccination routes (**Chapter 6**).

Inducing immune tolerance – methods to manipulate the immune system

Peptide therapy

Tolerance induction by administration of disease associated or tolerogenic antigens is an approach that is considered for a long time. Since the self-peptide that initiates

RA is unknown, other peptide therapies were investigated. In RA more than 90% of the patients carry at least one of the RA associated MHC class II alleles encoded by the HLA-DR β 1 genes (shared epitope). Therefore a peptide approach was tried in which a peptide mimic binds to the antigen-binding site of the shared epitope HLA molecules. This way, self-antigens cannot bind to the RA-associated HLA, meaning that immune responses towards this antigen cannot be elicited⁵. Next to blocking the HLA binding site, an approach in which peptides that can bind the TCR was used. In this vaccine, they combined four TCR peptides which specifically target the autoreactive TCR since it was found that in patients only a restricted repertoire of the TCR Va or V β was found. By modulating the autoreactive TCRs with peptides, disease symptoms could be abrogated. The development even went into phase II clinical trials, but no progress has been reported after that⁶.

Instead of targeting the immune responses in RA, others aimed to make use of inflammation induced components such as heat shock proteins (HSPs). As discussed (**Chapter 1**), HSPs are a family of proteins that are highly conserved between species and are produced under inflammatory conditions. It was found that by immunizing the rats with HSP60, rats were protected against adjuvant arthritis⁷⁻¹⁰. Later research showed that administration with a HSP70 peptide via tolerogenic routes also protected against experimental arthritis¹¹. HSP70 did not only stimulate Tregs but also induced immune-modulatory functions in dendritic cells (DCs)¹¹⁻¹³. For these reasons, we set out to study HSPs as surrogate auto-antigens in RA in combination with tolerogenic dendritic cells (tolDCs) (**Chapter 3 and 4**).

Tolerogenic dendritic cells

DCs are professional antigen presenting cells that are involved in the induction of immunity and in the maintenance of immune tolerance. Whether a DC is immunogenic or tolerogenic is largely dependent on maturation status but more importantly also from signals that they receive from their micro-environment. Damaging autoimmunity needs active silencing of autoreactive T cells. DCs are important players in this process. Since DCs are substantial orchestrators of the immune system, they can also be used for therapy. Besides developing DC vaccines to fight cancer (as reviewed in¹⁴), researchers are exploring the possibilities to use DC vaccination to restore immune tolerance. While there are several ways to generate tolDCs¹⁵⁻¹⁷, we investigated dexamethasone and 1,25-dihydroxyvitamin D3 induced tolDCs^{18,19}. In **chapter 3**, we have shown that tolDCs, generated by dexamethasone and 1,25-dihydroxyvitamin D3, dampen the activation and proliferation of CD4⁺ T cells. This results in overall more Tregs and an immune-regulatory state. Since the autoantigen in RA is unknown, we sought alternative autoantigens. Possibly HSPs

can be used as surrogate autoantigens, for this reason we investigated the CD4⁺ T cell response towards one or more HSP-peptides (**Chapter 4**). Since roughly eighty percent of both healthy donors and inflammatory arthritis patients showed a CD4⁺ T cell response towards HSPs, we reasoned that HSPs could be used to modulate CD4⁺ T cell responses in humans. Furthermore, tolDCs pulsed with HSP or control peptides induced a Tr1 phenotype in the CD4⁺ T cells. Next to this tolDCs inhibited NK cell proliferation via bystander suppression. The *in vivo* co-transfer studies (**Chapter 3**) also show decreased donor NK cell presence in the mice that received tolDCs, indicating bystander suppression by tolDCs possibly adding to restoration of immune tolerance. Several studies have shown that tolDCs spread tolerance via Tregs. This phenomenon, called infectious tolerance, entails that the regulatory phenotype of a Treg is transferred to another cell population. CD4⁺CD25⁺FoxP3⁺ Tregs transfer their regulatory state to other CD4⁺ T cells (as thus far known) via IL-10 and TGFβ^{20,21}. For Tregs to suppress activation and/or proliferation in other T cells cell-cell contact is needed, but to transfer their regulatory state cell-cell contact is not required. After the regulatory state transfer, CD4⁺CD25⁺ T cells produced IL-10 themselves and were unable to proliferate (anergic)²⁰. Furthermore, they managed to inhibit CD4⁺ T cell proliferation, in contrast to Tregs, without cell-cell contact. Another study shows that Tregs can even induce *de novo* Tregs from a naïve CD4⁺ T cell population in a TGFβ dependent manner²¹. For this process, cell-cell contact and activation of the Tregs was required. Since Tregs (CD4⁺CD25⁺FoxP3⁺) are involved in maintaining immune homeostasis, we needed a model to study antigen specific CD4⁺ T cells. As antigen specific CD4⁺ T cells comprise only a small population *in vivo* and we wanted to study primary T cell responses, we created a TCR transgenic mouse (**Chapter 2**). With this model we could study the activation, proliferation and differentiation of antigen specific CD4⁺ T cells²². In addition to transferring tolerance indirectly via Tregs, the results shown in **Chapter 3** and **4** demonstrate that tolDCs affect, next to CD4⁺ T cells, also other immune cells and thus it is plausible that they also influence other APCs. They might even induce new tolAPCs *in vivo* without first inducing Tregs. Already in the 90's, it was shown that DCs can prime B cells²³ and skew B cell class switching^{24,25}. More recent research shows that tolDCs induce the proliferation of immune suppressive B cells, or Bregs, via retinoic acid production²⁶.

TolDCs secrete many soluble factors that can communicate with other cells and thus influence other APCs. Next to immune regulatory cytokines (**Chapter 3** and **4**), extracellular vesicles (EVs) are an important factor of intercellular communication²⁷. These EVs from 50-200 nm contain proteins, lipids and RNAs that are representative of the cell they are derived of. By regulating the release and composition of these

EVs, parental cells can tightly control the message to other cells. Therefore, it is possible that EVs from tolDCs contain proteins or even RNAs²⁸ that are immune regulatory. Earlier studies have already shown that EVs derived from IDO over-expressing DCs and IL-10 treated DCs are able to abrogate experimental arthritis^{29,30}. This suggests that the content of the EVs can be immune regulatory, based on the nature of the EV releasing cell. By communicating with other APCs via EVs, tolerance could also be spread. This way, by spreading tolerance, long-term immune tolerance against a specific antigen may be achieved by providing a single dose of antigen-pulsed tolDCs.

Apart from the *in vivo* working mechanisms of tolDCs, many practical aspects concerning the tolDC therapy need to be investigated. There is not much known yet about the effective route of administration, the frequency of injections and the tolDC dose as discussed in **Chapter 3**. In most *in vivo* animal models, tolDCs were injected intravenously^{18,31,32,Chapter 3} which is mainly caused by the practical reasons that mice are too small to inject intranodal and tolDCs are too large and fragile to condense in such a volume that intradermal or intra-articular administration is an option. Furthermore, it is unclear if tolDCs are able to migrate *in vivo*. *In vitro* studies with both murine or human cells indicate that maturation of the tolDC is required for migratory abilities^{19,33}. A study from the cancer immunology field shows in what manner the route of administration influenced the migratory capacity of a DC; more DCs migrated after intranodal administration compared to intradermal administration³⁴. However, in 7 out of 24 patients, the DCs did not migrate at all. Thus it is important to investigate the effects and involved immune cells of a particular route of administration. In order to compare the immune cells involved in two non-traditional routes (intradermal and intranasal) of vaccination, we used a model vaccine in **Chapter 6**. As shown in **Chapter 6**, the model adjuvant R848 stimulated the innate immune system with both vaccination routes. However, the CD4⁺ T cell response after intradermal administration of the model vaccine was increased compared to the response after intranasal application. Furthermore, we noticed differences in cytokine production which illustrates that the microenvironment and immune response differ greatly between the several administration routes, and thus more research is needed on this topic. A mouse study in which tolDCs are administered via different routes could clarify which route is most optimal to reach immune tolerance.

Another question that needs to be addressed is the duration of the effect of one tolDC injection. In our studies, we followed the mice for three weeks after tolDC administration (**Chapter 3**). However, it is unclear if the efficiency of the tolDCs

is decreasing over time. Possibly, multiple injections are required to maintain the arthritis suppressing effects. If tolDCs do induce antigen specific infectious tolerance, creating a regulatory feedback loop, the effect of tolDCs is most likely long-lasting. In our studies, lowering the tolDC dose from 1×10^6 to 2×10^5 cells/injection did not affect the competence of tolDCs to modulate $CD4^+$ T cell responses (**Chapter 3**). However, increasing the dose to 20×10^6 tolDCs/injection can accelerate experimental arthritis symptoms in mice³⁵. In phase I clinical trials, up to 10×10^6 cells/injection were safe and without any side-effects^{36,37}.

As shortly discussed in the previous section, the autoantigen for RA is unknown. To be able to induce antigen-specific immune tolerance, surrogate autoantigens are explored (**Chapter 4**). **Chapter 3** shows that unloaded mtolDCs are also able to suppress arthritis in an experimental arthritis model. Furthermore, it was shown that tolDCs produce general immune suppressive cytokines and are able to inhibit NK cells via bystander suppression. However, a preliminary co-transfer study with unloaded mtolDCs and antigen-specific $CD4^+$ T cells suggests that mtolDCs might be able to pick up the antigen *in vivo* (unpublished observations). Studies show that the migratory capacities of (tol)DCs are limited *in vivo*, so one could argue that by local administration of tolDCs, inducing general immune tolerance would also be sufficient to suppress arthritic symptoms. However, the risk is that by inducing general immune tolerance, immune responses against invading pathogens is not elicited. Furthermore, if these non-antigen-pulsed tolDCs are able to take up antigen *in vivo*, the safety of these tolDCs is an issue. It cannot be excluded that non-antigen-pulsed tolDCs also take up other antigens that should not be targeted.

TolDC therapy seems promising, but there is also a downside. First of all, cell therapies are more labor intensive than off-the-shelf products. Secondly, tolDC therapy has been until now autologous. This means that every patient needs personalized medicine developed in a specialized medical center which is accompanied by high costs. Therefore, alternative ways of restoring immune tolerance are sought which are applicable to multiple patients. One of the options is to use drug delivery systems for local immune modulation.

Nanoparticles as drug delivery system

TNF is a pro-inflammatory cytokine that plays an important role in the pathogenesis of RA (**Chapter 1**). Currently the most effective therapy on the market are anti-TNF biopharmaceuticals, which are used for RA patients to treat their symptoms. The disadvantage of these anti-TNF antibodies or soluble TNF receptors is that their efficiency can be hampered by the production of antibodies against these anti-

TNF biopharmaceuticals³⁸. RNA interference therapy could be a solution to inhibit excessive TNF production while avoiding antibody production. However, to deliver siRNA intracellularly to the RNAi pathway in the cytosol of target cells a drug delivery system is needed, because siRNA cannot pass through cellular membranes. Drug delivery systems are applied to overcome delivery challenges as they protect the incorporated drug from degradation. For this, nanoparticles containing cationic lipids were developed at the University of Copenhagen^{39,40}. These nanoparticles, composed of poly(DL-lactic-co-glycolic acid) (PLGA) and the cationic lipid 1,2-dioleoyl-3-trimethylammonium propane (DOTAP), efficiently delivered siRNA to cells and mediated high transfection efficiency. Since toxicity for cells was a problem, lipidoids (lipid-like materials with a tetraamine backbone) nanoparticles were made as these are less toxic^{39,41}. Lipidoids can be formulated as long circulating stable nucleic acid lipid particles (SNALPS) or as lipid-polymer hybrid nanoparticles (LPNs). Considering that these nanoparticles are designed for drug delivery, the immunogenicity was tested in *in vitro* TLR activation and DC maturation experiments⁴². Especially in autoimmunity, the delivery system itself should not induce any additional (pro-inflammatory) immune responses. As shown by de Groot *et al.*, when the lipidoids were included into the structure of the nanoparticle to form LPNs, both TLR4 activation and APC maturation were abrogated. The SNALP nanoparticles, did activate TLR4 and APCs to some extent⁴².

The next step was to test if the LPNs and SNALPs, containing siRNA, were able to silence the target RNA *in vitro*. For this purpose, TNF siRNA was produced and enclosed into the nanoparticles, and first tested in a macrophage cell line (**Chapter 5**). Both nanoparticles containing TNF siRNA were able to silence TNF production. To assess whether TNF siRNA encapsulated by SNALPs or LPNs could silence TNF *in vivo* and abrogate arthritis, the experimental arthritis model was used⁴³. Both the SNALPs and LPNs containing TNF siRNA restrained arthritic symptoms after local administration, indicating that TNF was silenced *in vivo* (**Chapter 5**). However, while the nanoparticles were administered locally, the effect observed was systemic which suggests that the nanoparticles are transferred throughout the mouse. There is not a lot known about the migratory abilities of nanoparticles *in vivo*. The diffusion rate of a nanoparticle is dependent on its size, charge and content. Research about nanoparticles used as drug delivery system for tumors shows that smaller nanoparticles (20 nm and 40 nm) diffuse ten times further into a tissue-model than larger nanoparticles (100 nm and 200 nm)⁴⁴. A study that compared non-organic (e.g. silica and silver) and organic (e.g. liposomes and micelles) nanoparticles showed that nanoparticles that contain lipid-tails take longer timewise to migrate compared to the non-organic nanoparticles *in vitro*⁴⁵.

Furthermore, the encapsulated content could influence the migration time and double the migration time of the nanoparticle. Next to this, it was shown that after one intravenous injection with gold nanoparticles, the nanoparticles were found in lung (< 1 week after injection), liver, spleen (throughout the entire study; 2 months) and kidney. The nanoparticles were not measured in the brain, indicating that these nanoparticles could not cross the blood-brain barrier⁴⁶. These results imply that nanoparticle distribution occurs throughout the whole body, which could also be possible with lipid-like nanoparticles.

Next to distribution of the nanoparticles, the cellular uptake of nanoparticles determines their effects. Cellular uptake is partly dependent on nanoparticle size. Nanoparticles that are smaller than 100 nm can be more easily internalized than nanoparticles >100 nm. Furthermore, the charge, aggregation abilities and surface characteristics of a nanoparticle determine the efficiency of the cellular uptake⁴⁷. In **chapter 5**, we showed that macropinocytosis and clathrin-mediated endocytosis are possible mechanisms for the uptake of SNALPs and LPNs (both between 60-80 nm). This indicates that mainly APCs will take up LPNs or SNALPs, among which macrophages. Once engulfed by the cell, the siRNA needs to escape from the endosomes towards the target area. In the case of LPNs and SNALPs, which are both cationic lipid-based nanoparticles, one of the proposed escape mechanisms is the following: the cationic lipids of the nanoparticles interact with the anionic lipids of the endosome causing a flip-flop thereby destabilizing the endosome membrane⁴⁷. The cargo of the nanoparticles can then be released into the cytosol and target the TNF mRNA machinery.

Although the LPNs and SNALPs are probably actively taken up by APCs, we cannot exclude fusion of the nanoparticles with cell membranes of other cell types. To specifically target cells, tags could be attached to the nanoparticles. Small molecules such as peptides were added to nanoparticles to target murine heart endothelial cells or tumor cells. When adding the peptide directed to a receptor on the target cell, the uptake of nanoparticles by the target cells increased. Additionally, other non-targeted cell types engulfed lower amounts of nanoparticles^{48,49}. A study in transplant immunology shows that by conjugating α -human CD31-antibodies to the surface of their nanoparticles (poly(lactic acid)-poly(ethylene glycol)), the vascular retention of the nanoparticles increased⁵⁰. With these α CD31 coupled nanoparticles, accumulation of nanoparticles in the target cells, endothelial cells, was established and increased 5-10 fold compared to non-targeted nanoparticle accumulation⁵⁰. Small molecule-surface modification of nanoparticles even made it possible to target cells depending on their activation status (e.g. activated vs resting). This

way, it would be possible to directly target overactivated immune cells (e.g. TNF producing macrophages as in **Chapter 5**) in the arthritic joint.

Targeting specific cell types also provides new opportunities for the use of nanoparticles. If it is possible to directly target DCs *in vivo*, it would be possible to generate tolDCs in the patient without the need of modulating cells *ex vivo* in the laboratory. A study by Cruz *et al.* in 2012 indicates that direct targeting of DCs *in vivo* is possible. PLGA nanoparticles were coupled to several biotinylated ligands (carbohydrates, glycoproteins and antibodies) that could bind DC-SIGN⁵¹. DC-SIGN is a C-type lectin receptor that is mostly expressed by DCs. This receptor can internalize antigens which are presented to T cells and thus influence the immune response⁵². When comparing the different biotinylated ligands, it was found that the DC-SIGN antibodies were most efficient in binding DC-SIGN and thus provided the highest vaccine uptake efficiency⁵¹. In this study they used nanoparticles to deliver a vaccine, but since nanoparticles can carry different types of cargo they could also be used otherwise. More recently, researchers started to create tolerogenic nanoparticles (tNPs). These tNPs not only target specific cell types but also induce tolerance. The induction of tolerance via tNPs can be established in several ways and can be roughly divided in two: 1) tNPs directly target autoreactive cell populations such as T cells thereby restoring immune tolerance⁵³. 2) tNPs expressing inhibitory antibodies or antigens for an inhibitory receptor (cell specific tolerance), or tNPs encapsulating tolerogenic agents to target immature APCs and induce tolDCs^{54,55}.

To achieve immune tolerance via directly targeting autoreactive cells (1), tNPs were loaded with a disease-relevant peptide in pMHC multimers to directly target the T cell receptor. Next to this, inhibitory receptor-targeting antibodies (e.g. PD-L1 antibody) and 'self-marker' molecules (CD47) were co-presented to prevent uptake by APCs. After intravenous administration, tNPs reduced self-peptide reactive Th1 and Th17 cells by inducing apoptosis and inhibit proliferation and this ameliorated disease⁵³.

To induce tolDCs with tNPs (2), tolerogenic agents that have proven to induce tolDCs *in vitro* (**Chapter 3 and 4**) could be used. Loading tolerogenic microparticles (tMPs) with Vitamin D3 in combination with TGF β has shown to be effective in a type 1 diabetes study⁵⁶. DCs treated with tMPs encapsulating VitD3 and TGF β exhibited an immature phenotype and were able to functionally present antigen to CD4⁺ T cells. Furthermore, when NOD mice were injected subcutaneously with a combination of VitD3-, TGF β -, and insulin-encapsulated particles, the mice were protected from diabetes. After 15 weeks, some mice did develop diabetes indicating that

treatment needed repetition to prevent onset of disease⁵⁶. In addition to preventing diabetes, the percentage of regulatory cells was also increased in mice treated with a combination of VitD3, TGFβ-, and insulin-capsulated particles. Another study using tNPs shows that tNPs encapsulating rapamycin and disease-relevant peptide demonstrate regulatory capacities. Administering rapamycin tNPs reduced proliferation of CD4⁺ T cells and increased the amount of regulatory cells, similar to the study by Lewis *et al.* Moreover, therapeutic application of the tNPs inhibited experimental autoimmune encephalomyelitis (EAE)⁵⁷. Additionally, tolerance was transferrable via Tregs and the regulatory response that was induced was still functional after a substantial period (>4 weeks). The combined results from these studies^{56,57} indicate that inducing tolerance, possibly via the induction of tolDCs, by the use of tolerogenic particles is a realistic possibility.

Future perspectives on immune modulation

The immune tolerance inducing methods (**Chapter 3, 4 and 5**) described in this thesis explored two ways to dampen autoreactive and damaging cells while leaving other immune responses intact. However, to be able to restore immune tolerance in a clinical setting and circumvent the need of general immune suppressive drugs, more research regarding immune tolerance inducing methods seems required. Not only the exact working mechanisms of tolerance inducing therapies are important to unravel, also the practical side is extremely important. As we have seen, dose, frequency and especially route of administration partly determine the outcome of a treatment. It has been the aim of the studies presented in this thesis to expand on our knowledge about immune tolerance and ways of administration of treatment. The results in this thesis may bring us a step closer towards developing immune tolerance-inducing therapies for rheumatoid arthritis and possibly also other autoimmune diseases.

References

- Weinblatt ME, Maddison PJ, Bulpitt KJ, et al. CAMPATH-1H, a humanized monoclonal antibody, in refractory rheumatoid arthritis. an intravenous dose-escalation study. *Arthritis Rheum.* 1995;38(11):1589-1594.
- Ilan Y, Zigmund E, Lalazar G, et al. Oral administration of OKT3 monoclonal antibody to human subjects induces a dose-dependent immunologic effect in T cells and dendritic cells. *J Clin Immunol.* 2010;30(1):167-177. doi: 10.1007/s10875-009-9323-7 [doi].
- Nakou M, Katsikas G, Sidiropoulos P, et al. Rituximab therapy reduces activated B cells in both the peripheral blood and bone marrow of patients with rheumatoid arthritis: Depletion of memory B cells correlates with clinical response. *Arthritis Res Ther.* 2009;11(4):R131. doi: 10.1186/ar2798 [doi].
- Bar-Or A, Steinman L, Behne JM, et al. Restoring immune tolerance in neuromyelitis optica: Part II. *Neurol Neuroimmunol Neuroinflamm.* 2016;3(5):e277. doi: 10.1212/NXI.0000000000000277 [doi].
- Woulfe SL, Bono CP, Zacheis ML, et al. A peptidomimetic that specifically inhibits human leukocyte antigen DRB1*0401-restricted T cell proliferation. *J Pharmacol Exp Ther.* 1997;281(2):663-669.
- Moreland LW, Morgan EE, Adamson TC, 3rd, et al. T cell receptor peptide vaccination in rheumatoid arthritis: A placebo-controlled trial using a combination of Vbeta3, Vbeta14, and Vbeta17 peptides. *Arthritis Rheum.* 1998;41(11):1919-1929. doi: 10.1002/1529-0131(199811)41:11:1919-1929 [doi].
- van Eden W, Thole JE, van der Zee R, et al. Cloning of the mycobacterial epitope recognized by T lymphocytes in adjuvant arthritis. *Nature.* 1988;331(6152):171-173. doi: 10.1038/331171a0 [doi].
- Anderton SM, van der Zee R, Prakken B, Noordzij A, van Eden W. Activation of T cells recognizing self 60-kD heat shock protein can protect against experimental arthritis. *J Exp Med.* 1995;181(3):943-952.
- Prakken BJ, Roord S, van Kooten PJ, et al. Inhibition of adjuvant-induced arthritis by interleukin-10-driven regulatory cells induced via nasal administration of a peptide analog of an arthritis-related heat-shock protein 60 T cell epitope. *Arthritis Rheum.* 2002;46(7):1937-1946. doi: 10.1002/art.10366 [doi].
- Moudgil KD, Chang TT, Eradat H, et al. Diversification of T cell responses to carboxy-terminal determinants within the 65-kD heat-shock protein is involved in regulation of autoimmune arthritis. *J Exp Med.* 1997;185(7):1307-1316.
- van Herwijnen MJ, Wieten L, van der Zee R, et al. Regulatory T cells that recognize a ubiquitous stress-inducible self-antigen are long-lived suppressors of autoimmune arthritis. *Proc Natl Acad Sci U S A.* 2012;109(35):14134-14139. doi: 10.1073/pnas.1206803109 [doi].
- Borges TJ, Wieten L, van Herwijnen MJ, et al. The anti-inflammatory mechanisms of Hsp70. *Front Immunol.* 2012;3:95. doi: 10.3389/fimmu.2012.00095 [doi].
- Spiering R, van der Zee R, Wagenaar J, van Eden W, Broere F. Mycobacterial and mouse HSP70 have immuno-modulatory effects on dendritic cells. *Cell Stress Chaperones.* 2013;18(4):439. doi: 10.1007/s12192-012-0397-4.
- Saxena M, Bhardwaj N. Re-emergence of dendritic cell vaccines for cancer treatment. *Trends Cancer.* 2018;4(2):119-137. doi: S2405-8033(17)30240-6 [pii].
- Morita Y, Yang J, Gupta R, et al. Dendritic cells genetically engineered to express IL-4 inhibit murine collagen-induced arthritis. *J Clin Invest.* 2001;107(10):1275-1284. doi: 10.1172/JCI11490 [doi].
- Tan PH, Yates JB, Xue SA, et al. Creation of tolerogenic human dendritic cells via intracellular CTLA4: A novel strategy with potential in clinical immunosuppression. *Blood.* 2005;106(9):2936-2943. doi: 2005-05-1826 [pii].

17. Martin E, Capini C, Duggan E, et al. Antigen-specific suppression of established arthritis in mice by dendritic cells deficient in NF-kappaB. *Arthritis Rheum.* 2007;56(7):2255-2266. doi: 10.1002/art.22655 [doi].
18. Stoop JN, Harry RA, von Delwig A, Isaacs JD, Robinson JH, Hilken CM. Therapeutic effect of tolerogenic dendritic cells in established collagen-induced arthritis is associated with a reduction in Th17 responses. *Arthritis Rheum.* 2010;62(12):3656-3665. doi: 10.1002/art.27756 [doi].
19. Anderson AE, Swan DJ, Sayers BL, et al. LPS activation is required for migratory activity and antigen presentation by tolerogenic dendritic cells. *J Leukoc Biol.* 2009;85(2):243-250. doi: 10.1189/jlb.0608374 [doi].
20. Dieckmann D, Bruett CH, Ploettner H, Lutz MB, Schuler G. Human CD4(+)CD25(+) regulatory, contact-dependent T cells induce interleukin 10-producing, contact-independent type 1-like regulatory T cells [corrected]. *J Exp Med.* 2002;196(2):247-253.
21. Anderson AE, Sayers BL, Haniffa MA, et al. Differential regulation of naive and memory CD4+ T cells by alternatively activated dendritic cells. *J Leukoc Biol.* 2008;84(1):124-133. doi: 10.1189/jlb.1107744 [doi].
22. Jansen MA, van Herwijnen MJ, van Kooten PJ, et al. Generation of the first TCR transgenic mouse with CD4(+) T cells recognizing an anti-inflammatory regulatory T cell-inducing Hsp70 peptide. *Front Immunol.* 2016;7:90. doi: 10.3389/fimmu.2016.00090 [doi].
23. Bergtold A, Desai DD, Gavhane A, Clynes R. Cell surface recycling of internalized antigen permits dendritic cell priming of B cells. *Immunity.* 2005;23(5):503-514. doi: S1074-7613(05)00309-2 [pii].
24. Fayette J, Dubois B, Vandebeele S, et al. Human dendritic cells skew isotype switching of CD40-activated naive B cells towards IgA1 and IgA2. *J Exp Med.* 1997;185(11):1909-1918.
25. Wykes M, Pombo A, Jenkins C, MacPherson GG. Dendritic cells interact directly with naive B lymphocytes to transfer antigen and initiate class switching in a primary T-dependent response. *J Immunol.* 1998;161(3):1313-1319.
26. Di Caro V, Phillips B, Engman C, Harnaha J, Trucco M, Giannoukakis N. Retinoic acid-producing, ex-vivo-generated human tolerogenic dendritic cells induce the proliferation of immunosuppressive B lymphocytes. *Clin Exp Immunol.* 2013;174(2):302-317. doi: 10.1111/cei.12177 [doi].
27. Nolte-t Hoen EN, Wauben MH. Immune cell-derived vesicles: Modulators and mediators of inflammation. *Curr Pharm Des.* 2012;18(16):2357-2368. doi: CPD-EPUB-20120227-039 [pii].
28. Driedonks TAP, van der Grein SG, Ariyurek Y, et al. Immune stimuli shape the small non-coding transcriptome of extracellular vesicles released by dendritic cells. *Cell Mol Life Sci.* 2018. doi: 10.1007/s00018-018-2842-8 [doi].
29. Kim SH, Lechman ER, Bianco N, et al. Exosomes derived from IL-10-treated dendritic cells can suppress inflammation and collagen-induced arthritis. *J Immunol.* 2005;174(10):6440-6448. doi: 174/10/6440 [pii].
30. Bianco NR, Kim SH, Ruffner MA, Robbins PD. Therapeutic effect of exosomes from indoleamine 2,3-dioxygenase-positive dendritic cells in collagen-induced arthritis and delayed-type hypersensitivity disease models. *Arthritis Rheum.* 2009;60(2):380-389. doi: 10.1002/art.24229 [doi].
31. Creusot RJ, Chang P, Healey DG, Tcherepanova IY, Nicolette CA, Fathman CG. A short pulse of IL-4 delivered by DCs electroporated with modified mRNA can both prevent and treat autoimmune diabetes in NOD mice. *Mol Ther.* 2010;18(12):2112-2120. doi: 10.1038/mt.2010.146 [doi].
32. Mansilla MJ, Selles-Moreno C, Fabregas-Puig S, et al. Beneficial effect of tolerogenic dendritic cells pulsed with MOG autoantigen in experimental autoimmune encephalomyelitis. *CNS Neurosci Ther.* 2015;21(3):222-230. doi: 10.1111/cns.12342 [doi].
33. Ferreira GB, Vanherwegen AS, Eelen G, et al. Vitamin D3 induces tolerance in human dendritic cells by activation of intracellular metabolic pathways. *Cell Rep.* 2015. doi: S2211-1247(15)00026-1 [pii].
34. Lesterhuis WJ, de Vries IJ, Schreibeit G, et al. Route of administration modulates the induction of dendritic cell vaccine-induced antigen-specific T cells in advanced melanoma patients. *Clin Cancer Res.* 2011;17(17):5725-5735. doi: 10.1158/1078-0432.CCR-11-1261 [doi].
35. Lim DS, Kang MS, Jeong JA, Bae YS. Semi-mature DC are immunogenic and not tolerogenic when inoculated at a high dose in collagen-induced arthritis mice. *Eur J Immunol.* 2009;39(5):1334-1343. doi: 10.1002/eji.200838987 [doi].
36. Jauregui-Amezaga A, Cabezon R, Ramirez-Morros A, et al. Intraperitoneal administration of autologous tolerogenic dendritic cells for refractory crohn's disease: A phase I study. *J Crohns Colitis.* 2015;9(12):1071-1078. doi: 10.1093/ecco-jcc/jjv144 [doi].
37. Bell GM, Anderson AE, Diboll J, et al. Autologous tolerogenic dendritic cells for rheumatoid and inflammatory arthritis. *Ann Rheum Dis.* 2017;76(1):227-234. doi: 10.1136/annrheumdis-2015-208456 [doi].
38. Wolbink GJ, Vis M, Lems W, et al. Development of antiinfliximab antibodies and relationship to clinical response in patients with rheumatoid arthritis. *Arthritis Rheum.* 2006;54(3):711-715. doi: 10.1002/art.21671 [doi].
39. Colombo S, Cun D, Remaut K, et al. Mechanistic profiling of the siRNA delivery dynamics of lipid-polymer hybrid nanoparticles. *J Control Release.* 2015;201:22-31. doi: 10.1016/j.jconrel.2014.12.026 [doi].
40. Thanki K, Zeng X, Justesen S, et al. Engineering of small interfering RNA-loaded lipidoid-poly(DL-lactic-co-glycolic acid) hybrid nanoparticles for highly efficient and safe gene silencing: A quality by design-based approach. *Eur J Pharm Biopharm.* 2017;120:22-33. doi: S0939-6411(17)30565-9 [pii].
41. te Boekhorst BC, Jensen LB, Colombo S, et al. MRI-assessed therapeutic effects of locally administered PLGA nanoparticles loaded with anti-inflammatory siRNA in a murine arthritis model. *J Control Release.* 2012;161(3):772-780. doi: 10.1016/j.jconrel.2012.05.004 [doi].
42. de Groot A, Thanki K, Gangloff M, et al. Immunogenicity testing of lipidoids *In Vitro* and *in silico*: Modulating lipidoid-mediated TLR4 activation by nanoparticle design. . 2018;11:159-169.
43. Glant TT, Radacs M, Nagyri G, et al. Proteoglycan-induced arthritis and recombinant human proteoglycan aggrecan G1 domain-induced arthritis in BALB/c mice resembling two subtypes of rheumatoid arthritis. *Arthritis Rheum.* 2011;63(5):1312-1321. doi: 10.1002/art.30261 [doi].
44. Goodman TT, Olive PL, Pun SH. Increased nanoparticle penetration in collagenase-treated multicellular spheroids. *Int J Nanomedicine.* 2007;2(2):265-274.
45. Kato M, Sasaki M, Ueyama Y, et al. Comparison of the migration behavior of nanoparticles based on polyethylene glycol and silica using micellar electrokinetic chromatography. *J Sep Sci.* 2015;38(3):468-474. doi: 10.1002/jssc.201401086 [doi].
46. Balasubramanian SK, Jittiwat J, Manikandan J, Ong CN, Yu LE, Ong WY. Biodistribution of gold nanoparticles and gene expression changes in the liver and spleen after intravenous administration in rats. *Biomaterials.* 2010;31(8):2034-2042. doi: 10.1016/j.biomaterials.2009.11.079 [doi].
47. Adjei IM, Sharma B, Labhasetwar V. Nanoparticles: Cellular uptake and cytotoxicity. *Adv Exp Med Biol.* 2014;811:73-91. doi: 10.1007/978-94-017-8739-0_5 [doi].
48. Weissleder R, Kelly K, Sun EY, Shtatland T, Josephson L. Cell-specific targeting of nanoparticles by multivalent attachment of small molecules. *Nat Biotechnol.* 2005;23(11):1418-1423. doi: nbt1159 [pii].
49. Anabousi S, Bakowsky U, Schneider M, Huwer H, Lehr CM, Ehrhardt C. In vitro assessment of transferrin-conjugated liposomes as drug delivery systems for inhalation therapy of lung cancer. *Eur J Pharm Sci.* 2006;29(5):367-374. doi: S0928-0987(06)00202-8 [pii].
50. Tietjen GT, Hosgood SA, DiRito J, et al. Nanoparticle targeting to the endothelium during normothermic machine perfusion of human kidneys. *Sci Transl Med.* 2017;9(418):10.1126/scitranslmed.aam6764. doi: eam6764 [pii].

51. Cruz LJ, Tacken PJ, Pots JM, Torensma R, Buschow SI, Figdor CG. Comparison of antibodies and carbohydrates to target vaccines to human dendritic cells via DC-SIGN. *Biomaterials*. 2012;33(16):4229-4239. doi: 10.1016/j.biomaterials.2012.02.036 [doi].
52. Engering A, Geijtenbeek TB, van Vliet SJ, et al. The dendritic cell-specific adhesion receptor DC-SIGN internalizes antigen for presentation to T cells. *J Immunol*. 2002;168(5):2118-2126.
53. Pei W, Wan X, Shahzad KA, et al. Direct modulation of myelin-autoreactive CD4(+) and CD8(+) T cells in EAE mice by a tolerogenic nanoparticle co-carrying myelin peptide-loaded major histocompatibility complexes, CD47 and multiple regulatory molecules. *Int J Nanomedicine*. 2018;13:3731-3750. doi: 10.2147/IJN.S164500 [doi].
54. Maldonado RA, LaMothe RA, Ferrari JD, et al. Polymeric synthetic nanoparticles for the induction of antigen-specific immunological tolerance. *Proc Natl Acad Sci U S A*. 2015;112(2):E156-65. doi: 10.1073/pnas.1408686111 [doi].
55. Kishimoto TK, Maldonado RA. Nanoparticles for the induction of antigen-specific immunological tolerance. *Front Immunol*. 2018;9:230. doi: 10.3389/fimmu.2018.00230 [doi].
56. Lewis JS, Dolgova NV, Zhang Y, et al. A combination dual-sized microparticle system modulates dendritic cells and prevents type 1 diabetes in prediabetic NOD mice. *Clin Immunol*. 2015;160(1):90-102. doi: 10.1016/j.clim.2015.03.023 [doi].
57. LaMothe RA, Kolte PN, Vo T, et al. Tolerogenic nanoparticles induce antigen-specific regulatory T cells and provide therapeutic efficacy and transferrable tolerance against experimental autoimmune encephalomyelitis. *Front Immunol*. 2018;9:281. doi: 10.3389/fimmu.2018.00281 [doi].



Chapter 8

Addendum

Nederlandse lekensamenvatting
Dankwoord/Acknowledgements
Curriculum Vitae
List of publications



Nederlandse lekensamenvatting

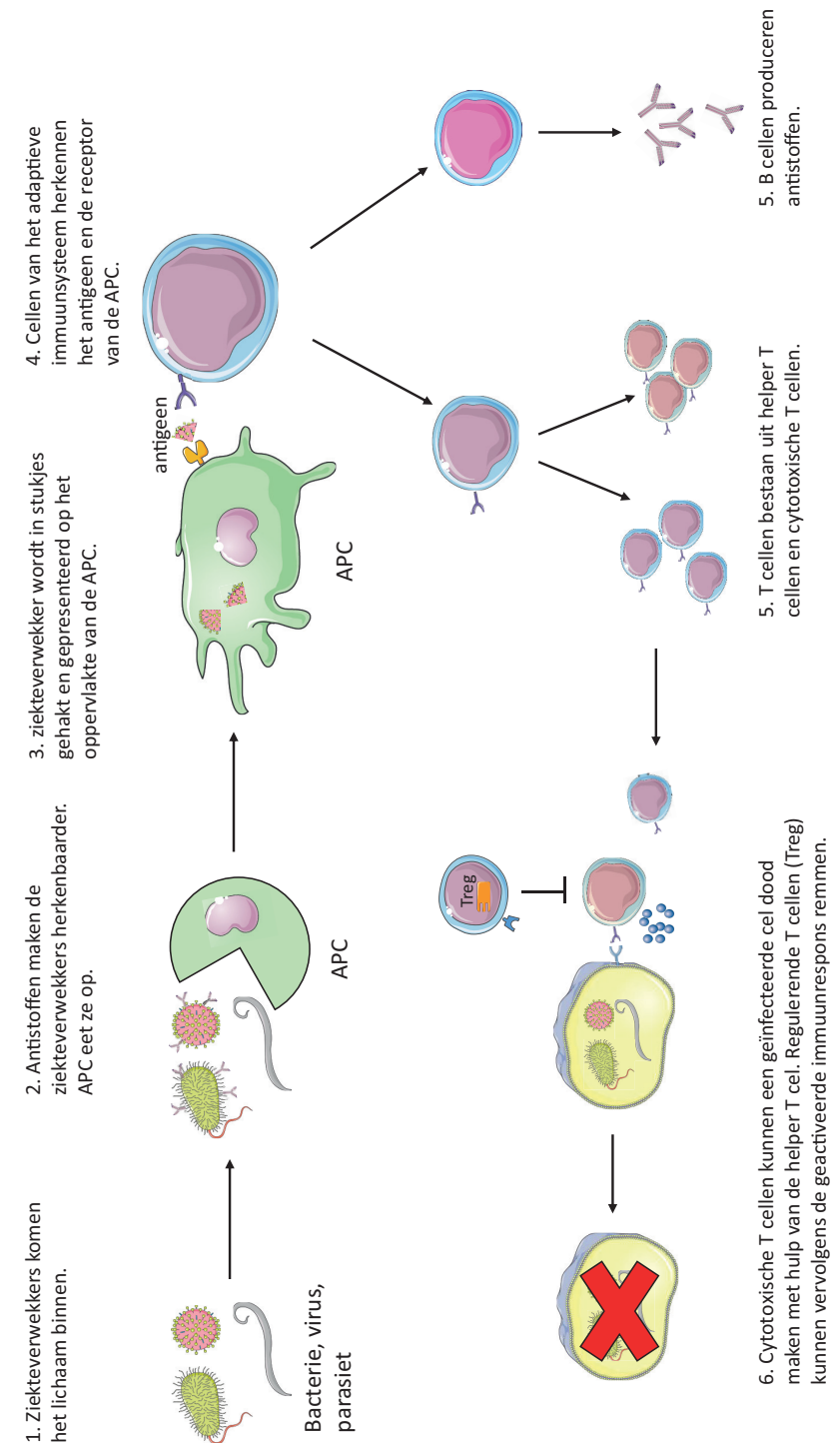
Het immuunsysteem

Ons afweersysteem (immuunsysteem) bestaat uit twee delen: het aangeboren en het adaptieve immuunsysteem. Het immuunsysteem is vooral belangrijk vanwege zijn mechanismen die er voor zorgen dat we niet ziek worden. Het beschermt ons lichaam tegen ziekteverwekkers zoals virussen, bacteriën en parasieten. Dit kan doordat het immuunsysteem bepaalde stukjes van ziekteverwekkers kan herkennen. Deze stukjes heten antigenen. Als een ziekteverwekker ons lichaam binnen komt zullen als eerste de cellen van het aangeboren immuunsysteem reageren. De cellen van het aangeboren immuunsysteem gaan ons hele lichaam door om te zoeken naar lichaamsvreemde dingen zoals ziekteverwekkers. Als deze cellen bepaalde gevaarsignalen die de ziekteverwekker met zich meebrengt herkennen, zullen ze de ziekteverwekker aanvallen. Zo wordt de ziekteverwekker gemakkelijker herkenbaar gemaakt door er dingen aan te plakken (zoals antistoffen) en eten de cellen de ziekteverwekker op en hakken het in stukjes (peptiden). Cellen laten deze peptiden dan op hun oppervlakte zien aan cellen van het adaptieve immuunsysteem. Deze cellen herkennen de peptiden en worden hierdoor actief. De verschillende soorten adaptieve immuuncellen, B en T cellen, gaan vervolgens de ziekteverwekker, of de cellen geïnfecteerd door een ziekteverwekker, opruimen om te voorkomen dat we ziek worden. B cellen doen dit vooral door antistoffen te produceren. T cellen bestaan uit twee groepen: de cytotoxische T cellen en de helper T cellen. De cytotoxische T cellen kunnen geïnfecteerde cellen dood maken en de helper T cellen helpen andere T cellen, maar ook B cellen en cellen van het aangeboren immuunsysteem. Zo werken alle cellen van het immuunsysteem samen.

Natuurlijk is het ook belangrijk dat de immuuncellen niet actief blijven als een ziekteverwekker is opgeruimd. Dit kan namelijk schade toe brengen aan weefsels en andere cellen in ons lichaam. Om deze reden bestaan er immuuncellen die de actieve immuuncellen kunnen remmen. Dit zijn voornamelijk de regulerende T cellen. Alle soorten T cellen hebben dus ieder een belangrijke rol in ons afweersysteem.

Immuun tolerantie en auto-immuniteit

Omdat immuuncellen ook stukjes van het eigen lichaam laten zien op hun oppervlakte bestaat er een proces wat immuun tolerantie wordt genoemd. Dit betekent dat T cellen niet reageren op de stukjes die uit ons eigen lichaam afkomstig zijn (zelf-antigenen). Kort gezegd houdt immuun tolerantie in dat de T cellen die zelf-antigenen sterk herkennen dood worden gemaakt. Maar als dit proces van tolerantie mis gaat dan kunnen cellen toch zelf-antigenen herkennen en wordt



er een immuun reactie op gang gebracht terwijl dat niet nodig is. Dit noemen we auto-immuniteit. Hierdoor kan schade ontstaan en afhankelijk van de plek waar dat gebeurt ontstaan er verschillende auto-immuunziekten. Voorbeelden zijn diabetes type I, multiple sclerose en reumatoïde artritis. In dit proefschrift kijken we specifiek naar reumatoïde artritis.

Reumatoïde artritis

Reumatoïde artritis (RA) is een chronische auto-immuunziekte die wordt gekarakteriseerd door continue ontstekingen in de gewrichten. Hierdoor ontstaat schade aan het gewricht en hebben patiënten vaak last van pijnlijke en stijve gewrichten. Hoe RA precies ontstaat is nog steeds onbekend en daarom zijn de huidige medicijnen vooral gericht op symptoombestrijding. Wat wel bekend is over de ontwikkeling van RA is dat twee signaalstoffen betrokken zijn bij het initiëren van ontsteking: tumor necrose factor (TNF) en interleukine 6 (IL-6). Om deze reden zijn de meeste medicijnen er op gericht om TNF of IL-6 te remmen. Het probleem is dat TNF en IL-6 niet specifiek zijn voor RA en dus ook nuttige functies hebben. In plaats van het algemeen remmen van de immuun reactie/ontsteking zou het beter zijn om immuuntolerantie te herstellen zoals in gezonde personen. Om immuuntolerantie te induceren zijn de laatste jaren verschillende manieren onderzocht. In dit proefschrift hebben we twee manieren onderzocht om RA te behandelen.

In dit proefschrift

Om immuuntolerantie te krijgen zouden dendritische cellen kunnen worden gebruikt. Dendritische cellen (DCs) zijn professionele antigen presenterende cellen en kunnen niet alleen het immuunsysteem activeren maar ook remmen. Door deze dubbele functie zijn DCs belangrijk in het aansturen van het immuunsysteem en kunnen ze ook worden gebruikt als therapie. DC therapie kan worden ingezet om kanker te bestrijden maar wordt nu ook onderzocht als manier om immuuntolerantie te bewerkstelligen. Er zijn verschillende manieren om zogenaamde tolerante dendritische cellen (tolDCs) te maken. In dit proefschrift hebben we één van deze manieren gebruikt en deze nader onderzocht. Om de effecten van tolDCs op helper T cellen te onderzoeken hebben we een model gemaakt. In **hoofdstuk 2** beschrijven we hoe we een muis hebben gemaakt die alleen maar helper T cellen heeft die een stukje van één eiwit herkennen. Op deze manier kunnen we kijken of de tolDCs antigeen-specifiek contact maken met de helper T cellen. Uit deze proeven kwam dat tolDCs er niet perse voor zorgen dat er nieuwe regulerende T cellen ontstaan maar wel dat helper T cellen minder actief zijn en minder delen. Hiernaast zijn de regulerende T cellen die in de aanwezigheid zijn van tolDCs meer actief. Hierdoor zijn er relatief gezien meer regulerende T cellen aanwezig en wordt de immuun

respons geremd (**Hoofdstuk 3**). Als we muizen injecteren met tolDCs krijgen ze minder ernstige artritis symptomen dan muizen die geen tolDCs krijgen. Dit laat zien dat tolDCs niet alleen in het laboratorium invloed hebben op T cellen maar dat ze ook in het lichaam (*in vivo*) immuun modulerend zijn.

Omdat het nog niet precies bekend is hoe RA ontstaat weet men nog niet wat de zelf-antigenen zijn die de onnodige immuun respons veroorzaken. Hierdoor is er een surrogaat antigeen nodig, iets dat ervoor zorgt dat de 'slechte' immuun respons die de klachten veroorzaakt wordt geremd, maar dat de 'goede' immuun respons intact laat. Een optie voor een surrogaat antigen zou één van de heat shock eiwitten (HSPs) kunnen zijn. HSPs zijn eiwitten die worden aangemaakt bij stress en dus ook bij een ontsteking. Ze zijn evolutionair erg geconserveerd, wat betekent dat deze eiwitten er in een bacterie bijna hetzelfde uitzien als in de mens. In patiënten met RA zijn HSPs veel aanwezig in hun gewrichten, veel meer dan bij gezonde mensen. In **hoofdstuk 4** hebben we gekeken of immuuncellen van RA patiënten en gezonde mensen kunnen reageren op HSPs. Dit bleek in bijna 80% van de gevallen zo te zijn. Ook laten we in **hoofdstuk 4** zien dat als we tolDCs laden met HSPs, deze tolDCs er voor zorgen dat de helper T cellen een soort regulerende T cellen worden. Daarnaast werd door de proeven duidelijk dat tolDCs meer regulerende signaalstoffen (cytokines) maken dan controle DCs.

Het gebruiken van tolDCs voor het herstellen van immuuntolerantie lijkt dus veel belovend. Een probleem is echter dat als we dit in patiënten willen gebruiken, de voorlopers van de tolDCs eerst uit het bloed van patiënten moeten worden gehaald. Deze worden dan vervolgens in tolDCs verandert in het lab en terug gegeven aan de patiënt. Dit kost veel tijd en geld omdat het voor iedere patiënt persoonlijk moet. Daarom zou een manier die voor alle (of in ieder geval meerdere) patiënten werkt kosten effectiever zijn. Om deze reden hebben we ook nanopartikels onderzocht. Nanopartikels zijn kleine blaasjes van ongeveer 50-100 nanometer groot. Deze worden vooral ontwikkeld om medicijnen af te leveren in het lichaam. Dit omdat veel medicijnen niet vanzelf het celmembraan kunnen passeren. Zoals eerder genoemd worden er op dit moment medicijnen gebruikt in RA om TNF te remmen. Wat helaas vaak voorkomt is dat het immuunsysteem van patiënten gaat reageren op deze medicijnen en antistoffen aanmaakt tegen het medicijn. Hier kunnen bijwerkingen door ontstaan of het medicijn kan hierdoor onwerkzaam worden. Een manier om dit te voorkomen is om TNF niet te remmen als het al geproduceerd is door een cel, maar om de hele productie te stoppen. Dit kan door middel van RNA interferentie. Voordat een eiwit, wat TNF is, kan worden gemaakt wordt er eerst RNA gemaakt van het DNA in de cel. Dit RNA kan worden geremd met zogenaamd

'klein interfererend RNA' (small interfering RNA oftewel siRNA). Er is speciaal siRNA gemaakt wat specifiek gericht is tegen RNA wat codeert voor TNF. Vervolgens is dit TNF siRNA in een nanopartikel gestopt. In **(hoofdstuk 5)** laten we zien dat cellen van het aangeboren immuunsysteem de nanopartikels met TNF siRNA op kunnen nemen en de TNF productie in deze cellen kan worden geremd. Daarnaast kunnen de TNF siRNA bevattende nanopartikels artritis symptomen in de muis remmen. Hoewel de nanopartikels lokaal (in het enkelgewricht) waren ingespoten, was er een systemisch effect. Dit betekent dat niet alleen de behandelde poot minder ontstoken was maar ook de andere poten. Hoe dit precies werkt is nog onbekend en daarvoor is verder onderzoek nodig.

Vaccins worden vaak in de spier (intramusculair) geïnjecteerd. Er zijn ook andere routes mogelijk die misschien voor tolerogene therapieën zoals de toIDCs of de nanopartikels gunstiger zijn. Daarom hebben we in **hoofdstuk 6** twee verschillende toedieningsroutes vergeleken met behulp van een model vaccin: intranasaal (in de neus) en intradermaal (net onder de huid). Het voordeel van deze routes, naast de traditionele intramusculaire route, is dat op beide plekken veel immuuncellen dichtbij zijn. Hoewel beide routes een immuun stimulerend effect laten zien met het model vaccin was er toch een duidelijk verschil. Na intra dermale toediening werd er meer antigen opgenomen door antigen presenterende cellen en was er dus ook meer T cel activatie te zien. De resultaten in **hoofdstuk 6** laten zien dat de werking van het vaccin mede wordt bepaald door de toedieningsroute.

Conclusie

Om mensen met RA te kunnen genezen zijn er andere medicijnen nodig dan er momenteel beschikbaar zijn. Omdat er een disbalans is in het immuun systeem moeten we zoeken naar mogelijkheden om deze disbalans in tolerantie te herstellen; toIDCs zijn een veel belovende mogelijkheid hiertoe. Met toIDCs zouden patiënten door een gepersonaliseerde therapie genezen kunnen worden. Hiernaast kunnen nanopartikels die TNF siRNA bevatten gebruikt worden om RA te remmen, maar zouden nanopartikels ook kunnen worden gebruikt om de immuun balans te herstellen. Er moet nog meer onderzoek worden gedaan om deze therapieën verder te ontwikkelen. Dit proefschrift draagt bij aan de kennis over toIDCs en nanopartikels en brengt de wetenschap een stap dichterbij het ontwikkelen van een specifieke therapie voor RA en mogelijk ook voor andere auto-immuunziekten.

Dankwoord

Het is voor mij alweer tijd om deze laatste bladzijdes van mijn proefschrift te schrijven. Ongelooflijk wat zijn die 4 jaar snel gegaan!

Allereerst wil ik graag **Femke** bedanken. Dankjewel voor je enthousiasme en positiviteit. Het was super fijn dat ik al mijn ideeën altijd kon spuien zonder me af te vragen of het geen stomme plannen waren. Ondanks dat je erg druk bent kon ik je altijd bereiken ook al moest je er zelfs een OK voor uitlopen.

Willem, bedankt voor de mogelijkheid om hier te promoveren en je 'insights' in de academische wereld.

Ook veel dank aan de **Immuno** afdeling; met veel taart, gezellige lunches, labuitjes, kerstborrels en vooral altijd beschikbare hulp heeft het mijn AIO-tijd een stuk gemakkelijker en leuker gemaakt. Ik hoop dat ik heb kunnen bewijzen dat je ook zonder koffie je AIO tijd prima door kan komen ;). Vooral ook dankzij mijn medemuizen AIOs: **Anouk, Marit** en **Suus**, die me hun kennis over hebben gedragen over de wondere wereld van het proefdieronderzoek. **Suus**, dankjewel voor al je hulp bij (non)AIO gerelateerde dingen en op de soms lange proefdagen, gelukkig maakten proefkoekjes veel goed. **Irene**, mijn paranimf en super-collega. Dankjewel voor al je hulp op het lab, bij de muizen maar vooral ook daarbuiten. Heel fijn om te weten dat er altijd iemand voor je klaar staat!

Dankjewel ook de andere AIO's van het lab, **Lindert, Eef, Peter, Charlotte** en **New**: thanks for all your advice and 'gezelligheid' at work, 'borrels', conferences and retreats. **Peter**, de uitstapjes naar the Village hebben de schrijfperiode zeker leuker gemaakt. Dankzij de 2016-lichting AIOs **Robin, Andreja, Nathalie** en **Qingkang**, kwamen er weer nieuwe ideeën en enthousiasme de afdeling binnen. **Nathalie**, bedankt dat je mijn paranimf wilde zijn. Ondanks dat we met verschillende diersoorten werken, hadden we toch veel overeenkomsten en dat was wel eens handig. Die nuchtere blik van jou is geweldig. En wanneer gaan we nou eindelijk eens samen fietsen?

Dan W442, mijn kamergenootjes: **Peter**, wat weet jij veel en allemaal uit je hoofd! Ondanks dat je met namen wel eens moeite hebt was het erg handig om 'mijn' muizenfok, hybridoma's en andere informatie die ik nodig had zo dichtbij te hebben. Daarnaast was je niet te beroerd om me advies te geven over hypotheek, fietsreparaties, bedrijven en nog veel meer. **Charlotte**, ondanks dat ik je vaak heb moeten missen (eerst alleen de CBG dagen, daarna verlof en welverdiende mama

dagen) vond ik het altijd erg gezellig als je er was! Dankje voor alle leuke gesprekken (met of zonder telcon ondertussen) en goede adviezen. **Robin, W442** werd weer een stukje gezelliger (met een zachte G!) met jou erbij.

Bedankt ook mijn studenten **Ashley** en **Thomas**, door jullie te begeleiden heb ik veel van jullie geleerd en dat is omgekeerd hopelijk ook zo.

Dan nog de dames van het GDL, **Ivonne, Anja** en **Nicky**, dankjewel voor jullie hulp en de goede zorg voor de muizen.

Ruben, Carlos, Lars en daarna **Nienke**, met jullie borrels organiseren voor I&I was elke keer weer een feestje. Naast kilo's Japanse mix en kin hechtingen zal ik me vooral de hele serieuze vergaderingen herinneren.

Naast de collega's op het lab heb ik ook veel samenwerkingen gehad. Een hele belangrijke was de samenwerking met **Catharien** en **Rachel** in Newcastle. Dankjewel voor de ontzettend nuttige skype meetings. Hier heb ik ontzettend veel aan gehad! Another collaboration was with the group in Copenhagen. Thank you, especially **Camilla, Xianghui** and **Kaushik** for the successful collaboration described in chapter 5.

In June 2016, I visited the lab of **Andrew Macdonald** in Manchester. Thank you for giving me the opportunity to visit your lab and learn about Flt3L DC cultures and multi-color flow (thanks **Alex!**). I had a great time!

Dit boekje was er nooit gekomen zonder de steun van familie en vrienden. Mijn 'oudste' vriendinnen, **Lieke, Juliette, Karin** en **Helmi**, super fijn dat jullie er na al die jaren (we moeten volgens mij nog steeds ons 10 jarig jubileum vieren, 5 jaar te laat) nog steeds zijn. Ook al was het soms onbegrijpelijk wat ik nou precies allemaal deed toch waren jullie altijd vol interesse en begrip.

Dan het BMW-groepje, **Liz, Tom, Chantal, Erik, Guido** en **Joost**, ondanks dat we elkaar niet meer zo veel zien als tijdens onze studie, is het nog steeds elke keer gezellig als we afspreken. **Liz** en **Tom**, altijd leuk om jullie te zien op de immunocongressen, veel herkenbare verhalen!

Fijn is het ook om zo'n warme schoonfamilie te hebben, **Arie, Dienne, Esther, Asanka, Ruwan, Bas** en **Soraya**, dankjewel voor alle belangstelling en gezellige weekendjes in Ommen.

Opa, ook al was er in het begin verwarring omdat ik bij diergeneeskunde werk toch vind je het nu maar wat interessant en vraag je dingen over reuma als je hier ergens iets over hebt gehoord. Dankzij de liters soep die ik van je heb gehad werd mijn lunch vaak lekkerder!

Pap, mam dank jullie wel voor alle lange telefoontjes, rotsvast vertrouwen en humor. Bij jullie thuis komen voelt nog steeds als een warm bad. Leuk om te horen dat jullie vol trots uit proberen te leggen aan andere mensen wat ik nou eigenlijk doe.

Hugo en Anne, fijn om altijd bij jullie terecht te kunnen in wat soms voelt als mijn 3^e huis. **Hugo**, dankjewel voor het lezen van de Nederlandse samenvatting, ik weet dat het soms niet gemakkelijk is met drie biomedici om je heen. **Zus**, tja hoe kan ik jou bedanken. Je bent er altijd als ik je nodig heb met advies, steun en heel veel gezelligheid. Super fijn!

Als allerlaatste, lieve **René**, dankjewel dat je mee ging als ik nog even mijn cellen moest voeren in het weekend onderweg naar familie. Dankje voor je vele knuffels, luisterend oor en bemoedigende toespraken. Ook al is er veel veranderd sinds we samen zijn (van student naar samen wonen in ons eigen huis), nog steeds sta je altijd achter me. Ik kijk uit naar onze volgende avonturen!

Curriculum Vitae

Manon Aleida Adriana Jansen was born on the 17th of November 1990 in Sint Michielsgestel, the Netherlands. In 2009 she graduated from Gymnasium Beekvliet (pre university education) in Sint Michielsgestel. In September 2009, she started her university education at Utrecht University. She obtained her bachelor degree in Biomedical sciences in 2012 after which she continued with her master Biology of disease (Utrecht University). During her masters in 2012-2013, she conducted an internship in the Wilhelmina Children's hospital under supervision of dr. Thijs Flinsenberg and dr. Marianne Boes on optimizing antigen cross presentation by human dendritic cells. In 2013, she also started a minor Science communication and education as part of her master. In 2014, she conducted an internship at the Inflammation research center in Ghent (in the lab of Bart Lambrecht) under supervision of dr. Mary van Helden on ILC3s in the murine gut. After this, she wrote her master thesis under supervision of Prof. dr. Roel de Weger and dr. Manon Huibers about Cardiac allograft vasculopathy. Manon obtained her master's degree in 2014.



In 2014, Manon started her PhD project at the Immunology division of the department Infectious diseases and Immunology, at Utrecht University under supervision of Prof. dr. Willem van Eden and Prof. dr. Femke Broere. She studied several therapeutic interventions for Rheumatoid arthritis and was part of multiple international collaborations (e.g. Newcastle University and Copenhagen University) and the European 'Action to Focus and Accelerate Cell-based Tolerance-inducing Therapies (AFACTT)' consortium. During her PhD, Manon received a short term scientific mission grant from AFACTT to join the lab of Prof. dr. Andrew MacDonald in Manchester to expand her knowledge on multi-color flow cytometry. Also during her PhD, Manon was an active member of the Veterinary PhD council, organizing lectures and workshops for fellow PhD students. The research conducted during her PhD is described in this thesis and published in peer-reviewed scientific journals. She will continue her scientific career as clinical scientist at the center for human drug research in Leiden.

List of publications

M.A.A. Jansen, R Spiering *et al.* Matured tolerogenic dendritic cells modulate pre-activated and naïve CD4⁺ T cells and ameliorate proteoglycan induced arthritis in mice. *Submitted.*

M.A.A. Jansen, L.H. Klausen *et al.* Lipidoid-Polymer hybrid nanoparticles loaded with TNF siRNA suppress inflammation after intra-articular administration in a murine experimental arthritis model. *Submitted.*

R Spiering, **M.A.A. Jansen** *et al.* Targeting of tolerogenic dendritic cells to heat-shock proteins in inflammatory arthritis. *Submitted.*

S van Aalst, **M.A.A. Jansen** *et al.* Routing dependent immune responses after experimental R848-adjuvated vaccination. *Vaccine*, 2018 Mar 36; 1405–1413.

W van Eden, **M.A.A. Jansen** *et al.* The immuno-modulatory potential of tolDCs loaded with heat shock proteins. *Frontiers in Immunology*, 2017 Nov 30;8:1690

W van Eden, **M.A.A. Jansen** *et al.* The Enigma of Heat Shock Proteins in Immune Tolerance. *Frontiers in Immunology*, 2017 Nov 21;8: 1599.

M.A.A. Jansen, Spiering R *et al.* Targeting of tolerogenic dendritic cells towards heat shock proteins: a novel therapeutic strategy for autoimmune diseases? *Immunology*. 2017 Aug 14.

M.A.A. Jansen, M.J.C. van Herwijnen *et al.* Generation of the first TCR transgenic mouse with CD4⁺ T cells recognizing an anti-inflammatory regulatory T cell-inducing HSP70 peptide. *Frontiers in Immunology* 2016 Mar 9;7:90.

M.A.A. Jansen, H.G. Otten *et al.* Immunological and Fibrotic Mechanisms in Cardiac Allograft Vasculopathy. *Transplantation*. 2015 Dec;99(12):2467-75.

T. Flinsenberg, L. Spel, **M. Jansen** *et al.* Cognate CD4 T-cell licensing of dendritic cells heralds anti-cytomegalovirus CD8 T-cell immunity after human allogeneic umbilical cord blood transplantation. *J. Virology* 2015 Jan 15;89(2):1058-69.

